Potentiating M1 and mGlu1 receptors to modulate prefrontal cortical dysfunction in psychiatric diseases

By

James Thomas Michael Maksymetz

Dissertation

Submitted to the Faculty of the

Graduate School of Vanderbilt University

in partial fulfillment of the requirements

for the degree of

DOCTOR OF PHILOSOPHY

in

Pharmacology

March 31st, 2020

Nashville, Tennessee

Approved:

P. Jeffrey Conn, Ph.D.

Craig W. Lindsley, Ph.D.

Brad A. Grueter, Ph.D.

Roger J. Colbran, Ph.D.

Sachin Patel, M.D., Ph.D.

ACKNOWLEDGEMENTS

There are countless people that have contributed scientifically and intellectually to the work described in this dissertation. First and foremost, I would like to sincerely thank my graduate mentor Dr. P Jeffrey Conn for all of his support and guidance. I am eternally grateful for the scientific, career, and life advice that Jeff has provided throughout my graduate career. I would also like to thank the members of my dissertation committee for their helpful feedback, for putting up with my ever-changing research directions, and for continuously supporting my scientific and career development.

Thank you to all of the members of the Conn lab, past and present, who have made the last few years a blast, through the good and the bad. In particular, I would like to thank the other half of “Shames”, Sean Moran, for his friendship and for being a great sounding board for ideas, problems, and terrible jokes. I will forever believe that our endless, pedantic arguments were essential for getting through graduate school. I would also like to thank Max Joffe for being a great friend and an amazing mentor in the lab. His help scientifically with the work in this dissertation has been invaluable but he is also an amazing role model for young scientists; he will without a doubt be an extraordinary professor. I would like to thank Branden Stansley for selflessly accompanying me to Italy and Aspen, but particularly for contributing to the fear conditioning work in this dissertation. A special thank you to Brianna Li for being a great trainee and for the genotyping, staining, and behavior you did! Likewise, I would like to thank Samantha Yohn, Jordan Galbraith, and Ellen Reith for collaborating on behavioral studies. Thank you to Nellie Byun for running the phMRI experiments, to Carrie Jones for providing the GluN1 KD mice, and to Craig Lindsley and all the members of the VCNDD who synthesized and provided an endless assortment of VU compounds for these studies. I would be remiss not to thank Nicole Fisher for her camaraderie in lab, in the Pharmacology department, and especially when we served on the PhGSA together. To all of the other members of the Conn Lab and VCNDD that I worked closely

with including Dan Foster, Mark Moehle, Shalini Dogra, Zixiu Xiang, Jerri Rook, Colleen Niswender, Rocco Gogliotti, Sheryl Vermudez, and many others: thank you for your support and feedback over the years.

I would like to acknowledge the amazing friends and colleagues I have made throughout graduate school who will undoubtedly be incredibly successful in all their future endeavors. I would also not be where I am today without the constant support of my family, persisting through the convoluted and likely incredibly boring descriptions of what I do but always being there when I need to talk and supporting me through thick and thin. Finally, none of this would have been possible without the constant support of my amazing partner Stephanie who has been there for me through it all. Thank you so much.

TABLE OF CONTENTS

LIST OF FIGURES

Page

CHAPTER I

STRUCTURE AND FUNCTION OF THE PREFRONTAL CORTEX

The neocortex is a collection of recently developed brain structures that expanded in size and complexity early in mammalian evolution to ultimately produce the collection of human cortices that define our intellectual and emotional abilities (*1*). During this expansion, the human prefrontal cortex (PFC) in particular underwent a significant increase in size as well as afferent and efferent connectivity compared to rodents and nonhuman primates (*2*, *3*). The PFC is an associational cortex that is critical for the integration of cortical and subcortical information and exertion of top-down control over the function of various downstream brain regions. The human PFC can be broadly subdivided into two functionally and anatomically distinct subregions: the orbitomedial and the dorsolateral PFC (*4*). The orbitomedial PFC is generally considered to be involved in emotional regulation while the dorsolateral PFC (dlPFC) is critical for cognitive functions. For the purposes of this dissertation, the discussion will focus on the dlPFC due to the wealth of information about its function and dysfunction in various disorders.

The dlPFC (corresponding to Brodmann areas 9 and 46 in humans) is involved in higher-order cognitive and executive functions including working memory and attention. Working memory is the ability to maintain relevant information over a short period of time to guide future actions while attention refers to the ability to appropriately respond to external and internal stimuli; these two functions operate together to allow for higher order behavioral and cognitive flexibility (*5*). The computational tasks performed by the dlPFC therefore allow for the temporal guidance of behavior based on previous and pertinent information. Evidence for the involvement of the dlPFC in these functions comes from early work from the labs of Fuster (*6*) and Goldman-Rakic (*7*), which identified that neurons in the non-human primate dlPFC were able to encode spatial working memory information by firing over a delay period in a given task, interpreted as holding information

"online" without the need for sensory input. Contemporaneously, clinical imaging work demonstrated that dlPFC activity increases during attentional (*8*) and working memory tasks (*9*) in healthy human volunteers providing further evidence that the dlPFC is responsible for these cognitive functions.

Lesion studies in both humans and primates have further shed light on dlPFC function and dysfunction. Perhaps the first and most famous example in the literature of a frontal lobe lesion is that of Phineas Gage, a railroad worker who survived a large iron rod driven through his skull and left frontal lobe and subsequently exhibited significant behavioral and personality changes (*10*, *11*). More specifically, lesions to the dlPFC in non-human primates and humans result in impaired working memory, increased distractibility, difficulties in rule and reversal learning, poor planning and organizational skills, and a loss of initiative or reduction in motivation (*12*). Together, these findings support the theory that the dlPFC is critical for executive functions, especially working memory and attention. Furthermore, many of the phenotypes observed after dlPFC lesions mimic symptoms of common psychiatric disorders that have been clinically linked to dlPFC dysfunction, including schizophrenia (*13*), major depressive disorder (MDD) (*14*), stress and anxiety disorders (*15*), autism spectrum disorders (ASDs) (*16*), and attention-deficit/hyperactivity disorder (ADHD) (*5*).

Based on the involvement of the dlPFC in everyday cognitive tasks and abundant evidence of its dysfunction in a variety of diseases, there has been a focus on pharmacological manipulation of the dlPFC to treat various psychiatric disorders (*17*). Ameliorating deficient dlPFC function in many psychiatric diseases is especially important as an increased severity of cognitive deficits is associated with poorer long-term functional outcomes for patients (*18*, *19*). While there are multiple psychiatric drugs with various mechanisms-of-action on the market for disorders such as schizophrenia, the vast majority were discovered serendipitously, they are not broadly efficacious across all symptoms of these disorders nor across the entire patient population, and they commonly have serious adverse effects leading to poor compliance and discontinued use

(*20*–*22*). Therefore there is a critical unmet need to identify novel pharmacological targets to modulate dlPFC function that have better efficacy profiles and improved therapeutic windows. To discover and characterize novel targets, it is essential to understand the molecular, cellular, and circuit-level biology of the dlPFC.

While the human dlPFC would be the ideal system in which to study and identify novel targets, for ethical, moral, and technical reasons we must rely on animal models to guide drug development and target validation (*23*). Likewise, non-human primates would be the ideal alternative due to functional and anatomical similarities between the human and primate dlPFC (*24*) but there are significant limitations on the use of non-human primates including cost, availability, and genetic tractability (*25*). Rodent models, on the other hand, provide an ideal preclinical framework in which to identify novel pharmacological targets. In addition to allowing for large sample sizes, rodent models permit the study of molecular, cellular, and circuit-level functions underlying psychiatric disorders in tandem or in combination with behavioral outputs (*23*). Specifically, the genetic tractability of mice, in particular, has led to their increased use in preclinical research, leveraging advances in cell-type specific genetic targeting, opto- and chemogenetics, and *in vivo* biosensors to investigate the necessity and sufficiency of certain genes, cell types, and neural circuits in behaviors relevant to psychiatric disorders and pharmacological manipulations.

Although rodent models present practical and technical advantages, an important caveat is that rats and mice do not have a granular dlPFC (*26*, *27*). While the human dlPFC is a hexalaminar region consisting of layers I through VI with a granular layer IV as a defining feature of the PFC (*28*), there exists no anatomical and functional dlPFC homolog in the rodent containing a granular layer IV (*29*). Rodents do however have collection of brain regions considered by many to be the PFC (Figure 1, Page 5) (*30*–*32*). These regions are typically defined as frontal cortical regions receiving input from the mediodorsal nucleus of the thalamus (MDT), as input from this region is largely restricted to the frontal cortex in primates and other mammals (*27*, *33*). This

corresponds to the medial regions of the rodent frontal cortex consisting of the prelimbic (PL), infralimbic (IL), and anterior cingulate (ACC) cortices (*34*, *35*). Typically, the PL and IL cortices are referred to together as the medial PFC (mPFC) and in addition to MDT innervation, rodent mPFC lesions produce similar deficits in working memory, attention, and emotional behaviors to primate dlPFC lesions (*36*). Furthermore, there is evidence that the more dorsal PL subregion is important for cognitive behaviors, functionally analogous to the human dlPFC, while the more ventral IL subregion is involved in emotional regulation, functionally similar to the human orbitomedial PFC (*36*, *37*). While there are clear reasons for why these regions are not perfect models for the human dlPFC (*29*), the functional similarities between the human and rodent PFC regions support the use of rodent models to study and identify novel pharmacological targets that, with proper translational and clinical validation, may yield life-changing therapeutics for patients suffering from psychiatric disorders. For this reason along with the functional similarities to the human dlPFC, the majority of the discussion in this chapter will focus on the rodent PL cortex.

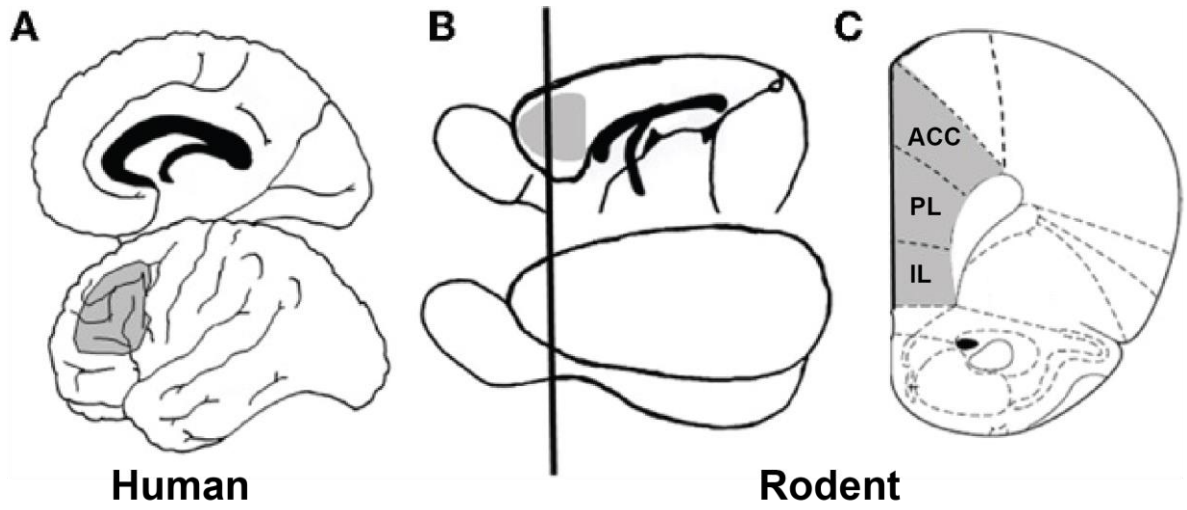

Figure 1: Structural differences between the human and rodent PFC. **(A)** The dorsolateral prefrontal cortex (dlPFC) is involved in executive and cognitive functions. Gray area denotes Brodmann area 46, part of the dlPFC along with Brodmann area 9. **(B)** A sagittal view of the rodent brain with the analogous rodent PFC denoted in grey. **(C)** A coronal view of the rodent PFC corresponding the black bar in panel B. The rodent PFC is denoted in grey and subdivided into the anterior cingulate cortex (ACC), prelimbic cortex (PL), and infralimbic cortex (IL). Adapted from (*38*).

1.1 PFC Macrocircuitry

The rodent PL cortex is agranular and consists of five main layers, I, II, III, V, and VI, with the notable exception of a granular layer IV. The flow of information through different cortical layers has been extensively studied in other cortical regions such as the somatosensory or visual cortices where thalamic afferents densely innervate the layer IV cells which then relay information to be integrated in layer II/III which then transmits the information to the output layer V neurons (*39*). Since the PL cortex lacks a layer IV, afferents from thalamic and other brain regions directly innervate the pyramidal neurons of layers II/III, V, and occasionally VI, all of which have dendrites spanning multiple layers including layer I. The PL cortex receives direct excitatory input from a vast array of other brain regions including cortical areas such as the orbital and IL cortices, limbic regions including the hippocampus and amygdala, and thalamic regions including the MDT and the nucleus reuniens (*35*, *40*). The PL sends direct output to multiple regions including cortical, limbic, thalamic, and neuromodulatory structures as well (*36*). It is through the processing of this diverse array of incoming information and the subsequent output to various regions involved in

cognitive function that the PL cortex is capable of mediating the various executive functions previously described.

Thalamic Connectivity

One of the defining features of the PL cortex (along with other PFC regions) is dense innervation from the MDT (Figure 2, Page 7). Input from the MDT primarily terminates in superficial layers I and III (*41*, *42*) where it forms functional synapses onto layer II/III pyramidal neurons (*43*) and the dendrites of layer V pyramidal neurons (*44*) in addition to certain inhibitory interneurons (*45*). The ventromedial thalamus (VMT) also send axons to the PL cortex and these inputs terminate densely in layer I, activating both layer I interneurons (*46*) and layer II/III and V pyramidal neurons (*44*). Axon labelling from both the MDT and the VMT are also found in deeper layers but it is unclear if these are functional terminals or just passing through to the more superficial layers (*41*, *44*). The nucleus reuniens (RE), another midline thalamic nuclei that forms reciprocal connections with the hippocampus and the PL cortex, sends axons that terminate densely in layer I and deep layers V and VI of the PL cortex (*47*). Stimulation of the RE *in vivo* produces depolarizing responses across PL layers indicating that functional synapses between the RE and PL cortex (*48*).

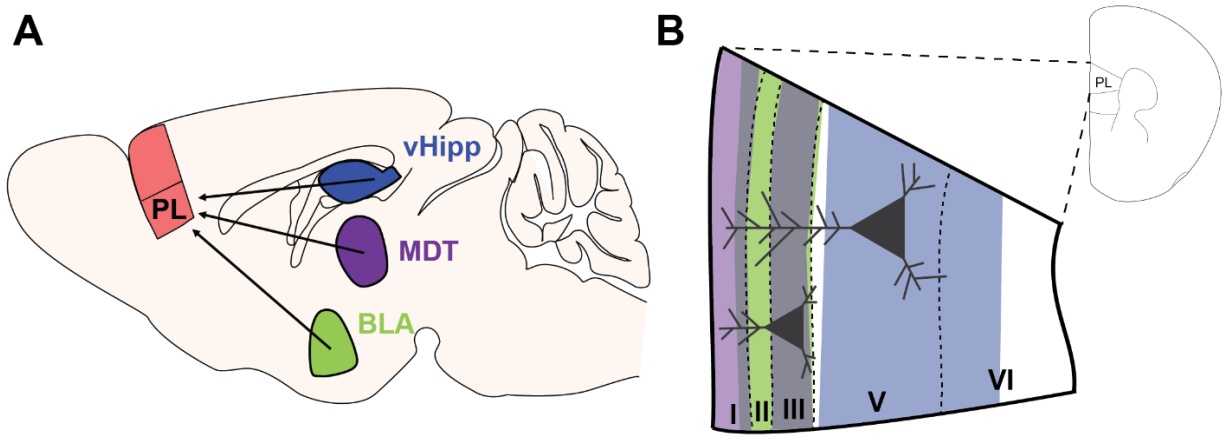

Figure 2: Thalamic and limbic projections to the prelimbic cortex. **(A)** Simplified schematic depicting three major projections to the rodent PL cortex including the ventral hippocampus (vHipp), mediodorsal thalamus (MDT), and basolateral amygdala (BLA). The ventral hippocampus is depicted to improve visualization but is actually closer to the location of the BLA. **(B)** Simplified schematic depicting the laminar structure of the PL cortex with a layer III and a layer V pyramidal neuron. Note the apical dendrites projecting up into the superficial layers. The major projection fields of the vHipp (blue), BLA (green) and MDT (purple) are depicted. These represent the areas with the densest labeling of axons from each respective region although inputs from all three regions can be found in all PL cortex layers. The BLA and MDT projection fields overlap in the superficial layers.

The PL cortex forms reciprocal connections with the MDT, VMT, and RE (*36*). These corticothalamic projections primarily originate from the deeper layers V and VI (*44*), consistent with cortical organization described in granular cortices (*49*). For both the MDT- and VMT-PL connection, there exists a closed loop circuit whereby thalamic input synapses onto the superficial layer II/III neurons, which in turn synapse onto thalamus-projecting layer V neurons. Additionally, thalamic input to layer V can directly synapse onto layer V corticothalamic pyramidal neurons (*44*, *50*).

At a functional level, thalamic connectivity with the mPFC is important for a variety of behavioral tasks (*51*). MDT lesions produce behavioral deficits similar to mPFC lesions in rodents, including deficits in working memory and attentional set-shifting (*52*, *53*). Similarly, chemogenetically inhibiting the MDT impairs behavioral flexibility, working memory, and PFC-MDT neuronal synchrony (*54*). Another study recently corroborated these behavioral findings and also found that chemogenetic MDT inhibition produced deficits in social preference (*55*). Specific

to PFC-MDT connectivity, chemogenetic or optogenetic inhibition of the PFC-MDT connection impairs goal-directed behaviors (*56*), behavioral flexibility (*57*), and spatial working memory (*58*). Finally, a recent study demonstrated that both PL and IL output to the RE is required for fear extinction retrieval, a top-down cognitive process that is impaired in multiple psychiatric disorders (*59*). Altogether, these findings support the role of MDT-PFC connectivity in various higher order cognitive tasks.

Limbic Connectivity

In addition to thalamic input, the mPFC also receives dense innervation from various limbic regions including the ventral region of the hippocampus (vHipp) and the basolateral amygdala (BLA) (Figure 2, Page 7) (*35*). Retrograde tracing studies demonstrate that the mPFC receives direct input from neurons in the ventral subiculum and CA1 regions of the vHipp with no observable afferents from the dorsal hippocampus. Anterograde labelling of vHipp projections revealed that vHipp afferents terminate primarily in the deep layers of the PL and IL cortices, with a denser innervation of the IL over the PL (*60*). The vHipp projections form monosynaptic, glutamatergic synapses onto PL pyramidal neurons as well as various interneurons throughout the PL cortex and are capable of mediated feed-forward inhibition (*61*, *62*). There is sparse vHipp axon labelling in the superficial layers of the PL cortex (*43*, *60*) and direct excitatory connections from the vHipp to PL cortex primarily target layer V pyramidal cells (*63*). Interestingly, unlike thalamic connectivity, there is no monosynaptic reciprocal connection from the PL cortex to the vHipp (*36*). The PFC-vHipp loop is formed by indirect circuits through regions such as the RE and the entorhinal cortex which receive projections from the PL cortex and in turn project to the hippocampal formation (*35*, *64*).

The BLA sends strong reciprocal connections to both the PL and IL cortices, primarily innervating the superficial layer II/III but also deeper layer V pyramidal neurons (Figure 2, Page 7) (*35*, *43*, *65*). *In vivo* stimulation of the BLA evokes both monosynaptic glutamatergic responses as well as strong, polysynaptic inhibitory responses in the mPFC (*66*), suggesting that BLA input

to the PFC drives robust feed-forward inhibition in the cortex (*65*, *67*). Unlike the vHipp but similar to the MDT, the mPFC projects back to the BLA to modulate its function (*36*). mPFC neurons that project to the BLA are primarily concentrated in superficial layers II and III (*65*, *68*) and typically receive strong glutamatergic input from the BLA as well as polysynaptic feed-forward inhibition (*65*). This suggests that the mPFC processes incoming emotional information from the BLA by heavily gating its input.

Functionally, the involvement of both the vHipp and BLA inputs to the mPFC in certain behaviors and pathological states has been extensively studied (*69*–*71*). Initial disconnection studies of the vHipp and mPFC resulted in spatial working memory deficits, consistent with a role of the hippocampus in spatial learning and memory (*72*, *73*). It has also been known for over a decade that the hippocampus and mPFC exhibit coordinated synchrony of neuronal oscillations, primarily in the theta frequency band (4-12 Hz) during spatial working memory tasks, suggesting functional interactions between these brains regions during behavior (*74*, *75*). This synchrony increases as animals learn a spatial working memory task and impairments correlate with deficits in behavioral performance (*76*), indicating that the mPFC-vHipp connectivity is critical for proper working memory function. Furthermore, optogenetic inhibition of vHipp terminals in the mPFC during a delayed non-match to place working memory task impairs behavioral performance (*77*), directly implicating the vHipp-to-mPFC synapse in spatial working memory. Furthermore, chemogenetically increasing vHipp-mPFC transmission impairs social recognition memory in mice (*78*).

Some of the most rigorously studied functions related to vHipp, BLA, and mPFC connectivity are fear learning and anxiety-like behaviors (*71*, *79*). Inactivation of the PL cortex does not affect acquisition but impairs the expression of fear learning, similar to inactivation of the BLA or vHipp (*80*). BLA and vHipp afferent activity also integrate in the mPFC during fear expression such that vHipp-mediated feed-forward inhibition gates BLA-induced mPFC activation to reduce fear expression and to mediate fear extinction behavior (*81*). Consistent with this,

optogenetically inhibiting PL cortex-projecting BLA neurons (*82*, *83*) or reducing BLA-mPFC synaptic strength by optogenetic induction of synaptic long-term depression (*84*) reduces fear expression and facilitates extinction while optogenetic activation of PL cortex-projecting BLA neurons increases fear behavior (*83*). From lesion and optogenetic studies, the vHipp-mPFC connection appears to be critically involved in contextual aspects fear and extinction, specifically context-dependent fear retrieval after extinction training (*70*). Disconnection by contralateral lesions of the vHipp and mPFC prevents post-extinction fear renewal in a novel context (*85*) and optogenetic inhibition of mPFC-projecting vHipp neurons reduces fear renewal (*86*). Additionally, optogenetic vHipp-to-mPFC inhibition is required for anxiety-like behaviors (*87*) and chemogenetic activation or inactivation of mPFC-projecting vHipp neurons birdirectionally modulates anxiety behaviors whereby decreasing vHipp-mPFC activity is anxiolytic (*88*). Similarly, optogenetic activation of mPFC-projecting BLA neurons increases anxiety whereas inhibition of these neurons reduces anxiety-like behaviors (*89*). Altogether, it is clear that vHipp/BLA-mPFC communication is critical for higher-order cognitive and emotional functions such as working memory, fear learning, and anxiety.

Finally, the mPFC also projects to the nucleus accumbens (NAc), a limbic region critical for reward and motivated behaviors, but does not receive direct NAc input (*35*, *36*, *90*, *91*). This mPFC-NAc connection is involved in goal-directed and reward related behaviors as well as mood regulation (*92*, *93*). Interestingly, a long-range GABAergic projection from the mPFC to the NAc exists and optogenetic activation of these projections results in avoidance behavior, suggesting these peculiar projections transmit negative valence (*94*). Conversely, optogenetic stimulation of glutamatergic PL cortex inputs to the NAc has been shown to reverse deficits in social interaction and anhedonia in addition to heightened anxiety (*95*), implicating the glutamatergic connection between the PL cortex and NAc in positive valence states. Furthermore, various forms of synaptic plasticity have been described at the mPFC-NAc synapse that are thought to contribute to motivational behaviors in normal and pathological states, such as drug seeking (*92*, *93*, *96*, *97*).

This implies that motivation and goal-directed behaviors are influenced both by the integration performed by NAc-projecting neurons in the mPFC as well as locally at the synaptic level in NAc. Through efferent connectivity to the NAc, the mPFC is therefore capable of modulating and exerting control over motivated behaviors.

Other Brain Regions and Neuromodulatory Connectivity

The PL cortex also forms connections with various other sensory and associative cortical regions such as the medial frontal polar cortex, insular cortex, orbitomedial cortex, IL cortex, and the contralateral PL and IL cortices (*35*, *36*). Consistent its cognitive function, the majority of connection to and from the PL cortex are from limbic-related cortices that are essential for various forms of cognition based on lesion and inactivation studies (*98*). Additionally, the PL cortex is heavily connected to the claustrum (*35*, *99*), a brain region that contributes to cognition and the coordination of other cortical areas.

In addition to excitatory, glutamatergic input from cortical and subcortical sources, the PL cortex receives a variety of neuromodulatory input (*35*) from regions that produce and release acetylcholine (ACh), dopamine (DA), norepinephrine (NE), and serotonin (5HT) (reviewed in (*100*)). The densest neuromodulatory input to the PL cortex is dopaminergic, primarily innervates deep layers, and arises from the ventral tegmental area (VTA), comprising part of the mesocortical DA pathway. Disruption or depletion of DA in the mPFC produces phenotypes similar to mPFC lesions including impairments in attentional set-shifting (*101*, *102*), working memory (*103*), and sensorimotor gating (*104*). The PL cortex also projects densely to the VTA, where it can either increase or decrease DA neuron activity, creating both a feedforward and feedback loop that can be differentially recruited in various cognitive and emotional situations (*105*). Terminals containing NE arising from the locus coeruleus are also found in both superficial and deep layers of the PL cortex and contribute to the higher-order functions of the region (*5*, *35*). Similar to the DA system, the PL cortex also projects back to the locus coeruleus and thus can regulate the activity of NE neurons. Pharmacological reductions in NE produce deficits in attention (*106*) and enhancing NE

signaling improves attentional set-shifting (*107*), working memory (*5*), and reversal learning (*108*). Interestingly, both DA and NE display an inverted-U dose response curve with respect to PFC function; too little or too much of either catecholamine will produce deficits in attention and other executive functions (*109*).

The PL cortex is also supplied with non-catecholamine neuromodulators such as 5HT and ACh. The dorsal raphe nuclei contain 5HT-producing neurons and project throughout the cortex, including to the PL. The dorsal raphe is also innervated by the PL, again forming a feedback loop for 5HT similar to DA and NE. In contrast to the other neuromodulators, depletion of 5HT in the mPFC does not impact attentional set-shifting performance in rodents but does impair reversal learning (*110*, *111*). Depletion of 5HT also increases impulsivity (*112*), potentially related to increased 5HT metabolite levels observed clinically in impulsive suicide attempters (*113*). Finally, the PL cortex is innervated by ACh-containing cholinergic fibers which originate in basal forebrain, primarily from the nucleus basalis (*114*). Additionally, there are local cholinergic interneurons that provide ACh in the cortex, although there are relatively few of them and their function in the mPFC is poorly understood (*115*). Interestingly, although various cortical regions receive cholinergic input, the mPFC is the major cortical region that sends projections to the basal forebrain and therefore is positioned to exert top-down control to regulate global cortical cholinergic tone (*116*). ACh is a critical neurotransmitter and neuromodulator for many PFC-related behaviors, especially attention. ACh levels in the mPFC increase during attention (*117*, *118*) and local cholinergic depletion in the mPFC impairs behavioral performance in visual attention-based tasks (*119*, *120*) . Furthermore, intracortical infusions of ACh receptor antagonists impair attentional set-shifting, working memory, and reversal learning (*120*, *121*). It is clear from these studies and others that ACh is essential for the proper function of the PL cortex and the mPFC in general. A more detailed description of cholinergic neuromodulation via actions on muscarinic ACh receptors will be covered in Chapter II.

1.2 PFC Microcircuitry

While the PL cortex receives input from and projects to a variety of brain regions, it is the intracortical processing that occurs within cortical microcircuits that allow for the proper integration of cortical and subcortical information to ultimately exert top-down control. As discussed, the PL cortex consists of five main layers, of which II, III, V, and VI contain the glutamatergic pyramidal neurons that make up approximately 80% of the local neurons; the other ~20% of PL neurons are local inhibitory GABAergic interneurons that reside in all five layers (*122*). This combination of pyramidal neuron and interneuron function confers incredible flexibility and complexity to the PL circuit, allowing for the gating of incoming information, intralaminar processing, and output control. Further expanding the processing power of the PL cortex is the diversity of neuronal subtypes as both the glutamatergic pyramidal neurons and GABAergic interneurons can be further subdivided based on their morphology, physiology, and molecular markers (*123*, *124*).

Pyramidal Neurons

The glutamatergic pyramidal neurons can be mainly classified based on their laminar distribution, with layer II/III and V neurons exhibiting distinct cellular properties. Layer II/III in the PL cortex acts similarly to layer IV in other granular cortices and is innervated by a variety of thalamic and cortical regions. Layer II pyramidal neurons are densely packed in a thin layer at the layer I border and have large, broad tufted apical dendrites that span a larger volume than their basal counterparts, a unique characteristic amongst PFC pyramidal neurons (*125*). They rest relatively hyperpolarized compared to neurons in other layers and exhibit a variety of firing patterns. Layer III neurons on the other hand occupy a less dense layer below layer II and are generally more heterogeneous (*125*). The basal dendritic tree is larger than in layer II and comparable to the size of the apical tree which extends and spreads out in layer I. Electrophysiologically, layer III neurons can be subdivided into regular spiking, adapting, or bursting types. This morphological and electrophysiology diversity likely allows for differential

integration of intracortical and subcortical input by the superficial layers by potentially segregating between neurons or within a single neuron where afferent information arrives (*43*).

The mPFC deep layer V pyramidal neurons are generally larger than the superficial neurons and can be broadly classified into two major groups based on their output: pyramidal tract (PT) neurons which project to the brain stem, and intratelencephalic (IT) neurons which do not send afferents to the brain stem but can innervate the contralateral cortex (*124*). PT cells contain corticopontine (CP) and corticothalamic (CT) neurons which typically have thick-tufted apical dendrites that span up to layer I. IT cells consist of corticocortical (CC) neurons and coritcostriatal (CS) neurons that project to the contralateral cortex and striatum, respectively while some IT cells project also to the ipsilateral striatum. IT cells generally have a thin-tufted apical dendrite and are electrophysiologically more diverse than PT neurons. PT neurons in general have a larger voltage sag, lower input resistance, and a more regular spiking pattern than IT neurons although diversity exists within each subcategory (*124*, *125*). Based on these subdivisions, layer V is commonly further separated into the more superficial layer Va and deeper layer Vb. Layer Vb typically receives denser thalamic innervation and contains more CP neurons that project to the spinal cord (*124*). With respect to intracortical connectivity, layer V neurons receive input from subcortical sources as well as layer II/III neurons and can form connections with one another. PT neurons, specifically CP neurons, have a high degree of reciprocal connectivity while IT cells tend to monodirectionally innervate PT cells. Finally, innervation from individual layer II/III neurons tends to stick to one of the two subclasses of layer V neurons, such that PT cells receive information from similar superficial cells while IT cells receive separate innervation from layer II/III (*124*).

Due to its relative heterogeneity, layer VI is the least characterized of the cortical layers with respect to pyramidal neuron diversity. There is a variety of morphological diversity in layer VI but electrophysiologically the pyramidal neurons are generally similar with high input resistances and excitability. Almost half of all layer VI neurons have apical dendrites that extend all the way

to layer I and approximately the same amount project to thalamic regions (*125*). Layer VI neurons do not receive strong input from superficial layers, therefore it is likely they receive mostly thalamic and subcortical information but the exact distribution of inputs to layer VI is unclear (*44*). Altogether, PL cortex pyramidal neurons are morphologically and functionally diverse in addition to their laminar distributions which may provide a level of complexity necessary for the sophisticated intracortical calculations performed by this brain region.

Inhibitory Interneurons

GABAergic inhibitory interneurons make up only a small proportion of the total number of neurons in the PL cortex but they are essential for the integration of afferent information and the precisely timed generation of output leading to the synchronization of ensembles of pyramidal neurons to produce neuronal oscillations such as theta and gamma oscillations (*126*). Cortical interneurons can be broadly subdivided into three distinct groups based on their morphology, electrophysiological properties, and molecular markers: parvalbumin-, somatostatin-, and $5HT_{3a}$ receptor-positive interneurons (Figure 3, Page 16) (*123*). It is important to note that these are not exclusive groups and there does exist some overlap between certain populations, although this classification accounts for nearly all cortical interneurons and segregates their function fairly well.

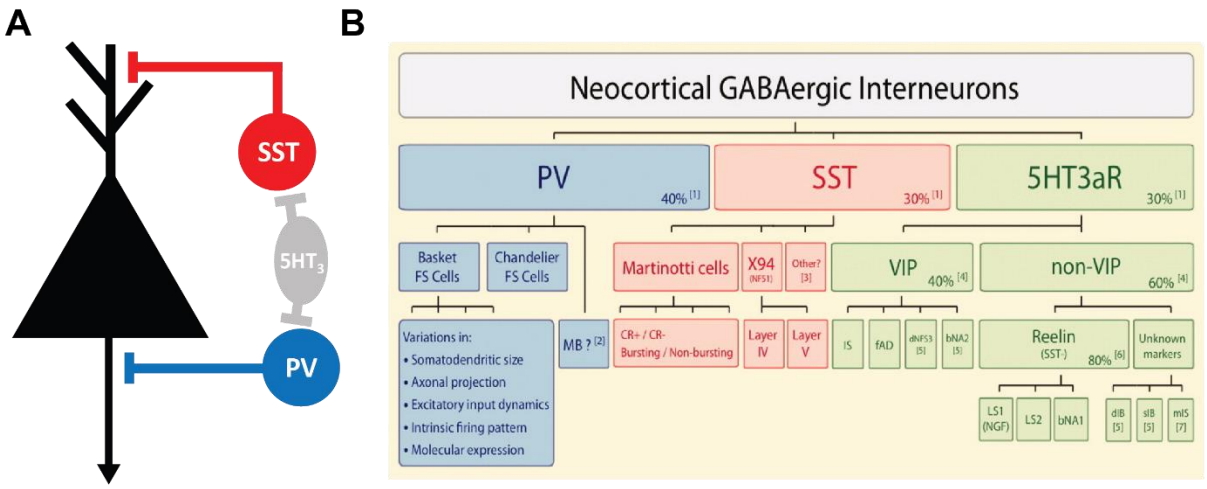

Figure 3: Cortical interneurons can be subdivided into PV, SST, and $5HT_{3a}R$ expressing subtypes. **(A)** Simplified schematic of the cortical microcircuit with an SST interneuron synapsing onto the distal dendrites of a pyramidal neuron (black) and a PV interneuron synapsing onto the axon initial segment, putatively a chandelier cell. PV basket cells typically innervate the cell body and proximal dendrites of pyramidal neurons. A $5HT_{3a}R$ interneuron is depicted synapsing onto both SST and PV interneurons, forming a disinhibitory circuit with respect to the pyramidal neuron. **(B)** Table adapted from (*123*) summarizing the major interneuron types and subdivisions within those broader categories defined largely by molecular markers, morphology, and synaptic connectivity.

The parvalbumin (PV)- positive interneurons are probably the most well characterized due to their role in feed-forward inhibition, the generation of gamma oscillations, and their putative dysfunction in various psychiatric disorders (*127*). These neurons account for approximately 40% of cortical interneurons and are identified based on their expression of the calcium-binding protein parvalbumin as well as their fast-spiking properties. Electrophysiologically, PV neurons have low input resistance, are capable of firing fast action potentials at very high (>100Hz) frequencies with large afterhyperpolarization (AHPs) potentials. PV neurons broadly provide perisomatic inhibition to pyramidal neurons, regulate the timing of their output, and are especially important for the generation of gamma oscillations due to their fast-spiking nature (*128*). They can be further subdivided into chandelier cells that target the axon initial segment and basket cells which target the soma and proximal dendrites of pyramidal neurons (*129*). Compared to basket cells, relatively little is known about the function of chandelier cells concerning their function and origin. Chandelier cells innervate pyramidal neuron axon initial segments throughout all cortical layers

and a single PV chandelier cell can innervate hundreds of neighboring pyramidal neurons (*130*). In the mouse PFC, chandelier cell bodies appear to be restricted to layer II (*131*). Interestingly, some studies have suggested that chandelier cells may be excitatory due to differences in the chloride reversal potential at the axon initial segment (*132*) but recent work using less invasive techniques has failed to replicate this finding and suggests that chandelier cells function as classical inhibitory neurons (*130*, *133*).

Due to their relative abundance and simpler identification, more is known about PV basket cells. Their cell bodies are found in both superficial and deep layers of the rodent PFC and PV basket cells can form synapses with almost every local pyramidal neuron, allowing for large-scale synchronization of cortical networks (*131*, *134*). Basket cell dendrites cross multiple cortical layers and receive input from subcortical sources as well as from local pyramidal neurons in both layer II/III and V. In addition to excitatory synapses, PV neurons are also innervated by inhibitory interneurons including other basket cells and they can form electrical gap junctions with each other (*128*). Functionally, this allows for synchronization of PV neurons via electrical synapses and may increase the receptive field of individual PV cells (*135*). PV basket cells receive input from multiple subcortical sources and have been shown to mediate feed-forward inhibition from the vHipp (*86*) and MDT (*45*), as well as contribute to feed-forward inhibition from the BLA (*65*, *67*) and contralateral cortex (*136*). PV neurons are thus situated to mediate feed-forward and feed-back inhibition to tightly control the output of PL cortex pyramidal networks.

Somatostatin (SST)-expressing interneurons make up approximately 30% of PL cortical interneurons and are morphologically and functionally distinct from PV neurons as well as more heterogeneous. They are defined by the expression of the neuropeptide SST which can be co-released with GABA and mediate neuromodulation through multiple G-protein coupled receptors (*137*). SST interneurons typically do not express PV while the majority express calbindin (CB) and some express calretinin (CR); subclassification based on the expression of these calcium-binding proteins has been proposed (*138*). Additionally, SST interneurons can express other

peptide markers such as neuropeptide Y (NPY) and neuronal nitric oxide synthase (nNOS) (*139*). Finally, morphologically, SST interneurons can be generally segregated into either Martinotti or non-Martinotti cells. Non-Martinotti neurons can be further subdivided into basket cells similar to PV neurons, double-bouquet cells similar to some $5HT_{3a}R$ neurons, and long-range projecting GABAergic neurons (*139*, *140*). RNA sequencing combined with functional data has identified anywhere from 10 to over 100 different subtypes of neocortical SST interneurons (*141*), but for the purposes of this dissertation, we will focus on the fairly well- characterized Martinotti neurons.

SST Martinotti neurons are the majority of SST interneurons in the rodent PFC and are found in both superficial and deep layers (*142*). Morphologically, they have diverse dendritic processes that, unique among cortical interneurons, have dendritic spines. All Martinotti cells have dense axonal processes that spread throughout layer I, making up approximately 75% of GABAergic axons in this superficial-most layer, and make inhibitory contacts with a large number of pyramidal neurons (*143*). Distinct from PV neurons, SST Martinotti neurons target the distal dendrites of layer II/III and V pyramidal neurons and function to gate incoming information. Electrophysiologically, SST Marintotti cells are low threshold-spiking neurons, with a more depolarized resting membrane potential, higher input resistance, large hyperpolarization-mediated voltage sag, and slower action potential kinetics than PV neurons. Unlike fast-spiking PV neurons, SST Martinotti cells exhibit action potential frequency adaptation and, commonly, overshoot spiking after release from hyperpolarization (*139*). Whereas excitatory synapses onto PV cells are depressing, pyramidal neuron synapses onto SST Martinotti neurons have a low release probability but are facilitating, allowing for summation of coincident and high frequency input (*144*). The majority of SST neuron input comes from local pyramidal neurons and therefore they mediate mainly feedback and lateral inhibition through a cortex-wide motif termed frequency-dependent disynaptic inhibition (*145*, *146*). PFC SST interneurons can also receive input from the BLA (*65*) and the contralateral cortex (*136*). The contribution of SST interneurons to feed-forward inhibition by vHipp (*86*) and MDT (*45*) inputs appears to be negligible although these experiments

were not performed with trains of stimulation to account for the facilitating properties of SST neurons. SST Martinotti neurons also receive inhibitory input, mainly from $5HT_{3a}R$ interneurons, and rarely form chemical synapses with each other but are connected via gap junctions (*147*). They also send inhibitory projections to PV basket cells, forming a disinhibitory circuit (*148*). SST interneuron therefore mediate distinct forms of cortical network control and are critical for the gating of afferent information to the distal dendrites of pyramidal neurons.

Finally, the remaining 30% of cortical interneurons are defined as expressing the ionotropic serotonin 3a receptor ($5HT_{3a}R$) and are equally or more diverse than SST interneurons (*123*). They are generally subdivided into vasoactive intestinal peptide (VIP)-positive or VIP-negative interneurons and are largely restricted to superficial layers; they are the only neuronal cell type found in layer I (*149*). $5HT_{3a}R$ interneurons generally synapse onto other interneurons, forming disinhibitory circuits preferentially with SST neurons but also with PV cells, although there is emerging evidence of their inhibitory control over the dendrites of pyramidal neurons (*150*). Additionally, $5HT_{3a}R$ interneurons contain cholecystokinin (CCK)-positive interneurons that are non-PV basket cells which inhibit pyramidal neurons at the soma and proximal dendrites, although these are more extensively characterized in the hippocampus compared to the PFC (*149*). VIP-positive neurons typically co-express CR and are enriched in layers II and III. VIP-negative neurons can co-express Reelin and are predominantly found in layer I where they mediate volume transmission of GABA rather than forming distinct inhibitory synapses. Electrophysiologically, $5HT_{3a}R$ interneurons have a very high input resistance, making them highly excitable, and typically have an irregular spiking phenotype. While diverse and understudied compared to PV and SST interneurons, the structure and function of $5HT_{3a}R$ interneurons has garnered recent interest and more will certainly be known about the role that these neurons play in behavior and cortical processing in the future (*149*). Distinct from other interneuron subtypes, $5HT_{3a}R$ interneurons play a critical role in PFC function by forming almost exclusively disinhibitory circuits to permit pyramidal cell integration and output and given their localization to layer I, likely play an

integral role in processing the higher-order associational cortical and thalamic input that synapses in this superficial most layer.

Functional Effects of Microcircuit Function

Given the large diversity of neuronal subtypes in the PL cortex and their relative roles in integration and cortical processing, manipulating the function of the PL microcircuit has a variety of behavioral effects. Using optogenetic approaches, increasing mPFC pyramidal neuron activity non-specifically has produced both procognitive effects and cognitive disruptions. Using a step-function opsin expressed under the control of the CaMKIIα promoter to increase pyramidal cell activity, Yizhar *et* al. found that increasing pyramidal cell activity produces deficits in social interaction and fear conditioning but does not affect open field activity or novel object recognition (*151*). On the other hand, another study found that increasing PFC pyramidal neuron activity improves object-in-place discrimination in rats (*152*). Optogenetic stimulation of PL pyramidal neurons using channelrhodopsin-2 (ChR2) impairs avoidance behavior (*153*) and inhibition of PL pyramidal neurons was found to impair trace fear conditioning, a PFC-dependent associative learning task (*154*). Interestingly, optogenetic inhibition of PL pyramidal neurons with halorhodopsin (NpHR) rescues working memory deficits in a chronic pain model that produces hyperactivity of the PFC (*155*). The fact that bidirectional modulation of pyramidal neuron activity can produce similar behavioral effects may be related to an artificially-induced imbalance between excitatory pyramidal neuron and inhibitory interneuron activity. Supporting this, Yizhar *et al*. was able to rescue the social deficit induced by increasing pyramidal neuron activity by concurrently optogenetically enhancing the activity of PV interneurons in the PL cortex (*151*).

Optogenetic and ablation studies have also shed light on the function of different interneuron populations in the PFC. As mentioned above, enhancing PV interneuron activity optogenetically to rebalance excitation and inhibition was able to reverse a social deficits (*151*). Additionally, optogenetically enhancing PV activity rescues social interaction deficits in a mouse model of ASD (*156*). PL cortex PV neurons have also been implicated in fear conditioning as

optogenetically stimulating these neurons suppresses and inhibiting them evokes conditioned fear behaviors, respectively (*157*). In wildtype mice, stimulating PL cortex PV neurons produces deficits in working memory (*158*), consistent with perturbations in the balance between excitatory and inhibitory neurons having functional consequences. Interestingly, inhibiting PFC PV interneurons in a similar working memory task had no effect on performance but inhibiting SST interneurons resulted in deficits during trials with long delays between the sample and choice phases (*159*). Another study found a corroborating increase in mPFC SST interneuron activity during the delay phase of a related spatial working memory task but contrastingly found that stimulating mPFC SST interneurons results in performance deficits (*160*). This discrepancy could be due to artificial stimulation of SST interneurons that may impair their function. In a spontaneous alternation task, ablation of PFC PV interneurons produces deficits whereas ablation of SST interneurons has no effect (*161*). The discrepancy between this study and the optogenetic findings may be related to task-specific differences or potential compensatory mechanisms due to long term inhibition of SST and PV interneuron signaling. This would be consistent with a further study that reported acute chemogenetic inhibition of PFC SST interneurons produces an anxiogenic phenotype whereas chronic inhibition or ablation results in the opposite, anxiolytic effect (*162*). Finally, optogenetic inhibition of mPFC VIP-positive interneurons reduces avoidance behavior resulting in an anxiolytic-like phenotype (*163*). Altogether, these studies illustrate that GABAergic interneurons play a critical role in regulating many mPFC-dependent functions.

Finally, mPFC microcircuits are capable of producing neuronal oscillations which are essential for the precise temporal control of synaptic integration and output of pyramidal neurons as well as for the coordinated activity of distant brain regions (*126*). Due to their fast-spiking properties, PV interneurons are involved in gamma oscillations which occur at 30-80Hz and correlate with working memory and cognitive demand (*164*). In a seminal study, Sohal *et al.* showed that inhibiting local PV interneurons suppresses mPFC gamma oscillations *in vivo* and that stimulating input onto PV interneurons can generate gamma rhythms (*165*). Further work has

suggested that input from local layer II/III, but not layer V, pyramidal neurons is required for the generation of gamma oscillations in the mPFC (*166*). In other brain regions, SST interneurons have been implicated in the generation and maintenance of slower oscillations such as theta and beta rhythms which are important for information processing and attention (*167*, *168*). In particular, spatial working memory is associated with increases in synchronized gamma and theta oscillations between the vHipp and mPFC and disruptions in this synchrony correlate with behavioral deficits (*76*, *77*). While the role of SST interneurons in mPFC neuronal oscillations remains unclear, optogenetic inhibition of mPFC interneurons impairs vHipp-mPFC theta synchrony, suggesting that they contribute to oscillations in this frequency band (*159*). Overall, the coordinated actions of the various pyramidal neuron and interneuron cell types in the mPFC allow for the emergence of neuronal oscillations that support and mediate the top-down processing abilities of this higher-order brain region.

1.3 Molecular mediators of neurotransmission

The pyramidal neurons and interneurons in the PL cortex communicate with one another and receive cortical and subcortical input primarily via glutamatergic and GABAergic neurotransmission. This section will briefly describe the molecular mediators of cortical neurotransmission.

Glutamatergic neurotransmission

PL pyramidal neurons as well as the thalamic, limbic, and cortical inputs to the mPFC all release glutamate as their primary neurotransmitter. Glutamate, the major excitatory neurotransmitter in the central nervous system, is synthesized in axon terminals either via α-ketoglutarate or primarily from glutamine supplied by astrocytes that is converted via the enzyme glutaminase (*169*). Glutamate is loaded into presynaptic vesicles by vesicular glutamate transporters (vGluTs) including vGluT1-3. vGluT1 is the main isoform found in cortical glutamatergic neurons while vGluT2 is found in thalamic neurons and their terminals in the mPFC

(*170*). Upon release into the extracellular space, glutamate binds to a variety of pre- and postsynaptic receptor subtypes while the temporal and spatial boundaries of this signaling is regulated by removal of glutamate by plasma-membrane bound glutamate transporters, the excitatory amino acid transports (EAATs) (*171*). EAAT2 is the primary glutamate transporter and is expressed predominantly is astrocytes. Along with EAAT1, these transporters actively pump glutamate into astrocytes where it is converted to glutamine by glutamine synthetase. This glutamine is then transported out of the astrocyte and into nearby axon terminals completing the glutamate-glutamine cycle (Figure 4, Page 24) (*169*). Glutamate can also be directly taken up into axon terminals, dendrites, and cell bodies by neuronal EAAT3 and EAAT4. The EAAT5 isoform exists but is restricted to the retina (*171*).

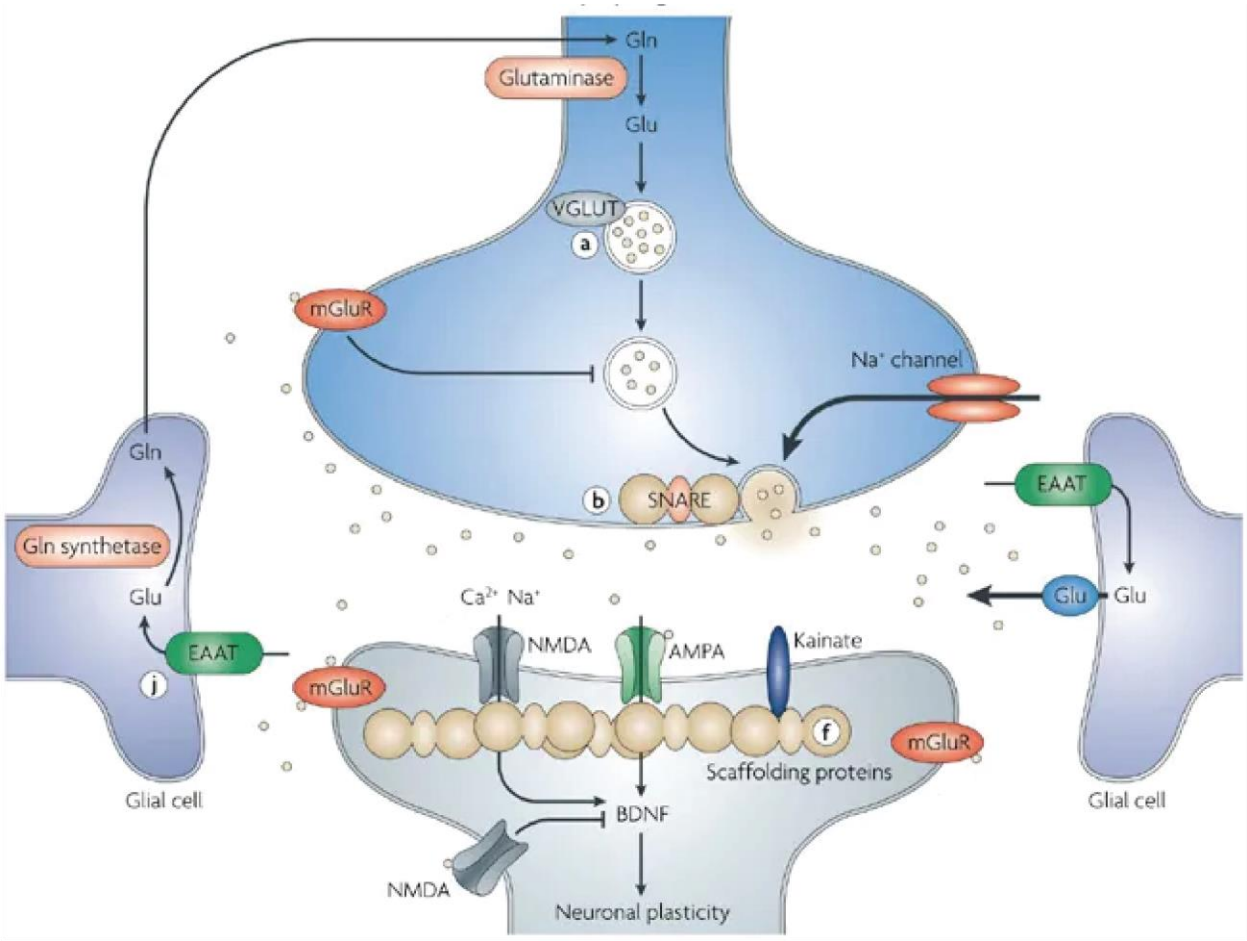

Figure 4: Components of a glutamatergic synapse. Glutamate (Glu) is synthesized in the presynaptic neuron from gluamatine (Gln) supplied by neighboring astrocytes. Glu is then packed into presynaptic vesicle by vGluTs and upon terminal depolarization, released into the synaptic cleft. It can bind to AMPA, NMDA, or kainite subtypes of ionotropic glutamate receptor to mediate fast excitatory neurotransmission or act at the G-protein coupled metabotropic glutamate (mGlu) receptors to mediate slow neuromodulation. Glu is cleared from the synapse primarily by astrocytic EAATs where it is converted to Gln and then transported back to the presynaptic neuron, completing the cycle. Adapted from (*172*).

Once in the synaptic and extracellular space, glutamate can bind to ionotropic and metabotropic glutamate receptors. The ionotropic glutamate receptors mediate fast neurotransmission as ligand-gated ion channels, allowing the influx of Na^+ and sometimes Ca^{2+} ions along with the efflux of K^+ to produce depolarizing changes in membrane potential termed excitatory postsynaptic potentials (EPSPs). The three members of the ionotropic glutamate receptors are the α-amino-3-hydroxy-5-methyl-4-isoxazoleproplionic acid (AMPA), N-methyl-D-

aspartate (NMDA), and kainate (KA) receptors. All three receptor subtypes are obligate tetramers formed by a combination of subunits (*173*).

AMPA receptors mediate the majority of fast glutamatergic neurotransmission in the cortex and are typically heterotetramers, commonly composed of a dimer of dimers with two GluA2 subunits and either two GluA1, GluA3, or GluA4 subunits (*173*, *174*). Most GluA2-containing AMPA receptors are Ca^{2+}-impermeable due to an RNA editing event that converts a glutamine residue to an arginine and only flux Na^{+} and K^{+}. GluA2-lacking AMPA receptors are Ca^{2+}-permeable and undergo rectification due to intracellular polyamines blocking the pore at depolarized potentials. Unedited GluA2-containing AMPA receptors can exist but are rare (*175*).

NMDA receptors play an essential role in synaptic plasticity and function as neuronal coincidence detectors for two reasons: at resting membrane potentials their pore is blocked by a Mg^{2+} ion, and they require the binding of either glycine or D-serine in addition to glutamate in order to open (*173*). NMDA receptors are heterotetramers requiring at least two GluN1 subunits that contain the co-agonist binding sites, one GluN2 subunit containing the glutamate binding site, and either another GluN2 or GluN3 subunit. There are multiple isoforms of GluN2 and GluN3 including GluN2A, GluN2B, GluN2C, GluN2D, GluN3A, and GluN3B which can differentially affect the kinetics and voltage-dependence of the receptor (*174*). NMDA receptors are Ca^{2+}-permeable but typically require depolarization to relieve the Mg^{2+} block therefore only flux ions during synaptic transmission paired with postsynaptic depolarization (*173*).

KA receptors are composed of either homo- or heterotetramers of GluK1, GluK2, and GluK3. The GluK4 and GluK5 subunits also exist and can form functional heterotetramers with GluK1-3 (*174*). KA receptors have not been as extensively characterized as AMPA or NMDA receptors but they seem to be important for the modulation of synaptic transmission and synaptic plasticity (*173*, *176*). In addition to ionotropic glutamate receptors that mediate fast excitatory neurotransmission, glutamate also binds to and signals through a family of G-protein coupled metabotropic glutamate (mGlu) receptors (*177*). There are eight subtypes of mGlu receptors,

$mGlu_1$–$mGlu_8$, classified into three groups (group I, $mGlu_{1,5}$; group II, $mGlu_{2,3}$; group III, $mGlu_{4,6,7,8}$) which will be discussed in Chapter II.

GABAergic neurotransmission

Inhibitory interneurons in the PL cortex synthesize and release the major inhibitory neurotransmitter γ-aminobutyric acid (GABA). GABA is synthesized primarily from its precursor glutamate by glutamic acid decarboxylase (GAD), of which there are two isoforms: GAD_{65} and GAD_{67} (*178*). Glutamate is provided to GABAergic neurons via astrocytes similar to in glutamatergic neurons or is directly imported via neuronal EAATs. After synthesis, GABA is packed into synaptic vesicle by the vesicular GABA transporter (vGAT) and once released into the extracellular and synaptic space can bind to pre- and postsynaptic receptors (*179*). Like glutamate, GABA neurotransmission is limited by clearance of GABA into presynaptic terminals and astrocytes by GABA transporters (GATs). In neurons, GABA is then either packed into presynaptic vesicles again or degraded by the enzyme GABA transaminase (GABA-T); in astrocytes, GABA is degraded by GABA-T and its metabolites enter the TCA cycle to ultimately produce glutamate then glutamine which can be transported back to the GABAergic axon terminals (Figure 5, Page 27) (*179*).

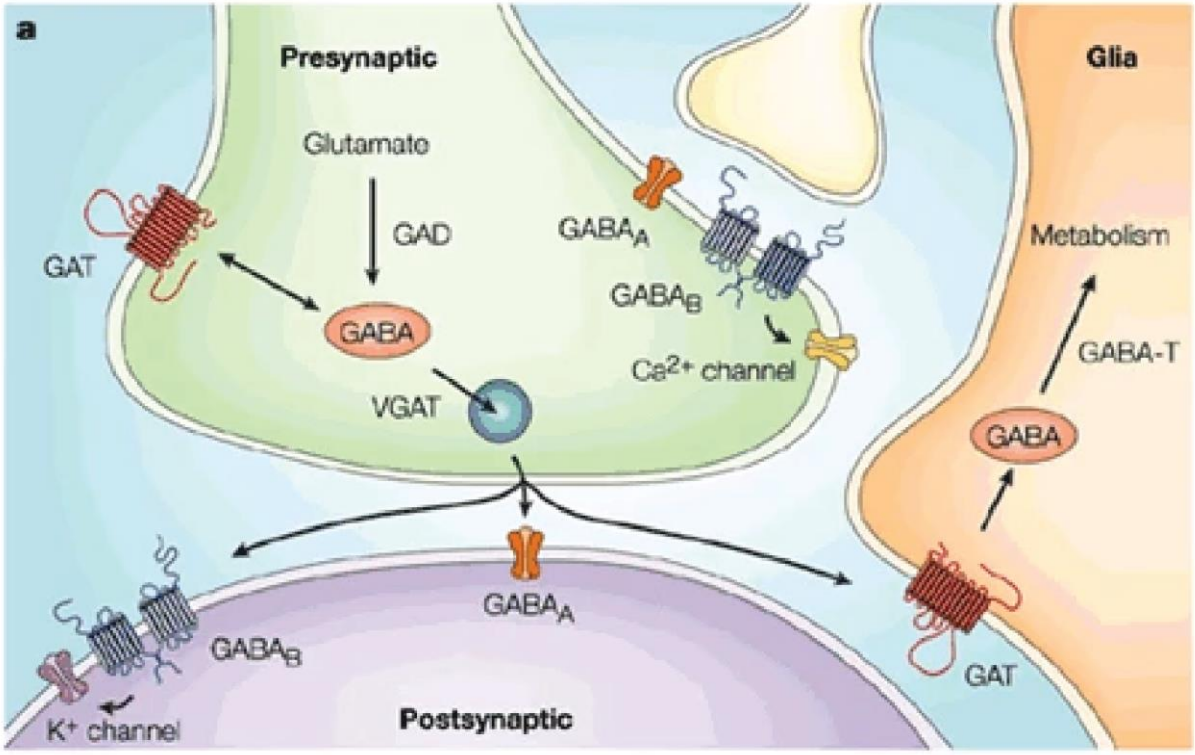

Figure 5: Components of a GABAergic synapse. GABA is synthesized from glutamate by GAD enzymes and then loaded into presynaptic vesicles via vGAT. Once released into the synapse or extracllular space, GABA can activate ionotropic $GABA_A$ receptors to mediate fast inhibitory neurotransmission or metabotropic $GABA_B$ receptors to modulate neuronal function. GABAergic transmission is limited by reuptake into presynaptic terminals and neighboring astrocytes via GAT. In neurons, it can be repackaged into vesicles while in astrocytes it is typically metabolized by GABA-T. Adapted from (*180*).

In the extracellular space and synaptic cleft, GABA can bind to both ionotropic and metabotropic GABA receptors to mediate fast neurotransmission and neuromodulation, respectively. GABA produces fast inhibitory neurotransmission via the $GABA_A$ receptor family of pentameric ligand-gated ion channels (*181*). $GABA_A$ receptors are selective for Cl^- ions, which in adult mammals flux into the postsynaptic neuron to hyperpolarize the membrane potential and produce inhibitory postsynaptic potentials (IPSPs). If the membrane potential and the Cl^- reversal potential are equivalent when $GABA_A$ receptors are activated, they can also mediate shunting inhibition without any net flux of Cl^- by decreasing local membrane resistance. There are twelve $GABA_A$ receptor subunits: α1-6, β1-4, γ1-3, δ, ρ1-3, ε, π and θ (*182*). $GABA_A$ receptors are commonly comprised of two of the same α subunits, two of the same β subunits, and one

alternative subunit. The majority of synaptic receptors contain a γ subunit while extrasynaptic $GABA_A$ receptors that mediate tonic inhibition and respond to GABA spillover typically contain the δ subunit. The relative subunit composition will affect channel gating kinetics as well as the pharmacology of the receptor with respect to modulation by exogenous compounds and drugs as well as by endogenous neurosteroids (*182*). Found almost exclusively in the retina, $GABA_C$ receptors are ligand-gated Cl^- channels that are formed the ρ subunits forming homo- or heteropentamers and differ in pharmacology from $GABA_A$ receptor although they still respond to GABA (*181*).

Similar to glutamate, GABA can also bind to and activate a G-protein coupled $GABA_B$ receptor. Unlike mGlu receptors, there are only two possible $GABA_B$ receptors assembled by the heterodimerization of a $GABA_{B1a}$ or $GABA_{B1b}$ and a $GABA_{B2}$ subunit (*183*). Each subunit is a class C G-protein coupled receptor (GPCR) with a large extracellular GABA binding domain but when expressed in isolation, individual subunits generally do not traffic to the cell surface and cannot couple to G-proteins. The two subunits dimerize via interactions at the C-terminal tail allowing surface expression and effector coupling although there exceptions to this have been obseved (*183*). Functionally, activation of $GABA_B$ receptor leads to mobilization of $G\alpha_{i/o}$ proteins which classically inhibit adenylyl cyclase activity to reduce cAMP and counteract activation of PKA. $GABA_B$ signaling also proceeds through liberation of Gβγ subunits which presynaptically reduces neurotransmitter release by inhibiting N-, L-, and T-type voltage-gated Ca^{2+} channels and postsynaptically induces a slow inhibitory response via activation of G-protein coupled inwardly rectifying K^+ channels (GIRKs) (*184*).

In conclusion, glutamate is the major excitatory neurotransmitter released by the majority of afferents and local pyramidal neurons while GABA is released by local inhibitory interneurons and mediates both fast and slow neurotransmission in the cortex. The precise balance between excitatory and inhibitory signaling in the cortex is critical for proper circuit function as subtle

perturbations from the ideal balance can contribute to and produce a variety of neurological and psychiatric consequences (*185*, *186*).

1.4 Synaptic plasticity of neurotransmission

In order to maintain the proper balance between excitation and inhibition in the mPFC, the relative strength of synaptic connections undergoes dynamic remodeling in a process termed synaptic plasticity (*187*). Synaptic strength can be strengthened and potentiated or alternatively weakened and depressed. This can occur over seconds or minutes, termed short-term potentiation (STP) and short-term depression (STD) or persist over much longer time scales in the case of long-term potentiation (LTP) and depression (LTD) (*188*). While the mPFC is typically thought to involve short-term information storage and processing to facilitate working memory and attention, both short- and long-term forms of synaptic plasticity occur and are important for cortical function (*189*). This section will review the general principles and mechanisms of synaptic plasticity and provide an overview of synaptic plasticity in the mPFC.

Short-term plasticity occurs on the scale of milliseconds to minutes and includes paired-pulse facilitation and depression as well as STP and STD after trains of synaptic stimulation (*190*). A common mechanism among forms of short-term plasticity is changes in intracellular Ca^{2+} levels in the presynaptic terminal that subsequently modifies neurotransmitter release (*190*). If two stimuli are provided with a short interstimulus interval, paired-pulse facilitation or depression can occur. At very short intervals, paired-pulse depression typically prevails likely due to inactivation of voltage-gated ion channels and depletion of neurotransmitter vesicles. At longer intervals (>20ms), an accumulation of Ca^{2+} from the first pulse combined with replacement of docked synaptic vesicles contribute to commonly observed paired-pulse facilitation. Whether a particular synapse displays facilitation or depression can be also be influenced by the initial release probability: high release probability synapses will more likely display depression whereas low release probability synapses will typically exhibit facilitation. During and after longer trains of

stimulation, STP and STD occur (*190*). Similar to paired-pulse plasticity, increases in intracellular Ca^{2+} concentrations are thought to lead to increases in release probability for STP and depletion of synaptic vesicles or neuromodulatory effects contribute to STD.

In the PL cortex, short-term plasticity has been studied using both *in vivo* and *ex vivo* techniques. Synapses from the contralateral cortex (*191*) and vHipp (*192*) display paired-pulse facilitation *in vivo* at 50-100ms interpulse intervals while at similar intervals MDT synapses exhibit paired-pulse depression (*193*). In *ex vivo* slice studies using optogenetic approaches, BLA-to-PL layer II synapses do not display paired pulse facilitation or depression (*194*) while BLA-to-PL layer V are facilitating (*195*). Similarly, vHipp-to-PL layer V synapses display paired pulse facilitation at baseline across a range of intervals (*196*). MDT-to-PL layer II/III synapses are depressing while VMT to layer II/III synapses are facilitating (*44*). Intracortical synapses are also generally facilitating, as layer II/III-to-V and layer V-to-V synapses in the same hemisphere exhibit paired pulse facilitation across a range of stimulus intervals (*197*). STP and STD on the order of seconds to minutes has also been observed in PL cortex. *In vivo* stimulation of the vHipp with a moderate intensity theta-burst protocol induces STP at vHipp-mPFC synapses that lasts for longer than 5 minutes and is DA D_1 receptor-dependent. Interestingly, *in vivo* theta-burst stimulation of superficial mPFC layers produced weak and transient STP measured in deep layers but stimulation of the same synapse in the gamma frequency range results in STP lasting longer than 5 minutes and is dependent on DA D_2 receptors, not D_1 (*198*). In *ex vivo* slices, PL cortex layer II/III-V synapses exhibit a frequency-dependent STP that lasts for around 1 minute, peaks in the gamma frequency range (*199*), and is also inhibited by DA D_1 receptors (*200*). Another form of STP lasting around 4 minutes occurs at this synapse and does not involve dopamine receptors (*197*, *200*). At layer V-to-V synapses, only the longer form of STP occurs but can be converted to LTD by blocking DA D_1 receptors (*200*). These forms of short term plasticity occur on similar time scales to cognitive functions of the PL cortex, such as working memory, and are likely important for storing and processing information over short time scales.

Certain inputs to the mPFC can also affect the relative strength of inputs arising from other regions in a form of synaptic 'gating'. This is typically through engagement of cortical microcircuitry feed-forward inhibition but may also involve biophysical mechanisms affecting dendritic signal propagation (*43*). Stimulation of vHipp inputs to the mPFC 10-500ms before stimulation of MDT inputs inhibits MDT-evoked firing of some mPFC neurons *in vivo*. The reverse is true but over a shorter range of interstimulus intervals, where MDT stimulation 25-100ms before vHipp activation decreases vHipp-evoked mPFC firing. On the other hand, if the MDT inputs are repetitively stimulated, a short-term enhancement of vHipp-evoked mPFC firing is observed that lasts for approximately 10 minutes (*193*). This suggests that MDT inputs gate vHipp input at low frequencies but when MDT-mPFC input is strongly recruited, it can increase the gain of the vHipp-mPFC synapse and could be related to why both MDT and vHipp input are required for working memory (*54*, *77*). BLA and vHipp inputs to the PL cortex can also interact with each other (*201*, *202*). Patterned stimulation of the BLA *in vivo* reduces the response of mPFC neurons to vHipp input, peaking at 20-50Hz and this can also gate input from other cortical regions to the mPFC (*202*). In contrast to MDT/vHipp interactions, stimulation of vHipp inputs did not affect BLA-evoked responses in this same study. This is interesting in light of work showing that the vHipp can gate BLA-evoked mPFC responses during fear extinction (*81*) and after prenatal toxin exposure (*203*), but not in naïve or control animals. vHipp stimulation can also depotentiate BLA-evoked responses but only after induction of LTP at the BLA-mPFC synapse (*204*). Therefore, under basal conditions the BLA unidirectionaly gates vHipp input while the vHipp can affect BLA input after the network state has been altered.

Long-term changes in synaptic strength also occur in the PL cortex and are commonly considered the molecular correlates of learning and memory. While cognitive processes like working memory take place over short time scales, mPFC functions such as rule and extinction learning as well as strategy planning occur over long time scales which could involve LTP and LTD (Figure 6, Page 32) (*189*). Long-term plasticity is a change in synaptic strength that persists

over hours, days, and weeks. The most extensively studies forms of plasticity are NMDA receptor-dependent LTP and LTD in the hippocampus and detailed research into their mechanisms contributes to understanding plasticity throughout the nervous system, including the mPFC.

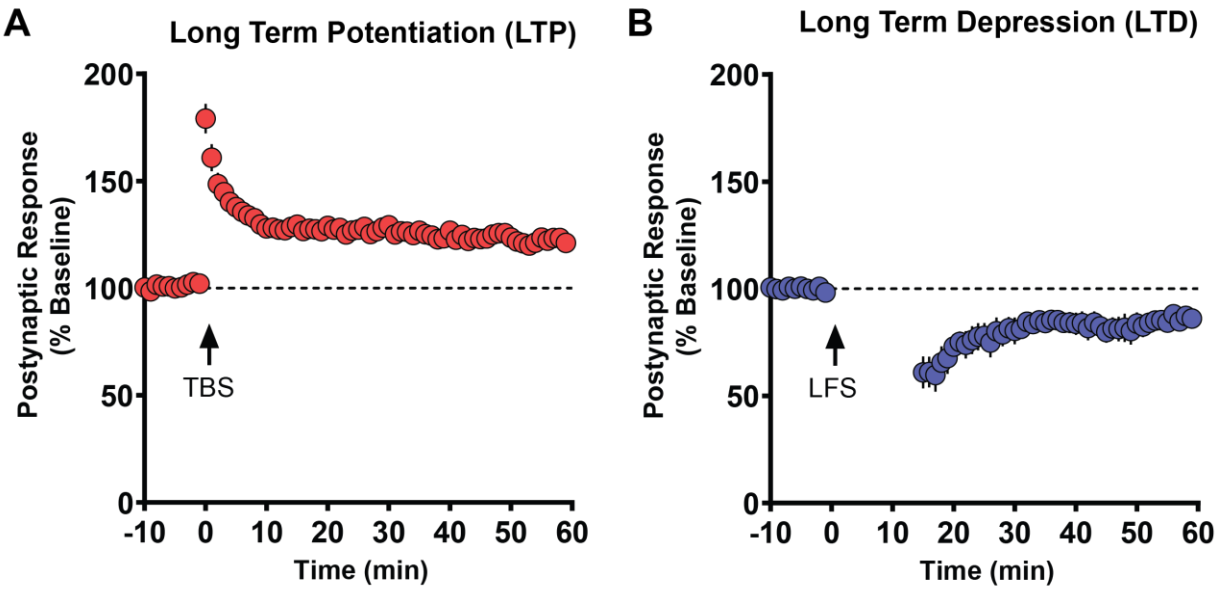

Figure 6: Examples of long term potentiation (LTP) and long term depression (LTD) of synaptic transmission. **(A)** LTP is induced by a theta-burst stimulation protocol modeled after the *in vivo* theta rhythm. This brief, strong presynaptic stimulation produces an initial post-tetanic potentiation that decays but does not return to baseline, resulting in a long term increase in the postsynaptic response. **(B)** LTD is induced by low frequency, 1 Hz stimulation over 15 minutes. This results in a post-tetanic depression that decays but does not return to baseline, resulting in a long term reduction in synaptic strength.

NMDA receptor-dependent LTP is typically induced by a short-duration, high frequency burst of afferent stimulation. Typical protocols involve either repeated bursts of 100Hz stimulation (*205*) or trains of theta-burst stimulation patterned after *in vivo* theta rhythms (Figure 6) (*206*). LTP can also be induced by coordinated timing of pre- and postsynaptic responses following the general rule that the postsynaptic response must occur within a tightly regulated time window after the presynaptic stimulus (*207*). In response to high frequency input, the postsynaptic dendritic spine sufficiently depolarizes via AMPA receptor activation to allow for Mg^{2+} to be removed from NMDA receptors. Once liberated from this block, activation of NMDA receptors

then permits the influx of Ca^{2+} into the postsynaptic compartment which activates CaMKII (*188*, *208*). CaMKII then phosphorylates a myriad of downstream effectors including postsynaptic density (PSD) proteins, AMPA receptors, AMPA receptor auxiliary proteins, and other signaling molecules to result in exocytosis of AMPA receptors at perisynaptic sites which then translocate and insert into the PSD (*209*). LTP that persists for under 2 hours does not involve protein synthesis whereas late-phase LTP that can persist for hours, days, and even weeks requires transcription of new mRNA and protein synthesis for its expression (*210*). This is commonly associated with structural remodeling of dendritic spines to increase the size of the PSD and allow for the increased AMPA receptor density to remain. The postsynaptic increase AMPA receptor density results in a larger postsynaptic response to the presynaptic release of glutamate, thus potentiating the synapse.

Conversely, if the presynaptic input is stimulated at a low frequency but for a long duration, such as 1Hz for 15 minutes, NMDA receptor-dependent LTD can be induced to weaken synaptic strength (Figure 6, Page 32). This form of plasticity also requires postsynaptic depolarization to relieve the Mg^{2+} block of NMDA receptors but the reduced frequency of stimulation over a long period of time results in a smaller rise in intracellular Ca^{2+} triggering different signaling cascades compared to LTP (*188*). A similar NMDA receptor-dependent slow rise in Ca^{2+} can be accomplished by timing a postsynaptic action potential before the presynaptic spike thus inducing a spike-timing dependent form of LTD (*207*). This slow rise in Ca^{2+} activates various protein phosphatases including calcineurin (or PP2B) and PP1 (*211*) which dephosphorylate PSD proteins including AMPA receptor auxiliary proteins that anchor the receptors to the PSD scaffolds (*212*). Additionally, the Ca^{2+}-independent phospho-T286-induced activity of CaMKII results in phosphorylation of AMPA receptors at a distinct serine residue compared to CaMKII activation by LTP-inducing stimuli to reduce AMPA receptor synaptic localization (*213*). This destabilization then allows for dynamin- and clathrin-mediated endocytosis of AMPA receptors and their removal from the synapse (*188*). LTD can be maintained by structural remodeling or removal of dendritic

spines as well as persistent signaling to prevent the reinsertion of AMPA receptors back into the PSD. Thus, a reduction in the number of AMPA receptors in the postsynaptic compartment results in a smaller EPSP in response to the same presynaptic stimulation.

Another commonly studied form of LTD in the brain involves the postsynaptic activation of group I mGlu receptors and does not require NMDA receptor activation (*214*). In *ex vivo* slice preparations, mGlu receptor-dependent LTD can be induced by group I mGlu agonism or with a paired-pulse low frequency stimulation protocol that presumably allows for glutamate spillover into the perisynaptic space where group I mGlu receptors are localized (*215*). This paired-pulse protocol can also involve the activation of M_1 muscarinic receptors, therefore coincident activation of $G\alpha_q$-coupled receptors may be required under endogenous circumstances to activate a sufficient amount of downstream LTD effectors (*216*). In contrast to NMDA receptor-dependent LTD, hippocampal mGlu receptor-dependent LTD induced by agonist application is Ca^{2+}-independent (*217*) although a similar form of LTD induced by afferent stimulation appears to involve Ca^{2+}-dependent signaling (*218*). In the hippocampus, mGlu receptor-dependent LTD requires activation of striatal-enriched tyrosine phosphatase (STEP) (*219*, *220*), which functions similarly to calcineurin and PP1 in NMDA receptor-dependent LTD although via dephosphorylation of different substrates (STEP is a tyrosine phosphatase while calcineurin/PP1 are serine/threonine phosphatases), to ultimately mediate the removal of AMPA receptors from the PSD. Through distinct mechanisms, both NMDA receptor- and mGlu receptor-dependent forms of LTD result in a decrease in AMPA receptor density at the synapse to decrease synaptic strength.

While most long-term plasticity has been studied in the hippocampus, there are multiple examples of LTP and LTD at mPFC synapses that have been identified from *in vivo* and *ex vivo* experiments. LTP was first identified at the vHipp-PL cortex synapse *in vivo* using high-frequency stimulation in anaesthetized rats (*221*) and was later confirmed to be NMDA receptor-dependent (*222*) and also present in mice (*192*). Additionally, LTD can be induced at the vHipp-PL cortex

input *in vivo* by low frequency stimulation (*223*). LTP and LTD have also been observed at the MDT- (*224*), BLA- (*225*), and contralateral cortex-mPFC (*191*) synapses *in vivo.* Supporting the role of these plasticity mechanisms in mPFC function, the MDT-mPFC synapse initial undergoes LTD and then switches to LTP *in vivo* during multiple days of fear extinction learning whereas the vHipp-mPFC synapse initially potentiates and then returns to baseline (*226*). Furthermore, *in vivo* BLA-mPFC LTP is impaired after acute stress (*225*). Interestingly, similar to the short-term interactions described above, high frequency stimulation of the vHipp inputs to the mPFC can produce LTP of both vHipp and MDT synapses (*227*). Therefore in addition to MDT input positively modulating vHipp-mPFC synapses in the short-term, strong vHipp activity can enhance the responsiveness of the mPFC to MDT input on longer time scales. Additionally, a modified high frequency protocol induces LTD at vHipp-PL cortex synapses that emerges during development and is dependent on intact mPFC GABAergic transmission (*228*). The same stimulation however induces LTP at BLA-PL cortex inputs that is GABA-independent, demonstrating how different synapses can undergo vastly different forms of plasticity in response to similar afferent activity patterns.

Ex vivo brain slice studies have been useful to study the molecular mechanisms of long-term plasticity in the mPFC. Both LTP and LTD can be induced in acute brain slices using similar protocols to those used *in vivo* (*196*, *229*). High frequency stimulation of superficial layers evokes either LTP or LTD of EPSPs measured in PL cortex layer V somewhat stochastically in acute slices. When LTP is induced, it is NMDA receptor- and Ca^{2+}-dependent (*230*). Theta-burst stimulation of the same synapse more reliably induces NMDA receptor-dependent LTP that can be modulated by mGlu receptors (*231*). In the presence of bath applied DA however, high frequency stimulation reliably induces or facilitates an NMDA receptor-independent form of LTD recorded in at layer II/III-to-V synapses (*232*, *233*). This form of LTD in the mPFC involves coordinated activity of mGlu receptors, as the facilitation of high frequency stimulation to induce LTD by DA is blocked by a pan-mGlu receptor antagonist (*234*). Furthermore, while bath

application of DA, activation of group I mGlu receptors, or tetanic stimulation in isolation have no long term effect, any combination of these stimuli will result in LTD in the mPFC (*234*). These studies also discovered that activation of group II mGlu receptors alone is sufficient to induce LTD at this synapse (*234*). This was later determined to be $mGlu_3$-dependent (*235*), involve cross-talk with $mGlu_5$ (*236*), and required PI3K, Akt, and GSK3 signaling (*237*). Furthermore, this form of LTD also occurs at BLA inputs to the PL cortex but not at the vHipp input (*195*). Intriguingly, if this synapse is initially primed with DA application and then stimulated after washout, the same afferent stimulation protocol that normally induced LTD produces LTP (*238*). Thus the balance of long term plasticity is under heavily neuromodulatory control by DA in PL cortex slices.

Plasticity in the PL cortex is under the control of various neuromodulators in addition to DA. At layer II/III-to-V synapses, genetic deletion or antagonism of the $5HT_{1A}$ receptor increases the likelihood of LTP induction following high frequency stimulation while a $5HT_{1A}$ receptor agonist shifts the balance towards LTD induction (*239*). DA D_1 receptor activation also increases the likelihood of LTP following high frequency stimulation, similar to the priming result described above, but this effect required $5HT_{1A}$ receptors (*240*), suggesting interplay between the dopaminergic and serotonergic systems. Conversely, it was also shown that DA D_2 receptor activation favored LTD induction in the PL cortex through a GSK3-dependent pathway (*241*). In addition to DA and 5HT, ACh can also modulate synaptic plasticity in the PL cortex (*242–244*). Activation of muscarinic receptors with pan-muscarinic agonists can induce LTD in mPFC slices at the layer II/III-to-V, layer V-to-V, and vHipp-PL cortex synapses (*242–246*). Furthermore, optogenetic stimulation of cholinergic terminals in the PFC paired with electrical stimulation can induce a muscarinic receptor-dependent form of LTD (*244*, *247*). Mechanistically, there has been disagreement on the induction and expression mechanisms of this LTD, although this could be explained by technical variations between labs. There is general agreement that this LTD is mediated by M_1 muscarinic receptors (*243*, *244*, *247*). Some groups have found that coincident synaptic stimulation is necessary for LTD induction (*246*, *247*) while others report that it is not

(*242*, *243*). Muscarinic LTD does not require NMDA receptors nor postsynaptic Ca^{2+} but there is disagreement on the requirements of mGlu receptor stimulation (*243*, *246*) although this may reflect species (rat vs. mouse) and developmental (young vs. adult) differences. Recently, it was reported that muscarinic LTD requires the activation of phospholipase D_1 while the involvement of the more canonical $G\alpha_q$-PLC pathway is unclear (*243*, *248*). Finally, a presynaptic component is likely involved in the expression of muscarinic LTD in the PL cortex as an increase in paired pulse ratio has been consistently observed (*243*, *244*, *247*) and at the layer V-to-V synapse, this form of LTD has been shown to be endocannabinoid-dependent (*247*). Based on these *ex vivo* slices, long-term plasticity in the PL cortex is heavily dependent on neuromodulation which may allow for an increased processing capacity depending on arousal states and environmental conditions.

Finally, inhibitory neurotransmission can also undergo synaptic plasticity. In the hippocampus, synapses from CCK-positive interneurons express the cannabinoid type 1 (CB_1) receptor onto pyramidal neurons and express a form of heterosynaptic plasticity referred to as inhibitory LTD (iLTD) (*249*). In the mouse PFC, inhibitory responses onto layer V pyramidal neurons evoked by both layer II/III and layer V stimulation are sensitive to CB_1 receptor activation but are resistant to iLTD induction. Consistent with aforementioned role of neuromodulation in mPFC plasticity, co-incident activation of DA D_2 receptors facilitates the induction of iLTD at these synapses in the PL cortex (*250*). Additionally, synapses from mPFC SST interneurons onto superficial pyramidal neurons exhibit a form of LTP induced by postsynaptic activation of NMDA receptors, rises in intracellular Ca^{2+}, and activation of CaMKII. This form of LTP is selective for SST synapses compared to PV and VIP interneurons and can be induced heterosynaptically by high frequency stimulation of MDT afferents (*251*). Finally, excitatory synapses onto interneurons can also undergo plasticity. Theta burst stimulation of the superficial layers that induces LTP in layer V pyramidal neurons also causes LTP at excitatory synapses onto deep layer PV interneurons (*252*). However, in the presence of an adenosine A_{2A} receptor antagonist the same

stimulation induces LTD onto PV neurons with no effect on pyramidal neuron synapses. Therefore, adenosine would be expected to reduce the magnitude of LTP at a network level and provide yet another example of the effect of neuromodulation of long term plasticity in the PFC.

In conclusion, the capacity of the PL cortex to receive afferent information, process and integrate that information together, and exert top-down control over efferent regions via precise regulation of pyramidal cell output is mediated through an intricate set of excitatory and inhibitory circuits that can undergo dynamic plasticity on short and long time scales. This plasticity is critically dependent on a number of neuromodulators with DA and ACh identified as major contributors; this is not surprising based on the dense innervation of the PL cortex by dopaminergic and cholinergic terminals. Thus, from the molecular, to the cellular, up to the macrocircuit level, the PL cortex is organized and regulated in an incredibly complex manner suited to the complexity of its cognitive and executive functions.

CHAPTER II

PFC DYSFUNCTION AND NOVEL TREATMENT APPROACHES

Portions of the following chapter have been published in the journals *Molecular Brain* (*253*) and *Trends in Pharmacological Sciences* (*254*).

The molecular and cellular complexity of the PFC confers its ability to perform higher order cognitive tasks but also presents multiple opportunities for dysfunction. The precise synaptic connectivity of the PFC microcircuitry and macrocircuitry appear to be particularly vulnerable to stress and other pertubations both during development and in adulthood which can lead to long-lasting effects on cognitive and emotional function (*255*). This chapter will provide an overview of two psychiatric disorders that involve dysfunction of the PFC: posttraumatic stress disorder (PTSD) and schizophrenia. Furthermore, M_1 muscarinic acetylcholine and $mGlu_1$ metabotropic glutamate receptors will be discussed as novel pharmacological targets to potentially treat and normalize cortical dysfunction in these disorders.

2.1 Posttraumatic stress disorder

PTSD is a debilitating stress-related disorder that affects 3-4% of the general population annually and 15% of combat-exposed populations (*256*, *257*). Clinically, the DSM-5 criteria for PTSD include: exposure to a traumatic event with intrusive symptoms, avoidance behavior, negative alterations in mood and cognition, and alterations in arousal and reactivity persisting for more than 1 month (*258*). Selective serotonin reuptake inhibitors (SSRIs) are the only clinically approved drugs for the treatment of PTSD but a large majority of patients fail to benefit

substantially from them (*259*). Thus there remains considerable room for improvement in developing novel treatments for PTSD.

Due to its dense innervation by neuromodulators that are involved in the stress response, namely DA and NE, the general functions of the PFC are susceptible to both acute and chronic stressors. dlPFC dysfunction has been observed using both functional magnetic resonance imaging (fMRI) and electroencephalography (EEG) recording, with deficits in cortical activation as well as theta and gamma oscillations found following stress (*260–262*). Uncontrollable stress also impairs working memory and attentional tasks (*260*, *261*, *263*), and PTSD patients perform worse than healthy controls in various PFC-dependent cognitive tasks (*264*). Chronic stress leads to decreased PFC grey matter as well as reduced connectivity and top down-control over subcortical structures (*265–267*). Neuroimaging studies in PTSD patients have also identified deficient structure and activation of the dlPFC as well as the related ventromedial PFC (vmPFC). During a working memory task, PTSD patients display deactivation of the dlPFC compared to activation in healthy controls (*268*) while PTSD patients have exaggerated vmPFC responses in a task of response inhibition (*269*). The dlPFC and vmPFC also exhibit reduced grey matter volume and functional connectivity in PTSD patients compared to controls (*270*, *271*). Thus, there is ample evidence of PFC dysfunction in PTSD.

While fear is a normal and adaptive response to a perceived threat, in PTSD paitents fear responses become disproportionate to the threat level and can impair everyday function (*272*). The induction of PTSD by exposure to a traumatic event represents an aberrant learning event and the persistence of this perceived threat through hypervigilance and hyperarousal to non-threatening situations can be thought of as inappropriate memory recall and a deficit in the extinction of a fearful memory (*273*). As described in chapter I, the PFC plays a critical role in extinction learning, particularly in concert with the vHipp and BLA, and PFC dysfunction has been implicated in the pathophysiology of PTSD (*274*). While there is a dearth of pharmacological treatments for PTSD, behavioral exposure therapy is commonly using in the clinic but with

relatively inconsistent results (*275*). Since exposure therapy is based on the concept of fear extinction, novel pharmacological approaches that enhance fear extinction may augment exposure therapy in the clinic and improve its therapeutic utility (Figure 7) (*276*).

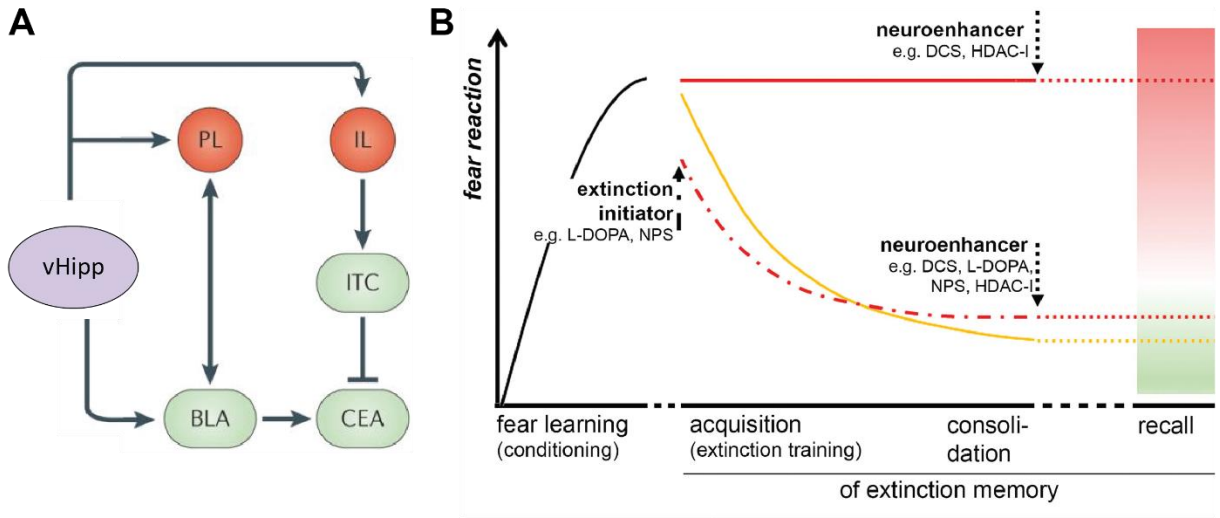

Figure 7: Fear circuitry and pharmacological approaches to augment fear extinction. **(A)** Fear acquisition and extinction involve the coordination of the vHipp-BLA-PFC circuit. During extinction, PL cortex activity decreases and IL cortex activity increases to mediate top-down control of the amygdala. The vHipp and BLA are both important for fear extinction as well. Adapted from (*277*). **(B)** Schematic depicting possible pharmacological augmentation of fear extinction. The solid red line represents a deficit in fear extinction compared to the normal extinction representation by the solid yellow line. Pharmacological interventions to initiate fear extinction or augment extinction and exposure therapy are being pursued for the treatment of PTSD and other anxiety disorders. Adapted from (*278*).

As discussed in chapter I, in rodent models both the PL and IL cortices play critical roles in the extinction of learned fear. PL cortex inactivation does not affect acquisition but impairs the expression of fear while IL inactivation impairs fear extinction and the consolidation and recall of that extinction memory (*80*). While the PL cortex is analogous to the dlPFC, it is also functionally similar to the human dorsal anterior cingulate cortex (dACC) and PTSD patients exhibit exaggerated dACC activity that correlates with poor fear extinction (*279*, *280*). Conversely, the vmPFC which is functionally similar to the rodent IL displays reduced activation during an extinction task in PTSD patients (*280*). These clinical results are consistent with studies in rodent

PFC which would suggest that PL hyperactivity and IL hypoactivity would cause a heightened fear responses and impair extinction. Therefore, either reducing the activity of the PL cortex during fear extinction or enhancing the activity of the IL may have therapeutic value for the augmentation of fear extinction and exposure therapy in the clinic. Furthermore, PTSD patients demonstrate enhanced BLA activation during fear acquisition (*281*, *282*) and combat veterans with PTSD exhibit increased BLA, hippocampal, and vmPFC activity in a fear extinction task (*283*). Since the BLA and vHipp innervate the mPFC, hyperactivity of these circuits may also contribute to extinction deficits and the pathophysiology of PTSD and therefore mechanisms to reduce their activity could be therapeutic.

Exposure to an intense bout of acute stress – a traumatic event or series of events – can induce a phenotype in animals that model many of the clinical aspects of PTSD and are useful in evaluating the etiology of the disorder (*284*). These include exposure to inescapable footshocks over a short or long period of time, exposure to predator odors, single prolonged stress, and various chronic stress models. A common theme among all of these models is an exaggerated fear response after conditioning and impaired extinction mechanisms (*285*). Single prolonged stress impaires extinction consolidation and retention of both contextual and cued fear (*286*) and similar to clinical fMRI studies, this is associated with an increased activation of the BLA although no PL cortex differences from control animals were observed (*287*). Stress-enhanced fear learning also produces impaired extinction and enhanced BLA activation has been shown to be required for expression of enhanced fear in this model (*272*). Likewise, BLA activity was increased in a subgroup of susceptible, extinction-deficient animals after shock exposure and stimulation of the IL cortex facilitates extinction and reduces BLA activity in these rodents (*288*). While there have been few studies into the circuit-based mechanisms of aberrant activity in the PL cortex in PTSD-like models, consistent observations of BLA hyperactivity suggest that mechanisms that could depress BLA-mPFC synapses could facilitate fear extinction and potentially lead to novel treatments for PTSD. One study that has investigated PL cortex physiology used predator odor

exposure which produces susceptible, extinction-deficient animals (*289*) and found enhanced excitatory drive specifically in PL cortex at both superficial and deep layers in these animals (*290*), suggesting PL cortical hyperactivity following traumatic stress.

Both clinical and preclinical studies have implicated PFC dysfunction in the pathophysiology of PTSD, especially concerning deficits in fear extinction and exposure therapy. Furthermore, a hyperactive BLA and hippocampus also appear to contribute to clinical deficits in PTSD patients. Given the intricate macrocircuitry between the PFC, BLA, and vHipp, novel pharmacological mechanism that could selectively modulate these circuits could be useful to augment exposure therapy in the clinic and improve the lives of patients living with PTSD. While some pharmacological agents have been identified that can enhance fear extinction (*291–294*), more work is needed to identify novel, hypotheses that can be tested in the clinic.

2.2 Schizophrenia

Schizophrenia is a devastating psychiatric disorder that afflicts approximately 1% of the worldwide population, affects women and men equally, and spans all socioeconomic groups (*295*). The disease is characterized by three major symptom domains: positive, negative, and cognitive symptoms (*296*). Current antipsychotics are effective at treating the positive symptoms such as auditory and visual hallucinations, delusions, and disorganized thoughts; however, they do not address the negative nor the cognitive symptoms. Negative symptoms (e.g. flattened affect, social withdrawal) and cognitive symptoms (e.g. deficits in working memory, and cognitive flexibility) are believed to be the best predictors of long-term outcome and are estimated to cost the U.S. healthcare system over $60 billion per year (*19*, *297*, *298*). Additionally, most patients discontinue current treatments due to adverse effects including extrapyramidal side effects (EPS) (i.e. dystonia, akathisia, parkinsonism, bradykinesia, tremor, and tardive dyskinesia) induced by first-generation typical antipsychotics and metabolic side effects (i.e. weight gain, type II diabetes, and hyperlipidosis) induced by second generation atypical antipsychotics (*299–301*).

The currently available antipsychotic medications on the market typically act via antagonism of dopamine D_2 receptors and serotonin $5HT_{2A}$ receptors (*302*). The efficacy of first generation typical antipsychotics was initially discovered serendipitously when a French surgeon noticed the anxiolytic and sedative-like effects of novel antihistamine drugs, leading to the development of chlorpromazine, later marketed as Thorazine, which produced a state of "artificial hibernation" in surgical patients (*303*). Clozapine was developed in late 1960s as a novel, atypical antipsychotic that retained efficacy but did not induce EPS (*304*) and despite a side effect profile that limited its clinical use, this led to the development of atypical antipsychotics including risperidone, olanzapine, and quetiapine that are all used today (*303*). Thorazine was introduced in 1954 and the efficacy of clozapine was demonstrated in the late 1960s but it took decades for any molecular mechanism to be attributed to these drugs (*305*–*308*). While their clinical value should not be discounted, it is clear from the lack of efficacy across all symptoms that there remains a significant unmet need to develop better treatments.

This desire has been significantly bolstered by an improved understanding of the underlying pathophysiology of the disease at the molecular, cellular, and brain-wide level. As a result, two major hypotheses have been proposed to explain the progression of the disease involving DA and glutamate. The dopaminergic hypothesis of schizophrenia is based on the discovery that dopamine receptors are blocked by typical antipsychotics (*305*, *308*) and posits that excessive dopamine release in striatal regions leads to overactivation of dopamine D_2 receptors and aberrant activity in the associative dorsal striatum, leading to psychosis (*309*). In postmortem tissue from schizophrenia patients, elevated dopamine and increased markers of dopaminergic transmission (*310*, *311*) have been observed in the dorsal and ventral striatum (*312*, *313*) compared to healthy controls. Positron emission tomography (PET) and related imaging studies subsequently demonstrated a significant increase in dopamine synthesis and release in the striatum of schizophrenia patients (*314*). While it was originally hypothesized that excessive DA in the NAc was responsible for the positive symptoms, higher resolution imaging studies have

now demonstrated that DA dysfunction is greatest in associative and sensorimotor striatal regions, with little evidence for deficient NAc DA transmission (*314–316*).

To explain the cognitive deficits in schizophrenia, a “revised” dopamine hypothesis has been proposed that posits a hyperactivity of nigrostriatal DA signaling with a concurrent hypoactivity of mesocortical DA signaling (*317*). The cognitive deficits in schizophrenia essentially encompass all of functions mediated by the PFC, including deficits in working memory, attention, behavioral flexibility, episodic memory, and response inhibition (*318*). As described in Chapter I, the PFC receives dense dopaminergic innervation from the VTA and dopamine is critical for proper plasticity induction and cognitive and executive functions. Postmortem studies have demonstrated a reduction in markers of dopaminergic innervation in the dlPFC while PET studies have shown a reduction in dopamine release capacity (*319*) and alterations in dopamine D_1 receptor availability in the dlPFC of schizophrenia patients (*320–322*). In further support of hypodopaminergic signaling in the dlPFC, enhancing dopamine release with amphetamine can improve cognitive function in schizophrenia (*323*), although it can also exacerbate psychotic symptoms precluding its therapeutic use (*324*).

There is a large body of evidence that supports glutamate dysfunction as a contributing factor to schizophrenia (*325*, *326*). For example, administration of the NMDA receptor antagonist phencyclidine (PCP) induces a schizophrenia-like state that presents clinically with all three symptom domains in healthy individuals (*327*). Similar clinical results have been found with administration of other NMDA receptor antagonists such as ketamine (*328*) and NMDA receptor antagonists can exacerbate or precipitate controlled symptoms when administered to schizophrenia patients (*329*). Additionally, a form of encephalitis where patients express circulating antibodies against GluN1/GluN2-containing NMDA receptors presents with schizophrenia-like symptoms (*330*). These clinical observations have formed the basis for the NMDA receptor hypofunction and glutamate hypothesis of schizophrenia.

A genome-wide association study in a large cohort of schizophrenia patients identified various glutamatergic loci associated with schizophrenia including the genes encoding GluA1, GluN2A, $mGlu_3$, and serine racemase, an enzyme responsible for the production of the NMDA receptor co-agonist D-serine (*331*). Microarray analyses have found reduced mRNA encoding the NMDA receptor subunits GluN1, GluN2A, and GluN2C as well as the AMPA receptor subunits GluA1, GluA2, and GluA4 in the dlPFC of schizophrenia patients (*332*–*335*), but this has not been consistently replicated (*336*–*339*). There have also been mixed results investigating protein levels of glutamate receptors with some studies finding decreased GluN1, GluA1 and GluA2 protein in the dlPFC of schizophrenia patients (*333*, *340*) while others have found no change (*341*).

In animal models, genetic reduction or antagonism of NMDA receptor function produces behavioral phenotypes that are related to schizophrenia-like symptoms including deficient sensorimotor gating, hyperactivity, and social and cognitive deficits (*342*, *343*). Underlying these behavioral effects are a variety of morphological and physiological phenotypes that mimic the clinical syndrome. Acute NMDA receptor antagonism causes excessive glutamate release in the rodent mPFC (*344*) that models increased glutamate levels in early schizophrenia patients (*345*). Animals treated subchronically or chronically with NMDA receptor antagonists also exhibit morphological changes in the mPFC that mirror findings from postmortem schizophrenia patients. One of the more replicated results from postmortem samples is a reduction in dendritic arborization and spine density of the superficial and deep layer dlPFC pyramidal neurons of schizophrenia patients (*346*–*351*). Recapitulating this, subchronic treatment with the NMDA receptor antagonists PCP, ketamine, or MK-801 reduces dendritic spine density in the rat and mouse mPFC (*352*, *353*). Additionally, mice with a genetic reduction in NMDA receptors or serine racemase also have reduced dendritic spine density in cortical pyramidal neurons (*354*, *355*), suggesting that NMDA receptor hypofunction may contribute to the development of cortical abnormalities in schizophrenia. These morphological abnormalities likely disrupt proper afferent

integration and synaptic plasticity mechanisms in the dlPFC, contributing to cognitive and executive deficits.

Acute administration of NMDA receptor antagonists to rodents or healthy human subjects cause a widespread increase brain activity assessed by *in vivo* electrophysiology and fMRI, respectively, particularly in the PFC (*356*–*360*). This recapitulates clinical fMRI studies in early schizophrenia patients that found hyperactivity and overactivation of the dlPFC during working memory tasks (*361*, *362*). In rodents, seminal work from Bita Moghaddam's lab demonstrated that the acute NMDA receptor antagonist-induced increase in mPFC pyramidal neuron firing was accompanied by a reduction in the firing of putative PV interneurons (*356*). This finding suggests that cortical GABAergic interneurons are particularly sensitive to NMDA receptor antagonism which reduces their activity, resulting in a disinhibition of mPFC pyramidal neurons and consequent cortical hyperexcitabilty (*363*). Corroborating this, acute and subchronic NMDA receptor antagonism in rodents reduces the expression of proteins associated with GABAergic transmission such as GAD67 and PV as well as producing functional inhibitory (*364*–*366*). Additionally, in the hippocampus and certain cortical regions including the PFC, GABAergic interneurons are more sensitive than pyramidal neurons to NMDA receptor antagonism (*367*–*372*). Together, these data form the basis for the hypothesis that NMDA receptor hypofunction on GABAergic interneurons contributes to the etiology of schizophrenia (*363*, *373*).

Likely the most consistent pathophysiological finding from postmortem studies is a reduction in the mRNA and protein levels of GAD67 in the dlPFC of schizophrenia patients compared to healthy controls (Figure 8, Page 49) (*374*–*377*). Additionally, mRNA of various interneuron markers including PV, SST, and CCK are reduced in the dlPFC of schizophrenia patients (*378*, *379*). Importantly, the total number and density of interneurons is not different between schizophrenia patients and healthy controls as well as the number of GABAergic synapses onto pyramidal neurons (*380*, *381*). Therefore the capacity of these interneuron to perform normal microcircuit functions is thought to be impaired due to disrupted GABA

homeostasis via reductions in GAD67 expression. These deficits appear to target specific interneuron subtypes as approximately half of dlPFC PV interneurons lack detectable GAD67 mRNA in schizophrenia samples (*382*). Furthermore, alterations in PV mRNA and protein in dlPFC PV basket cells is hypothesized to contribute to their dysfunction as PV protein is involved in modulating intracellular Ca^{2+} during fast action potential spiking and deficient levels may predispose interneurons to oxidative stress (*364*, *383*). Interneuron dysfunction in schizophrenia has also been implicated at a functional level. Some PET studies have found lower GABA levels in the dlPFC in schizophrenia patients (*384–386*), but these results have been inconsistent (*387*, *388*). Deficits in interneuron function have also been indirectly inferred from EEG studies. In healthy individuals, gamma oscillation power in the dlPFC increases during working memory tasks (*389*) however in patients with schizophrenia, this increase is blunted (*390–392*). These clinical findings support the theory that cortical GABAergic interneuron dysfunction plays a critical role in the pathophysiology of schizophrenia.

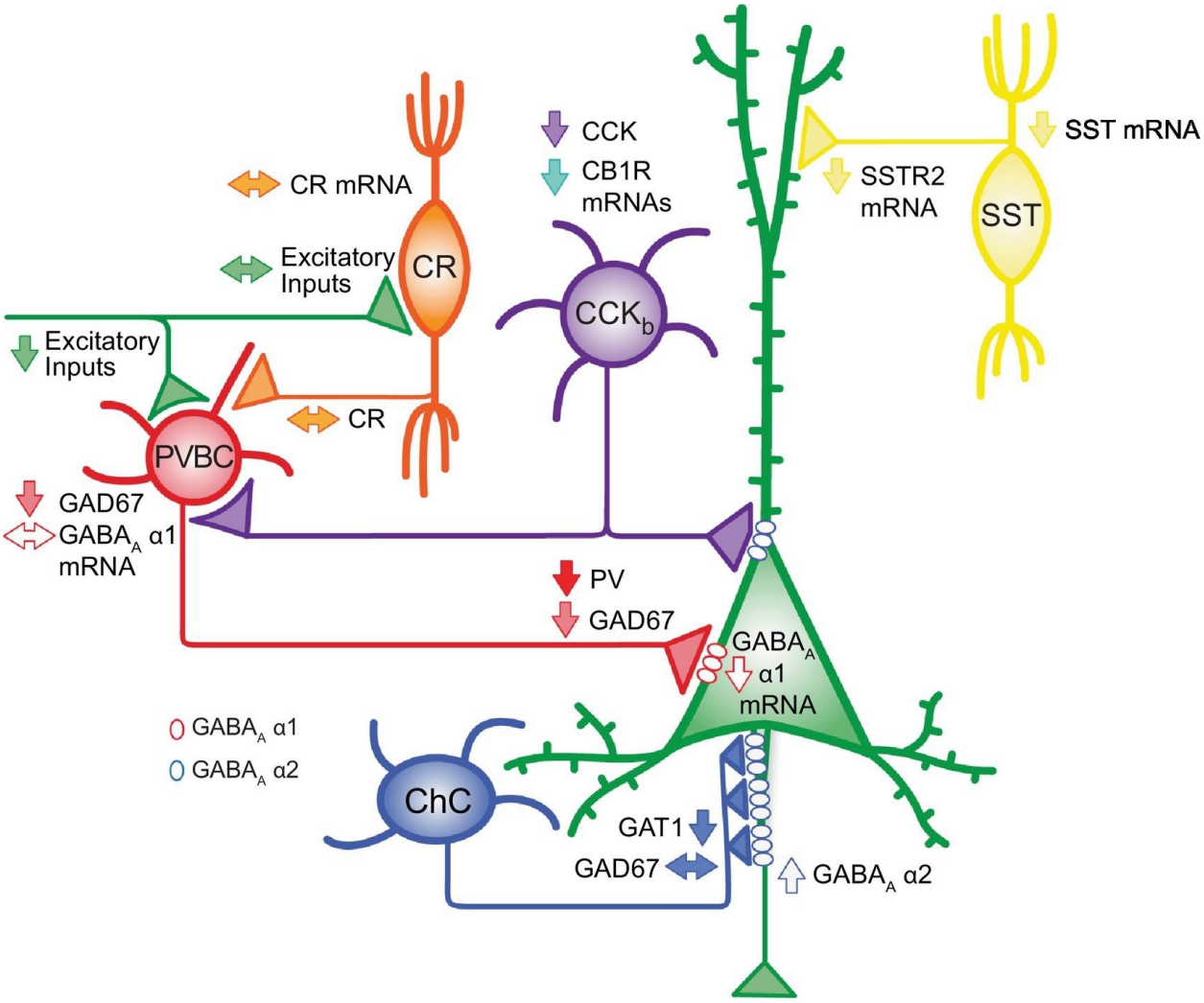

Figure 8: Summary of inhibitory deficits observed in the dlPFC of postmortem samples from schizophrenia patients. Reductions in GAD67 mRNA and protein levels, particularly in PV interneurons, are some of the most consistent pathophysiological findings in schizophrenia and suggest a reduced inhibitory capacity of the dlPFC microcircuit. Additionally, alterations in the expression of various other interneuron-specific transcripts and proteins all suggest impaired GABAergic inhibition. Adapted from (*393*).

While acute and subchronic NMDA receptor antagonism produce similar interneuron phenotypes in rodents, genetic manipulations of NMDA receptors also result in physiological and behavioral deficits consistent with interneuron dysfunction. Deletion of GluN1 from approximately 50% of cortical and hippocampal interneurons results in schizophrenia-like behavioral phenotypes including impaired prepulse inhibition, deficient working memory, asociality, and hyperactivity (*394*, *395*). These mice also have impaired evoked cortical gamma oscillations, consistent with

the clinical data. PV-specific deletion of GluN1 also produces spatial working memory deficits and impaired gamma oscillations in mice (*396*, *397*). Intriguingly, many of these behavioral changes only emerge after social isolation or similar stressful challenges, suggesting that NMDA receptor hypofunction alone is insufficient to produce schizophrenia-like phenotypes. This is consistent with a hypothesis put forth by John Lisman and colleagues that coincident stress and NMDA receptor hypofunction may be required to hyperactivate a thalamo-hippocampal-VTA loop that leads to the development of schizophrenia (*398*). This would also be consistent with epidemiological studies indicating early-life stress increases the chance of developing schizophrenia and the results of various “double-hit” models (*399*). This may also suggest that NMDA receptor hypofunction occurs upstream of dopamine dysregulation and may reconcile the dopaminergic and glutamatergic hypotheses of schizophrenia. In support of this idea, NMDA receptor antagonism or genetic manipulations increase DA signaling in subcortical regions (*395*, *400*, *401*).

Finally, etiologically distinct models of schizophrenia also produce behavioral deficits and dysfunctional cortical inhibitory transmission, consistent with clinical findings and arguing that this may be a common mechanism underlying the development of the disease. The neonatal ventral hippocampal lesion model results in working memory and other cognitive deficits, asocial and aggressive behaviors, and hyperactivity and deficits in prepulse inhibition (*402*). This model also exhibits decreases in PFC GAD67 expression (*403*) and hyperactivity of PFC pyramidal neurons (*404*). Prenatal administration of the mitotoxin MAM also produces schizophrenia-like behavioral phenotypes as well as deficits in BLA inhibitory gating of vHipp inputs, similar to NMDA receptor antagonism (*203*). Furthermore, the MAM model results in NMDA receptor hypofunction early in adolescence (*405*). Maternal immune activation produces schizophrenia-like behavioral effects as well as disrupted development of PV, SST and CB-positive interneurons (*406*). Finally, genetic models in mice that mimic a large chromosome deletion associated with schizophrenia display

deficits in PFC GAD67 and PV expression, gamma oscillations, impaired vHipp-mPFC theta synchrony, as well as working memory and social deficits (*76*, *407*).

Altogether, glutamatergic dysfunction, specifically involving NMDA receptor hypofunction, is thought to lead to cortical interneuron dysfunction that disrupts the ability of the dlPFC to function properly, resulting in the cognitive and negative symptoms and contributing to DA dysregulation that contributed to the positive symptoms of schizophrenia. With an improved understanding of the pathophysiology of schizophrenia, various novel pharmacological targets and mechanisms can be identified to rescue dlPFC dysfunction by targeting NMDA receptor hypofunction and inhibitory deficits to ultimately generate more efficacious treatments for schizophrenia patients.

2.3 Targeting M_1 muscarinic receptors for the treatment of psychiatric disorders

As described in chapter I, cholinergic innervation of the dlPFC plays a critical role in supporting various cortical functions including attention and working memory. ACh signals through two distinct classes of receptors that include the nicotinic receptors which are ligand-gated ion channels and G-protein-coupled muscarinic ACh receptors (mAChRs). While both play important roles in central and peripheral systems, ACh acts primarily through mAChRs in the brain as a neuromodulator to shape ensembles of neurons and alter neuronal firing in response to changing environmental conditions (*408*, *409*). The mAChR family consists of M_1, M_3 and M_5, which primarily couple to $G\alpha_q$, and M_2 and M_4, which primarily couple to $G\alpha_{i/o}$. Considerable evidence suggests that mAChRs are critically involved in modulating complex behaviors such as cognition and motivation and their localization both pre- and postsynaptically throughout the CNS make mAChRs uniquely situated as potential targets for the treatment of multiple CNS disorders (Figure 9, Page 52) (*410*, *411*).

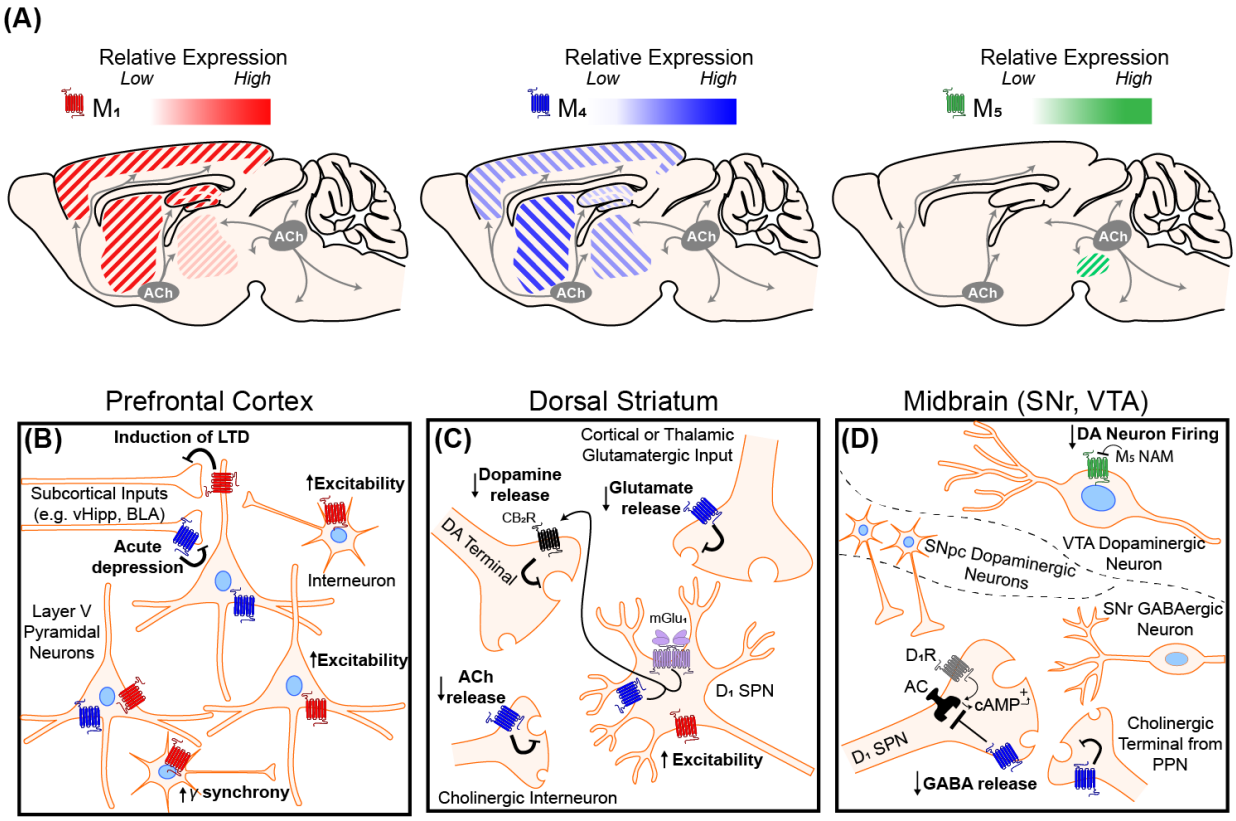

Figure 9: Muscarinic receptor distribution and molecular mechanisms relevant to the treatment of psychiatric disorders. **(A)** Distribution of M_1, M_4, and M_5 muscarinic acetylcholine (ACh) receptors in brain regions implicated in neurological dysfunction. The relative expression of each receptor subtype is indicated by its respective color gradient. M_1 mAChRs are highly expressed in the cortex, hippocampus, and dorsal and ventral striatum, and are expressed at low levels in thalamic areas. M_4 mAChRs are highly expressed in striatal regions, moderately expressed across the cortex and thalamus, and are lowly expressed in the hippocampus. M_5 mAChR expression is restricted to the midbrain. Cholinergic projection neurons derive from two distinct clusters – the basal forebrain nuclei (grey circle, left) which innervates cortical, hippocampal, and thalamic areas, and the brain stem nuclei (grey circle, right) which innervates midbrain, hindbrain, thalamic, and cerebellar areas. Cholinergic tone in the dorsal and ventral striatum is primarily provided by large cholinergic interneurons. **(B)** In the PFC, M_1 mAChR activation induces a form of long-term depression (LTD) of glutamatergic inputs. M_1 mAChR activation also increases the excitability of pyramidal neurons and GABAergic interneurons to increase gamma oscillation synchrony in the cortex. M_4 mAChRs can acutely inhibit neurotransmitter release. **(C)** In the dorsal striatum, M_4 mAChRs expressed on direct pathway D_1 receptor-positive spiny projection neurons (SPNs) interact with metabotropic glutamate receptor 1 ($mGlu_1$) to produce endocannabinoids which then bind to cannabinoid type 2 (CB_2) receptors to inhibit local dopamine release. In addition, M_4 activation can reduce both ACh release from local cholinergic interneurons and act as a heteroreceptor on glutamatergic terminals from the cortex and thalamus to reduce glutamate release. M_1 mAChRs expressed on D_1-SPNs increase the excitability of these neurons. **(D)** In the midbrain, cholinergic modulation of dopaminergic (DA) neurons in the ventral tegmental area (VTA) and direct pathway input into the substantia nigra reticulata (SNr) are relevant to neurological disorders. In the VTA (top), M_5 mAChRs are expressed on VTA DA neurons and M_5 NAMs are hypothesized to reduce DA neuron firing. In the SNr (bottom), M_4 mAChR activation on direct pathway D_1-SPN terminals directly opposes increased GABA release mediated through D_1-receptor activation by DA released from the substantia nigra pars compacta (SNpc, middle). M_4 can also act as an autoreceptor and reduce ACh release from cholinergic projection terminals. From (*254*).

Of the mAChRs, M_1 and M_4 have attracted the most attention as potential targets for novel treatments of psychiatric disorders based on preclinical and clinical findings. This interest was significantly enhanced by the results of two clinical trials with the M_1/M_4-preferring agonist xanomeline. In a phase III clinical trial in over 300 patients with behavioral disturbances associated with Alzheimer's disease, xanomeline significantly reduced vocal outbursts, agitation, and the psychosis-related symptoms of hallucinations and delusions (*412*). Based on those antipsychotic-like effects, a small, phase II trial was run in 20 schizophrenia patients. Xanomeline significantly improved schizophrenia symptoms as assessed by the Brief Psychiatric Rating Scale (BPRS) compared to placebo and excitingly, demonstrated cognition-enhancing effects in tests of verbal learning and short-term memory (*413*). Despite this promising clinical efficacy, peripheral adverse effects attributed to activation of M_2 and M_3 receptors (*414*) were dose-limiting and Eli Lily decided to halt development. In late 2019, Karuna Therapeutics released results from a phase II clinical trial (NCT03697252) of KarXT, a combination of xanomeline formulated with a peripherally-restricted pan-mAChR antagonist. In 182 adults with schizophrenia, they report a statistically and clinically significant reduction in symptoms using the Positive and Negative Syndrome Scale (PANSS) score in patients receiving KarXT compared to placebo and importantly, discontinuation rates were similar between KarXT and placebo. These results confirm the earlier phase II trial conducted by Eli Lilly (*413*) in a larger patient population and provide further clinical support for ongoing M_1 and M_4 drug development efforts. The initial clinical findings with xanomeline have led to significant efforts to develop subtype selective ligands for M_1 and M_4 mAChRs without activity at M_2 and M_3 in order to avoid dose-limiting side effects. For the purposes of this dissertation, this section will focus on M_1 receptors.

Based on observations of cholinergic dysfunction in the dlPFC in schizophrenia (*415*, *416*) and the discovery that a subset of patients display a reduction of dLPFC M_1 receptor density (*417*, *418*), M_1 selective ligands have been pursued as potential cognition-enhancing therapeutics for schizophrenia. M_1 receptors have been shown to modulate the activity of PFC pyramidal neurons

and GABAergic interneurons (*419–422*) and genetic deletion of M_1 receptors causes deficits PFC-dependent behaviors including working memory and visual discrimination learning (*423*, *424*). M_1 receptor activation can also positively modulate NMDA receptor function (*425*) and has been implicated in the clinical efficacy of clozapine (*426*). Additionally, M_1 receptor activation can induce a form of LTD in the mPFC that could be therapeutically useful to reduce PFC hyperactivity (*244*).

Pursuit of M_1 selective activators ultimately led to the discovery of benzyl quinolone carboxylic acid (BQCA) as a selective M_1 positive allosteric modulator (PAM) with favorable pharmacokinetic properties for preclinical work (*427*). Studies with BQCA have demonstrated that M_1 potentiation is pro-cognitive in a variety of PFC- and hippocampal-dependent tasks (*421*, *424*, *427–429*), consistent with M_1 expression in these regions (*430*, *431*). Development of PQCA, an analog suitable for non-human primate studies, has also demonstrated that M_1 potentiation in higher species can improve attention and cognitive performance (*432*, *433*). While Merck and Pfizer have both pursued M_1 PAM development, subsequent investigation of their lead compounds MK-7622 (*434*) and PF-06827443 (*435*) identified that these compound exhibited intrinsic agonist activity in addition to PAM activity, as so called ago-PAMs (*436*, *437*). Previous reports have suggested that agonist activity of $G\alpha_q$-coupled receptors modulators results in adverse effect liability (*438*) and overactivation of M_1 receptors was recently found to produce deficits in PFC function in non-human primates (*439*). A phase II clinical trial with MK-7622 in Alzheimer's disease was recently terminated due to lack of efficacy (*440*) supporting the idea that M_1 agonist activity may disrupt cognition, while pure PAM activity is optimal for procognitive effects (*437*). It will be interesting to see whether this hypothesis is corroborated following the disclosure of clinical results from other M_1 agonist programs such as HTL0018318 developed by Sosei Heptares (NCT03456349).

Subsequent development efforts have led to M_1 PAMs with improved pharmacodynamics and pharmacokinetic properties including VU0453595 (*244*), VU6004256 (*441*), and VU0486846 (*442*) that have pro-cognitive efficacy and lack agonist activity. VU0453595 rescues subchronic

PCP-induced physiological as well as cognitive and social deficits (*244*). Additionally, VU6004256 reverses physiological and cognitive deficits in the GluN1 knockdown genetic model of schizophrenia (*441*). Together, these results suggest that M_1 PAMs could be effective treatments for the cognitive and negative symptoms of schizophrenia. The M_1 PAM VU'319 is in an ongoing phase I clinical trial (NCT03220295) and TAK-071 (NCT02769065) has just concluded a phase I study. As the remaining M_1 PAMs in clinic, the results of subsequent trials will be important to clinically validate the hypothesis that M_1 PAM are procognitive.

In addition to efficacy in reversing cognitive and social deficits in schizophrenia-like models, M_1 PAMs are also efficacious in models of Alzheimer's disease and other neurodegenerative disorders (*421*, *443–445*). The M1 PAM BQCA also improves learning and memory deficits in a rodent model of traumatic brain injury (*446*) and M_1 receptors may be a viable target for substance use disorders based on findings that M_1 activation reduces cocaine discrimination (*447*). Altogether, the procognitive effects of M_1 PAMs warrant further preclinical and clinical investigation and may prove to be effective therapeutics for schizophrenia and other psychiatric disorders.

2.4 Targeting $mGlu_1$ receptors for novel treatments of schizophrenia

Based on the NMDA receptor hypofunction hypothesis of schizophrenia, pharmacological agents that enhance NMDA receptor function are not only valuable tools in preclinical animal models but could also provide therapeutic benefits to patients with schizophrenia. Unfortunately, direct activation of NMDA receptors using traditional orthosteric agonists induces adverse effects such as excitotoxicity and seizures (*448–452*). Furthermore, treatments with NMDA receptor obligate co-agonists such as glycine or serine failed to have consistent efficacy across multiple clinical trials (*453*).

In addition to NMDA receptors and other ionotropic glutamate receptors, glutamate also binds to and signals through a family of G-protein coupled metabotropic glutamate (mGlu)

receptors (*177*). There are eight subtypes of mGlu receptors, $mGlu_1$–$mGlu_8$, classified into three groups (group I, $mGlu_{1,5}$; group II, $mGlu_{2,3}$; group III, $mGlu_{4,6,7,8}$). mGlu receptors are class C GPCRs which function primarily as dimers and modulate glutamatergic, GABAergic, and neuromodulatory neurotransmission throughout the central nervous system (CNS) (*177*). Group I mGlu receptors primarily coupled to $G\alpha_q$, while group II and III mGlu receptor preferentially signal through activation of $G\alpha_{i/o}$ to inhibit adenylyl cyclase activity and $G\beta\gamma$ to modulate a variety of ion channels, similar to $GABA_B$ receptor described in chapter I. All three groups of mGlu receptors have been pursued as putative targets for novel antipsychotics due to their ability to directly alter NMDA receptor function or other aspects of glutamatergic signaling (Figure 10, Page 57). For the purposes of this dissertation, this section will focus on the function of and development of ligands for $mGlu_1$ receptors.

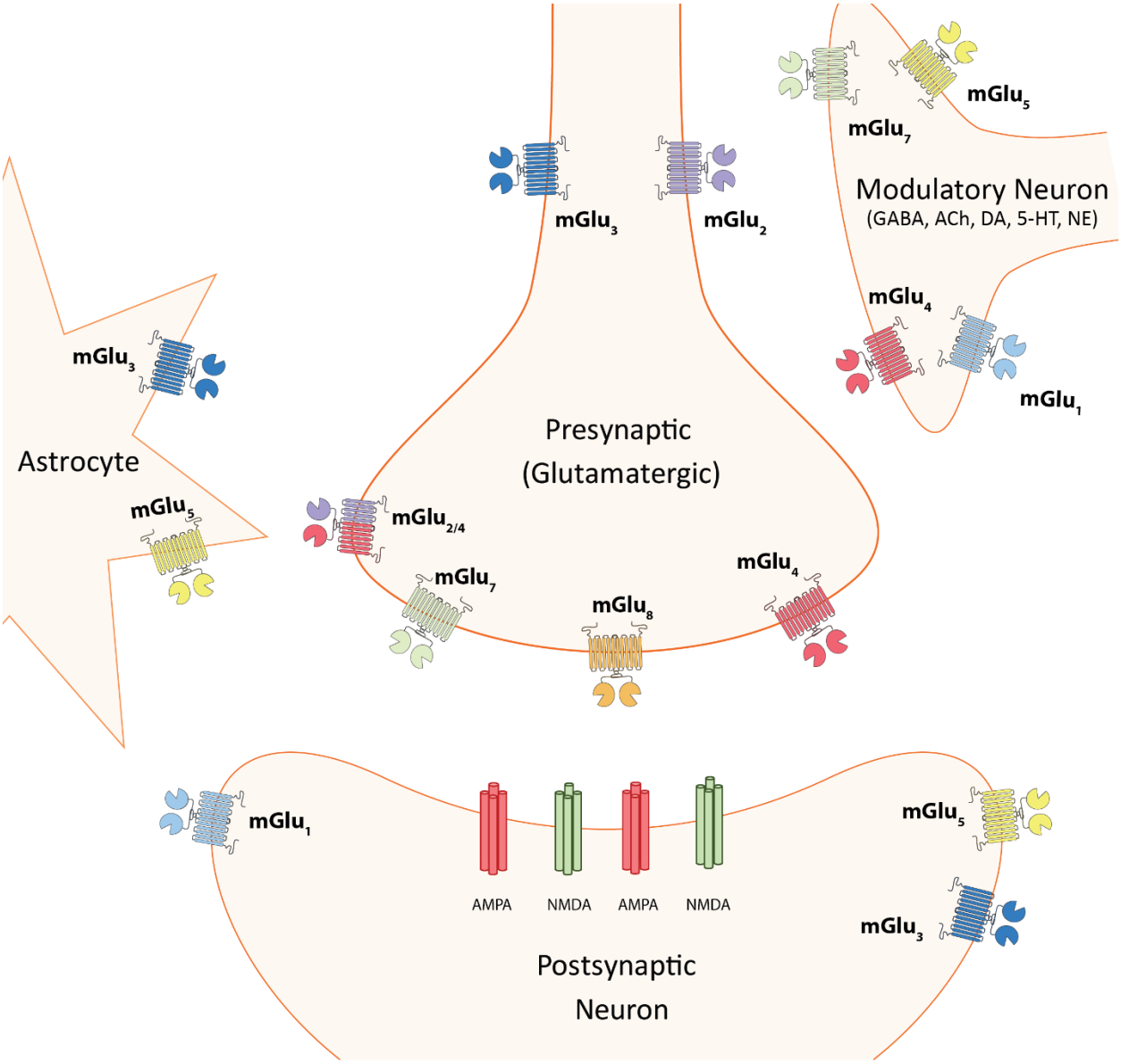

Figure 10: Localization of mGlu receptor subtypes. $mGlu_1$ (light blue) is found on postsynaptic glutamatergic neurons as well as on GABAergic neurons. $mGlu_5$ (yellow) can be located on the same neurons as $mGlu_1$ as well as on glia. $mGlu_2$ (purple) is found primarily presynaptically as both a homodimer as well as a heterodimer with $mGlu_4$ (red). $mGlu_3$ (dark blue) is found on both presynaptic and postsynaptic glutamatergic, GABAergic, and neuromodulatory neurons as well on glia. $mGlu_4$ is localized to both modulatory neurons as well as on presynaptic glutamatergic neurons as either a homodimer or heterodimer. $mGlu_7$ (green) is localized to presynaptically neurons as well as GABAergic neurons. Lastly, $mGlu_8$ (orange) is primarily localized presynaptically and $mGlu_6$ is not shown since it is restricted to the retina. From (*253*).

The highly conserved orthosteric glutamate binding site among mGlu receptor subtypes has generally precluded the design of subtype-specific receptor agonists or antagonists. This problem has been addressed by designing small molecule modulators that bind to distinct and subtype-unique allosteric sites within the 7 transmembrane domains of mGlu receptors allowing unprecedented selectivity against other glutamate receptors (*454*). PAMs generally do not activate the receptor directly but instead potentiate responses to endogenous glutamate. Conversely, NAMs act as non-competitive antagonists and may also have inverse agonist activity, reducing constitutive activity of the receptor in the absence of glutamate (*455*, *456*).

Group I mGlu receptors include $mGlu_1$ (*457*, *458*) and $mGlu_5$ (*459*) and are primarily coupled to the $G\alpha_q$ subunit of the heterotrimeric G-proteins. Canonical $G\alpha_q$ signaling activates phospholipase C and causes downstream activation of protein kinase C (PKC) via the generation of the second messengers diacylglycerol (DAG) and inositol triphosphate (IP_3). The group I mGlu receptors have emerged as attractive targets, initially based on their close coupling to the NMDA receptor via intracellular signaling pathways and scaffolding proteins including Homer, SHANK, and GKAP-PSD95 (*460–462*) and their ability to potentiate NMDA responses in acute brain slices (*463*). $mGlu_1$ and $mGlu_5$ are predominantly postsynaptic receptors, but they have also been identified on presynaptic terminals of GABAergic and glutamatergic neurons (*464*). Group I mGlu receptors are found primarily as homodimers via interactions at the large extracellular N-terminal Venus flytrap domain of each monomer (*465*). Emerging evidence points to group I mGlu receptors existing as monomers with distinct neurodevelopmental patterns which may impact their pharmacological profiles at specific ages (*466*). While the potential role of dimeric versus monomeric expression may have interesting implications for schizophrenia, further studies are required to investigate this phenomenon.

Two recent independent studies have identified 12 rare deleterious nonsynonymous single nucleotide polymorphisms in the *GRM1* gene encoding for $mGlu_1$ in schizophrenia (*467*, *468*). Further support for $mGlu_1$ dysregulation in schizophrenia is evidenced by postmortem

findings in which $mGlu_1$ mRNA expression is altered compared to controls (*469*). Preclinically, *Grm1* knockout mice display deficits in prepulse inhibition (PPI), a behavioral assessment of sensory gating which is the process of filtering unnecessary stimuli from total sensory stimuli and which is impaired in schizophrenia patients (*342*, *470*). Interestingly, recent studies reveal that *GRM1* mutations associated with schizophrenia reduce $mGlu_1$ signaling in cell lines and that selective $mGlu_1$ PAMs can partially rescue the reduction in glutamate-mediated calcium signaling *in vitro* (*471*). Therefore, enhancing $mGlu_1$ signaling through selective agents has the potential to rescue deficits in schizophrenia patients with deleterious *GRM1* mutations.

Potent first generation $mGlu_1$ PAMs were developed in the early 2000s, but poor drug metabolism and pharmacokinetic (DMPK) profiles limited their use in preclinical studies (*472*, *473*). More recent efforts yielded VU6000799, VU6000790, and VU6004909 as potent, highly selective $mGlu_1$ PAMs with improved DMPK properties and brain penetrance, and are therefore better suited for *in vivo* studies (*474–478*). In the future, it will be important to evaluate these compounds in a range of animal models that are relevant to all three symptom domains of schizophrenia.

In addition to rescuing $mGlu_1$ signaling deficits, activators or PAMs of $mGlu_1$ may also act to counteract the hyperdopaminergic signaling in the striatum in schizophrenia patients (*479*, *480*). Multiple studies have demonstrated that the pan-mGlu receptor agonist trans-ACPD is able to attenuate stimulation-induced dopamine release in the dorsal striatum (*481*), the substantia nigra (*482*), and the NAc (*483*). In a follow up study, $mGlu_1$ was identified as the subtype responsible for this effect in the dorsal striatum (*484*). Therefore, $mGlu_1$ activation may have the potential to produce similar antipsychotic effects as D2 dopamine receptor antagonist antipsychotics. Consistent with this, it was recently reported that co-activation of $mGlu_1$ is required for both the M_4 muscarinic receptor PAM-mediated reductions in dopamine release (*485*) and the *in vivo* antipsychotic efficacy of M_4 PAMs in an amphetamine-induced model of the positive symptoms of schizophrenia (*486*). Furthermore, the $mGlu_1$ PAM VU6004909 alone reduces local

striatal dopamine release *in vivo* and reverses amphetamine-induced hyperlocomotion and disruptions in PPI (*486*), supporting the hypothesis that $mGlu_1$ PAMs have antipsychotic-like efficacy.

Important to the potential utility of $mGlu_1$ PAMs to treat schizophrenia, it has been reported that the $mGlu_1$ NAMs FTIDC and CFMTI are efficacious in animal models predictive of antipsychotic activity, including reducing psychostimulant and NMDA receptor antagonist-induced hyperlocomotion and deficits in PPI as well as reversing deficits in social interaction induced by the NMDA receptor antagonist MK-801 in rats (*487*, *488*). The contrasting findings of $mGlu_1$ PAMs, NAMs, and *Grm1* knockout animals illustrate the potential complexity of $mGlu_1$ ligands. Regionally restricted $mGlu_1$ signaling may explain the discrepancy between the $mGlu_1$ PAM and NAM behavioral data. $mGlu_1$ is expressed in dopaminergic neurons in the midbrain and local activation leads to depolarization and burst firing of dopaminergic neurons (*489–491*). Consequently, activation of $mGlu_1$ *in vivo* by direct infusion of a group I agonist into the midbrain produces increases in dopamine release in the striatum and cortex (*492*, *493*). The reduction in striatal dopamine release observed with the $mGlu_1$ PAM occurs locally in the striatum via a cannabinoid CB_2 receptor-mediated reduction in dopamine release from dopaminergic terminals (*485*, *486*). Therefore, an $mGlu_1$ NAM may produce antipsychotic-like effects by antagonizing $mGlu_1$ postsynaptically on midbrain dopamine neurons while the antipsychotic efficacy of $mGlu_1$ PAMs could be due to local actions in the striatum that circumvent the predicted increase in dopamine neuron activity. Importantly, $mGlu_1$ NAMs also produce cognitive disruptions (*494*) that may be related to a global decrease in dopamine release, therefore the local actions of an $mGlu_1$ PAM in the striatum may increase the therapeutic window of $mGlu_1$ receptor modulation.

Finally, $mGlu_1$ is expressed on GABAergic interneurons in the hippocampus and cortex (*215*, *495*, *496*). In hippocampal stratum oriens lacunosum-moleculare interneurons, postsynaptic $mGlu_1$ activation mediates a form of LTP of glutamatergic transmission onto these cells (*497*). Additionally, $mGlu_1$ activation in the cortex can lead to an increase in inhibitory transmission (*498*,

499). In neuronal culture systems, $mGlu_1$ has also been shown to enhance NMDA receptor currents (*462*). Taken all together, these data imply that $mGlu_1$ could enhance NMDA receptor function and GABAergic interneuron activity in the PFC, potentially rescuing the deficits observed in schizophrenia. While the antipsychotic actions of an $mGlu_1$ PAM have recently been disclosed, it remains to be tested whether $mGlu_1$ PAMs have efficacy in models of the cognitive and negative symptoms of schizophrenia.

2.5 Outline of Current Studies

In psychiatric disorders including PTSD and schizophrenia, aberrant PFC activity correlates with cognitive and emotional deficits that are thought to involve dysfunctional integration of afferent information and intracortical processing. Current treatments for these disorders have limited efficacy, especially concerning dlPFC-dependent cognitive functions; therefore, there is a critical need to identify novel pharmacological mechanisms to restore PFC function in these disorders. Overall, we hypothesize that modulation of PFC neurotransmission by M_1 and $mGlu_1$ PAMs will ameliorate cortical hyperactivity and have procognitive effects in models of PTSD and schizophrenia, respectively.

Stress-induced loss of fear extinction can impair recovery from trauma and is thought to play a critical role in sustaining pathological fear in PTSD. The PFC is essential for fear extinction by integrating information from the vHipp and the BLA. This raises the possibility that M_1 LTD could play a role in fear extinction learning and that M_1 PAMs could potentially be adjunct therapies to augment exposure therapy in the clinic. It is currently unknown whether M_1 LTD is expressed at synapses in the vHipp-PFC-BLA circuit that have been implicated in fear and extinction learning. Additionally, the role of M_1 in fear learning and extinction is unclear. In Chapter III, we used a combination of optogenetics, acute brain slice electrophysiology, cued and contextual fear conditioning, and the SEFL model of PTSD to test the hypothesis that M_1

muscarinic receptors modulate fear-related subcortical inputs to the PFC and that an M_1 PAM will be efficacious in a model of PTSD.

Intracortical processing involving inhibitory GABAergic interneurons is critical for proper PFC function. One of the most consistent pathophysiological findings in schizophrenia is postmortem and functional evidence of inhibitory interneuron dysfunction. $mGlu_1$ has been genetically linked to schizophrenia, is expressed in cortical interneurons, and activation of postsynaptic group I mGlu receptors increases neuronal activity. Targeted enhancement of $mGlu_1$ function therefore may rescue inhibitory deficits and lead to novel therapeutics for cognitive dysfunction in schizophrenia but the effects of $mGlu_1$ potentiation in the PFC are unknown. Furthermore, the behavioral effects of $mGlu_1$ PAMs on cognition in a schizophrenia-like model have not been investigated. In Chapter IV, we used a combination of whole-cell electrophysiology, optogenetics, functional magnetic resonance imaging, and behavioral assays to test the hypothesis that $mGlu_1$ potentiation enhances inhibitory transmission in the PFC and has procognitive efficacy in an NMDA receptor hypofunction model of schizophrenia.

CHAPTER III

M_1 MUSCARINIC RECEPTORS MODULATE FEAR-RELATED INPUTS TO THE PREFRONTAL CORTEX: IMPLICATIONS FOR NOVEL TREATMENTS OF POSTTRAUMATIC STRESS DISORDER

The following chapter has been published as titled in the journal *Biological Psychiatry* (*500*).

3.1 Abstract

Background: The prefrontal cortex (PFC) integrates information from multiple inputs to exert “top down” control allowing for appropriate responses in a given context. In psychiatric disorders such as posttraumatic stress disorder (PTSD), PFC hyperactivity is associated with inappropriate fear in safe situations. We previously reported a form of muscarinic acetylcholine receptor (mAChR)-dependent long-term depression (LTD) in the PFC that we hypothesize is involved in appropriate fear responding and could serve to reduce cortical hyperactivity following stress. However, it is unknown if this LTD occurs at fear-related inputs.

Methods: Using optogenetics with extracellular and whole-cell electrophysiology, we assessed the effect of mAChR activation on the synaptic strength of specific PFC inputs. We used selective pharmacological tools to assess the involvement of M_1 mAChRs in conditioned fear extinction in control mice and in the stress-enhanced fear learning (SEFL) model.

Results: M_1 mAChR activation induced LTD at inputs from the ventral hippocampus and basolateral amygdala but not the mediodorsal nucleus of the thalamus. We found that systemic M_1 mAChR antagonism impaired contextual fear extinction. Treatment with an M_1 PAM enhanced contextual fear extinction consolidation in SEFL-conditioned mice.

Conclusions: M_1 mAChRs dynamically modulate synaptic transmission at two PFC inputs whose activity is necessary for fear extinction and M_1 mAChR function is required for proper contextual fear extinction. Furthermore, an M_1 PAM enhanced the consolidation of fear extinction in the SEFL model suggesting M_1 PAMs may provide a novel treatment strategy to facilitate exposure therapy in the clinic for the treatment of PTSD.

3.2 Introduction

The prefrontal cortex (PFC) integrates information from a diverse set of cortical and subcortical sources (*35*, *36*) and is a central structure involved in higher-order cognitive functions (*501*, *502*). Normal function of the PFC is critical for "top down" processing of internal and external signals to inhibit inappropriate thoughts, emotions, and actions, and allows for relevant behavioral responses in appropriate contexts (*503–505*). To properly integrate synaptic information and facilitate executive functions, input to the PFC undergoes dynamic regulation via mechanisms of synaptic plasticity including long-term potentiation and long-term depression (LTD) of synaptic strength. These forms of synaptic plasticity are commonly considered the molecular correlates of learning and memory (*189*, *195*, *244*) and are critical in directing PFC activity to guide emotional and behavioral responses (*277*, *503*).

The PFC plays a critical role in extinction of fear conditioning by integrating information from the ventral hippocampus (vHipp) and the basolateral amygdala (BLA), key regions for encoding conditioned fear and regulating emotional responses to fearful stimuli (*277*, *506*). Interestingly, multiple studies suggest that exposure to acute or repeated stress can induce disruptions in PFC function (*504*, *505*) and can dramatically inhibit normal fear extinction (*276*). Stress-induced loss of fear extinction can impair recovery from trauma and is thought to play a critical role in sustaining pathological fear in post-traumatic stress disorder (PTSD) patients (*276*).

Preclinical and clinical studies suggest that cholinergic projections to the PFC from the basal forebrain play important roles in the extinction of fear learning (*507*). Acetylcholine (ACh)

acts in large part through the five subtypes of muscarinic acetylcholine receptors (mAChRs), M_1-M_5, of which the primarily $G\alpha_q$-coupled M_1 and $G\alpha_i$-coupled M_4 subtypes are the most abundant in the PFC (*431*). mAChRs are involved in working memory (*508*), attention (*509*), as well as appropriate fear (*510*) and emotional responses (*511*). These roles of mAChRs in the PFC have been studied primarily using non-selective *pan*-mAChR antagonists such as scopolamine (*508*, *510*, *511*), but the relative contribution of each subtype to cognitive and affective functions has remained elusive, in part due to a dearth of subtype-selective compounds. We and others have recently developed selective ligands for mAChR subtypes, including highly selective agonists (*512*), antagonists (*513*), and positive allosteric modulators (PAMs) (*244*, *427*, *437*, *441*, *442*, *514*) for the M_1 mAChR. Using these new tools, along with genetic manipulations (*515*, *516*), we recently reported that M_1 mAChR activation induces a form of LTD in the rodent prelimbic (PL) PFC (*244*). This is especially interesting in light of studies suggesting that PFC neurons display robust firing during states of high fear, and that depression of excitatory inputs to the PFC may be important for fear extinction learning (*81*, *235*, *517*). This raises the possibility that M_1 LTD could play a role in mAChR regulation of fear extinction learning. If so, this could provide important new insights that are relevant for the treatment of PTSD and other disorders in which fear extinction learning is disrupted. However, the PFC receives input from multiple subcortical areas (*35*, *43*) and it is not known whether M_1 LTD is expressed at synapses in the vHipp-PFC-BLA circuit that have been implicated in fear conditioning and extinction learning.

We now report a series of studies in which we found that M_1 mAChR activation induces LTD at the vHipp-PFC and BLA-PFC synapses but not at synapses from the mediodorsal nucleus of the thalamus (MDT). Further studies utilizing viral-mediated deletion of M_1 from pyramidal cells revealed that vHipp-PFC mAChR LTD requires postsynaptic M_1 in PFC pyramidal neurons. Interestingly, selective blockade of M_1 impaired contextual fear extinction. Finally, we found that an M_1 PAM was able to reverse deficits in contextual fear extinction in a rodent model of PTSD, implying that M_1 PAMs may have clinical efficacy as an adjunct to exposure therapy. These results

are especially exciting in light of the development of M_1 PAMs as potential therapeutics for psychiatric and neurodegenerative disorders.

3.3 Materials and Methods

Animal Use

C57BL/6J mice were obtained from Jackson Laboratories (Bar Harbor, ME, USA), allowed to acclimate to the housing facility for at least one week and were then used for experiments. *Chrm1*$^{loxP/loxP}$ mice (*516*) were bred in-house and maintained as homozygous breeding pairs. All experiments were performed in mice 8-12 weeks of age. Mice were group-housed (2–5 per cage) on a 12-h light cycle (lights on at 6:00 a.m.). Food and water were available *ad libitum*. All experimental protocols were approved by the Vanderbilt Institutional Animal Care and Use Committee.

Viral Injections

At 4-5 weeks of age, C57BL/6J mice were anesthetized with 3% isoflurane, positioned in a stereotaxic frame (Kopf Instruments, CA) and maintained on 1-2% isoflurane for the remainder of the procedure. Briefly, an incision was made and the skin and muscle atop the skull was pulled to the side. A craniotomy was made above the sites of the injections. Mice were then injected with 0.8µL (ventral hippocampus, vHipp) or 0.4µL (basolateral amygdala, BLA, or mediodorsal nucleus of the thalamus, MDT) of AAV5-CaMKIIa-ChR2-EYFP (UNC Viral Core, NC) per injection site at a rate of 0.1µL/min using a 28G needle attached to a 10µL Hamilton syringe (Hamilton Co., NV). The coordinates for injections relative to Bregma are as follows (in mm): vHipp, AP -3.4, ML ±3.4, DV -4.0; BLA, AP –1.4, ML ±2.9, DV –4.7; MDT, AP –1.2, ML ±0.3, DV –3.0. The needle remained in place for 5 min following injection and was then slowly retracted. The scalp was closed with VetBond (3M, MN) and mice were returned to their home cage.

At 4-5 weeks of age, *Chrm1*$^{loxP/loxP}$ mice underwent a similar procedure with the following modifications. A unilateral injection of 0.8µL AAV5-CaMKIIa-ChR2-EYFP (0.1µL/min) was made

into the left vHipp (coordinates above) and a subsequent injection of 0.8µL AAV5-CaMKIIa-Cre-mCherry or AAV5-CaMKIIa-mCherry was made into the ipsilateral PFC (coordinates in mm relative to Bregma: AP, +1.9, ML -0.3, DV -2.0). All mice that underwent surgery were monitored and administered carprofen (10 mg/kg) for 48 hours post-surgery.

Electrophysiology

Extracellular field and whole-cell patch clamp recordings were performed as previously reported (*244*). Briefly, 4-5 weeks (C57BL/6J mice) or 6 weeks (*Chrm1*$^{loxP/loxP}$ mice) following surgery, mice were anesthetized with 5% isoflurane and transcardially perfused with ice-cold NMDG-HEPES artificial cerebrospinal fluid (aCSF) containing (in mM): 92 NMDG, 2.5 KCl, 1.25 NaH_2PO_4, 30 $NaHCO_3$, 20 HEPES, 25 glucose, 2 thiourea, 5 Na-ascorbate, 3 Na-pyruvate, 0.5 $CaCl_2 \cdot 2H_2O$, and 10 $MgSO_4 \cdot 7H_2O$, titrated to pH 7.3-7.4 with HCl. The brain was rapidly removed from the skull, blocked, and the brain was mounted to the cutting stage of a Vibratome (Leica VT1200S, Leica Camera, Germany). Coronal sections containing the PFC were cut at 400µm (field recordings) or 300µm (whole-cell recordings) in ice-cold NMDG-HEPES aCSF and transferred to 32^{o}C for 10-12 min. Slices containing the injection site (vHipp, BLA, MDT) were obtained to confirm efficient and accurate viral injection then discarded. Following recovery, PFC slices were transferred to a holding chamber containing artificial cerebrospinal fluid composed of (in mM): 126 NaCl, 2.5 KCl, 1.25 Na_2PO_4, 26 $NaHCO_3$, 10 glucose, 2 $CaCl_2$, 1 $MgSO_4$, supplemented with 500µM sodium ascorbate at room temperature for a minimum of 1 hour.

For recording, slices were transferred to a submerged recording chamber (Warner Instruments, CT) and continually perfused with aCSF maintained at 31±1^{o}C using an in-line heater (Warner Instruments, CT) at a rate of 2mL/min. Extracellular recording pipets were pulled from capillary tubes to a resistance of 1-3MΩ, filled with aCSF, and placed approximately 50µm beneath the surface of the slice in layer V prelimbic cortex. Paired 1ms pulses of 470nm light (50ms interpulse interval; LEDD1B, Thor Labs, NJ) were administered through a 40X immersion objective via the epillumination port of an Olympus BX51 inverted microscope to the region around

the recording electrode to activate ChR2 at a rate of 0.05Hz. For electrically-evoked fEPSPs, a concentric bipolar stimulating electrode (CBARC57, FHC Inc., ME) was placed in layer II/III between the recording electrode and the pia surface. 100μs duration electrical paired pulses (50ms interpulse interval) were administered at a rate of 0.05Hz at a stimulation intensity range of 50 to 200μA using a constant-current isolated stimulator (Digitimer Ltd., UK). Extracellular field potentials were amplified using an Axoclamp 700B amplifier, digitized with a Digitdata 1550B, and collected and recorded using Clampex 10.6 software on a PC running Windows 7. All data analysis was performed offline using Clampfit 10.6 (Molecular Devices, CA).

For whole-cell patch clamp recordings in *Chrm1*$^{loxP/loxP}$ mice, 300μm coronal slices of the PFC were obtained as above. Virally-infected pyramidal neurons in PFC layer V were targeted and confirmed by visualization of mCherry fluorescence in response to brief illumination with 545nm light. Pipets pulled to a resistance of 3-5 MΩ were filled with a K-Gluconate-based internal solution (in mm: 125 K-gluconate, 4 NaCl, 10 HEPES, 4 MgATP, 0.3 NaGTP, 10 Tris-phosphocreatine). After obtaining a >1GΩ seal, whole-cell configuration was achieved in mCherry-positive neurons and their cellular identity was confirmed by assessing spiking characteristics in response to a brief (1s) depolarizing current injection in current clamp. Optically-evoked excitatory postsynaptic currents (oEPSCs) were evoked with paired 1ms pulses of 470nm light as above to activate ChR2 at a rate of 0.1Hz. 300 ms of spontaneous EPSCs (sEPSCs) were recorded prior to the first light pulse. Access resistance, membrane resistance, and holding current were monitored throughout the recording. Cells where the access resistance changed more than 20% throughout the recording were excluded from analysis. Electrophysiology experiments were performed in male and female mice and no significant sex differences were observed so the data were combined.

Image Acquisition and Immunofluorescence

Epifluorescence images of the injection sites (vHipp, BLA, or MDT) and terminal expression in corresponding slices of the medial PFC were acquired on an Olympus BX51

inverted microscope through a 10X lens. Slices were briefly illuminated with 470nm light through the epillumination port and images were acquired with a Cool Snap HQ2 camera (Photometrics, AZ) and Lambda 10–2 shutter (Sutter Instruments, CA) controlled by Metamorph 10.4 software (Molecular Devices, CA).

5-6 weeks post-injection, *Chrm1*$^{loxP/loxP}$ mice were anesthetized with 5% isoflurane, transcardially perfused with ice-cold phosphate-buffered saline (PBS) supplemented with 2g/L glucose followed by 4% paraformaldehyde (PFA) in PBS. Brains were dissected and post-fixed for 24hrs in 4% PFA at 4^{o}C then transferred to increasing concentrations of sucrose-containing PBS (10, 20, then 30% sucrose *w/v*) and then rapidly frozen in chilled (-50^{o}C) 2-methylbutane and stored at -80^{o}C until sectioning. 40µm sections of the PFC and vHipp were cut using a freezing microtome and stored in cryoprotective buffer until staining. Free-floating sections were blocked with 5% normal donkey serum and 0.1% Triton X-100, then incubated overnight at 4^{o}C with a goat anti-RFP (1:1000 in blocking buffer, Cat. No. 43590, Cell Signaling Technology, MA) and chicken anti-GFP (1:2000 in blocking buffer, Cat. No. ab13970, Abcam, UK) primary antibody mixture. Sections were washed, incubated with appropriate secondary antibodies (donkey anti-goat conjugated to Cy3 and donkey anti-chicken conjugated to Alexa488, Jackson ImmunoResearch Laboratories, PA), then incubated with the far-red DNA dye DRAQ5 (Cell Signaling Technology) and mounted on slides using ProlongGold (Thermo Fisher Scientific, MA). Images were obtained at 10X using a confocal microscope (Leica LSM520).

Behavior – Cued and Context Fear Conditioning and Extinction

8-10 week-old C57BL/6J mice underwent classical Pavlovian fear conditioning after at least 1 week of acclimation to the housing facility. An initial cohort of female mice did not acquire sufficient contextual fear conditioning to study extinction so male mice were used for all behavioral studies. Mice were handled and injected with 0.9% saline for at least 2 days prior to fear conditioning to minimize handling and injection stress. The percent of time spent freezing was

used as a measure of learned fear and was analyzed using VideoFreeze software (Med Associates, St. Albans, VT).

On day 1, mice were transported to the conditioning room where the house lights were on and allowed to habituate for 1 hour. Mice were individually placed into “context A”, which was a brightly lit conditioning chamber (Med Associates), with a shock grid floor, no wall coverings, scented with 1mL of 10% vanilla extract, and cleaned with 70% ethanol. Following a 2 min baseline period, mice were administered 5 tone-shock pairings that consisted of a 30s tone (90dB, 5000Hz) that co-terminated with a mild foot-shock (0.7mA, 1s duration). Tone-shock pairings were separated by 30 seconds. On day 2, mice were transported to the conditioning room and allowed to habituate for 1 hour with the house lights off and a red light on to illuminate the room. 30 min prior to being placed in the conditioning chamber, mice were injected with vehicle (20% β-cyclodextrin in sterile water), 3, 10, or 30 mg/kg VU0255035 (formulated at 0.01mL/g body weight; administered *intraperitoneally*). These doses were selected based on previous pharmacokinetic studies with VU0255035 and the top dose of 30mg/kg is predicted to have good brain exposure but below full occupancy of the M_1 receptor (*513*). Mice were then placed in “context B” which was a dark conditioning chamber (infrared light used for video monitoring) with a hard white plastic sheet placed over the grid floor, two hard black plastic sheets forming a tent covering the chamber walls, scented with 1mL 10% almond extract, and cleaned with 10% MB-10 solution. Baseline freezing was assessed for 1 min and then a series of 12 30s tones were played, separated by 5s. On day 3, mice were placed back in context B, baseline freezing was assessed for 1 min and then 9 tones were played to assess the consolidation and recall of auditory fear extinction. On day 4, mice were transported to the conditioning room in the same manner as day 1. 30 min prior to being placed in the context A conditioning chamber, mice were injected with vehicle, 3, 10, or 30 mg/kg VU0255035. The doses were randomized so that a single mouse did not receive the same dose as on day 2. Mice were then placed in context A for 12 min. On day 5, mice were placed back in context A for 3 min to assess the consolidation and recall of contextual fear extinction.

For auditory cued fear conditioning, freezing on days 1, 2, and 3 were measured during the baseline periods and then during each 30s tone. For days 2 and 3, freezing for 3 tones blocks were averaged together. Mice were excluded from cued extinction analysis if baseline freezing to context B was greater than 30%. For contextual fear conditioning, freezing on days 1, 4, and 5 were measured during the baseline period (day 1), during each tone (day 1), and then in 3 min bins (days 4 and 5).

Behavior – Stress-enhanced fear learning and contextual fear extinction

8-10 week-old C57BL/6J mice were exposed to stress-enhanced fear learning (SEFL) conditioning after at least 1 week of acclimation to the housing facility. For SEFL conditioning on day 1, 4 mice were placed in each conditioning chamber context A (as above) and administered 10 random foot-shocks (0.7mA, 1s duration) over 1 hour. For controls, 4 mice were placed in context A for 1 hour with no shocks delivered. On day 2, mice were transported to the conditioning room and allowed to habituate for 1 hour with the house lights off and a red light on to illuminate the room. Individual mice were then placed in context B (as above, but no hard white plastic sheet over floor grid) and after 2 min of baseline activity, were administered 2 tone-shock pairings. On day 3, mice were transported as on day 2 and SEFL mice were administered either vehicle (20% β-cyclodextrin) or 10 mg/kg of VU0453595 (formulated at 0.01mL/g body weight; administered *intraperitoneally*). 10 mg/kg VU0453595 was used as it has previously been determined to reach unbound concentrations in the brain approaching the *in vitro* PAM EC_{50} and has been shown to have behavioral efficacy in multiple paradigms (*244*). Mice were then placed in context B for 15 min to undergo contextual fear extinction. On day 4 mice were placed back in context B for 3 min to assess the consolidation and recall of extinction.

Compounds

Oxotremorine-M was obtained from Tocris Bioscience (MN) and a stock solution was prepared in diH_2O. VU0255035, VU0364572, and VU0453595 were synthesized in-house. For electrophysiology experiments, stock solutions were prepared in DMSO and diluted in aCSF to a

final concentration (≤ 0.1% DMSO). VU0255035 was used for electrophysiology experiments at 10μM, a concentration that is predicted to fully inhibit M_1 in brain slices (*244*, *421*, *513*) and has been shown to be selective for M_1 while having no effect on responses that are mediated by activation of other mAChR subtypes, including M_4, M_5, and presumed M_2/M_3 mediated responses (*518*, *519*).

Data Analysis

The number of mice in each experiment is denoted by "N" and the cells or slices by "n". Data are presented as mean ± standard error of the mean (SEM). Statistical analyses were performed using GraphPad Prism (La Jolla, CA). A paired or unpaired two-tailed Student's t-test, one/two-way ANOVA, or repeated measures two-way ANOVA with Bonferroni's post-test were used where appropriate. Results of statistical analyses are presented in the figure legends.

3.4 Results

Muscarinic LTD in the PFC is Input-Specific

Our lab and others previously reported that the cholinergic agonist carbachol induces LTD of extracellular field excitatory postsynaptic potentials (fEPSPs) recorded in layer V in response to electrical stimulation of layer II/III in PL PFC slices (*243*, *244*). We first confirmed that this LTD is induced by the mAChR-selective agonist oxotremorine-M (OxoM) (*520*) in acute slices of the mouse PFC. Bath application of OxoM (10μM) induced a robust LTD of electrically-evoked fEPSPs measured after drug washout (Figure 11 A, E, Page 73), consistent with our previous carbachol data and confirming that LTD in the PFC can be induced by a more selective mAChR agonist.

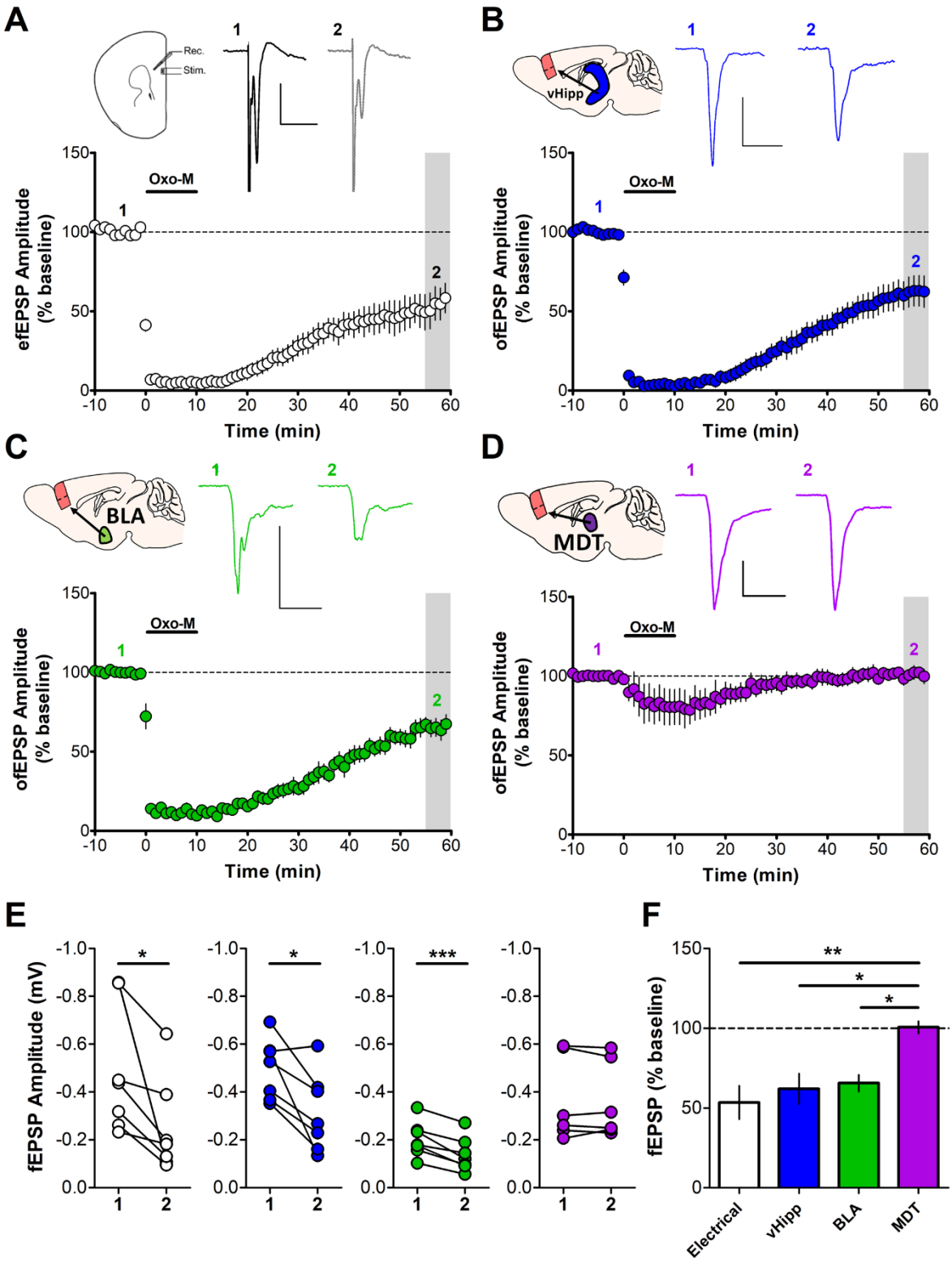
A
Rec.
Stim.
1
2
Oxo-M
efEPSP Amplitude (% baseline)
Time (min)
B
vHipp
ofEPSP Amplitude (% baseline)
C
BLA
D
MDT
E
fEPSP Amplitude (mV)
F
fEPSP (% baseline)
Electrical
vHipp
BLA
MDT

Figure 11: Muscarinic LTD in the PFC is input-specific. Acute slices of the mouse PFC were prepared 4 weeks after AAV-CaMKIIa-ChR2-eYFP was injected into the vHipp (blue), BLA (green) or MDT (purple). **(A)** Electrical stimulation of PL layer II/III evoked field excitatory postsynaptic potentials (efEPSPs) recorded in layer V (inset, sample traces). Application of 10μM OxoM induces an acute depression followed by LTD of efEPSPs measured 55-59 min post-drug add. (53.49 ± 10.47%; n = 7) **(B)** Optical stimulation of afferents from vHipp-ChR2 injected mice with paired pulses of 470nm blue light (1ms pulse duration; 50ms interpulse interval) elicited ofEPSPs that also underwent induction of LTD following bath application of OxoM (10μM). (62.01 ± 9.50%; n = 7) **(C)** ofEPSPs evoked from stimulation of BLA-ChR2 afferents were also sensitive to OxoM (10μM) and expressed LTD. (65.61 ± 5.28%; n = 7) **(D)** ofEPSPs evoked in MDT-ChR2 mice exhibited a small acute depression in the presence of OxoM (10μM) but rapidly returned to baseline, not expressing LTD. (100.6 ± 3.72%; n = 6). Sample traces for A-D correspond to baseline (1) and grey shaded area (2). Scale bars: 0.2mV and 20ms. **(E)** Summary data of change in fEPSP amplitude for each input; 1 = baseline amplitude, 2 = amplitude at 55-59min post-drug add corresponding to the grey shaded regions in A-D. Paired student's t-test: Electrical, vHipp *$p < 0.05$, BLA ***$p < 0.001$, MDT $p = 0.778$. **(F)** Summary data of fEPSP amplitude corresponding to grey shaded regions expressed as a percent of baseline compared across inputs. One-way ANOVA: $F_{3,23} = 6.228$, $p = 0.003$. Bonferroni's post-test: Electrical vs. MDT: ** $p < 0.01$, vHipp vs MDT and BLA vs MDT: * $p < 0.05$, Electrical vs. vHipp: $p > 0.05$; Electrical vs. BLA: $p > 0.05$; BLA vs. vHipp: $p > 0.05$. Sean P Moran contributed some efEPSP data to this figure.

We then determined whether OxoM would induce LTD at distinct subcortical inputs to the PFC. We used an optogenetic approach whereby we injected mice with virus encoding the expression of eYFP-tagged channelrhodopsin-2 (ChR2) into the afferent region of interest and prepared acute PFC slices 3-4 weeks later. Corroborating previous reports (*43*), we detected terminals from the vHipp, BLA, and the MDT throughout the PFC (Figure 12, Page 76). After establishing a stable baseline of optically-evoked fEPSPs (ofEPSPs), bath application of OxoM (10μM) induced LTD of vHipp-evoked ofEPSPs (Figure 11 B, E, Page 73) and BLA-evoked ofEPSPs (Figure 11 C, E, Page 73) but not of MDT-evoked ofEPSPs (Figure 11 D, E, Page 73). The LTD of electrically-evoked fEPSPs and vHipp- and BLA-evoked ofEPSPs were of similar magnitude but were all significantly different from the MDT input (Figure 1F, Page 73). Together, these data suggest that mAChR LTD of glutamatergic transmission in the PFC exhibits input specificity, and is observed at specific inputs from the BLA and vHipp.

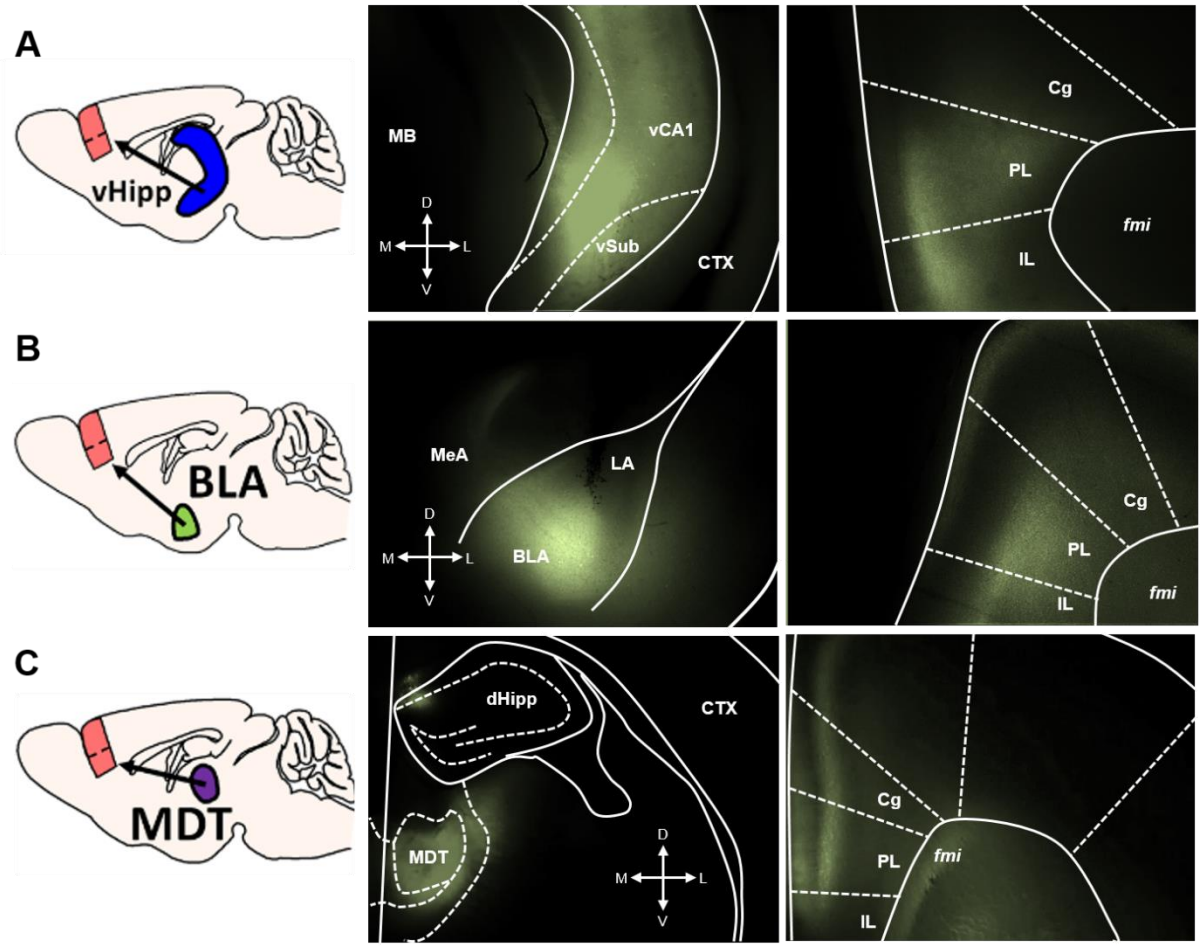

Figure 12: Viral injection sites and terminal expression of eYFP-tagged ChR2 in prefrontal cortex (PFC) slices**. (A)** Left, cartoon of ventral hippocampus (vHipp) projecting to PFC. Middle, eYFP expression in ventral CA1 and subiculum. Right, corresponding vHipp terminals detected throughout the PFC. **(B)** Left, cartoon of basolateral amygdala (BLA) projecting to PFC. Middle, eYFP expression in the BLA. Right, corresponding eYFP BLA terminals in the PFC. **(C)** Left, cartoon of mediodorsal nucleus of the thalamus (MDT) projecting to PFC. Middle, eYFP expression in the MDT. Right, eYFP MDT terminals expressed throughout the PFC. MB = midbrain, vCA1 = ventral CA1, vSub = ventral subiculum, CTX = cortex, Cg = cingulate cortex, PL = prelimbic cortex, IL = infralimbic cortex, fmi = forceps minor of the corpus callosum, MeA = medial nucleus of the amygdala, LA = lateral amygdala, dHipp = dorsal hippocampus.

Input-Specific mAChR LTD is mediated by M_1 Receptors

Next, we assessed whether M_1 mediates mAChR LTD at vHipp-PFC and BLA-PFC synapses. Consistent with prior studies using electrical stimulation (*244*), OxoM-induced LTD at the vHipp input was blocked in the constant presence of the M_1 antagonist VU0255035 (10µM), at a concentration selective for M_1 over other mAChR subtypes (*244*, *513*, *518*, *519*) (Figure 13, A,C, Page 77). Furthermore, we found that bath application of the selective M_1 allosteric agonist

VU0364572 (*512*) (30μM) was sufficient to induce LTD at the vHipp-PFC synapse (Figure 13, B, C). Similarly, BLA-PFC mAChR LTD was significantly attenuated by VU0255035 (Figure 13, D, F) and was induced by the allosteric agonist VU0364572 (Figure 13 E, F). This is consistent with the role of M_1 in mediating mAChR LTD of electrically-evoked fEPSPs and confirms that M_1 is the subtype mediating mAChR LTD at inputs from the vHipp and BLA to the PFC.

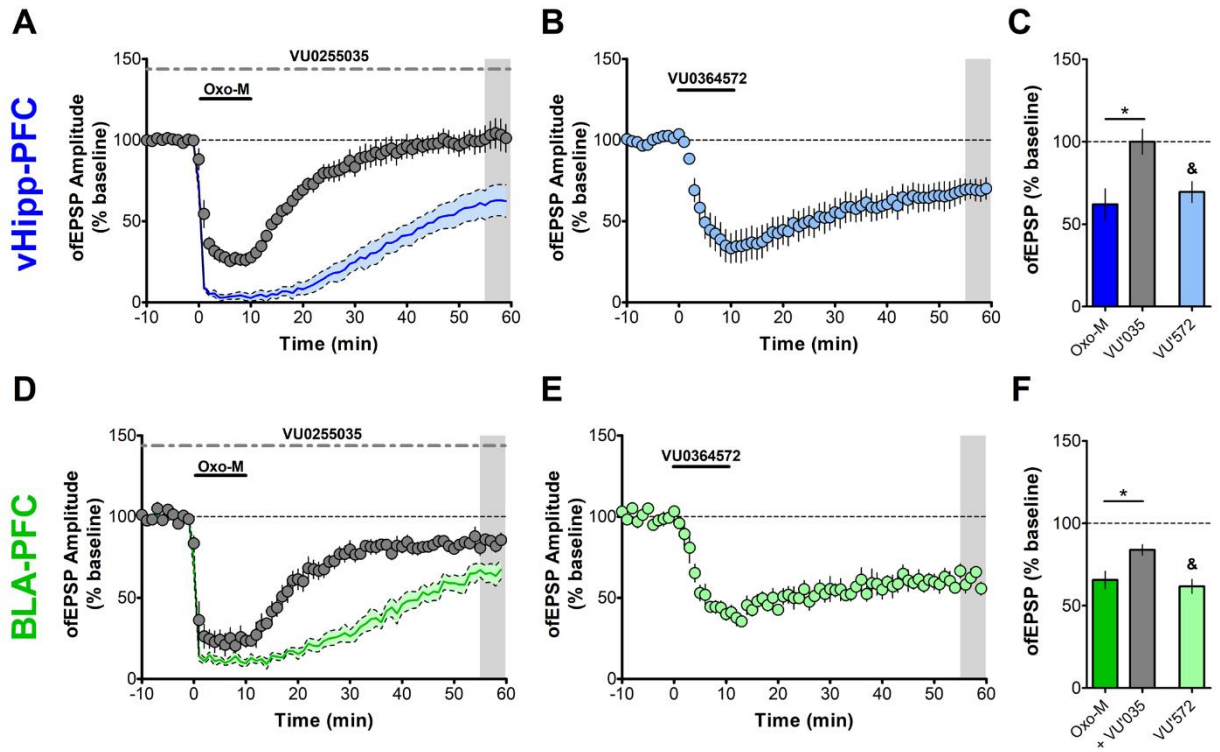

Figure 13: Input-Specific mAChR LTD is mediated by M_1 Receptors. Recordings from vHipp-ChR2 or BLA-ChR2 injected mice. **(A)** In the constant presence of the selective M_1 antagonist VU0255035 (VU'035, 10μM), OxoM (10μM) induced an acute depression of ofEPSPs PL layer V evoked from vHipp afferents but mAChR LTD was blocked. (99.96 ± 7.67%; n = 5). **(B)** Bath application of the selective M_1 allosteric agonist VU0364572 (VU'572, 30μM) for 10 min also induces LTD of ofEPSPs elicited from vHipp afferent stimulation (69.48 ± 6.38%; n = 5). **(C)** Summary data for vHipp ofEPSP amplitude 55-59 min post-drug add. Unpaired student's t-test, OxoM vs. OxoM + VU'035: * $p < 0.05$; paired student's t-test comparing baseline to shaded area in B: &, $p < 0.05$. **(D)** LTD of ofEPSPs evoked from BLA-ChR2 expressing afferents in response to OxoM (10μM) was also blocked in the constant presence of VU'035 (83.86 ± 3.34%; n = 6). **(E)** Bath application of VU'572 for 10 minutes also induces LTD of ofEPSPs elicited from BLA afferent stimulation (61.71 ± 4.24%; n = 5). **(F)** Summary data for BLA ofEPSP amplitude 55-59 min post-drug add. Unpaired student's t-test, OxoM vs. OxoM + VU'035: * $p < 0.05$; paired student's t-test comparing baseline to shaded area in E: &, $p < 0.05$. Shaded time courses in A and D correspond to OxoM alone from Fig 1. Solid colored line represents mean ofEPSP amplitude and grey shaded region around line is ± SEM.

vHipp-PFC mAChR LTD Requires Postsynaptic M_1 Receptors

Previously, we reported that mAChR LTD of electrically-evoked fEPSPs correlated with increased inhibition onto layer V pyramidal neurons and that this may contribute to M_1 LTD (*246*). As M_1 is expressed on both PFC glutamatergic pyramidal neurons and GABAergic interneurons (*419*, *521*, *522*), this brings into question the localization of M_1 involved in M_1 LTD. To address this, we used a viral-mediated knockdown approach allowing for selective deletion of M_1 receptors from glutamatergic pyramidal neurons in the PFC. 5-6 weeks post-injection, we prepared slices to confirm viral expression and observed cell bodies labelled with mCherry and terminals positive for eYFP throughout the PFC (Figure 14).

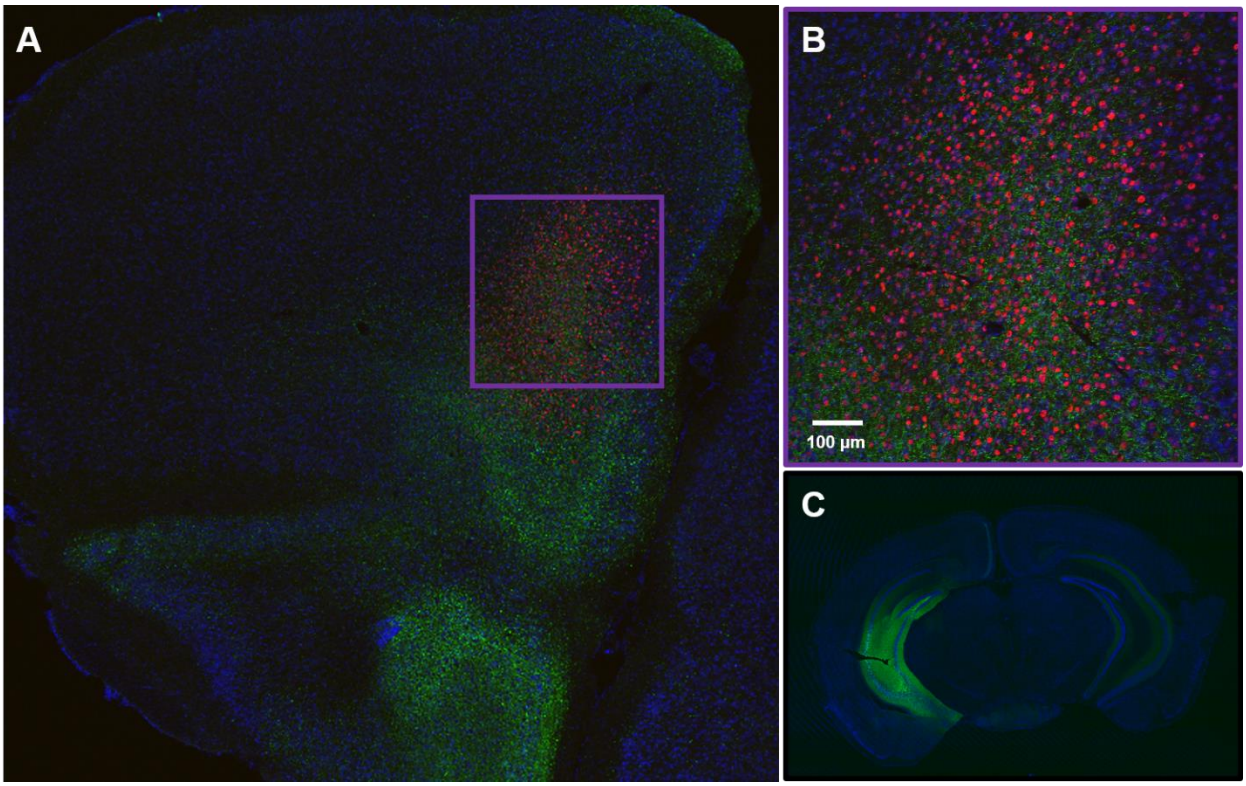

Figure 14: Viral injection sites and expression of mCherry-positive cell bodies and eYFP-positive terminals from the vHipp in the medial PFC of Chrm1$^{loxP/loxP}$ mice. Representative confocal images of vHipp and medial PFC slices 5-6 weeks post-viral injection. **(A)** eYFP-positive terminals from the vHipp are detected throughout the medial PFC and mCherry-positive cell bodies of neurons infected with AAV-Cre-mCherry are detected in the prelimbic region of the medial PFC. **(B)** Image containing the prelimbic cortex corresponding to the purple box in A. **(C)** Robust eYFP-staining is observed unilaterally in the CA1 and subiculum regions of the vHipp. Blue = DRAQ5-stained nuclei, Red = mCherry, Green = eYFP.

Using whole-cell electrophysiology in acute slices, we confirmed the genetic deletion of M_1 by monitoring the depolarizing inward current induced by a cholinergic agonist, previously shown to be dependent on postsynaptic M_1 receptors (*421*). In mCherry-positive neurons from CaMKIIα-mCherry infected mice, OxoM (10 μM) induced a depolarizing inward current while in mCherry-positive neurons from CaMKIIα-Cre-mCherry infected mice, OxoM did not cause any change in the holding current (Figure 15 B, Page 80). OxoM caused a significant increase in the frequency of spontaneous excitatory postsynaptic currents (sEPSCs) during OxoM add that returned to baseline levels upon washout (Fig 15 C, Page 80) in control-infected cells. In Cre-infected cells, the OxoM-induced increase in sEPSC frequency was abolished and, interestingly, we observed a significant decrease in sEPSC frequency that persisted following drug washout (Figure 15 D, Page 80) which might be due to activation of other, inhibitory mAChRs (*431*). These data functionally confirm deletion of M_1 from PFC pyramidal cells, validating our genetic approach.

Having confirmed deletion of M_1 from pyramidal cells, we then determined whether postsynaptic M_1 receptors were required for mAChR LTD at the vHipp-PFC synapse. We selected the vHipp-PFC input based on the complete blockade of LTD by the M_1 antagonist (Figure 13 A, Page 77) compared to the significant but incomplete block of BLA-PFC LTD (Figure 13 D, Page 77). Furthermore, to control for the effects of incomplete viral infection on extracellular field recordings (Figure 16, Page 81), we used whole-cell patch clamp recordings to measure optically-evoked EPSCs (oEPSCs) from vHipp terminals. In mice infected with control virus, OxoM (10 μM) induced an LTD of oEPSCs (Figure 15 E, G, Page 80). Compared to controls, LTD induced by OxoM in mice infected with Cre virus was significantly attenuated (Figure 15 F, H, I, Page 80). These data indicate that postsynaptic M_1 mediates mAChR LTD at vHipp-PFC synapses.

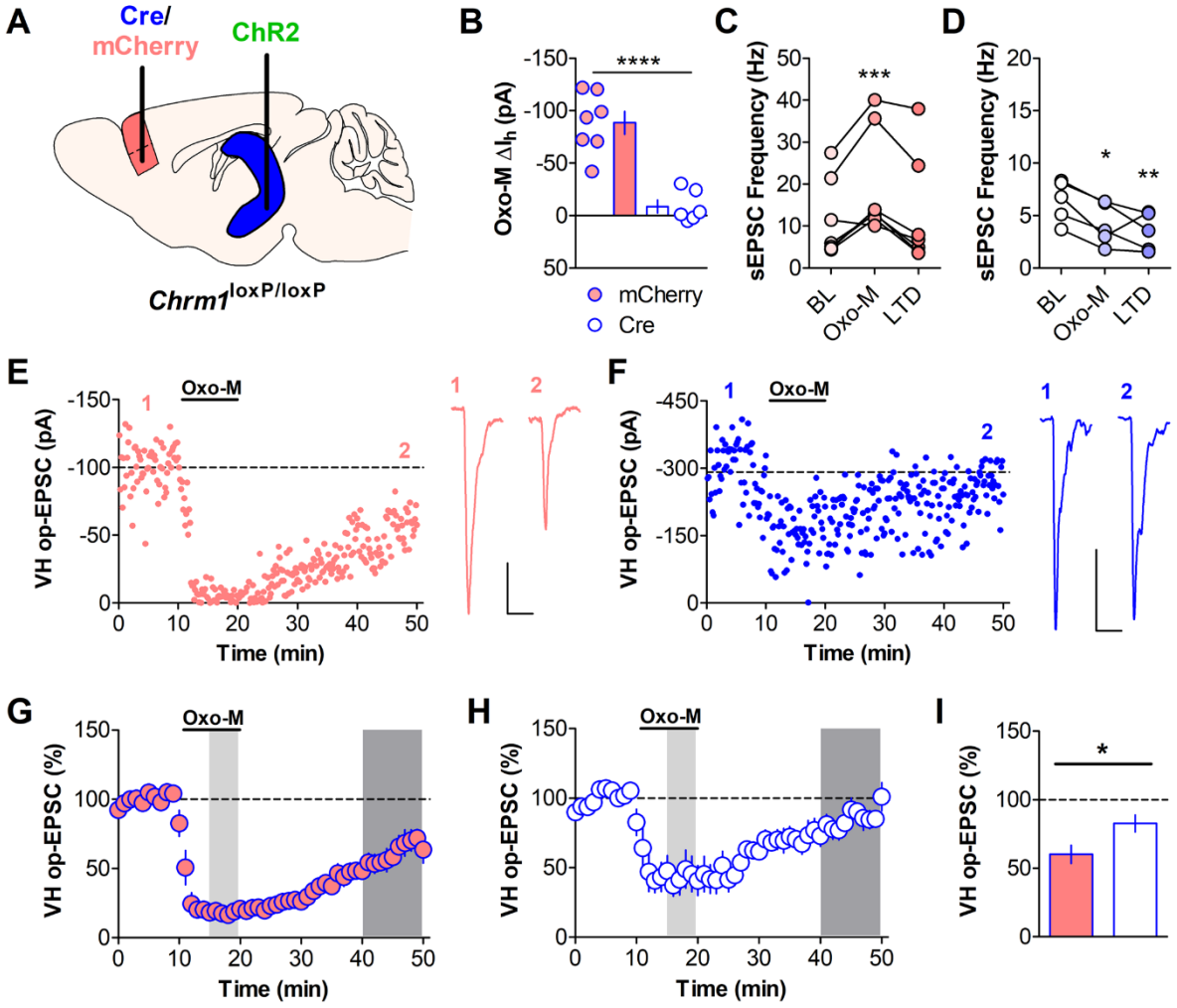

Figure 15: vHipp-PFC mAChR LTD requires postsynaptic M_1 receptors. **(A)** Chrm1$^{loxP/loxP}$ mice were injected with AAV-CaMKIIa-Cre-mCherry (white with blue outline throughout) or AAV-CaMKIIa-mCherry (red with blue outline throughout) into the PFC and co-injected with AAV-CaMKIIa-ChR2-eYFP into the vHipp. Recordings were performed 5-6 weeks post-injection. **(B)** OxoM (10μM) induced an inward current in neurons from control mCherry-infected mice (-88.55 ± 10.92 pA; n = 7) but failed to elicit an inward current in neurons from Cre-mCherry infected mice (-8.651 ± 6.06 pA; n = 6). (Student's t-test, mCherry vs. Cre **** $p < 0.0001$). **(C)** OxoM (10μM) induced a significant increase in sEPSC frequency recorded before optical stimulation in mCherry neurons. (One-way repeated measures ANOVA**,** $F_{2,6} = 13.52$, $p < 0.001$, Bonferroni's post-test *** $p < 0.001$ baseline (BL) vs OxoM, n = 7). **(D)** Conversely, OxoM induced a significant decrease in sEPSC frequency in Cre-mCherry neurons. (One-way repeated measures ANOVA, $F_{2,4} = 11.49$, $p < 0.01$, Bonferroni's post-test * $p < 0.05$ BL vs OxoM, ** $p < 0.01$ BL vs LTD, n = 5). **(E)** A representative experiment for an mCherry-infected neuron (scale bar: 25pA and 25ms) and **(F)** a Cre-infected neuron (scale bar: 100pA and 25ms). **(G)** Summary time course for control mCherry mAChR LTD experiments. Bath application of OxoM (10μM) induced a long-term depression of oEPSCs evoked from vHipp-ChR2 terminals in mCherry-infected neurons (60.15 ± 6.67%; n = 7). **(H)** Summary time course for Cre LTD experiments. LTD of oEPSCs was attenuated in Cre-mCherry infected neurons (82.66 ± 6.13%; n = 6). In both G and H, light shaded areas correspond to the time at which Oxo-M sEPSC measurements were taken for C and D. Dark shaded areas correspond to the time at which LTD sEPSC measurements were taken for C and D and for quantification in I. **(I)** Summary data for oEPSC amplitude 40-49 min post-OxoM add. Unpaired student's t-test, * $p < 0.05$. Max E Joffe contributed to this figure.

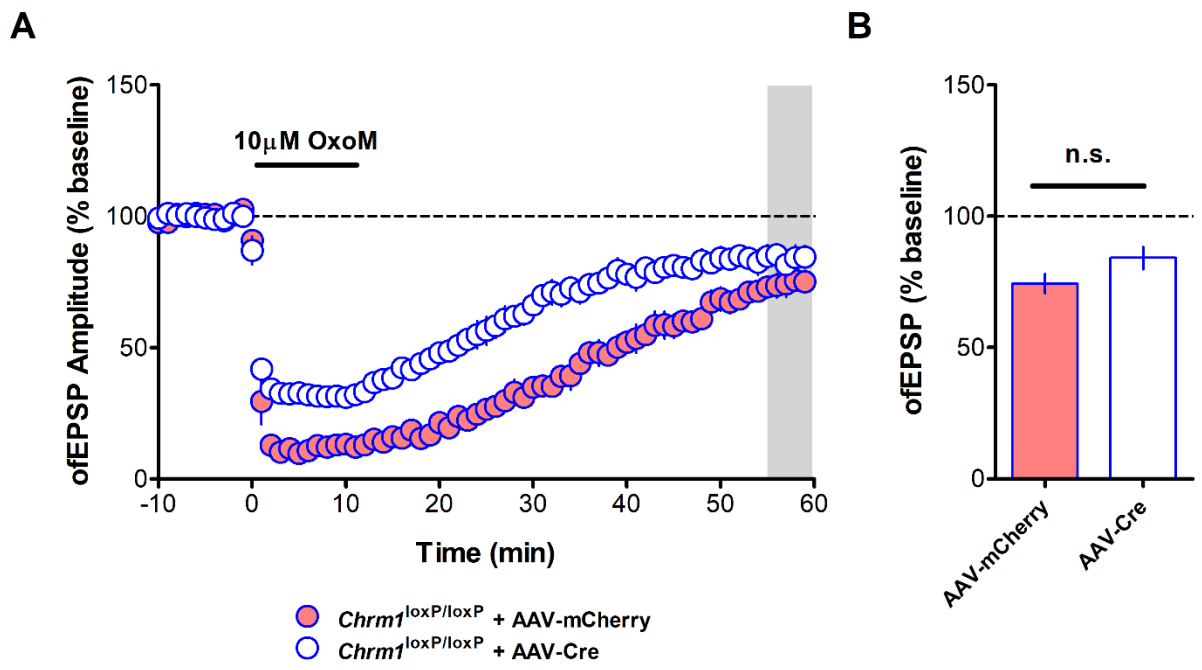

Figure 16: Incomplete effect of viral-mediated knockdown on muscarinic long-term depression measured using extracellular field recordings in Chrm1$^{loxP/loxP}$ mice. **(A)** Time courses of optically-evoked field excitatory postsynaptic potentials (ofEPSPs) measured in slices from mCherry- or Cre-injected Chrm1$^{loxP/loxP}$ mice. The recording electrode was placed in layer V in an area of high mCherry-expression in the prelimbic PFC and brief pulses of 470nm light were used to activate ChR2 in vHipp terminals. Bath application of 10μM OxoM induces a long-term depression of ofEPSPs in both control mCherry- (n = 6) and Cre-infected (n = 6) slices. **(B)** Summary data of the ofEPSP amplitude in the grey shaded region in (A) relative to baseline. Student's t-test, $p > 0.05$.

M_1 Receptor Function is Necessary for Contextual but not Cued Fear Extinction

Together, these data demonstrate that M_1 is poised to regulate synaptic transmission at two long-range inputs to the PFC. Given the established role of mAChRs and inputs from the BLA and vHipp in extinction of fear conditioning, we hypothesized that the *in vivo* relevance of this input-specific modulation may relate to fear extinction. We implemented a five-day fear conditioning protocol to assess the effects of M_1 antagonism on both auditory cued and contextual fear extinction (Figure 17 A, Page 83). Mice were conditioned on day 1. During cued extinction on day 2 and context extinction on day 4, mice were administered vehicle (20% β-cyclodextrin) or 3, 10, or 30 mg/kg VU0255035 *i.p.* 30 minutes prior to being placed into the extinction context. There was no significant effect of M_1 antagonism within the cued fear extinction session nor on

cued extinction recall on day 3 (Figure 17 B, Page 83). Interestingly, there was a significant effect of M_1 antagonism on within-session contextual fear extinction and mice administered 30 mg/kg VU0255035 prior to contextual fear extinction on day 4 displayed significantly higher freezing to the context on recall day 5 compared to vehicle-treated mice (Figure 17 C, Page 83). Importantly, the maximal dose of 30 mg/kg VU0255035 did not affect freezing in animals that were not exposed to foot-shocks on day 1 (Figure 18, Page 84). Overall, these data suggest that M_1 activation is not required for auditory cued fear extinction but is required for contextual fear extinction.

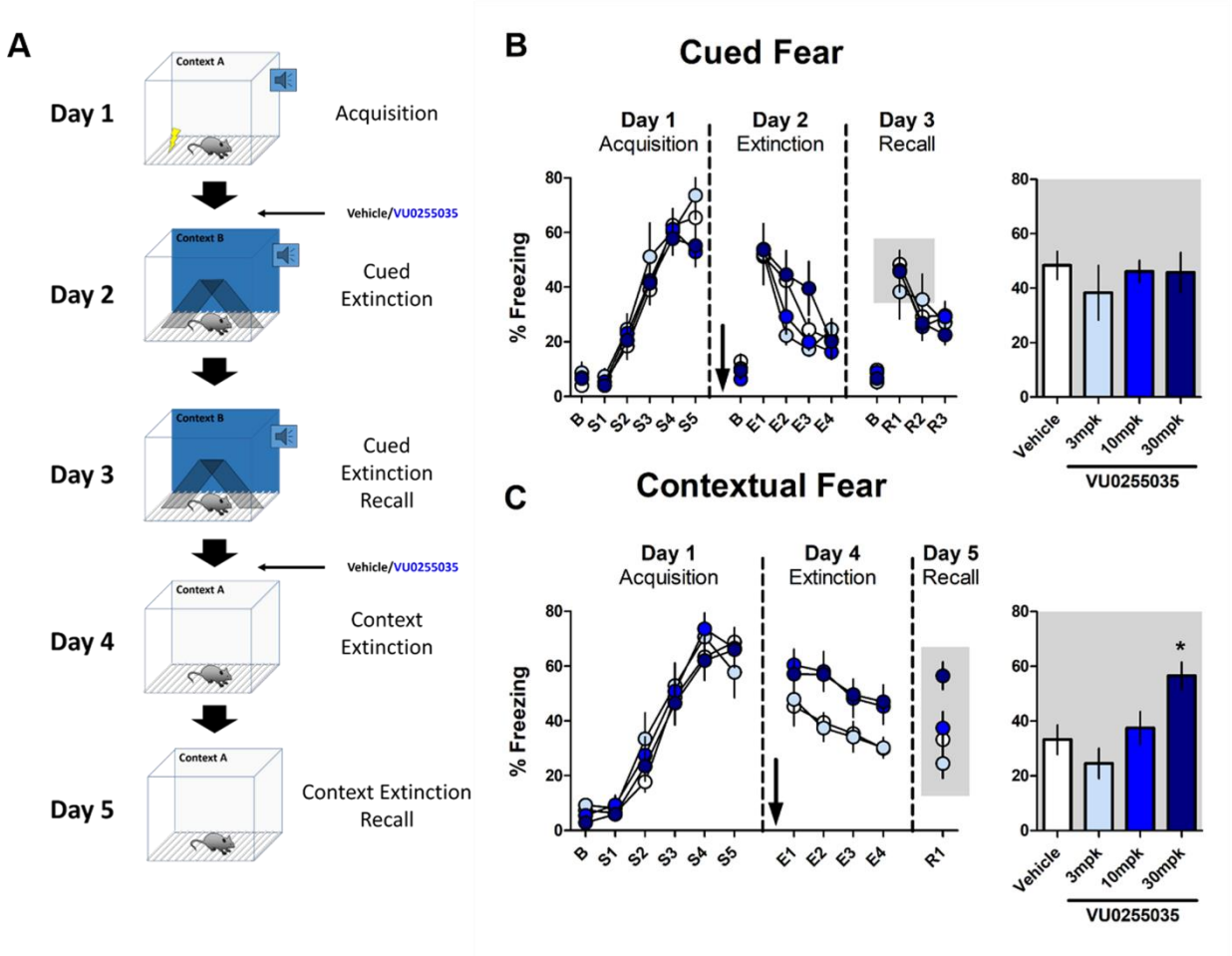

Figure 17: M_1 receptor function is necessary for contextual but not cued fear extinction. Effect of systemic M_1 antagonism on cued and contextual fear extinction in mice. **(A)** Schematic depicting the training and testing procedure used. Mice were conditioned in Context A with 5 mild footshocks, each preceded by a 30s tone. On day 2, mice were administered the M_1 antagonist VU0255035 (3, 10, 30 mpk, i.p.) or vehicle (20% β-cyclodextrin) 30 minutes before being exposed to a series of 12 tones in a novel Context B to assess extinction of auditory cued fear. On day 3, mice were placed back in Context B and exposed to 9 tones to assess consolidation of cued fear extinction. On day 4, mice were again administered VU0255035 or vehicle and placed in Context A for 12 minutes to assess contextual fear extinction. On day 5, mice were placed back in Context A for 3 minutes to assess contextual fear extinction consolidation. **(B)** At all doses VU0255035 had no effect on auditory cued fear extinction on extinction day 2 (two-way repeated-measures ANOVA, Effect of drug: $F_{3,35} = 0.960$, $p = 0.423$; Effect of tone block: $F_{3,35} = 36.00$, $p < 0.0001$; Interaction, $F_{9,35} = 1.787$, $p = 0.079$) or on recall day 3 (one-way ANOVA, $F_{3,35} = 0.350$, $p = 0.789$). Data for days 2 and 3 are binned by 3 tones and mice were excluded from analysis if baseline freezing was >30%. Bar graph depicts average % freezing to the first three tones on recall day 3, corresponding to the grey shaded box. (N, Veh = 13, 3 mpk = 5, 10 mpk = 12, 30 mpk = 9) **(C)** Systemic M_1 antagonism impairs within-session contextual fear extinction (two-way repeated-measures ANOVA, Effect of drug: $F_{3,39} = 3.663$, $p = 0.020$; Effect of time block: $F_{3,39} = 12.56$, $p < 0.0001$; Interaction: $F_{3,39} = 0.317$, $p = 0.968$) and 30 mpk VU0255035 significantly impaired contextual extinction recall on day 5 (One-way ANOVA, $F_{3,39} = 5.177$, $p < 0.01$; Bonferroni's post-test, Veh vs. 30 mpk * $p < 0.05$). Extinction on days 4 and 5 are depicted as 3 min bins. Bar graph depicts R1. (N, Veh = 14, 3 mpk = 7, 10 mpk = 11, 30 mpk = 11).

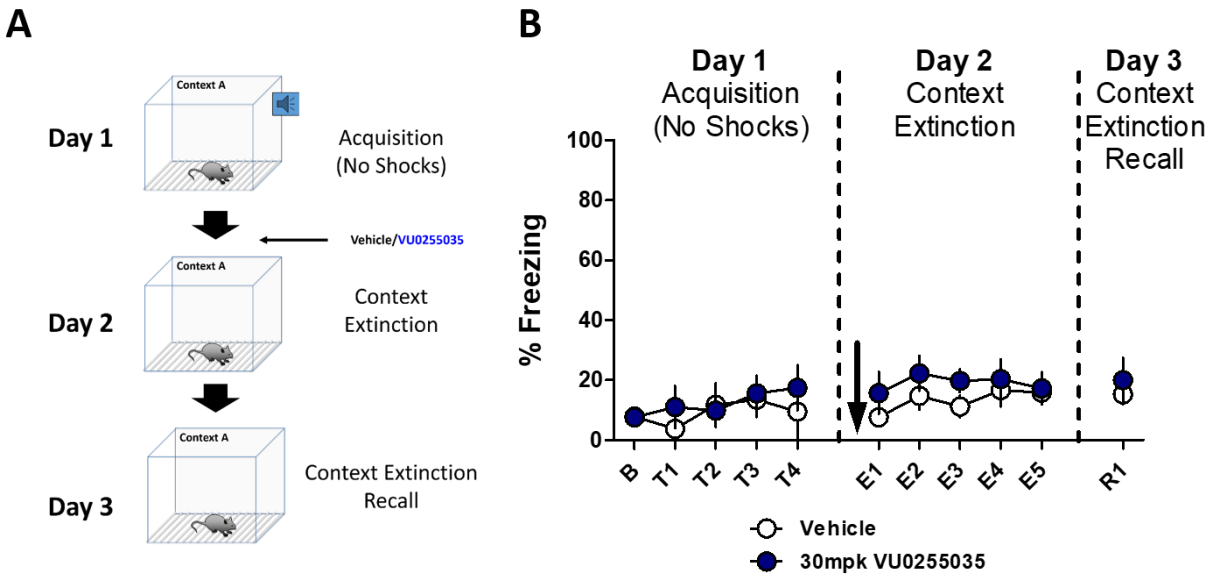

Figure 18: The M_1 antagonist VU0255035 alone does not affect freezing. **(A)** Schematic depicting the training and testing procedure used. Mice were conditioned in Context A with 5 30s tones, with no foot-shocks. On day 2, mice were administered VU0255035 (30 mpk i.p.) or vehicle (20% β-cyclodextrin) and placed in Context A for 15 minutes to assess the effects of VU0255035 on freezing behavior. On day 3, mice were placed back in Context A for 3 minutes to assess the effect of VU0255035 on freezing 24hrs after dosing. **(B)** No effect of VU0255035 was observed within session on Day 2 (Two-way repeated-measures ANOVA: Effect of drug, $F_{1,6} = 0.9034$, $p = 0.379$) or on Day 3 (Unpaired student's test, $p = 0.581$). (N, Veh = 4, 30 mpk = 4).

M_1 Potentiation Enhances Fear Extinction in a Model of PTSD

Impaired fear extinction is a hallmark of anxiety-related disorders including PTSD, estimated to affect 3.5% of the US population annually (*272*). Exposure therapy is one of the most common treatment paradigms for PTSD and shares many similarities with Pavlovian fear extinction used in rodents (*523*). Pharmacological manipulations that enhance the acquisition and/or consolidation of fear extinction therefore may be beneficial for use in conjunction with exposure therapy. Based on our findings, we hypothesized that enhancing M_1 function with a PAM may enhance contextual fear extinction in a rodent model of PTSD.

To test this, we used the extensively validated SEFL model, which produces phenotypes in rodents that mimic PTSD symptoms in the clinical population (*272*) (Figure 19 A, Page 86). On day 1, mice underwent SEFL conditioning and exhibited greater freezing during fear acquisition

in a novel context (context B) on day 2 (Fig 5B) and when exposed to context B on day 3 (Fig 5C). SEFL conditioned mice then received either vehicle (20% β-cyclodextrin) or the M_1 PAM VU0453595 (10 mg/kg) prior to contextual fear extinction in context B on day 3. Pretreatment with VU0453595 had no effect on the expression of contextual fear assessed during the first 3 minutes in context B and no effect on within-session extinction (Figure 19 D, Page 86). When mice were tested for the consolidation of extinction on day 4, PAM-treated mice froze significantly less compared to vehicle-treated mice (Figure 19 D, Page 86), indicating that VU0453595 enhanced the consolidation of contextual fear extinction in SEFL-conditioned mice.

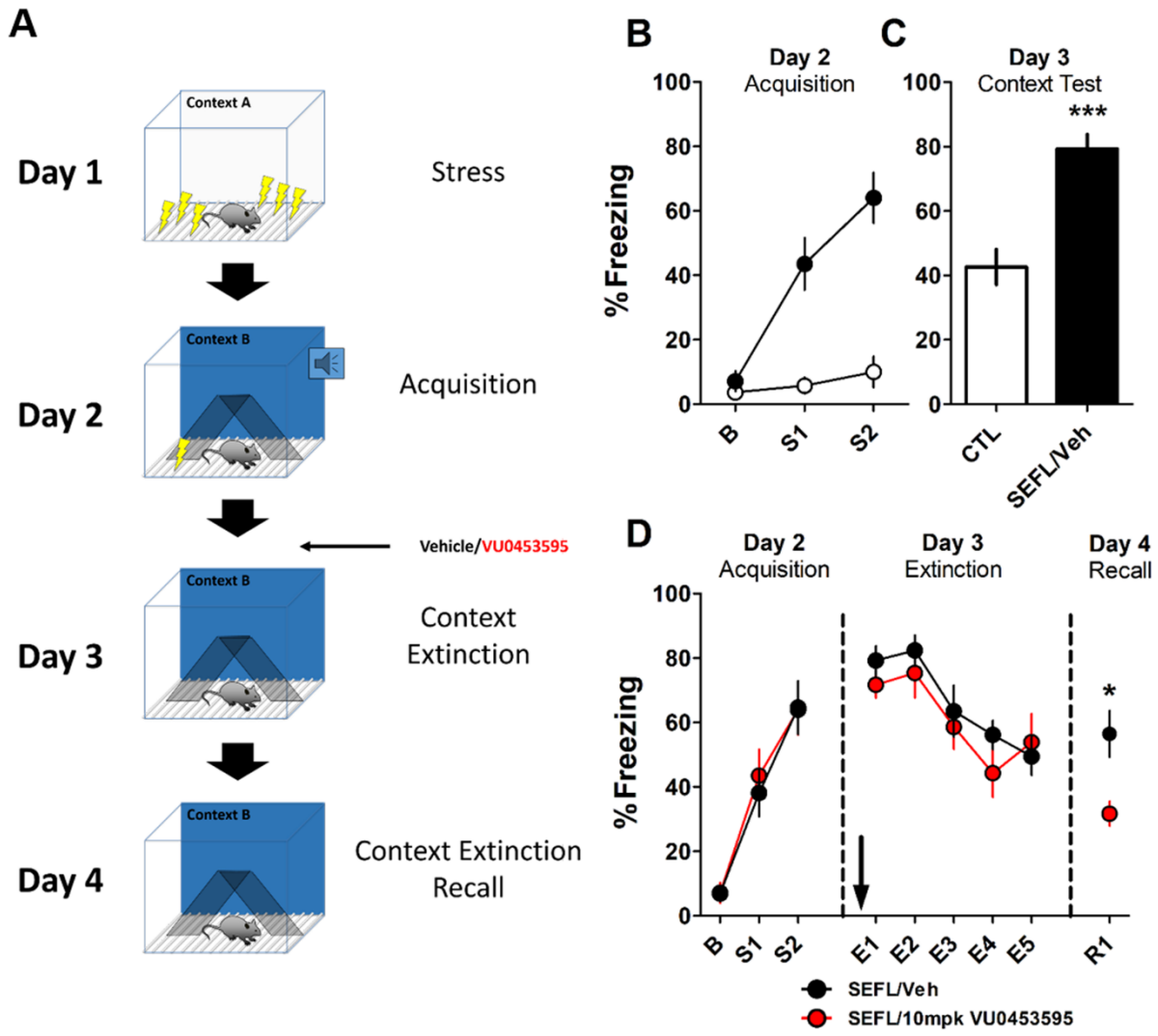

Figure 19: M_1 potentiation enhances fear extinction in a model of PTSD. **(A)** Schematic illustrating the SEFL model and experimental design. On day 1, mice underwent SEFL conditioning in Context A where they received 10 footshocks at random intervals over 1 hour. Control mice were placed in Context A for 1 hour. Days 2, 3, and 4 were performed in a novel Context B. On day 2, mice were conditioned with 2 mild footshocks in Context B. On day 3, SEFL-conditioned mice were administered vehicle (20% β-cyclodextrin) or 10 mpk VU0453595 i.p. 15 min before being placed back in Context B where they underwent a 15 min context extinction session. On day 4, mice were placed back in Context B for 3 min to assess context extinction consolidation. **(B)** Mice that received SEFL on day 1 froze significantly more on day 2 during acquisition and **(C)** on day 3. Bar graph depicts first 3 min in Context B on day 3. (Unpaired student's t-test, ***$p < 0.001$). **(D)** Administration of 10 mpk VU0453595 had no effect on within-session extinction on day 3 (Two-way repeated-measures ANOVA: Effect of Drug: $F_{1,18} = 5.033$, $p = 0.440$; Effect of time block: $F_{4,18} = 15.15$, $p < 0.0001$; Interaction: $F_{4,18} = 0.782$, $p = 0.541$) but enhanced consolidation of contextual fear extinction measured on day 4. (Unpaired student's t-test, *$p < 0.05$. N, CTL = 8, SEFL/Veh = 10).

3.5 Discussion

In the present studies, we found that mAChR activation induces LTD at synapses onto PL PFC layer V from the vHipp and BLA inputs but not from the MDT. Furthermore, we confirmed that M_1 mediates LTD at both inputs and that postsynaptic M_1 is required for LTD at the vHipp-PFC synapse. This suggests that M_1 activation modulates fear-related inputs to the PFC in an input-selective manner. Based on the roles of the vHipp, BLA, and PFC in fear extinction, we further identified M_1 as necessary for contextual fear extinction. Finally, we demonstrated that M_1 potentiation enhances fear extinction in a rodent model of PTSD, suggesting that M_1 PAMs have potential clinical utility in the treatment of PTSD and stress-related disorders.

Dysregulated connectivity of subcortical regions to the PFC is present in multiple psychiatric disorders (*524–526*). Understanding the functional consequences of this has been a major focus of psychiatric-related research and has been aided by novel circuit-based techniques including optogenetics (*527*). There have been tremendous advances in establishing the circuitry underlying specific behaviors and how these circuits might be perturbed in psychiatric disorders. However, there is a critical need to identify circuit-specific targets to translate preclinical observations into clinically effective treatments (*528*). We took advantage of these circuit-based approaches and found that activation of M_1 selectively induces LTD at the vHipp and BLA inputs to the PFC, identifying M_1 as a potential therapeutic target to modulate these circuits.

Intact communication between the hippocampus, amygdala, and PFC is essential for proper fear extinction in both humans (*529*) and rodents (*80*) and is dysregulated in anxiety-related disorders such as PTSD (*280*). In animal models, BLA and vHipp inputs to the PFC are involved in anxiety-related behaviors (*87*, *89*, *527*) and inactivation studies demonstrate that the vHipp, BLA, and PFC are all required for fear extinction (*80*) while the vHipp-PFC pathway gates fear after extinction learning (*81*). Thus, it is clear that the vHipp and BLA inputs to the PFC are important for fear extinction and may be disrupted in anxiety-disorder models.

Our observation that M_1 activation induces LTD at the vHipp-PFC and BLA-PFC synapses along with work demonstrating that PFC mAChRs are required for fear extinction (*510*) suggested that these two phenomena are related. Consistently, we found that M_1 antagonism impairs contextual fear extinction but had no effect on the extinction of auditory cued fear. Our data does not definitively identify M_1 in the PFC as the mediator of these behavioral effects due to technical limitations including that muscarinic LTD measured extracellularly was still intact in Cre-injected *Chrm1*$^{loxP/loxP}$ mice. This suggests incomplete viral knockdown of M_1 therefore testing the necessity of PFC M_1 for the observed behavioral effects remains elusive. Nonetheless, our approach identified the involvement of M_1 in fear extinction and that an M_1 PAM could enhance fear extinction in a model of PTSD, thus translating circuit-based neuroscience to a potential therapeutic mechanism.

Concerning the potential mechanism, the hippocampus communicates contextual information to the PFC via monosynaptic connections from the ventral pole (*69*). M_1 LTD at the vHipp-PFC synapse may therefore reflect a modulation of contextual information flowing into the PFC and be more related to regulation of contextual aspects of fear rather than non-spatial cued fear (*530*). This is consistent with our observation that M_1 antagonism blocks LTD at the vHipp-PFC synapse and impairs contextual fear extinction. Furthermore, single-unit recordings in PL indicate that decreased activity of PL pyramidal neurons corresponds with reduced fear responses (*81*), consistent with a reduced afferent drive into the PL via an LTD-like mechanism. M_1 LTD of vHipp-PL PFC transmission could be required to reduce fear responses during contextual fear extinction by reducing vHipp-mediated excitation of PL neurons. While we identified postsynaptic M_1 as necessary for mAChR LTD at the vHipp-PFC synapse, the molecular mechanisms mediating vHipp-PFC M_1- LTD are still unknown. Future work investigating signaling downstream of M_1 necessary for the induction, expression, and maintenance mechanisms will be instrumental to investigate how this plasticity changes after fear extinction and will identify targets and mechanisms that could improve the treatment of disorders with dysfunctional vHipp-PFC

connectivity. M_1 also enhances the output of infralimbic (IL) cortex pyramidal neurons and fear extinction correlates with enhanced activity of IL neurons (*510*, *531*) thus M_1 PAMs might enhance fear extinction via actions in the IL in addition to LTD in the PL. It is possible that both mechanisms contribute to extinction and investigating the differential involvement of M_1 in the PL and IL to fear extinction is an interesting future direction.

vHipp afferents increase feedforward inhibition (FFI), contributing to the decreased activity of PL pyramidal neurons during reduced fear responding during extinction (*81*). We found that M_1 LTD at the vHipp-PFC synapse occurs at excitatory inputs onto PL pyramidal neurons recorded under whole-cell conditions where the contribution of inhibition is negligible. Therefore, vHipp-PL LTD may occur simultaneously with enhanced vHipp-mediated FFI to synergistically reduce the activity of PL pyramidal neurons. M_1 activation enhances PFC interneuron activity (*419*) and an M_1-driven increase in FFI may also contribute to fear extinction. Our previous finding that M_1 LTD of electrically-evoked fEPSPs correlates with enhanced inhibition onto PL pyramidal neurons (*246*) may suggest this, and the contribution of muscarinic modulation of inhibition to fear extinction is an interesting future direction as our results do not rule out contributions of both enhanced FFI and M_1 LTD mechanisms to fear extinction. M_1 is expressed in pyramidal neurons in human cortex (*417*, *430*, *532*) but M_1 in GABAergic interneurons has only been demonstrated in rodent (*419*, *522*) and non-human primate (*533*) cortex. Therefore, while our results pertaining to M_1 in PFC pyramidal neurons are likely relevant to humans, the clinical implications of M_1 modulation of inhibitory transmission are unknown and would require identification of M_1 in human cortical interneurons.

Systemic and intracortical delivery of the *pan*-muscarinic antagonist scopolamine impairs the consolidation of cued fear extinction in rats (*510*). In contrast to these findings, the M_1 antagonist VU0255035 did not impair cued fear extinction in the present studies. While M_1 mAChR activation promotes cued fear consolidation (*534*), our findings suggest that M_1 is not necessary for cued fear extinction and other muscarinic subtypes may contribute to extinction of cued fear.

Our present studies provide insight into this hypothesis. M_1 antagonism or genetic deletion does not impair the acute depression of fEPSPs at vHipp/BLA-PFC synapses. This transient depression may be permissive for cued, but not contextual, fear extinction. Additionally, although the M_1 antagonist attenuated mAChR LTD at the BLA-PFC synapse, we did not observe a complete block. Other muscarinic receptors such as M_4 likely contribute to mAChR LTD at the BLA-PFC synapse and M_1-independent depression may be sufficient for cued fear extinction. The involvement of M_4 in fear extinction is an intriguing future direction given the aforementioned scopolamine effect and the relatively high expression of M_4 in the PFC.

The rodent PL PFC shares connectivity and anatomical similarities to the human dorsal anterior cingulate cortex (dACC) and thus, the LTD we observed could relate to decreased activity of the human dACC observed during fear extinction (*535*). In an fMRI study, PTSD patients exhibited dACC and amygdala hyperactivity and hippocampal hypoactivity compared to controls during a fear extinction task (*280*). Hyperactivity of the dACC and amygdala might reflect a deficit in mechanisms similar to mAChR LTD while reductions in hippocampal activity could relate to deficits in the previously described hippocampal LTD-to-LTP switch (*536*), a reduction in vHipp-mediated FFI, and/or a deficit in vHipp-PFC M_1 LTD. The aforementioned functions of M_1 suggest it could be a valid therapeutic target to rescue deficient extinction in PTSD and imply together with M_1 expression in human cortex that our findings have translational relevance to humans.

M_1 potentiation could possibly reduce dACC hyperactivity in PTSD patients via LTD of hyperactive amygdala inputs and shifting vHipp input towards inhibition via enhanced FFI and LTD of excitatory transmission. This hypothesis is consistent with our finding that the M_1 PAM VU0453595 enhances contextual fear extinction in the SEFL model. Mimicking the disrupted circuitry in PTSD, rodents exposed to stressors including SEFL exhibit hyperactivity of the PL and BLA and hypoactivity of the hippocampus (*276*), suggesting these models exhibit excellent face validity with respect to the human disorder. Treatment with an M_1 PAM before extinction enhanced the consolidation and recall of contextual fear extinction, suggesting that M_1 PAMs may be

effective therapeutics to enhance exposure therapy in the clinic. Dysfunctional connectivity between the hippocampus, amygdala, and PFC (*525*, *537*) and impaired fear extinction (*538*) are present in many psychiatric disorders therefore these results and potential translatability may be relevant to disorders other than PTSD. This is especially exciting as M_1 PAMs have entered or completed Phase I trials (see ClinicalTrials.gov Identifiers NCT03220295 and NCT02769065) with schizophrenia and Alzheimer's disease as intended therapeutic indications. Excitingly, our findings suggest that PTSD might be another promising therapeutic area for these novel drugs.

Altogether, we report that activation of M_1 induces LTD of fear-related inputs from the vHipp and BLA to the PFC. This is consistent with previous studies demonstrating mAChR LTD at hippocampal inputs to the PFC (*245*, *246*) and further identifies the BLA, but not the MDT, as another input that expresses this form of synaptic plasticity. We also show that M_1 activation is required for contextual fear extinction and that potentiating M_1 *in vivo* with a PAM enhances contextual fear extinction in the SEFL model of PTSD. Our results add M_1 LTD at the vHipp and BLA inputs to the extensively studied functions of M_1 in the PFC, however future studies are necessary to determine the role of M_1-dependent input-specific modulation in other PFC-dependent processes. Overall, these results demonstrate that M_1 is poised to regulate fear-related information processing and suggest M_1 PAMs could modulate aberrant limbic inputs to the PFC and be useful as adjunct therapeutics to facilitate exposure therapy for PTSD in the clinic.

CHAPTER IV

METABOTROPIC GLUTAMATE RECEPTOR SUBTYPE 1 POTENTIATION ENHANCES CORTICAL INHIBITION TO RESCUE SCHIZOPHRENIA-LIKE PHYSIOLOGICAL AND BEHAVIORAL DEFICITS

4.1 Abstract

Evidence for GABAergic dysfunction in the prefrontal cortex (PFC) is one of the most consistent finding in schizophrenia and may contribute to cognitive deficits. Recent preclinical and clinical studies suggest that the $mGlu_1$ subtype of metabotropic glutamate (mGlu) receptor regulates cortical inhibition; however, the effects of an $mGlu_1$ positive allosteric modulator (PAM) on PFC microcircuit function and cognition is unknown. We now report a series of electrophysiology, optogenetic, functional magnetic resonance imaging, and animal behavior studies demonstrating that activation of $mGlu_1$ increases inhibitory transmission in the PFC by selective excitation of somatostatin-expressing (SST) interneurons. Furthermore, an $mGlu_1$ PAM reverses cortical hyperactivity and concomitant cognitive deficits induced acutely by NMDA receptor antagonism. Using in vivo optogenetics, we further show that PFC SST interneurons are necessary for $mGlu_1$ PAM efficacy. Collectively, these findings suggest that $mGlu_1$ PAMs could reverse cortical GABAergic deficits and have efficacy in treating cognitive dysfunction in schizophrenia.

4.2 Introduction

While currently available antipsychotic medications reduce the positive symptoms of schizophrenia in some patients, there remains a critical unmet need for therapeutic agents to treat the negative symptoms and cognitive deficits in this debilitating neuropsychiatric disorder (*19*,

539). Chronic cognitive dysfunction strongly predicts long-term functional outcomes for patients with schizophrenia, interfering with employment and interpersonal relationships (*540*). Furthermore, while contemporary antipsychotics minimize or prevent psychosis in many patients by modulating monoaminergic systems, recent evidence suggests that these approaches may exacerbate cognitive impairments (*20*). Therefore, identifying novel therapeutic targets is necessary to develop more efficacious treatments for all symptom domains of schizophrenia.

Cognitive deficits in schizophrenia patients include impairments in working memory and attention which critically depend on the function of the dorsal lateral prefrontal cortex (dlPFC). Suggestive of cortical dysfunction, one of the most consistent pathophysiological findings in studies of postmortem brain tissue from schizophrenia patients is a reduction in glutamic acid decarboxylase 67 (GAD67) mRNA and protein in the dlPFC (*541*). GAD67 is an enzyme that produces the inhibitory neurotransmitter γ-aminobutyric acid (GABA), and multiple clinical and preclinical studies support the hypothesis that dysfunction of GABAergic inhibitory transmission plays a critical role in the pathophysiological changes underlying the cognitive deficits in schizophrenia (*393*). Thus, enhancing the function of cortical GABAergic interneurons represents a promising potential therapeutic strategy to address unmet clinical needs for schizophrenia patients.

GABAergic inhibitory interneurons in the prefrontal cortex (PFC) can be subdivided into various subclasses based on physiology, morphology, and the expression of molecular markers with the vast majority classified by the expression of either somatostatin- (SST), parvalbumin- (PV), or the serotonin receptor 3a with minimal overlap (*123*). While there has historically been a focus on fast-spiking PV interneurons in schizophrenia (*127*), recent clinical and preclinical findings have suggested a significant role of the lesser-studied SST interneurons in PFC function, working memory, and the pathophysiology of schizophrenia. Acute, optogenetic inhibition of PFC SST interneurons impairs PFC-dependent behaviors (*159*, *542*), suggesting the involvement of SST interneurons in higher-order cognitive function. Furthermore, acute administration of an N-

methyl-D-aspartate (NMDA) receptor antagonist used to model cortical inhibitory deficits (*356*) suppresses PFC SST interneuron activity and produces corresponding schizophrenia-like behavioral deficits (*543*). Multiple studies have also found reduced *SST* mRNA in postmortem brain tissue from patients with schizophrenia (*378*, *379*), specifically with working memory networks (*544*), implicating their potential dysfunction in the pathophysiology of the disease. Altogether, these findings raise the possibility that enhancing PFC SST interneuron function may be effective in rescuing GABAergic and cognitive deficits in schizophrenia, although there is currently a dearth of pharmacological targets to selectively augment SST interneuron activity.

Early studies in rodents and non-human primates revealed that the $G\alpha_{q/11}$-coupled metabotropic glutamate (mGlu) receptor subtype 1 ($mGlu_1$) is expressed in GABAergic interneurons in the prefrontal cortex (PFC) (*545*, *546*) and in the hippocampus and other cortical regions, $mGlu_1$ is highly expressed in SST interneurons (*496*, *547*). Activation of postsynaptic group I mGlu receptors, consisting of $mGlu_1$ and $mGlu_5$, can increase neuronal activity via several mechanisms (*253*, *548*), raising the possibility that $mGlu_1$ activators could enhance the output of cortical SST interneurons. Consistent with this hypothesis, group I mGlu receptor activation enhances feedforward inhibition onto glutamatergic pyramidal neurons in acute PFC slices, an effect attributed to $mGlu_1$ (*499*). The potential role of $mGlu_1$ in regulating PFC interneuron function is especially interesting in light of human genetic and subsequent functional studies revealing multiple loss-of-function mutations in the gene encoding human $mGlu_1$, *GRM1*, associated with schizophrenia (*467*, *468*, *471*). These studies suggest that reduced $mGlu_1$ signaling may contribute to disease pathology in some patients. However, the precise role of $mGlu_1$ in regulating inhibitory transmission in the PFC and the potential of selective $mGlu_1$ activators to reverse cognitive deficits in schizophrenia models have not been evaluated.

Recently, our group and others have discovered highly selective $mGlu_1$ positive allosteric modulators (PAMs) that bind to and act at distinct, less-conserved allosteric sites (*471*, *474*, *475*). Furthermore, we recently reported that the $mGlu_1$ PAM VU6004909 achieves high brain exposure

after systemic administration and reverses amphetamine-induced hyperlocomotion and disruption of sensorimotor gating in rodents, suggesting potential antipsychotic-like efficacy of $mGlu_1$ PAMs (*486*). If $mGlu_1$ PAMs can also reverse deficits in inhibitory transmission in the PFC by augmenting SST interneuron function, these combined actions could provide a novel approach that could reduce positive symptoms and also treat cognitive deficits in schizophrenia patients, providing an exciting improvement over current antipsychotics. Thus, we took advantage of this novel $mGlu_1$ PAM tool compound, along with electrophysiological, functional magnetic resonance imaging, behavioral, and in vivo optogenetic approaches to test the hypothesis that potentiating $mGlu_1$ function augments SST interneuron output, enhances PFC inhibitory transmission and reverses deficits in an NMDA receptor hypofunction model of cortical pathophysiology relevant to specific cognitive impairments in schizophrenia patients.

4.3 Materials and Methods

Animal Use

All experiments were approved by the Institutional Animal Care and Use Committee for Vanderbilt University. Adult (>8 week) transgenic and C57BL/6J mice (Cat No. 000664) were obtained from Jackson Laboratories (Bar Harbor, ME, USA) and were allowed to acclimate to the housing facility for at least 1 week. SST-Cre::Ai9 and PV-Cre::Ai9 mice were generated by crossing either homozygous SST-Cre mice (Cat No. 013044) or PV-Cre mice (Cat No. 008069) with homozygous Ai9 reporter mice (Cat No. 007909) which carry a Cre-dependent tdTomato allele inserted into the ROSA26 locus. Experimental SST-Cre mice were generated by crossing homozygous SST-Cre mice with C57BL/6J mice. For phMRI experiments, adult (250-275g) Sprague-Dawley rats were obtained from Envigo (Indianapolis, IN, USA) and allowed to acclimate the housing facility for at least 1 week before preparation for phMRI studies. Both male and female mice were used for all studies and we did not observe any significant effects of sex therefore the data were combined. Male rats were used for the phMRI studies. Animals were cared for in

accordance with the National Institutes of Health *Guide for the Care and Use of Laboratory Animals*, were provided with food and water *ad libitum,* and maintained on a 12-hour light/dark cycle. Experiments were performed during the light cycle and all animals were group housed for the duration of the studies, with the exception of rats after catheter implantation.

Compounds

DHPG (S-3,5-dihydroxyphenylglycine) was purchased from Hello-Bio Inc. (Princeton, NJ, USA). (+)-MK-801 maleate, MTEP hydrochloride, and LY367385 were purchased from Tocris Bioscience (Minneapolis, MN, USA). VU6004909 was synthesized in-house as previously described (*475*). Stock solutions were prepared in deionized water for DHPG and MTEP, 0.9% saline for MK-801, 1.1 equivalents of NaOH for LY367385, and DMSO (<0.01% final concentration) for VU6004909.

Stereotaxic Surgeries and Fiber Implants

At 5 weeks of age, SST-Cre or SST-Cre::Ai9 mice were anesthetized with 3% isoflurane, positioned in a stereotaxic frame (Kopf Instruments, CA) and maintained on 1-2% isoflurane for the remainder of the procedure. Briefly, an incision was made and the skin and muscle atop the skull was pulled to the side and cleaned. A bilateral craniotomy was made above the prefrontal cortex. Mice were then bilaterally injected with AAV5-Ef1α-DIO-eNpHR3.0-eYFP provided as a generous gift from Karl Deisseroth (Addgene viral prep # 26966-AAV5; http://n2t.net/addgene:26966 ; RRID:Addgene_26966) at a volume of 0.6µL of per injection site at a rate of 0.1µL/min using a 28G needle attached to a 10µL Hamilton syringe (Hamilton Co., NV). The needle remained in place for 5 min following injection and was then slowly retracted. For *ex vivo* optogenetic experiments, the PFC stereotaxic coordinates were (in mm relative to Bregma): AP, +1.80, ML ±0.35, DV -2.00. The scalp was then closed with VetBond (3M, MN), mice were returned to their home cage, and received 10mg/kg carprofen for 48 hours.

For *in vivo* optogenetic experiments, PFC stereotaxic coordinates were (in mm relative to Bregma, 10^{O} angle): AP, +1.80, ML ±0.85, DV -2.25. Following bilateral viral injection, two

anchoring screws were secured to the caudal part of the skull and two 2mm long, 200 µm core, 0.22 NA fiber optic cannulae (ThorLabs, Newton, NJ, USA) were implanted above the injection sites. Cannulae were secured to the skull with C&B Metabond dental adhesive (Parkell, Edgewood, NY, USA) followed by a layer of dental cement (Integrity Temporary Crown and Bridge Material, Patterson Dental, St. Paul, MN, USA) and the scalp was then closed around the headcap with VetBond. Mice were returned to their home cage and received 10mg/kg carprofen for 48 hours.

Fluorescence in situ hybridization

Fluorescence *in situ* hybridization experiments were performed using RNAScope probes and reagents supplied by Advanced Cell Diagnostics (Minneapolis, MN, USA) using the fresh-frozen protocol available online. Probe sets were directed against mouse messenger RNA and included *Grm1* (Cat. No. 449781, channel C1, accession number NM_016976.3, target region 1420-2372), *Slc17a7* (Cat. No. 416631-C3, C3, NM_182993.2, target region 464-1415), *Slc32a1* (Cat. No. 319191-C2, C2, NM_009508.2, target region 894-2037), *Sst* (Cat. No. 404631-C2, C2, NM_009215.1, target region 18-407), and *Pvalb* (Cat. No. 421931-C3, C3, NM_013645.3, target region 2-885). A set of negative control probes were directed against DapB of *Bacillus subtilis* (Cat. No. 320871).

C57BL/6J mice were anesthetized using 5% isoflurane, decapitated, and brains were rapidly dissected and submerged in ice-cold artificial cerebrospinal fluid (in mM: 126 NaCl, 2.5 KCl, 1.25 Na2PO4, 26 NaHCO3, 10 glucose, 2 CaCl2, 1 MgSO4). Brains were then rapidly frozen in Tissue-Tek O.C.T. Compound using dry ice and stored at -80^{o}C until sectioning. 16µm, coronal sections containing the PFC were cut using a Leica Cryostat CM1950 (Leica Biosystems, Buffalo Grove, IL, USA), mounted onto Fisherbrand Superfrost Plus slides (Fisher Scientific), and stored at −80°C until processing. Slides containing PFC sections were fixed for 15 min in ice-cold 4% paraformaldehyde (PFA), followed by a sequence of dehydration steps by submersion in 50%, 70%, 100%, 100% ethanol at room temperature. Slides were then air-dried and a hydrophobic

barrier was drawn around the sections using an ImmEdge PAP Pen (Vector Laboratories, Burlingame, CA, USA). Sections were incubated with Protease IV solution for 30 minutes at room temperature, washed twice in phosphate-buffered saline (PBS) and incubated in a mixture of either *Grm1, Slc17a7, and Slc32a1* or *Grm1, Sst, and Pvalb* RNAScope probes for 2 hrs at 40^{o}C in a humidified chamber. Slides were washed in Wash Buffer and then underwent a series of amplification steps at 40^{o}C with AMP 1-FL (30 min), AMP 2-FL (15 min), AMP 3-FL (30 min) and either AMP 4-Alt C-FL (for *Slc17a7/Slc32a1* slides, 15 min) or AMP 4-Alt B-FL (for *Sst/Pvalb* slides, 15 min), washing twice for 5 min in between each incubation. Following a final wash step, sections were incubated with DAPI and then coverslipped using Fluoromount Aqueous Mounting Medium (Millipore-Sigma, St. Louis, MO, USA). Slides were sealed and stored at 4^{o}C until imaging. For each experimental section, a PFC section from the same mouse underwent the same protocol using the 3-plex negative control probe.

Sections were imaged with an inverted Nikon ECLIPSE Ti-E microscope (Nikon Instruments Inc, Melville, NY, USA) using a 20x objective and an Andor Zyla sCMOS camera (Andor USA, Concord, MA, USA). Images were acquired with 405, 488, 561, and 647nm diode lasers and stitched together using NIS-Elements software. Images were analyzed with Fiji software (*549*), using the negative control-treated sections to adjust brightness and contrast settings to minimize the visualization of bacterial transcripts and autofluorescence. Regions-of-interest (ROIs) were defined using the C2 or C3 channels and overlaid onto the C1 channel, corresponding to *Grm1* transcript. For each section, the optical density of the C1 channel was calculated within each ROI along with the average optical density of putative single transcripts identified as distinct, round dots with clearly decaying intensity on all sides. Following background correction, the number of “dots per cell” was then calculated by dividing the optical density in a given ROI by the average optical density of a single transcript, or “dot”. A cell was determined to be *Grm1* positive if it contained >2 dots of *Grm1* transcript within the ROI. Values for “dots per cell” for each hemisphere were averaged together and all comparisons were conducted within

animal. All representative images are displayed without the DAPI channel to improve visualization.

Immunohistochemistry

Mice were anesthetized with 5% isoflurane, transcardially perfused with ice-cold PBS with 2g/L glucose followed by 4% PFA. Brains were dissected and post-fixed for 24hrs in 4% PFA at 4ºC and then washed three times in PBS. Free-floating, 40-60µm coronal PFC sections were obtained using a Vibratome (Leica VT1200S, Leica Biosystems, Buffalo Grove, IL, USA) and stored in PBS until processing. Sections were washed with PBS, blocked with 5% normal donkey serum and 0.3% Triton X-100 for 2 hrs at room temperature, and then incubated with primary antibody diluted in blocking buffer overnight at 4ºC as follows: goat anti-RFP (Cat. No. 200-101-379, Rockland Immunochemicals, Inc., Limerick, PA) at 1:1000, chicken anti-GFP (Cat. No. ab13970, Abcam, Cambridge, MA, USA) at 1:2000. Slices were washed and then incubated with appropriate secondary antibodies for 2 hrs at room temperature as follows at 1:500 dilutions: donkey anti-goat-Cy3 (Cat. No. 705-165-147) and donkey anti-chicken-Alexa488 (Cat. No. 703-545-155, Jackson ImmunoResearch Inc., West Grove, PA, USA). Slices were washed, incubated with DRAQ5 (Cat. No. 4084) for 5 min at room temperature, and then mounted and coverslipped onto Fisherbrand Superfrost Plus slides using Fluoromount Aqueous Mounting Medium. Sections were imaged as performed for the fluorescence *in situ* hybridization experiments.

Electrophysiology

Adult mice were anesthetized with 5% isoflurane and the brain was rapidly removed from the skull, blocked, and mounted to the cutting stage of a Vibratome. Coronal sections containing the PFC were cut at 300 µm and hemisected in ice-cold NMDG-HEPES artificial cerebrospinal fluid (aCSF) containing (in mM): 92 NMDG, 2.5 KCl, 1.25 NaH2PO4, 30 NaHCO3, 20 HEPES, 25 glucose, 2 thiourea, 5 Na-ascorbate, 3 Na-pyruvate, 0.5 CaCl2·2H2O, and 10 MgSO4·7H2O, titrated to pH 7.3-7.4 with HCl. Slices were then transferred to 32ºC for 10-12 min and following recovery, transferred to a holding chamber containing aCSF composed of (in mM): 126 NaCl, 2.5

KCl, 1.25 Na2PO4, 26 NaHCO3, 10 glucose, 2 CaCl2, 1 MgSO4, supplemented with 500µM sodium ascorbate, at room temperature for a minimum of 1 hr before commencing recording.

For recording, slices were transferred to a submerged recording chamber (Warner Instruments, CT, USA) and perfused with aCSF maintained at 31±1^{o}C using an in-line heater (Warner Instruments, CT, USA) at a rate of 2mL/min. Whole-cell patch clamp recordings were performed in the prelimbic cortex from visually-identified layer V pyramidal neurons or tdTomato-positive SST or PV neurons in response to brief illumination with 565nm light. To record membrane properties, spontaneous excitatory postsynaptic currents (sEPSCs) and current-clamp responses to compound application, pipets pulled to a resistance of 3-5 MΩ were filled with a K-Gluconate-based internal solution (in mM: 125 K-gluconate, 4 NaCl, 10 HEPES, 4 MgATP, 0.3 NaGTP, 10 Tris-phosphocreatine). After obtaining a >1GΩ seal, fast capacitance was compensated for and whole-cell configuration was achieved. Cells were allowed to dialyze for 5 min while voltage clamped at -70 mV. To confirm cellular identity and assess membrane properties and spiking characteristics, the responses to a series of current injections ranging from -150pA to +400pA (25pA increments) were recorded for each cell in current clamp. sEPSCs were recorded in voltage clamp at -70mV near the reversal potential for $GABA_A$ receptor-mediated currents. Current-clamp recordings of membrane properties and compound application were performed with no current injected and with series resistance compensated for. To record spontaneous inhibitory postsynaptic currents (sIPSCs) and within-cell ratios of sIPSCs-to-sEPSCs, patch pipets were filled with Cs-based internal solution (in mM: 140 $CsMeSO_3$, 5NaCl, 10 HEPES, 0.2 EGTA, 2 MgATP, 0.2 NaGTP, 5 QX-314). sEPSCs and sIPSCs were recorded at -70mV and +10mV, respectively, adjusted for the liquid junction potential. sIPSCs were confirmed to be $GABA_A$ mediated as they were abolished by bath application of 50µM picrotoxin while sEPSCs were eliminated by bath application of 20µM CNQX and 50µM D-AP5. For within-cell ratios, baseline sEPSCs were recorded for 2 minutes at -70mV, then voltage was stepped up to +10mV where sIPSCs were recorded at baseline and in response to compound application, then

the cell was stepped back to -70mV to obtain a 2 minute sEPSC recording in the presence of test compounds. Recordings of tdTomato-positive neurons from SST::Ai9 mice were discarded if they displayed putative PV-like fast-spiking and membrane properties due to potential marker expression in PV neurons in this line (*550*). Access resistance, membrane resistance, and holding current were monitored throughout the recording. Cells where the access resistance changed more than 25% throughout the recording were excluded from analysis.

For *ex vivo* optogenetic experiments in voltage-clamp, 565nm light (M565L3, Thor Labs, NJ) was delivered through a 40X immersion objective via the epillumination port of an Olympus BX51 inverted microscope with a duration of 100ms at 5Hz to the region around the recording electrode to activate NpHR3.0 for the duration of the compound administration experiments. For current-clamp experiment to verify NpHR-mediated hyperpolarization and inhibition of action potential firing, constant 565nm light was delivered for 2 s or in the same manner used for the voltage-clamp experiments.

All recordings were amplified using an Axoclamp 700B amplifier, digitized with a Digitdata 1550B at 20kHz, low-pass filtered at 1.6kHz, and recorded using Clampex 10.7 software (Molecular Devices, San Jose, CA, USA) on a PC running Windows 10. sEPSC and sIPSC characteristics as well as baseline values used to calculate changes in holding current were analyzed using MiniAnalysis (Synaptosoft, Fort Lee, NJ, USA). Membrane properties and action potential characteristics were analyzed using ClampFit 10.7.

For sEPSC, sIPSC, and current-clamp recordings of compound application, baseline and compound values were quantified over a 2 min span directly before addition of compound and at the end of a 5 min compound bath application. For current-clamp recordings of compound application, cells were considered to fire persistent action potentials (APs) if AP frequency was greater than 1 Hz. For membrane properties, resting membrane potential (V_m) was calculated as the average voltage directly preceding a current step for all sweeps. Input resistance was determined by the average steady-state voltage (V_{ss}) of the negative current injections. Sag ratio

was calculated by the average of $(V_{sag} - V_{ss})/(V_{sag} - V_m)$ for all negative current steps, where V_{sag} is the peak negative deflection of a negative current step. Adaptation ratio was determined as the average ratio of the last and first interspike intervals across current steps initiating APs where there were more than 2 spikes, such that larger values indicate greater adaptation.

Pharmacological Functional Magnetic Resonance Imaging (phMRI)

phMRI studies were performed as described previously (*551*, *552*). Contrast-enhanced cerebral blood volume (CBV) functional MRI was used to obtain *in vivo* measures of drug-induced changes in neural activity. Isoflurane anesthetized Sprague-Dawley rats with preimplanted jugular vein catheters underwent endotracheal intubation (14G plastic catheter), followed by insertion of i.p. and s.c. catheters (22G), and mechanical ventilation (Kent Scientific, Litchfield, CT) delivering isoflurane in a 1:2 O_2:N_2O gas mixture. Animals were securely placed in a bite bar (transimaging.com, Raleigh, NC) and pulse rate, respiration rate and pattern, and rectal temperature were continuously monitored (PhysioPro; transimaging.com, Raleigh, NC) and temperature maintained through an air-heating unit (SAM-PC; SA Instruments, Encinitas, CA). End-tidal carbon dioxide was monitored (Invivo Research, Orlando, FL) and maintained. For each scan session, animals were anesthetized under 0.9% isoflurane with neuromuscular blockade (pancuronium bromide, 1 mg/kg). Functional MR images were acquired using a horizontal 9.4T Magnex magnet interfaced with a Varian/Agilent spectrometer and a Doty litz 38-mm transmit-receive radiofrequency coil (Doty). Magnetic field homogeneity was optimized by automatic global shimming followed by local shimming over the rat brain. High-resolution fast spin- echo (FSE) anatomical images were collected with the following parameters: repetition time [TR] 2550 ms; effective echo time [TEeff] 40 ms; number of excitations [NEX] 2; 128 × 128 matrix; 35 × 35 mm2 field of view [FOV]; 14 1.0 mm thick contiguous slices. Pre-contrast reference images and post-contrast functional images were acquired (FSE: TR 2600 ms; TEeff 36 ms; NEX 2; 64 × 64 matrix). To determine target engagement and the effects of VU6004909 on the NMDA receptor antagonist-induced regional responses, either vehicle (10% Tween-80 in sterile water) or 60

mg/kg VU6004909 (i.p.) was administered 30 min before scan initiation. To measure changes in CBV, Molday iron oxide nanoparticles (MION, 30 nm; 20 mg/kg, i.v.; BioPAL, Worcester, MA) were injected. After equilibration of MION, post-contrast baseline data were collected for 10 minutes, and then MK-801 was injected (0.3mg/kg, s.c.) and fMRI data were continuously acquired.

phMRI data were first pre-processed using Analysis of Functional NeuroImages (AFNI; afni.nimh.nih.gov). All brain masked, motion corrected (AFNI 2dreg) images were coregistered to an anatomical template (AFNI 3dreg). Data were processed using in-house MATLAB code (Mathworks); fractional CBV changes were calculated on a voxel-wise basis for each brain slice using the equation $\Delta CBV(t)/ CBVo = [\ln S(t) - \ln So]/[\ln So - \ln Spre]$, where S(t) is the signal measured at time t, So is the post-contrast baseline signal, and Spre is the pre-contrast baseline signal (*553*). Regions of interest (ROIs) that were pre-defined on an anatomical template based on the Paxinos & Watson rat brain atlas (*34*), were propogated through all slices for all subjects. Mean fractional CBV changes were calculated for each ROI (left / right hemispheres averaged).

Animal Behavior

Behavioral experiments were performed in adult, C57BL/6J mice with the exception of the *in vivo* optogenetic experiments which were performed in SST-Cre/SST-Cre::Ai9 mice following surgery. Experiments were performed in part through the use of the Murine Neurobehavior Core lab at the Vanderbilt University Medical Center.

Spontaneous alternation was performed in a Y-shaped maze with clear, plexiglass walls. Mice were injected with vehicle (10% Tween-80) or VU6004909 (60 mg/kg, i.p.) 40 min before injection with either vehicle (0.9% saline) or MK-801 (0.18 mg/kg, i.p) 20 min prior to the start of the behavioral session. Mice were then placed in one arm of the maze, facing away from the center and allowed to freely explore for 10 min. The start arm for each mouse was alternated and the maze was cleaned with 70% ethanol between each mouse. Animal tracking was performed using ANY-maze software with zones for each arm of the maze predetermined. The number and

order of entries into each of the three arms were analyzed. A correct spontaneous alternation occurred when the mouse entered a different arm in each of three consecutive arm entries (e.g. ABC or CAB is correct, ABA or CAC is incorrect). Percent alternation was calculated as: (Total correct spontaneous alternations) / (Total arm entries – 2) X 100.

In vivo Optogenetics

In vivo optogenetic manipulations of spontaneous alternation performance were performed similar to spontaneous alternation studies in C57BL/6J mice with the following modifications. 6 weeks after viral injection and cannula implantation, mice were habituated to a bifurcated patch cable (BFYL1LF01, Thor Labs). Each fiber optic cannula was wiped clean with 70% isopropyl alcohol and the two ends of the patch cable were connected to the implanted cannulae with ceramic sleeves. Mice were then allowed to explore a novel cage for 5 minutes before being disconnected.

To assess the effects of PFC SST inhibition on Y-maze performance, mice were randomized to light ON or OFF groups. Both groups were allowed to explore the maze for 8 minutes, split into two, 4 min trials. For the light ON group, the first 4 min were conducted with the light off, then a 560nm LED (Doric Lenses, Quebec, Canada) connected to the other end of the patch cord was turned on for the second 4 min. For the light OFF group, the mice were connected to the patch cord but the light was not turned on. 560nm light (5mW measured at the end of each patch cord cable) was delivered similar to the *ex vivo* slice studies, 100ms duration at 5Hz for 4 min. Mice were placed into an arm of the Y-maze facing away from the center, the start arm was alternated, and the maze was cleaned with 70% ethanol between each mouse.

To assess the effects of PFC SST inhibition on $mGlu_1$ PAM efficacy, mice were injected with vehicle (10% Tween-80) or VU6004909 (60 mg/kg, i.p.) 40 min before injection with either vehicle (0.9% saline) or MK-801 (0.18 mg/kg, i.p) 20 min prior to the start of the behavioral session. All mice were exposed to 560nm light as described above and mice were randomized to have the light ON during the first or second 4 min trial. Mice were initially connected to the patch

cable and placed in a novel cage for 30 s. For mice randomized to receive light ON first, the LED was turned on and then mice were placed into the Y-maze. After 4 min, the LED was turned off. For mice receiving light OFF first, mice were placed into the Y-maze from the novel cage and after 4 min, the LED was turned on.

Videos of the sessions were recorded and total arm entries and order were analyzed by an observer blinded to treatment groups. Zones were marked in the same way as experiments performed in wildtype mice. To control for inaccurate measurements of performance with few zone entries, mice that failed to perform more than 6 arm entries in either 4 min trial were excluded from analysis.

Upon completion of the *in vivo* optogenetic experiments, brains were collected and verification of cannula placement and NpHR expression was assessed as described in the immunohistochemistry methods. Mice with improper cannula placement or lack of expression of NpHR in both hemispheres around the cannula tips were excluded from analysis.

Statistical Analysis

The number of animals in each experiment is denoted by “N” and the cells or slices by “n”. Data are presented as mean ± standard error (SEM). Statistical analyses were performed using GraphPad Prism (La Jolla, CA). A paired or unpaired two-tailed Student’s t-test, two-tailed Mann-Whitney test, one -way ANOVA, or repeated measures one- or two-way ANOVA with suitable post-tests were used where appropriate. Results of analyses including relevant statistical values are presented in the figure legends.

4.4 Results

$mGlu_1$ expression is enriched in PFC somatostatin-expressing interneurons

While $mGlu_1$ is expressed in SST interneurons in the hippocampus and various cortical regions, it is expressed in multiple cell types and the relative distribution of $mGlu_1$ amongst the diverse neurons in the rodent PFC is not well understood. We therefore used an *in situ*

hybridization approach to visualize the expression and colocalization of mRNA encoding $mGlu_1$, *Grm1*, with distinct neuronal markers throughout the mouse prelimbic (PL) PFC (Figure 20 A, B, Page 107), a region that is functionally analogous to the human dlPFC. *Grm1* mRNA was detectable in the majority of putative glutamatergic vGluT1 (*Slc17a7*)-positive (76%, 7079/9275 cells) and GABAergic vGAT (*Slc32a1*)-positive (72%, 1600/2237) cells in the PL PFC (Figure 20 C, D, Page 107) although *Grm1* expression was significantly enriched in vGAT- compared with vGluT1-positive neurons (Figure 20 E, Page 107).

Based on the greater expression of $mGlu_1$ transcript in GABAergic neurons, we then determined the interneuron subtypes that express *Grm1,* focusing our subsequent experiments on SST and PV interneurons which account for ~70% of all GABAergic neurons in the PL PFC and are the predominant subtypes that exert inhibitory control over glutamatergic pyramidal neurons (Figure 20 B, Page 107). We found that 88% (332/377) of SST-positive neurons expressed *Grm1* whereas only 50% (201/204) of PV neurons were *Grm1*-positive (Figure 20 F, G, Page 107). Furthermore, when we compared relative expression within *Grm1*-positive neurons, we observed a marked enrichment of *Grm1* mRNA puncta in SST-positive neurons compared to PV-positive cells (Figure 20 H, Page 107). Together, these data demonstrate that $mGlu_1$ expression is enriched in SST interneurons in the rodent PFC.

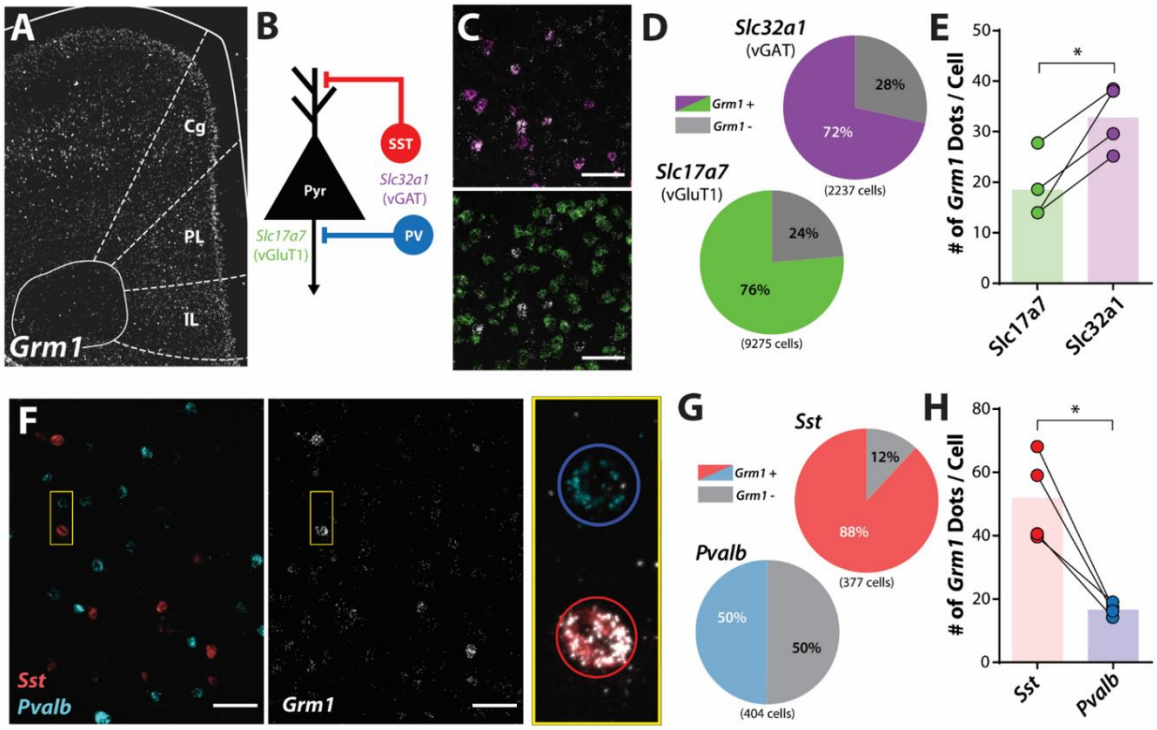

Figure 20: $mGlu_1$ expression is enriched in prefrontal cortical somatostatin interneurons. **(A)** In situ hybridization of Grm1 mRNA in a coronal slice of the mouse prefrontal cortex with distinct regions outlined in white. Cg = cingulate, PL = prelimbic, IL = infralimbic. **(B)** Simplified schematic of cortical microcircuitry with in situ hybridization mRNA markers for each neuronal population including glutamatergic pyramidal neurons (Pyr; Slc17a7, mRNA for vGluT1) and GABAergic interneurons (Slc32a1, mRNA for vGAT), consisting of somatostatin (SST)-positive (Sst), and parvalbumin (PV)-positive interneurons (Pvalb). **(C)** Representative images of deep layer V PL PFC. Top, colocalization of Slc32a1 (magenta) and Grm1 (white) mRNA. Bottom, colocalization of Slc17a7 (green) and Grm1 mRNA. Scale bar = 50µm. **(D)** Percentage of Grm1 mRNA colocalization with Slc32a1- and Slc17a7-positive cells. **(E)** Quantification of number of Grm1 mRNA puncta (dots) per Slc32a1- and Slc17a7-positive cell (two-tailed paired t-test, $p = 0.023$, $N = 4$ mice). **(F)** Representative images of deep layer V PL PFC. Left, Sst-positive (red) or Pvalb-positive (cyan) cells. Middle, same image displaying Grm1 mRNA (white). Right, magnification of pair of cells outlined in yellow box with Grm1, Sst, Pvalb mRNA overlaid. SST-positive neuron outlined in red circle, PV-positive neuron outlined in blue circle. Scale bar = 50µm. **(G)** Percentage of Grm1 mRNA colocalization with Sst- and Pvalb-positive cells. **(H)** Quantification of number of Grm1 mRNA puncta (dots) per Sst- and Pvalb-positive cell (two-tailed paired t-test, $p = 0.015$, $N = 4$ mice). * $p < 0.05$.

$mGlu_1$ activation enhances SST interneuron output in the PFC

To assess the functional consequences of $mGlu_1$ expression differences between PFC SST and PV interneurons, we generated mice expressing a Cre-dependent tdTomato reporter protein in SST or PV neurons. tdTomato-positive neurons from SST-Cre::Ai9 and PV-Cre::Ai9 mice were distributed throughout the PFC (Figure 21 A, Page 109). Additionally, tdTomato-positive neurons from SST-Cre::Ai9 and PV-Cre::Ai9 slices exhibited functional properties

consistent with SST and PV interneurons, respectively (Figure 21 B, C, Page 109). Action potentials induced by positive current injection in SST neurons were initiated with less current and plateaued at a lower frequency compared to the fast-spiking output of PV neurons (Figure 21 C, Page 109). SST neurons had a relatively depolarized resting membrane potential, higher input resistance, greater hyperpolarization-induced voltage sag, and higher adaptation ratio compared to PV interneurons (Figure 21 D-G, Page 109). These data are consistent with previous functional characterizations of PFC SST and PV interneurons (*65*, *554*).

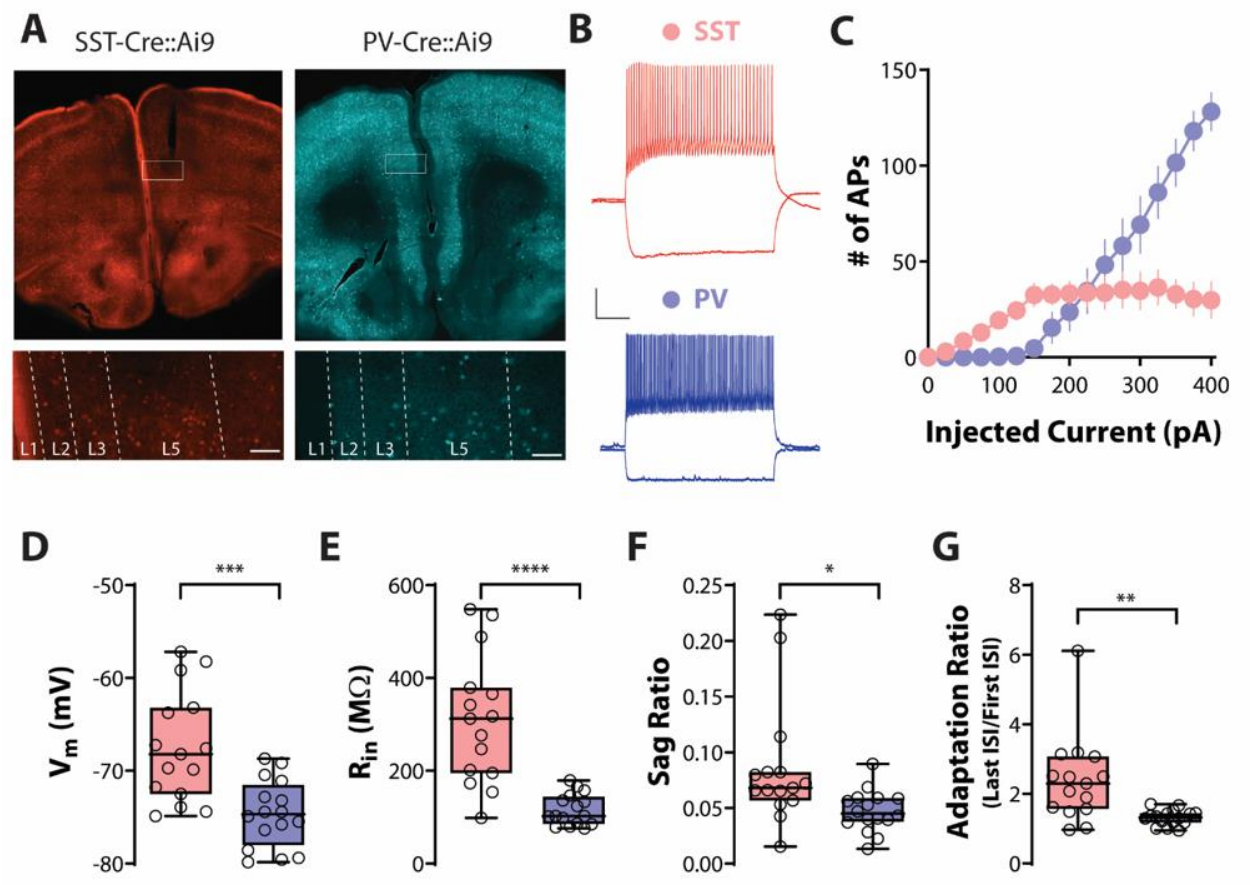

Figure 21: Properties of prelimbic cortex SST and PV interneurons. **(A)** Representative images of SST and PV interneuron distribution in coronal slices containing the PFC from SST-Cre::Ai9 and PV-Cre::Ai9 mice, respectively. *Bottom*, distributions of SST and PV neurons in the PL cortex, with laminar subdivision. Scale bar = 100 µm. **(B)** Representative current-clamp traces of the firing properties of SST and PV interneurons. **(C)** Input-output curve of action potential (AP) firing in response to positive current injection. **(D)** SST interneurons have a more depolarized resting membrane potential ($p = 0.0003$), **(E)** higher input resistance ($p < 0.0001$), **(F)** larger voltage sag ratio ($p = 0.014$), and **(G)** higher adaptation ratio ($p = 0.002$) compared to PV interneurons (two-tailed unpaired Student's t-tests; n = 15 – 16 cells per group). * $p < 0.05$, ** $p < 0.01$, *** $p < 0.001$, **** $p < 0.0001$.

To pharmacologically isolate $mGlu_1$ activation, we bath applied the group I mGlu receptor agonist DHPG in the constant presence of the $mGlu_5$ negative allosteric modulator (NAM) MTEP while recording from PFC SST or PV interneurons (Figure 22 A, C, Page 111). In SST interneurons, we observed a concentration-dependent increase in spontaneous excitatory postsynaptic current (sEPSC) frequency and a depolarizing change in the holding current, with no significant change in sEPSC amplitude (Figure 22 B, Page 111). In PV interneurons, we observed similar concentration-dependent effects on sEPSC frequency and holding current but with a reduced magnitude compared to those in SST interneurons (Figure 22 D, Page 111).

Based on the functional differences between SST and PV interneurons (Figure 21, Page 109), namely the higher input resistance and lower action potential threshold of SST interneurons, we hypothesized that $mGlu_1$ activation would have a greater effect on the output of SST neurons. To test this, we recorded from neurons in current-clamp configuration. $mGlu_1$ activation led to depolarization of both interneuron populations while SST interneurons exhibited greater depolarization compared to PV neurons (Fig 22 F, Page 111). Furthermore, $mGlu_1$ activation induced persistent action potential firing in the majority of SST neurons (7/10) while only 1/10 PV neurons depolarized sufficiently to persistently fire (Figure 22 G, Page 111). Altogether, these data demonstrate that activation of $mGlu_1$ preferentially increases the output of PFC SST interneurons.

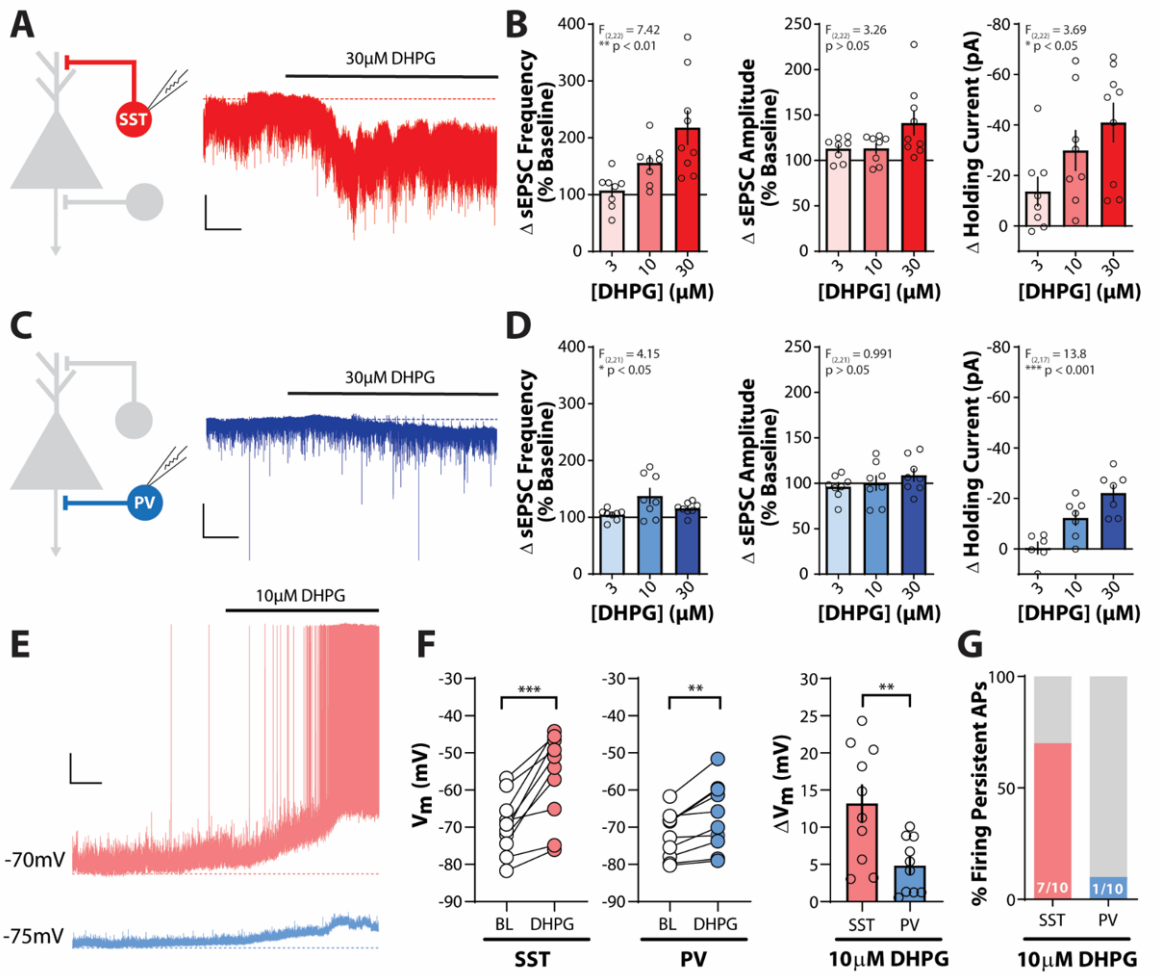

Figure 22: $mGlu_1$ activation enhances SST interneuron output in the PFC. **(A)** Left, schematic depicting whole-cell recording of SST interneurons. Right, sample trace of voltage-clamp recording of a SST interneuron in response to bath application of 30μM DHPG represented by bold black line above trace. Dashed red line represents baseline holding current. Scale bar = 50pA, 50sec. **(B)** Change in sEPSC frequency (one-way ANOVA main effect of DHPG concentration, $F_{(2,22)} = 7.42$, $p = 0.0034$, n/N = 8-9 slices/3-7 mice per group) and amplitude (one-way ANOVA main effect of DHPG concentration, $F_{(2,22)} = 3.26$, $p = 0.058$, n/N = 8-9 slices/3-7 mice per group) expressed as a percentage of baseline and change in holding current (one-way ANOVA main effect of DHPG concentration, $F_{(2,22)} = 3.69$, $p = 0.042$, n/N = 8-9 slices/3-7 mice per group) in response to bath application of DHPG in SST interneurons. **(C)** Left, schematic depicting whole-cell recording of PV interneuron. Right, sample trace of voltage-clamp recording of a PV interneuron as in panel A. Dashed blue line represents baseline holding current. Scale bar = 50pA, 50sec. **(D)** Change in sEPSC frequency (one-way ANOVA main effect of DHPG concentration, $F_{(2,21)} = 4.15$, $p = 0.030$, n/N = 8 slices/4-5 mice per group) and amplitude (one-way ANOVA main effect of DHPG concentration, $F_{(2,21)} = 0.991$, $p = 0.38$, n/N = 8 slices/4-5 mice per group) and change in holding current (one-way ANOVA main effect of DHPG concentration, $F_{(2,17)} = 13.80$, $p = 0.0003$, n/N = 6-7 slices/4-5 mice per group) in response to bath application of DHPG in PV interneurons. **(E)** Sample traces of current-clamp recordings from an SST (red) and PV (blue) interneuron in response to bath application of 10μM DHPG. Dashed lines represent baseline membrane potential. Scale bar = 10mV, 1min. **(F)** Change in membrane potential in SST (left) and PV (middle) neurons induced by 10μM DHPG (two-tailed paired t-test, SST: $p = 0.0005$, PV: $p = 0.0024$, n/N = 10 slices/4 mice per cell-type). Right, comparison of magnitude of change in membrane potential between SST and PV neurons (two-tailed Student's t-test, $p = 0.0066$, n/N = 10 slices/4 mice per cell-type). **(G)** Percentage of cells firing persistent action potentials in response to 10μM DHPG. Number of cells responding/total cells recorded denoted in each bar. (Two-sided Fisher's exact test, $p = 0.020$). ** $p < 0.01$, *** $p < 0.001$.

$mGlu_1$ activation increases inhibitory transmission onto layer V pyramidal neurons via actions on SST interneurons

Interneurons in the PFC are critical for the integration of incoming afferent activity and for the modulation and synchronization of glutamatergic pyramidal neurons. Thus, we next focused on the functional effects of $mGlu_1$ activation on layer V pyramidal neurons (Figure 23 A, Page 113), the primary output neurons of the PFC (*49*). Consistent with the expression of $mGlu_1$ in vGluT1-positive neurons (Figure 20 D, Page 107) and recurrent excitatory loops within layer V, $mGlu_1$ activation caused a small increase in sEPSC frequency onto layer V pyramidal cells compared to baseline although this was not statistically concentration-dependent (Figure 23 B, Page 113). We then isolated GABAergic spontaneous inhibitory postsynaptic currents (sIPSCs) and found that activation of $mGlu_1$ resulted in a robust, concentration-dependent increase in sIPSC frequency onto layer V pyramidal neurons with no change in amplitude (Figure 23 C, Page 113). The selective $mGlu_1$ antagonist LY367385 blocked the effect of 30µM DHPG on sIPSC frequency, confirming an $mGlu_1$-dependent mechanism (Figure 23 D, Page 113). These data indicate that $mGlu_1$ activation preferentially increases inhibitory transmission onto layer V pyramidal cells, consistent with previous findings (*499*).

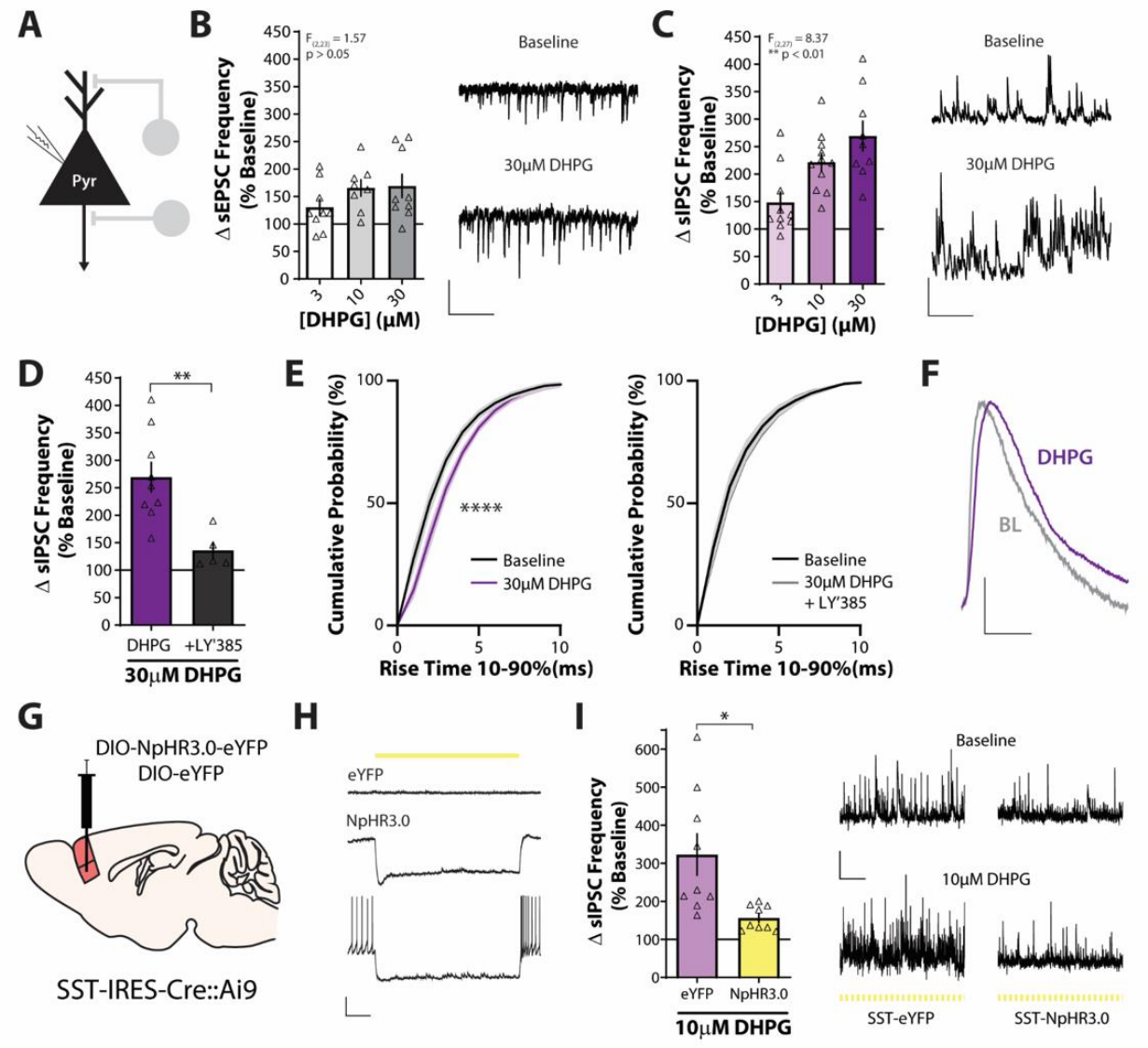
A
Pyr
B
$F_{(2,23)} = 1.57$
$p > 0.05$
Δ sEPSC Frequency (% Baseline)
[DHPG] (μM)
Baseline
30μM DHPG
C
$F_{(2,27)} = 8.37$
** $p < 0.01$
Δ sIPSC Frequency (% Baseline)
[DHPG] (μM)
Baseline
30μM DHPG
D
**
Δ sIPSC Frequency (% Baseline)
DHPG
+LY'385
30μM DHPG
E
Cumulative Probability (%)
****
Baseline
30μM DHPG
Rise Time 10-90%(ms)
Cumulative Probability (%)
Baseline
30μM DHPG
+ LY'385
Rise Time 10-90%(ms)
F
DHPG
BL
G
DIO-NpHR3.0-eYFP
DIO-eYFP
SST-IRES-Cre::Ai9
H
eYFP
NpHR3.0
I
*
Δ sIPSC Frequency (% Baseline)
eYFP
NpHR3.0
10μM DHPG
Baseline
10μM DHPG
SST-eYFP
SST-NpHR3.0

Figure 23: $mGlu_1$ activation increases pyramidal cell inhibition via actions on SST interneurons. **(A)** Schematic depicting whole-cell recording of layer V pyramidal neuron. **(B)** Left, change in sEPSC frequency in layer V pyramidal neurons in response to bath application of DHPG expressed as a percentage of baseline (one-way ANOVA main effect of DHPG concentration, $F_{(2,23)} = 1.57$, $p = 0.23$, n/N = 8-9 slices/4-6 mice per group). Right, sample traces showing sEPSCs recorded in voltage clamp at -70mV during baseline and in the presence of 30µM DHPG. Scale bars = 20pA, 500ms. **(C)** Left, change in sIPSC frequency in response to bath application of DHPG (one-way ANOVA main effect of DHPG concentration, $F_{(2,27)} = 8.37$, $p = 0.0015$, n/N = 9-11 slices/6-9 mice per group). Right, sample traces showing sIPSCs recorded in voltage clamp at +10mV during baseline and in the presence of 30µM DHPG. Scale bars = 50pA, 500ms. **(D)** Effect of 100µM LY367385 on change in sIPSC frequency induced by 30µM DHPG (two-tailed unpaired Student's t-test, $p = 0.0047$, n/N = 5-9 slices/2-6 mice per group). **(E)** Cumulative probability plots of sIPSC rise time during baseline and after bath application of 30µM DHPG alone (left; two-way repeated measures ANOVA, main effect of drug, $F_{(1,88)} = 67.5$, $p < 0.0001$) or in the presence of 100µM LY367385 (right; two-way repeated measures ANOVA, main effect of drug, $F_{(1,44)} = 2.65$, $p = 0.11$). **(F)** Scaled, average sIPSCs at baseline (BL) and after 30µM DHPG from panel C. Scale bars = scaled amplitude, 10ms. **(G)** Schematic depicting approach for viral-mediated expression of NpHR3.0-eYFP or eYFP in PFC SST interneurons. **(H)** Representative current-clamp recordings from control eYFP- (top) or NpHR3.0-eYFP-infected (middle and bottom) SST neurons. Delivery of 565nm yellow light is depicted by the yellow line. **(I)** Left, effect of 10µM DHPG on sIPSC frequency recorded in layer V pyramidal neurons in the presence of 565nm light (100ms duration, 5Hz) from control eYFP- or NpHR3.0-infected mice (two-tailed unpaired Student's t-test with Welch's correction, $p = 0.015$, n/N = 9 slices/3-5 mice per group). Right, sample traces showing sIPSCs during baseline and 10µM DHPG in constant yellow light in control and NpHR3.0-infected slices. Scale bars = 50pA, 2sec. * $p < 0.05$, ** $p < 0.01$.

SST interneurons preferentially synapse onto the distal dendrites of layer V pyramidal neurons (*123*) and IPSCs generated from synapses farther away from the somatic recording site exhibit slower kinetics than those originating from perisomatic synapses (*65*, *555*). We observed a slower sIPSC rise time following DHPG application that was blocked by LY367385 (Figure 23 E, Page 113), consistent with $mGlu_1$ activation augmenting SST interneuron output. Next, we directly tested whether SST interneuron activity is necessary for the $mGlu_1$-mediated increase of inhibitory drive onto layer V pyramidal cells using an optogenetic approach. We injected an adeno-associated virus expressing a Cre-dependent inhibitory chloride pump halorhodopsin (NpHR3.0) into the PFC of SST-Cre::Ai9 mice (Figure 23 G, Page 113). After allowing for sufficient expression, we observed NpHR3.0-positive neurons throughout the PL PFC colocalized with tdTomato (Figure 24 A, Page 116). Brief pulses of 565nm light selectively hyperpolarized NphR3.0/tdTomato-positive SST neurons and were sufficient to block action potential firing (Figure 23 H, Page 113). We then recorded sIPSCs from nearby layer V pyramidal neurons and activated $mGlu_1$ while inhibiting SST interneurons with yellow light (Figure 24 B, Page 116). In control, eYFP-infected slices we replicated a robust increase in sIPSC frequency onto layer V pyramidal cells (Figure 23 I, Page 113), while this effect was significantly attenuated in NpHR3.0-infected slices (Figure 23 I, Page 113). DHPG also increased sIPSC rise time in eYFP- but not in NpHR3.0-infected slices (Figure 24 D, Page 116). Therefore, the $mGlu_1$-mediated increase of GABAergic transmission onto PFC pyramidal neurons requires SST interneuron activity.

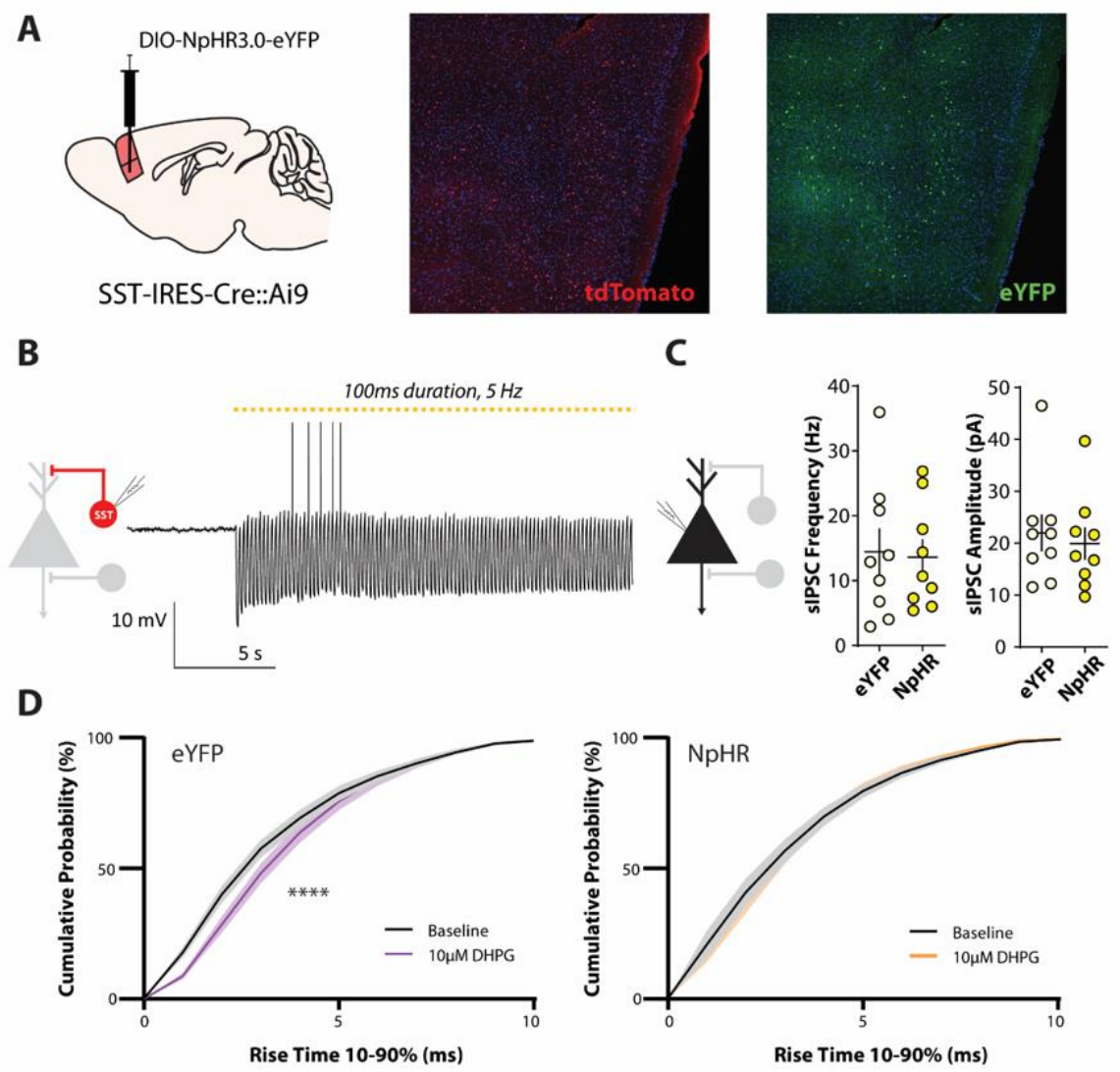

Figure 24: Validation of NpHR3.0-mediated inhibition of PFC SST interneurons *ex vivo*. **(A)** Schematic depicting the viral injection strategy to selectively express NpHR3.0 in SST interneurons in the PFC. *Right,* representative images of tdTomato-expression in SST neurons from SST-Cre::Ai9 mice and eYFP-tagged NpHR3.0. **(B)** Representative current-clamp recording of an tdTomato-postiive/eYFP-positive neuron from an NpHR3.0 infected mouse demonstrating 5Hz 565nm light inhibits SST interneurons over a long period of time. **(C)** Baseline sIPSC frequency ($p = 0.853$) and amplitude ($p = 0.660$) recorded in layer V pyramidal neurons did not differ between eYFP- and NpHR3.0-infected slices in the presence of 565 nm light ($n = 9$ slices per group). **(D)** Cumulative probability plots for eYFP- and NphR3.0-infected slices in response to 10μM DHPG bath application in the presence of 565 nm light (eYFP, two-way repeated measures ANOVA, main effect of drug, $F_{(1,88)} = 17.0$, $p < 0.0001$; NpHR, , two-way repeated measures ANOVA, main effect of drug, $F_{(1,88)} = 0.086$, $p = 0.77$). **** $p < 0.0001$.

The $mGlu_1$ positive allosteric modulator VU6004909 shifts PFC I-E balance towards inhibition

Based on our previous results and to test the hypothesis that potentiating $mGlu_1$ function will selectively enhance PFC inhibition, we took advantage of the recently developed $mGlu_1$ PAM tool compound VU6004909 that exhibits excellent subtype-selectivity ($mGlu_1$ PAM EC_{50} 25nM; other mGlu receptor subtypes > 10μM) and optimal pharmacokinetic properties for *in vivo* use (*475*). To test whether the $mGlu_1$ PAM VU6004909 potentiates cortical inhibition in native tissue, we again recorded from either SST interneurons (Fig 25 A, Page 118) or layer V pyramidal cells (Fig 25 E, Page 118). In SST neurons, a submaximally efficacious concentration of DHPG (3μM) was not sufficient to induce action potential firing alone (Fig 25 D, Page 118). Conversely, pretreatment of slices with the $mGlu_1$ PAM VU6004909 (10μM) significantly increased the depolarization (Fig 25 C, Page 118) and proportion of SST interneurons that fired persistent action potentials in response to 3μM DHPG (Fig 25 D, Page 118), indicating that an $mGlu_1$ PAM can enhance the activity of SST interneurons.

In layer V pyramidal neurons, VU6004909 had no effect on the change in sEPSC frequency (Fig 25 F, Page 118) but significantly potentiated the effect of 3μM DHPG on sIPSC frequency (Fig 25 G, Page 118). Furthermore, we compared the ratio of sIPSC to sEPSC frequency at baseline and after drug wash-on within the same pyramidal neuron and observed a significant increase in the inhibitory-excitatory (I-E) ratio induced by the combination of 3μM DHPG and VU6004909 (Fig 25 H, Page 118). These data demonstrate that an $mGlu_1$ PAM preferentially potentiates PFC inhibitory transmission and raise the possibility that VU6004909 could rescue I-E imbalance *in vivo*.

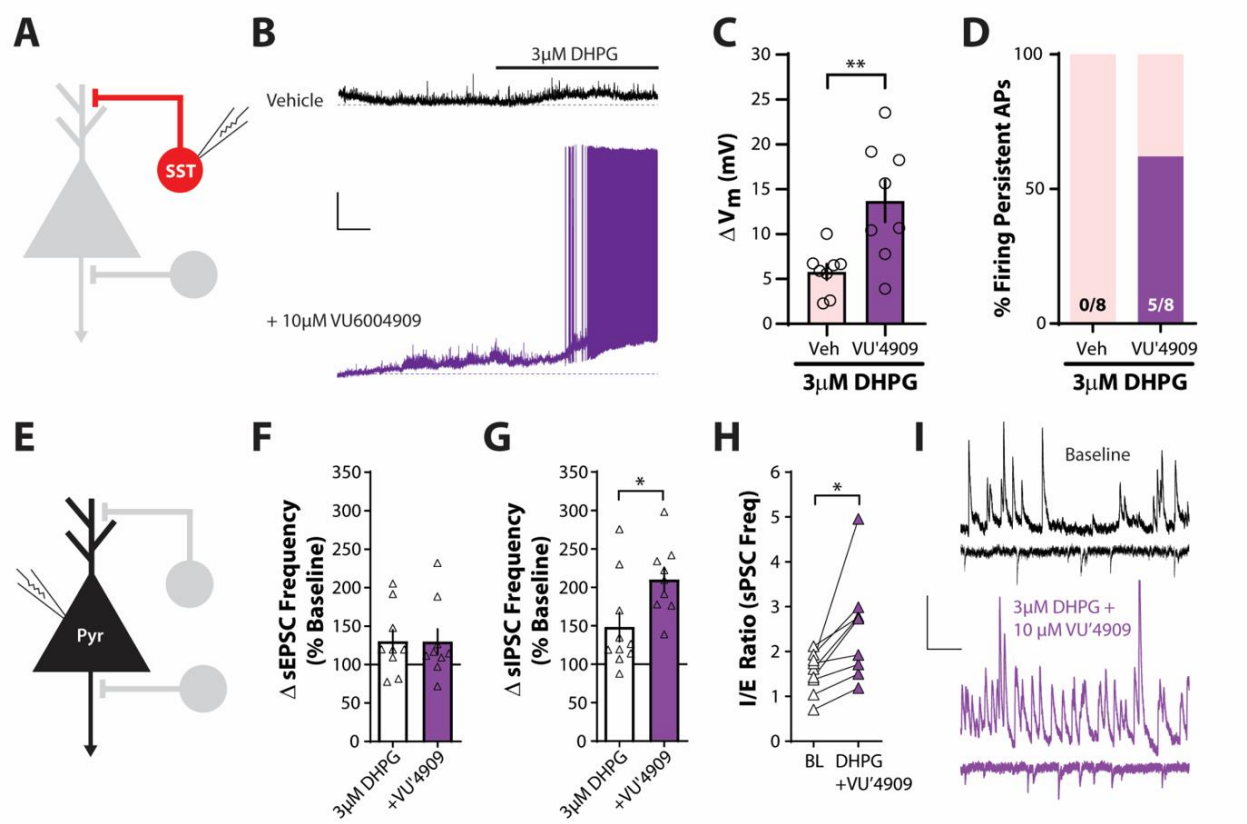

Figure 25: The $mGlu_1$ PAM VU6004909 shifts I-E balance towards inhibition. **(A)** Schematic depicting whole-cell recording of SST interneurons. **(B)** Sample traces of current-clamp recordings from SST interneurons in response to bath application of 3μM DHPG in the presence of vehicle (black) or 10μM VU6004909 (purple). Dashed lines represent baseline membrane potential. Scale bar = 10mV, 1min. **(C)** Comparison of magnitude of change in SST membrane potential in response to 3μM DHPG in the presence of vehicle and 10μM VU6004909 (two-tailed unpaired Student's t-test, p = 0.0067, n/N = 8 slices/4 mice per group). **(D)** Percentage of cells firing persistent action potentials in response to 3μM DHPG with and without VU6004909. Number of cells responding/total cells recorded denoted in each bar. (two-sided Fisher's exact test, p = 0.026). **(E)** Schematic depicting whole-cell recording of layer V pyramidal neuron. **(F)** Change in sEPSC frequency in layer V pyramidal neurons in response to bath application of 3μM DHPG with and without 10μM VU6004909 expressed as a percentage of baseline (two-tailed unpaired Student's t-test, p = 0.98, n/N = 9 slices/4 mice per group). **(G)** Change in sIPSC frequency in response to bath application of 3μM DHPG with and without 10μM VU6004909 (two-tailed unpaired Student's t-test, p = 0.023, n/N = 9-10 slices/4-7 mice per group). **(H)** Ratio of sIPSC to sEPSC frequency in the same layer V pyramidal neuron during baseline and in the presence of 3μM DHPG and 10μM VU6004909 (two-tailed paired t-test, p = 0.012, n/N = 9 slices/4 mice). **(I)** Sample traces of sIPSCs and sEPSCs in layer V pyramidal neurons during baseline and in the presence of 3μM DHPG and 10μM VU6004909. Scale bars = 20pa, 250ms. * $p < 0.05$, ** $p < 0.01$.

$mGlu_1$ potentiation ameliorates cortical hyperactivity induced by NMDA receptor hypofunction

To examine the efficacy of an $mGlu_1$ PAM *in vivo*, we used an NMDA receptor hypofunction model of schizophrenia. NMDA receptor antagonists, like MK-801, induce schizophrenia-like symptoms including cognitive deficits in healthy individuals (*328*) and can precipitate symptoms in schizophrenia patients. Converging with the GABAergic dysfunction hypothesis, administration of the NMDA receptor antagonist MK-801 in rodents increases PFC pyramidal neuron firing while decreasing the activity of PV and SST interneurons (*356*, *543*), suggesting that NMDA receptor antagonism induces disinhibition and disrupts cortical I-E balance, modelling schizophrenia-like functional deficits in inhibitory transmission (*556*).

Accompanying the behavioral effects of NMDA receptor antagonism is a widespread increase brain activity in healthy volunteers, particularly in the dlPFC (*357*) that is similar to cortical hyperactivity observed in schizophrenia patients during working memory tasks (*361*). To model this effect in rodents in a translationally-relevant preclinical assay, we used pharmacological functional magnetic resonance imaging (phMRI) to assess the physiological effects of an $mGlu_1$ PAM on MK-801-induced cortical hyperactivity. We measured cerebral blood volume (CBV) changes that indirectly reflect alterations in neural activity and assessed cortical, hippocampal, striatal, and thalamic areas (Figure 26 A, Page 120, and Figure 27 A, Page 121). In line with previous findings (*557*), injection of a behaviorally active dose of MK-801 led to sustained increases in CBV across cortical areas including the PFC (Figure 26 B, Page 120), cingulate cortex (Cg) (Figure 26 C, Page 120), and retrosplenial cortex (RSC) (Figure 26 D, Page 120) as well as the dorsal and ventral striatum, thalamic nuclei, and hippocampus (Figure 27 B-H, Page 121). Pre-treatment with VU6004909 (60 mg/kg, i.p.) significantly reversed MK801-induced cortical and subcortical hyperactivity. These reversals were significant in the PFC, Cg, and RSC (Figure 26 B-D, Page 120) as well as in the nucleus accumbens (Figure 27 D, Page 121) but not in the hippocampus (Figure 27 H, Page 121). VU6004909-mediated effects on the MK-801 response in the motor circuit (i.e. motor cortex, substantia nigra, caudate-putamen) were not

significant (Figure 27 B, C, G, Page 121), potentially due to a dampening of brain responses by the anesthesia necessary to immobilize animal during the scans. Furthermore, no effect of VU6004909 was observed in thalamic regions (Figure 27 E, F, Page 121). The cortical data however demonstrate that an $mGlu_1$ PAM can reverse the schizophrenia-like cortical hyperactivity *in vivo* and are consistent with $mGlu_1$ PAMs shifting cortical I-E balance in favor of inhibition.

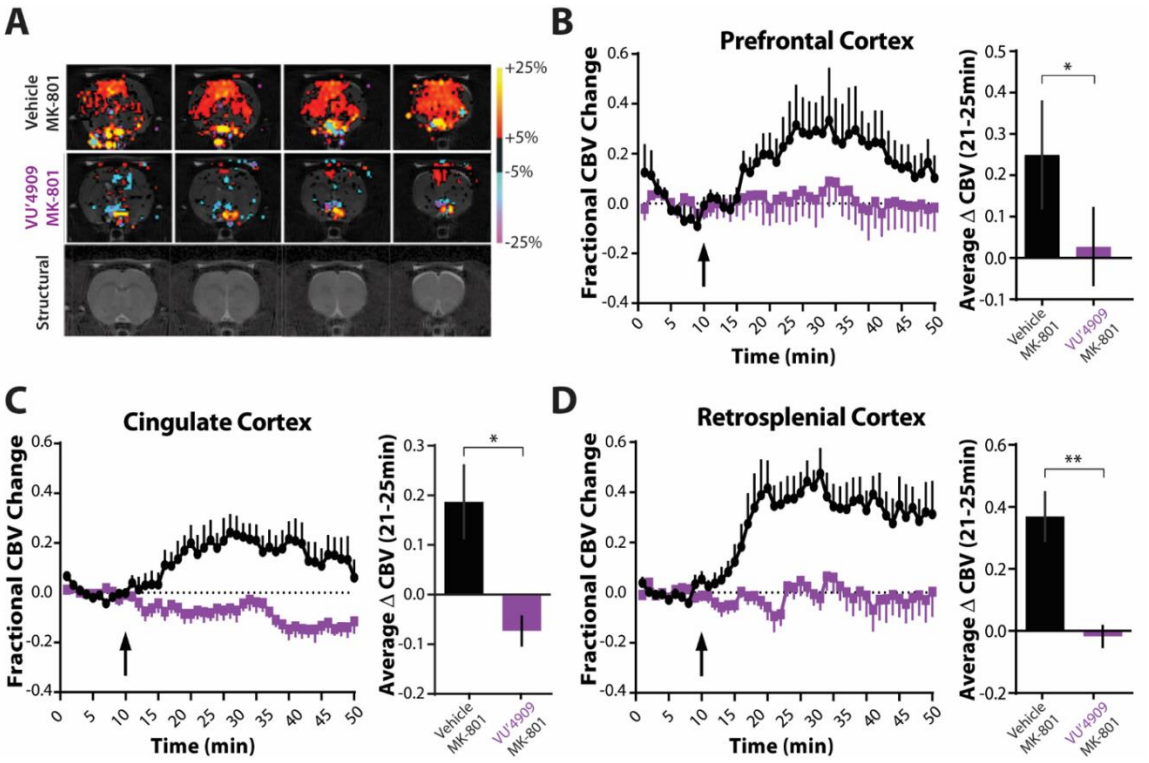

Figure 26: $mGlu_1$ potentiation reverses NMDA receptor antagonist-induced cortical hyperactivity. **(A)** Representative cerebral blood volume (CBV) and structural T2-weighted MRI template images of male Sprague-Dawley rat anesthetized and then treated with vehicle (i.p., 10% Tween-80) or 60 mg/kg VU6004909 and then 0.3 mg/kg MK-801 (s.c., 0.9% saline). In the group activation maps, the red to yellow bar range represents increased CBV, indicating increased neuronal activity, while blue to purple color bar range represents decreased CBV, indicating decreased neuronal activity. **(B-D)** Time courses and bar graphs of CBV changes after MK-801 injection (arrow) in rats pretreated with vehicle or VU6004909 from **(B)** prefrontal cortex (PFC), **(C)** cingulate cortex (Cg), or **(D)** retrosplenial cortex (RSC). Time courses show fractional changes in CBV ($\Delta CBV(t)/CBV_o$). For bar graphs, fractional CBV values were averaged between 21 and 25 min for each animal (two-tailed Mann Whitney test, PFC: $p = 0.041$; Cg: $p = 0.015$; RSC: $p = 0.0043$, N = 6 rats per group). * $p < 0.05$, ** $p < 0.01$. Nellie E Byun contributed this figure.

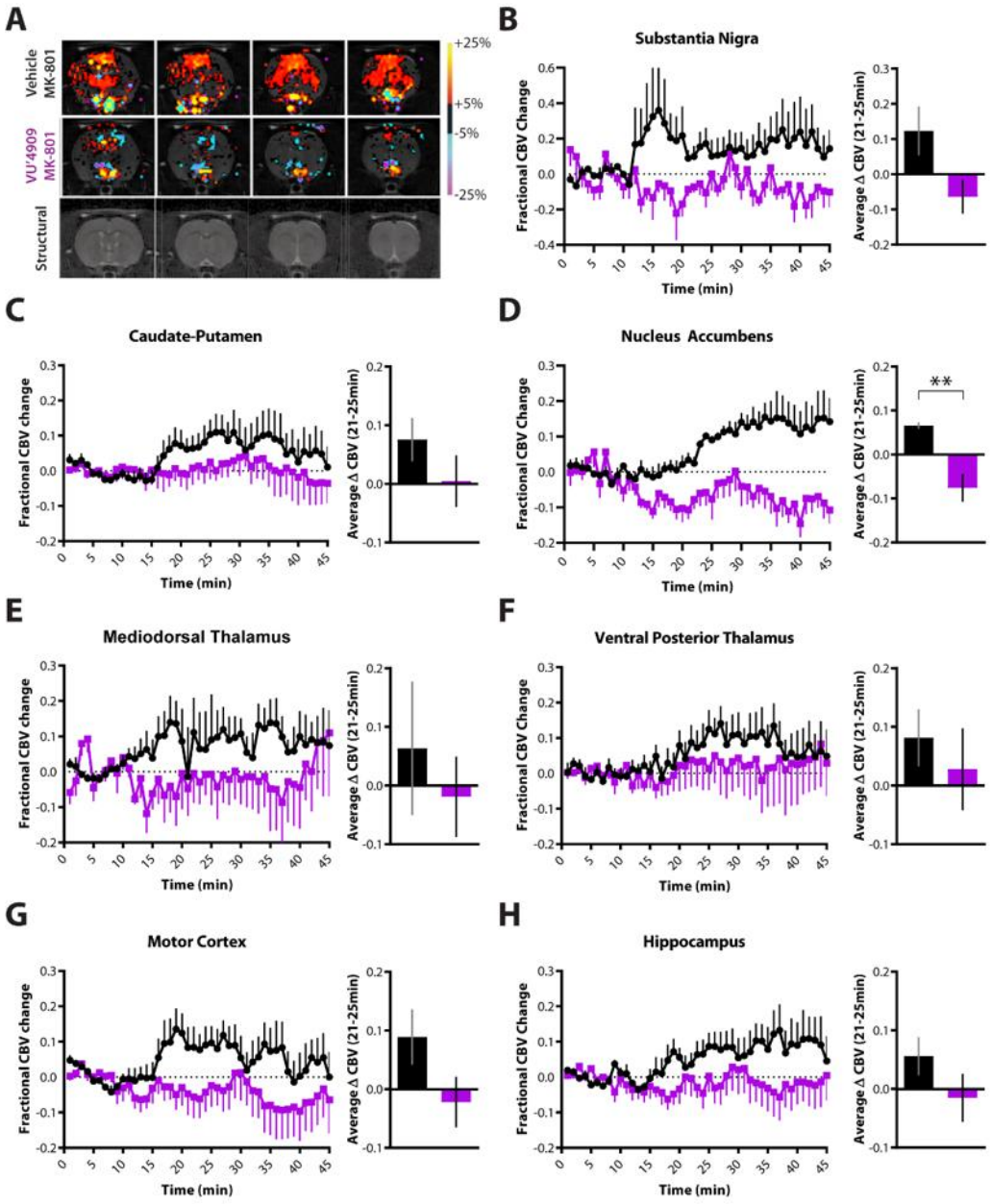

Figure 27: phMRI results of MK-801 and VU6004909 effects in other cortical and subcortical brain regions. **(A)** Representative CBV and structural T2-weighted MRI template images. Scale bar as in Figure 26. **(B-H)** Time courses and bar graphs of CBV changes after MK-801 injection (arrow) in rats pretreated with vehicle or VU6004909. 60 mg/kg VU6004909 reversed MK-801-induced hyperactivity in the nucleus accumbens ($p = 0.0022$, $N = 6$ rats per group). ** $p < 0.01$. Nellie E Byun contributed this figure.

The $mGlu_1$ PAM VU6004909 reverses MK-801-induced behavioral deficits

In addition to modeling physiological dysfunction in schizophrenia, systemic administration of NMDA receptor antagonists induce a range of behavioral deficits relevant to the cognitive symptoms of schizophrenia (*343*). Therefore, we next determined if the $mGlu_1$ PAM VU6004909 has efficacy in reversing an MK-801-induced deficit in PFC-dependent cognitive function. We assessed spatial working memory in mice by monitoring spontaneous alternation in the Y-maze (Figure 28 A, Page 123), a task that requires PFC interneuron function (*161*). We observed a significant deficit in spontaneous alternation induced by MK-801 that was rescued by pretreatment with VU6004909 (Figure 28 B, Page 123). Importantly, this was not accompanied by a reduction in locomotion as assessed by total arm entries (Figure 29 A, Page 125), demonstrating a procognitive effect of the $mGlu_1$ PAM. These data suggest that an $mGlu_1$ PAM may be effective in treating the cognitive deficits in schizophrenia.

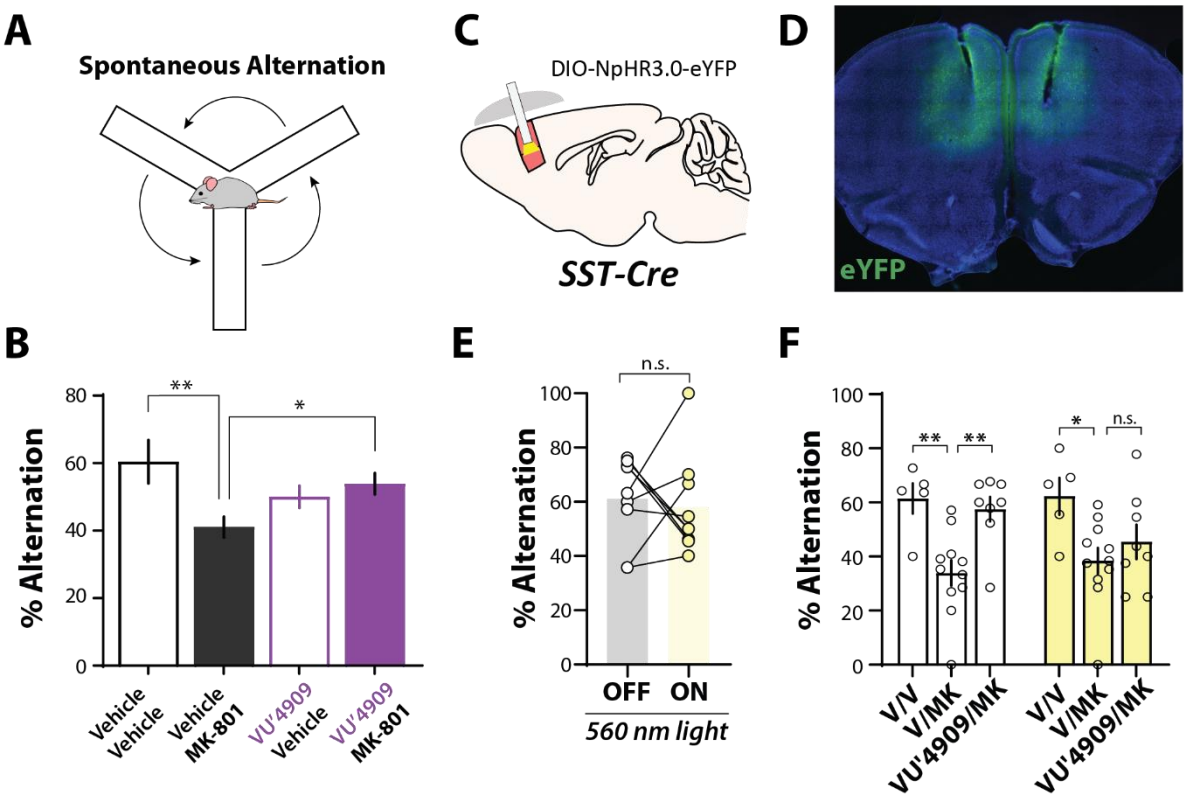

Figure 28: The $mGlu_1$ PAM VU6004909 reverses an MK-801-induced working memory deficit via actions on PFC SST interneurons. **(A)** Schematic of spontaneous alternation in the Y-maze. **(B)** Average % spontaneous alternation for mice in mice pretreated with vehicle or 60 mg/kg VU6004909 (i.p., 10% Tween-80) prior to administration of vehicle or 0.18 mg/kg MK-801 (i.p., 0.9% saline) 20 minutes before behavioral test (one-way ANOVA main effect, $F_{(3,36)} = 4.06$, $p = 0.014$; post-hoc Bonferroni's test: Vehicle/Vehicle vs. MK-801/Vehicle, $p = 0.0036$; MK-801/Vehicle vs. VU'4909/Vehicle, $p = 0.043$; N = 8-12 mice per group). **(C)** Schematic depicting strategy to optogenetically inhibit SST interneurons in vivo. **(D)** Representative image of bilateral NpHR3.0-eYFP expression throughout the PFC and bilateral fiber tracts terminating in the prelimbic PFC. **(E)** Effect of 560nm yellow light delivered to the PFC during the Y-maze. Mice underwent an 8 minute trial with 4 minutes of light ON and 4 minutes of light OFF, randomized to either receive ON first or OFF first. No effect of light order was observed (see Fig 29) therefore data is presented as pooled OFF and ON trials (two-tailed paired t-test, $p = 0.74$, N = 9 mice). **(F)** Effect of 560nm yellow light on Y-maze performance in mice dosed with vehicle, 0.18 mg/kg MK-801 (i.p., 0.9% saline), or 60 mg/kg VU6004909 (i.p., 10% Tween-80) pretreated before MK-801. White bars represent performance during light OFF trials and yellow bars represent performance during light ON trials (two-way repeated-measures ANOVA, main effect of drug, $F_{(2,21)} = 9.33$, $p = 0.0013$; post-hoc Bonferonni's multiple comparisons test: OFF trials: Vehicle/Vehicle vs. Vehicle/MK-801, $p = 0.0037$; Vehicle/MK-801 vs. VU'4909/MK-801, $p = 0.0039$; ON trials: Vehicle/Vehicle vs. Vehicle/MK-801, $p = 0.013$; Vehicle/MK-801 vs. VU'4909/MK-801, $p = 0.67$; N = 5-11 mice per group). * $p < 0.05$, ** $p < 0.01$.

PFC SST interneuron activity is necessary for the $mGlu_1$ PAM rescue of spatial working memory deficits

Lastly, we set out to determine whether the procognitive effects of an $mGlu_1$ PAM involve PFC SST interneurons. We used an optogenetic approach, bilaterally expressing NpHR3.0 in PFC SST interneurons and implanting fiber optic cannulae above the PL PFC to activate NpHR3.0 *in vivo* (Figure 28 C, D, Page 123). We then used the Y-maze task to test the hypothesis that PFC SST interneuron activity is required for $mGlu_1$ PAM efficacy. We first tested if PFC SST interneuron activity was necessary for spatial working memory in the Y-maze with mice performing half of the task with the light off and the other half with the light on (Figure 29 B, Page 125), using the same light stimulation parameters that we previously characterized in slices (Figures 23, 24). Although mice decrease the number of arm entries over the session, this did not affect performance in mice that did not receive light but were connected to the fiber (Figure 29 C, Page 125). Consistent with ablation studies (*161*), optogenetic inhibition of PFC SST interneurons had no effect on spontaneous alternation performance (Figure 28 E, Page 123).

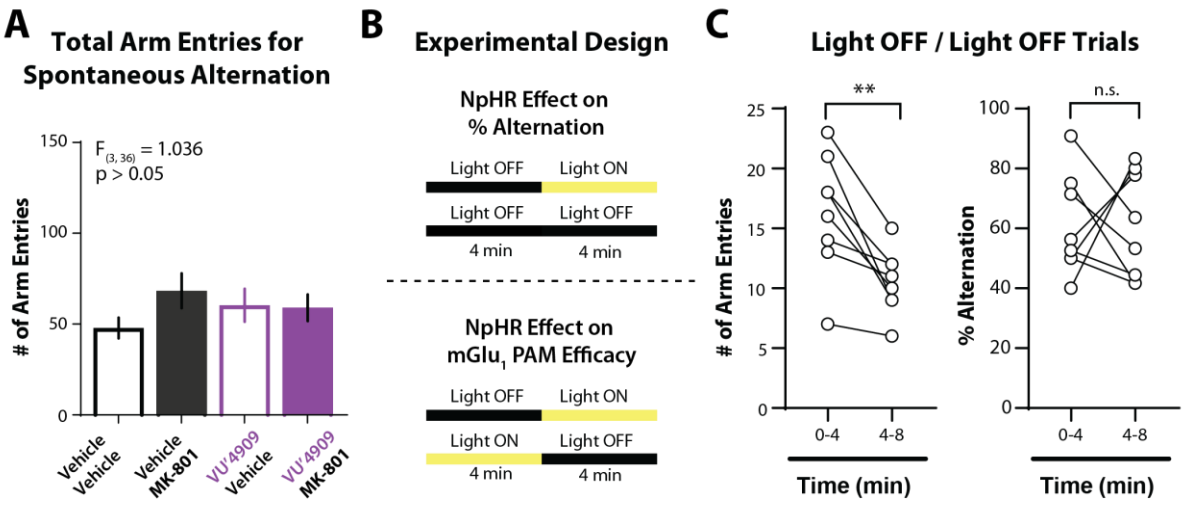

Figure 29: MK-801 and VU6004909 effects on arm entries in the Y-maze and experimental design for *in vivo* optogenetic experiments. **(A)** Neither 0.18 mg/kg MK-801 (*i.p.*, 0.9% saline), 60 mg/kg VU6004909 (*i.p.*, 10% Tween-80), nor the combination affects number of arm entries in the Y-maze (one-way ANOVA, $F_{(3,36)} = 1.04$, $p = 0.39$; N = 8 -12 mice per group). **(B)** Schematic depicting the experimental design for the two *in vivo* optogenetic experiments. To assess if inhibiting PFC SST interneurons affects Y-maze performance, mice either performed the entire 8 min session with the light OFF or 4 min with the light OFF followed by 4 min of light ON. To test if PFC SST interneurons are required for $mGlu_1$ PAM efficacy, all mice performed 4 min light ON and 4 min light OFF but the order was randomized. **(C)** Control data from Light OFF/OFF trials showing that arm entries decrease over the 8 minute session (two-tailed paired t-test, $p = 0.0041$) but performance does not ($p = 0.99$, N = 8 mice).

With no effect on general alternation behavior, we were then able to test the hypothesis that PFC SST interneurons are required for the $mGlu_1$ PAM efficacy. Mice were randomized to receive light on during the first or second half of the task (Figure 29 B). In vehicle-treated mice, we observed no difference in performance depending on the order of NpHR3.0 stimulation therefore all the data were pooled and presented as light-off versus light-on trials. Replicating our previous findings in the light off condition, we observed a significant deficit in performance induced by MK-801 compared to vehicle-treated animals. Again, this deficit was rescued by the $mGlu_1$ PAM VU6004909 in control light-off conditions (Figure 28 F, Page 123). However, in the light-on condition when PFC SST interneuron activity was inhibited, VU6004909 did not reverse MK-801-induced deficits (Figure 28 F, Page 123). These data provide a causal association between $mGlu_1$ PAM procognitive efficacy and the activity of PFC SST interneurons, consistent with our mechanistic data in brain slices (Figures 22 - 25).

4.5 Discussion

In this study, we found that $mGlu_1$ activation and potentiation enhances inhibitory neurotransmission in the PFC via actions on SST interneurons. Furthermore, we demonstrate that an $mGlu_1$ PAM can reverse cortical hyperactivity and has efficacy in reversing working memory deficits induced by NMDA receptor antagonism *in vivo*, an effect dependent on the function of PFC SST interneurons. To our knowledge, this is the first report than an $mGlu_1$ PAM reverses physiological and cognitive deficits in a schizophrenia-relevant model. The current data support the potential of $mGlu_1$ PAMs to provide procognitive efficacy for the treatment of schizophrenia.

Based on consistent observations of inhibitory deficits, modulation of the GABAergic system has been pursued as a novel therapeutic approach for schizophrenia (*558–561*). While the $GABA_A$ receptor has garnered substantial attention (*562–567*), enhancing interneuron function has lagged presumably due to a lack of druggable targets selective for these distinct neuronal populations. Our data identify $mGlu_1$ as a novel target to preferentially increase PFC SST interneurons activity, providing an alternative means to rescue deficient inhibitory transmission in schizophrenia patients. The current findings also add to accumulating evidence suggesting enhancing SST interneuron activity can improve cognitive function. Synaptic transmission between SST and pyramidal neurons is predominantly mediated by α_5-containing $GABA_A$ receptors (*568*), and α_5 $GABA_A$ receptor PAMs have procognitive efficacy in preclinical studies (*564*, *569*). Other procognitive therapeutics augment SST interneuron function, particularly α7 nicotinic and M_1 muscarinic acetylcholine receptor modulators (*570*)(*522*, *571*, *572*). α7 PAMs have had promising early clinical results for the treatment of cognitive deficits in schizophrenia (*573*) while M_1 PAMs reverse cognitive deficits in NMDA receptor hypofunction animal models (*244*, *441*) and early clinical results suggest that M_1 PAMs are procognitive (*574*). While the relative contribution of SST neuron modulation to these *in vivo* effects remain to be determined,

these in addition to our current results provide strong evidence for further drug discovery efforts directed at modulating SST interneurons.

It is intriguing that targeting PFC SST interneurons reverses schizophrenia-like deficits in light of abundant evidence of PV interneuron dysfunction in schizophrenia (*127*, *356*, *364*, *407*, *575*). Therefore, our results might indicate that SST interneurons are impaired in NMDA receptor antagonist models of schizophrenia. In adult rodents, the NMDA receptor contribution to excitatory transmission onto PV neurons is weak compared to low-threshold, putative-SST interneurons (*65*, *576*, *577*), therefore SST interneurons may be more susceptible to the effects of an NMDA receptor antagonist. Consistent with this, a recent study found that acute systemic ketamine reduced the activity of SST interneurons and increased pyramidal neuron activity *in vivo* in the cingulate cortex (*543*). Furthermore, genetic reduction of NMDA receptors in pyramidal neurons impairs SST-pyramidal neuron inhibitory transmission (*251*, *578*). Interestingly, we found no deficit in Y-maze performance upon optogenetic inhibition of PFC SST neuron activity, consistent with previous work demonstrating ablation of PFC SST interneurons does not impair spontaneous alternation (*161*). Additionally, in a delayed non-match to sample task, inhibiting PFC SST interneurons only impaired performance at long delays (*159*) that animals likely do not experience during spontaneous alternation. Therefore, PFC SST interneurons appear to be dispensable for baseline performance in the spontaneous alternation task while potentiating their activity is capable of rescuing the MK-801-induced behavioral deficit. Whether this is via a rescue of SST interneuron dysfunction or a potential compensatory mechanism is unclear.

How SST interneuron dysfunction in NMDA receptor hypofunction models might relate to the clinical aspects of schizophrenia is unclear. In other cortical regions, SST interneurons contribute to low-frequency theta and beta oscillations which are abnormal in schizophrenia patients (*579*). Additionally, SST mRNA is reduced in the dlPFC of schizophrenia patients (*378*, *379*, *580*) and may imply a clinical deficit that could be rescued by $mGlu_1$ potentiation. Supporting the translatability of our results, a recent study in human temporal cortex found that group I mGlu

receptor activation increased the output of putative-SST interneurons and enhanced inhibition onto layer II/III pyramidal neurons (*581*). This suggests that the functional effects of $mGlu_1$ potentiation we observed are conserved between rodents and humans and that an $mGlu_1$ PAM could engage similar circuitry in schizophrenia patients.

Although our *ex vivo* and *in vivo* results demonstrate the $mGlu_1$ PAM efficacy in reversing working memory deficits are primarily mediated through an SST interneuron mechanism in the PFC, our data do not rule out that *in vivo* $mGlu_1$ potentiation could modulate other neuronal populations. PV interneurons might be required for the efficacy of $mGlu_1$ PAMs similar to recent data demonstrating that the antidepressant-like efficacy of ketamine requires the coordinated activity of both SST and PV interneuron subtypes (*582*). In addition to interneurons, whether $mGlu_1$ receptors in other brain regions or other cell types contribute to the *in vivo* efficacy of $mGlu_1$ PAMs remains an exciting hypothesis for future studies. Our fMRI studies suggest that $mGlu_1$ PAMs can reverse effects of NMDA receptor hypofunction in other brain regions. Actions on PFC SST interneurons may contribute to this; alternatively, potentiation of discrete populations of $mGlu_1$ receptors in other brain regions may be responsible and could predict $mGlu_1$ PAM efficacy across other behavioral modalities. For example, the $mGlu_1$ PAM attenuated nucleus accumbens hyperactivity, suggesting that an $mGlu_1$ PAM could be effective to ameliorate motivational deficits schizophrenia (*583*). Therefore, determining the mechanisms of $mGlu_1$ activation in other brain regions and potential efficacy in other behaviors relevant to schizophrenia are exciting future directions. The continued development of $mGlu_1$ subtype selective ligands and the generation of genetic tools to selectively and conditionally restrict $mGlu_1$ expression will serve to help address these questions and further our understanding of $mGlu_1$ biology and its potential as a therapeutic target.

An important limitation of our work is the use of an acute pharmacologically-induced deficit model. Here, we sought to specifically model the inhibitory deficits (*541*) and cortical hyperactivity (*361*) observed clinically in schizophrenia patients by using acute NMDA receptor antagonism to

produce a disinhibition-like state in rodents (*356*). The etiology of schizophrenia involves a complex interaction of genetic and environmental factors so that preclinical animal models often fail to recapitulate the entirety of the disease (*343*). It will therefore be important to test $mGlu_1$ PAMs in a variety of other schizophrenia-related models (*343*). Another caveat is that the $mGlu_1$ PAM efficacy was studied after a single, acute dose. An effective symptomatic treatment for schizophrenia will necessitate long-term dosing therefore future studies will need to investigate the effects of chronic $mGlu_1$ PAM treatment. Finally, the motor and learning deficits of global $mGlu_1$ knockout mice (*584*, *585*) preclude their use for validation of $mGlu_1$ PAM on-target activity. Although VU6004909 is highly selective for $mGlu_1$ over other mGlu receptor subtypes (*475*), the development of chemically-distinct $mGlu_1$ PAMs as well as improved genetic approaches to conditionally restrict $mGlu_1$ expression in the future will help to confirm on-target efficacy of this approach.

Here, we describe $mGlu_1$ as a novel target to preferentially enhance GABAergic transmission and rescue cortical inhibitory deficits in schizophrenia. Augmenting receptor function *in vivo* with an $mGlu_1$ PAM reversed cortical hyperactivity and reversed a working memory deficits relevant to cognitive dysfunction in schizophrenia. As $mGlu_1$ PAM development efforts continue towards producing a clinical candidate, our study provides preclinical proof-of-concept that $mGlu_1$ PAMs have not only antipsychotic-like efficacy (*486*), but are able to rescue cognitive deficits as well. Based on our mechanistic work, it is possible that $mGlu_1$ PAMs will have broad utility in other disorders where I-E balance is perturbed such as epilepsy, autism, and Alzheimer's disease (*586*–*588*). Altogether, these data suggest that clinically, $mGlu_1$ PAMs have the potential to confer broad efficacy to improve the lives of patients living with schizophrenia.

CHAPTER V

DISCUSSION AND FUTURE DIRECTIONS

Aberrant cortical processing is a hallmark of multiple psychiatric diseases but there has been a lack of therapeutic development concentrated on ameliorating PFC dysfunction. In this work, we focused on the function of two neuromodulatory GPCRs in regulating PFC macro- and microcircuit function to identify novel pharmacological targets. Using subtype-selective PAMs in preclinical animal models, we were then able to validate these targets as potential novel treatments for psychiatric disorders. In Chapter III, we found that M_1 muscarinic receptors are poised to regulate fear-related afferents to the PFC and that M_1 potentiation may be a novel approach to enhance the efficacy of exposure therapy in PTSD. In Chapter IV, we observed that $mGlu_1$ activation preferentially enhances PFC inhibitory transmission through actions on SST interneurons and that $mGlu_1$ potentiation may be a novel therapeutic approach to rescue inhibitory deficits and treat cognitive deficits in schizophrenia. Therefore, the work described in this dissertation identifies and validates M_1 and $mGlu_1$ PAMs as potential pharmacological approaches to rescue cortical dysfunction. These findings contribute to ongoing translational and clinical development efforts with the goal of providing better treatments to people living with debilitating psychiatric diseases.

5.1 M_1 Muscarinic Receptors and PTSD

Using an optogenetic approach, we identified that M_1 muscarinic receptor activation induces a form of LTD at vHipp and BLA, but not MDT, inputs to layer V of the PL cortex. Based on the involvement of muscarinic receptors (*510*) as well as the PL cortex, vHipp, and BLA in fear learning and extinction (*80*), we observed that M_1 muscarinic receptor function is required for

contextual but not cued fear extinction. Finally, we demonstrated that the M_1 PAM VU0453595 enhanced contextual fear extinction recall in the SEFL model of PTSD, suggesting that M_1 PAMs may have clinical utility to enhance exposure therapy for PTSD patients. These findings are interesting in light of recent clinical trials investigating M_1 PAMs as treatments for Alzheimer's disease and schizophrenia. Our work in Chapter III therefore identifies PTSD as another disease in which these compounds may have clinical efficacy. While exciting, there are still many outstanding questions surrounding the mechanism and utility of M_1 PAMs for this indication.

An important caveat of our findings is the lack of a causative link between our *ex vivo* slice studies and the *in vivo* behavioral effects of M_1 receptor manipulation. Our *in vivo* investigation of M_1 function involved systemic administration of the compounds and M_1 receptors are expressed in other cortical regions, the hippocampus, the dorsal and ventral striatum, and thalamic regions (*431*). Therefore, it is possible that the actions of M_1 antagonism and potentiation in our work are due to modulation of M_1 receptor signaling in brain regions other than the PFC. While we attempted to address this with a viral-mediated approach to knockdown M_1 selectively in the PL cortex, we were unable to achieve sufficient genetic deletion to eliminate the muscarinic LTD measured using extracellular recordings thus preventing us from using this approach in our behavioral assays. Future development and optimization of a technique to allow for a more complete knockout of M_1 that is still spatially-restricted is therefore necessary. Direct site infusion of an M_1 antagonist may circumvent this issue but we have observed that compounds such as VU0255035 and VU0453595 tend to precipitate and produce necrosis in the surrounding tissue when used in this manner. Therefore, demonstrating causation will be difficult until subtype-selective antagonists are developed that are more amenable to this approach. Alternatively, an improved understanding of the molecular mechanism(s) underlying muscarinic LTD may allow for PL cortex-specific genetic or pharmacological approaches that are more achievable with currently available tools.

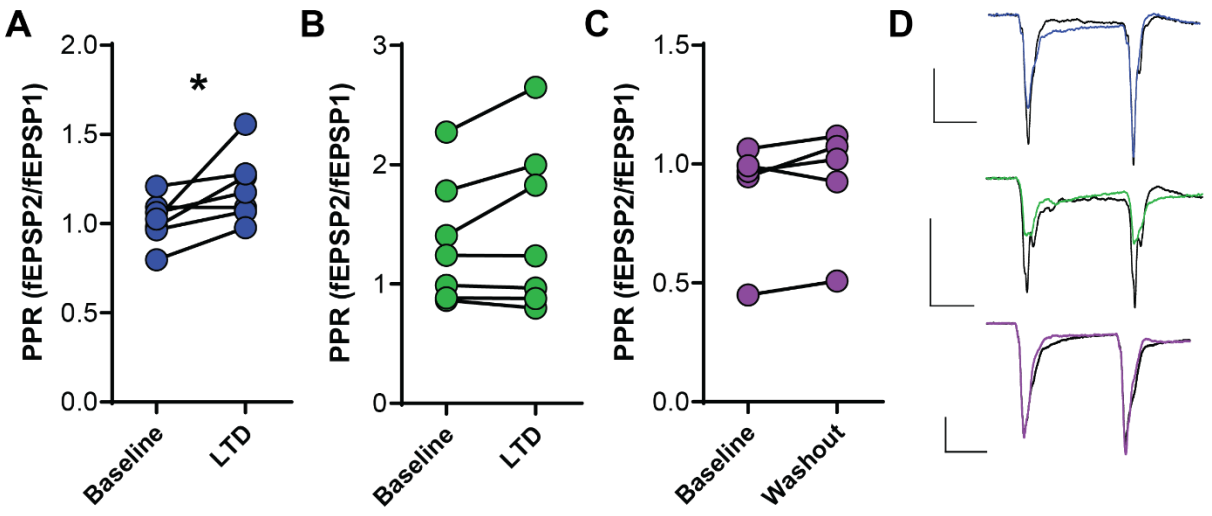

Figure 30: Paired-pulse ratio values at different inputs to the PFC related to Figure 11. **(A)** OxoM bath application results in a long-term increase in PPR after drug washout that correlates with LTD at vHipp-PFC synapse (*blue*, two-tailed paired t-test, p = 0.034). **(B)** No significant change in PPR was observed at the BLA-PFC synapse (green, p = 0.14) at the time point when LTD is present. **(C)** No change in PPR at the MDT-PFC synapse (*purple*) was observed (p = 0.23). **(D)** Sample traces of paired pulse recordings. Baseline is depicted in black, LTD/washout time point is depicted in the corresponding color for each input. Scale bars = 0.2mV and 20ms.

As described in Chapter I, muscarinic LTD in the PL cortex has been described by various labs with differing mechanistic explanations (*242–244*, *247*). Our observation of input-specificity further adds to the complexity and may indicate different mechanisms are occurring at different synapses. While our work in Chapter III did not focus on the molecular mechanisms involved in vHipp- or BLA-PFC LTD, we did observe a significant increase in the paired-pulse ratio (PPR) of fEPSPs at the LTD time point at vHipp- but not at the BLA- or MDT-PFC input (Figure 30), suggesting involvement of a presynaptic mechanism at the vHipp-PFC synapse. Our group and others have reported an increase in PPR that correlates with muscarinic LTD of fEPSPs recorded in layer V in response to both superficial and deep layer stimulation (*244*, *247*), therefore vHipp-PFC muscarinic LTD may share a presynaptic mechanism with LTD induced in the local PFC circuits. One group has suggested that muscarinic LTD of layer V-to-V synapses is mediated by the postsynaptic production of the endocannabinoid 2-arachidonylglycerol (2-AG) which activates CB_1 receptors on the presynaptic terminal to reduce glutamate release (*247*) but it remains to be

seen if this is true for vHipp-PFC muscarinic LTD. Recently, we reported that M_1 receptor-mediated LTD at layer II/III-to-V synapses requires phospholipase D (PLD) activity while other M_1-dependent effects do not (*248*). This finding could provide a useful way to selectively investigate the involvement M_1 plasticity in behavioral effects while not perturbing other M_1-mediated physiological responses although the involvement of PLD in input-specific muscarinic LTD is still unclear and inhibiting the ubiquitously-expressed enzyme in a spatially-restricted manner may be difficult. Overall, there is still a lack of mechanistic knowledge about muscarinic LTD, especially at the vHipp and BLA synapses in the PL cortex, but identification of necessary molecular mediators in the future will hopefully allow for the identification of behaviors that require these forms of plasticity and studies to corroborate our correlative findings.

At a microcircuit level, it is possible that muscarinic LTD is mediated by an increase in feedforward inhibition from the vHipp and BLA. Both the vHipp and BLA inputs synapse onto PFC interneurons and can drive feedforward inhibition onto deep layer pyramidal neurons (*63*, *65*). M_1 muscarinic receptors are expressed on both PV and SST interneurons therefore it is possible that M_1 activation induces an LTP of vHipp and BLA excitatory drive onto PFC GABAergic interneurons that results in a network-level LTD of synaptic transmission measured extracellularly. While our whole-cell experiments of vHipp-PFC LTD were performed with recording conditions where the contribution of $GABA_A$ receptor-mediated Cl^- flux should be negligible, we did not record in the presence of a $GABA_A$ receptor channel blocker and shunting inhibition could still be involved in the LTD. Similarly, our extracellular recordings were performed in the absence of a $GABA_A$ receptor antagonist leaving open the possibility of a GABAergic mechanism of muscarinic LTD. To address this, we performed preliminary experiments in GABAergic neuron-specific M_1 knockout mice by crossing GAD2-Cre mice expressing Cre recombinase under the GAD65 promoter with *Chrm1*$^{loxP/loxP}$ mice. There was no effect of this genetic manipulation on muscarinic LTD at the vHipp-PFC synapse (Figure 31, Page 134), arguing against interneuron involvement at this synapse. However, we cannot rule out compensatory mechanisms that occur upon genetic

deletion that may mask a role of the GABAergic system. Furthermore, we cannot exclude a role of interneuron M_1 receptors in the behavioral effects of M_1 receptor manipulation on fear extinction but these mice will be useful to determine the effects of M_1-mediated interneuron modulation on behavior in future studies.

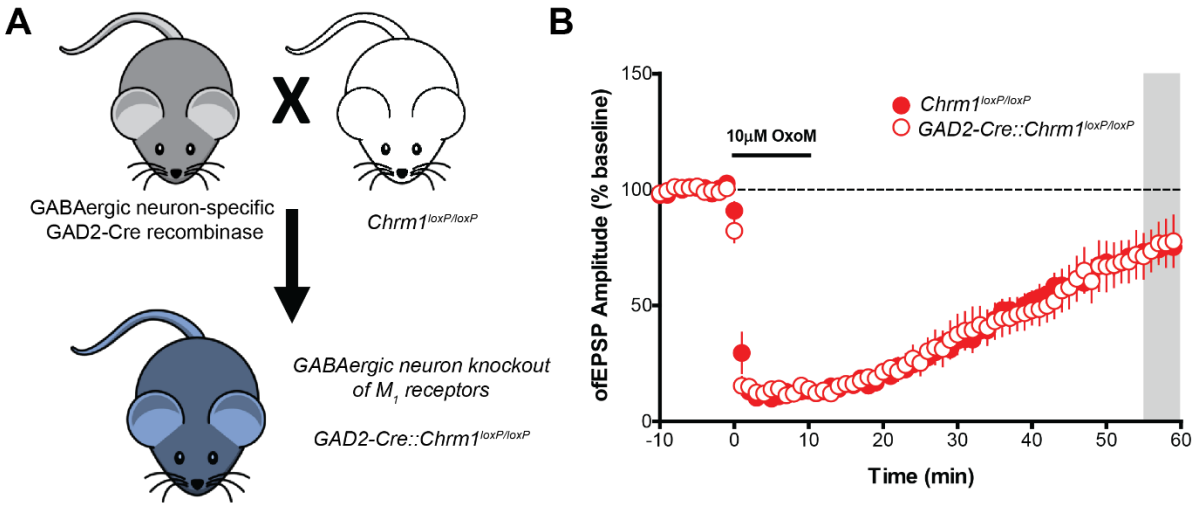

Figure 31: Mice genetically lacking M_1 muscarinic receptors in GABAergic neurons still exhibit vHipp-PFC muscarinic LTD. **(A)** Breeding scheme to generate interneuron-specific M_1 knockout mice by breeding GAD2-Cre mice with *Chrm1*$^{loxP/loxP}$ mice. **(B)** Time course of OxoM-induced LTD of vHipp-evoked ofEPSPs recorded in layer V PL cortex. No difference was observed between littermate controls and GAD2-Cre::*Chrm1*$^{loxP/loxP}$ mice (n / N = 5-6 slices from 3 – 4 mice per group).

Our *ex vivo* results with the M_1 antagonist VU0255035 also identified a potential role of other muscarinic receptors at the BLA-PFC synapse. While VU0255035 completely blocked the OxoM-induced LTD at the vHipp input, it only partially attenuated the LTD at the BLA input. This suggests that there is another form of LTD at this synapse that is mediated by muscarinic receptors other than M_1. It has been suggested that M_2 receptors might mediate LTD in the PFC (*245*) although the compounds used in this study exhibit poor subtype selectively. In addition to M_1 receptors, M_4 muscarinic receptors are abundantly expressed in the PFC (*431*) and M_4 PAMs have been shown to have procognitive efficacy in PFC-dependent tasks (*589*, *590*). We therefore utilized a recently-developed M_4 selective antagonist VU6013720 to test the hypothesis that M_4

muscarinic receptors mediate the M_1-independent muscarinic LTD at the BLA-PFC synapse. Our preliminary data indicate that M_4 antagonism alone partially attenuates the Oxo-M-induced LTD at this synapse, comparable to LTD observed in the presence of the M_1 antagonist (Figure 32). Furthermore, a combination of VU0255035 and VU6013720 completely blocked BLA-PFC muscarinic LTD suggesting that there is an M_4-dependent LTD at this synapse. It will be interesting in the future to determine if M_4 is acting pre- or postsynaptically to mediate this effect and the functional consequences of this form of plasticity.

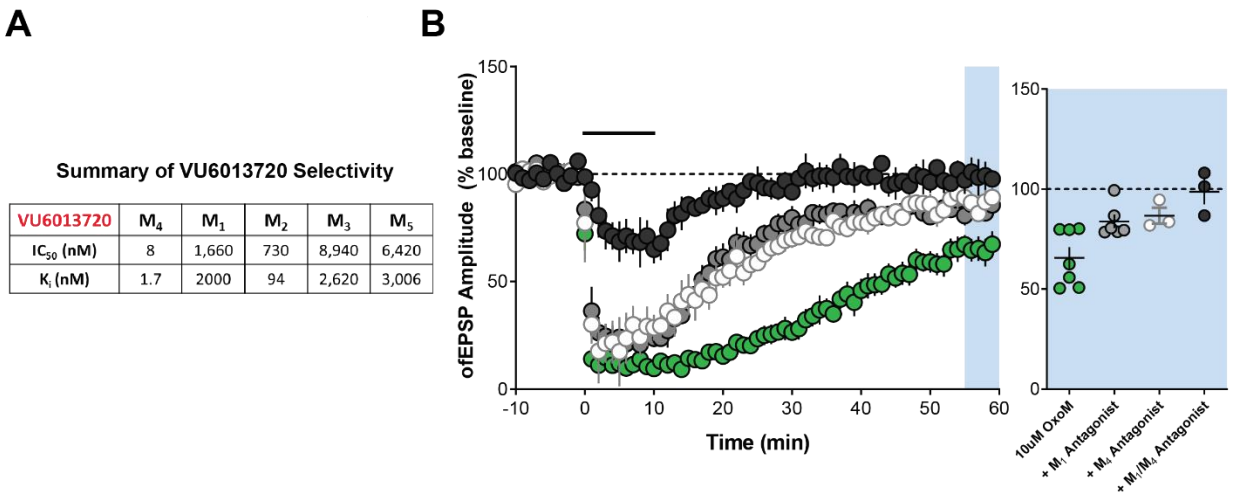

Figure 32: M_4 muscarinic receptors may mediate a form of LTD at the BLA-PFC synapse. **(A)** *In vitro* characteristics of the M_4 antagonist VU6013720. **(B)** Time course and summary of LTD induced by 10μM OxoM at the BLA-PFC synapse in the presence of the M_1 antagonist (10μM VU0255035), M_4 antagonist (500nM VU6013720), or a cocktail of both antagonists.

In relation to the involvement of M_4 in this circuit, a previous study reported that systemic administration of the pan-muscarinic receptor antagonist scopolamine before cued fear extinction impairs cued extinction recall (*510*). Interestingly, we found no effect of systemic administration of a selective M_1 muscarinic receptor antagonist on cued fear extinction. Taken together, these data may suggest that a different muscarinic receptor subtype is required for cued fear extinction. The possible involvement of M_4 in the BLA-PFC muscarinic LTD may be related to this behavioral effect and M_4 receptors may be necessary for cued fear extinction while M_1 receptors are

necessary for contextual fear extinction. It will be important to replicate these scopolamine findings but the future development of an M_4 antagonist that has suitable pharmacokinetic properties for *in vivo* use would allow to test this hypothesis. While VU6013720 exhibits properties that complicate its *in vivo* use, there are multiple M_4 PAMs with excellent *in vivo* characteristics that can be used to test whether M_4 potentiation could enhance cued fear extinction or rescue deficits in PTSD models.

Inactivation studies have revealed that the PL cortex is required for fear expression while the IL cortex is necessary for the acquisition and recall of fear extinction (*80*). We identified that M_1 receptor-mediated LTD of vHipp and BLA inputs occurs in the PL cortex and hypothesize that this LTD would decrease the activity of the PL cortex during extinction learning and consolidation, therefore reducing fear expression during recall. The vHipp, BLA, and MDT all densely innervate the IL cortex as well (*35*) and subsequent studies will be necessary to assess the functional consequences of M_1 activation at these synapses. Demonstrating a role of muscarinic receptors in the IL cortex in fear learning, systemic administration of an M_1/M_3-preferring agonist cevimeline enhances cued fear extinction while direct site infusion of scopolamine into the IL cortex impairs cued extinction recall (*510*). These behavioral effects were attributed to a muscarinic receptor modulation of IL cortex pyramidal neuron excitability (*510*) but the cevimeline effect could reflect engagement of the PL cortex LTD mechanisms we described as well as increases in IL cortex excitability. While we found that cued fear extinction is not M_1 receptor-dependent, it is possible that M_1 activation or potentiation could augment cued extinction via similar synaptic mechanisms that are recruited during contextual fear extinction and this could be tested with subtype selective PAMs. M_1 receptor activation also increases the excitability of PL cortex pyramidal neurons (*420*, *421*) but combined with LTD induction at the vHipp and BLA synapses, this may selectively increase PL cortex output in response to other inputs, such as from the MDT or contralateral cortex. Similar network level mechanisms could occur in the IL cortex but it will be necessary to investigate whether M_1 LTD is present and its input-specificity in the IL cortex first.

While the specificity of muscarinic LTD to the vHipp and BLA inputs to the PFC is interesting, the lack of LTD at the MDT input is equally as intriguing. As described in chapter I, the PL cortex has been historically defined as a region that receives dense innervation from the MDT, which primarily terminates in layer I and III forming synapses with both superficial and deep layer pyramidal neurons (*35*, *36*). We did not investigate the reasons underlying a lack of LTD at MDT-PFC synapses and without a mechanistic understanding of muscarinic LTD at other synapses, it will be difficult to determine why this synapse is resistant to LTD induction by muscarinic agonists. It is possible that MDT synapses do not contain the necessary molecular components or that they are not localized in a manner conducive to LTD induction. The simplest explanation is that dendritic spines targeted by MDT inputs do not express M_1 muscarinic receptors though this would likely require investigation by super-resolution or electron microscopy. Functionally, we interpreted the input-specificity of muscarinic LTD as a selective modulation of inputs related to certain behavioral states but it may also produce a heterosynaptic increase in the gain of MDT drive. Therefore, a pyramidal neuron that receives input from all three afferent areas may be more responsive to MDT inputs after M_1 activation, especially based on the more distal dendritic localization of MDT synapses compared to vHipp- and BLA inputs onto the same cell (*43*). Behaviorally, this could relate to cholinergic modulation of attention and working memory, both of which require intact MDT-PFC communication (*58*, *120*). While other input-specific forms of plasticity have been observed in the PL cortex (*195*), the biochemical and behavioral consequences of the lack of LTD at certain inputs still remain unclear and warrant future investigation.

Our work demonstrating that an M_1 PAM can enhance fear extinction consolidation in the SEFL model of PTSD suggests that M_1 PAMs may be efficacious adjunct treatments to improve the efficacy of exposure therapy in the clinic. Pharmacological interventions so far have had some success in the clinic when used to augment exposure therapy. The SSRI paroxetine combined with prolonged exposure therapy was found to be more efficacious than exposure therapy alone

in a small clinical trial of PTSD patients (*591*). In patients that were resistant to both exposure therapy and SSRIs, enhancing dopamine and serotonin release with MDMA (recreationally known as Ecstasy) significantly enhanced the efficacy of exposure therapy (*592*) and the majority of patients treated with MDMA experienced long-lasting reductions in PTSD symptoms years later (*593*). These results have led the FDA to grant Breakthrough Therapy status to MDMA for the treatment of PTSD and multiple phase III trials are currently ongoing. The effect of augmenting NMDA receptor function with D-cycloserine on exposure therapy in PTSD has also been clinically tested based on initial results in patients with phobias (*594*) but there have been mixed results in PTSD (*595*), although patients with severe symptoms appear to receive some clinical benefit from the combination compared to exposure therapy alone (*596*, *597*). These compounds also enhance fear extinction in preclinical rodent models (*595*), supporting the predictive validity of using fear extinction in animal models to develop novel pharmacological approaches to augment exposure therapy in the clinic. Excitingly, multiple M_1 PAMs are currently completing or have completed phase I safety trials in humans and therefore clinical efficacy trials in PTSD patients with M_1 PAMs may be possible in the future.

Finally, we focused our preclinical efficacy studies on a model of PTSD based on M_1-mediated modulation of the vHipp-BLA-PFC fear circuitry but these circuits as well as fear learning are also perturbed in other psychiatric diseases. In addition to PTSD, other stress and anxiety disorders produce heightened fear and reactivity and augmenting exposure therapy has some clinical efficacy in patients with panic disorder, social anxiety disorder, and debilitating phobias (*595*). Therefore, M_1 PAMs may be efficacious in other anxiety disorders in addition to PTSD. Furthermore, fear extinction is impaired in patients with schizophrenia (*538*, *598*) and this is recapitulated in preclinical animal models (*599*). Relevant to our findings, the induction of LTD at the BLA-PFC synapse *in vivo* is impaired in the MAM-model of schizophrenia, correlating with fear extinction deficits in these animals (*599*). Therefore, based on our discovery of an M_1 receptor-mediated LTD at the BLA-PFC synapse, M_1 PAMs may be able to rescue this LTD deficit.

We have also observed *ex vivo* muscarinic LTD deficits in subchronic PCP-treated mice and GluN1 knockdown mice (*244*, *441*). Interestingly, M_1 PAMs can rescue the LTD deficits in both of these models and can reverse multiple cognitive deficits *in vivo*. Based on these results and the clinical efficacy observed with xanomeline (*413*), it is hypothesized that M_1 PAMs could be effective treatments for the cognitive and negative symptoms of schizophrenia. Our work suggests that they may also be effective in treating aberrant emotional reactivity and fear extinction deficits in patients with schizophrenia.

5.2 $mGlu_1$ receptors and Schizophrenia

Using whole-cell electrophysiology, we established that $mGlu_1$ activation and potentiation preferentially enhanced inhibitory transmission in the PFC, shifting the balance between excitation and inhibition in favor of inhibition. Furthermore, utilizing fMRI and behavioral assays we found that an $mGlu_1$ PAM reversed schizophrenia-like physiological and behavioral deficits induced by NMDA receptor hypofunction. Finally, we determined that $mGlu_1$ activation increased PFC inhibition via actions on SST interneurons and using *in vivo* optogenetics, we observed that the ability of an $mGlu_1$ PAM to rescue spatial working memory deficits was dependent on the function of these cells. The work described in Chapter IV suggests that $mGlu_1$ PAMs may be effective at treating the cognitive deficits of schizophrenia, providing an improvement over currently available antipsychotics. Furthermore, our work describes the identification and validation of $mGlu_1$ as a novel target to preferentially rescue cortical inhibitory deficits in patients with schizophrenia. Compared to M_1 PAMs, the translational and clinical efforts focusing on $mGlu_1$ PAMs are still in the early stages but our work supports future validation efforts and the continued development of $mGlu_1$ PAM clinical candidates.

Molecular and functional observations of inhibitory deficits in the dlPFC of schizophrenia patients are some of the more replicated clinical findings and it has been hypothesized that modulating the GABAergic system will have procognitive and antipsychotic efficacy (*558–561*).

An initial study found that an $\alpha_{2/3}$-selective $GABA_A$ receptor partial agonist improved cognitive performance and electrophysiological endpoints in a small set of chronic schizophrenia patients (*562*) but this effect was lost in a larger study (*600*), potentially due to the partial efficacy of the compound. PAMs of α_5-containing $GABA_A$ receptors have shown preclinical procognitive and antipsychotic efficacy (*563*, *564*, *569*) although intriguingly, α_5-selective NAMs also have procognitive effects in animal models (*565*, *601*) and are currently in clinical trials for cognitive impairments associated with schizophrenia (NCT02953639). Furthermore, increasing brain GABA concentrations with a GABA ester prodrug BL-1020/CYP-1020 demonstrated efficacy preclinically (*602*, *603*) and clinically (*566*) although a more recent clinical trial was terminated due to a lack of efficacy (NCT01363349). Finally, the GAT-1 inhibitor tiagabine is currently in a phase III trial (NCT00179465) for patients with early-stage schizophrenia and early disclosures have been promising (*567*). Therefore, there have been mixed results with pharmacological modulation of the GABAergic synapse though there are still promising clinical trials and preclinical development efforts underway.

An alternative approach to augment GABAergic transmission in the PFC is direct modulation of GABAergic interneuron activity. While hypothetically possible, identification of interneuron-specific druggable targets has proven difficult. To circumvent this issue, many groups have utilized opto- and chemogenetic approaches to selectively enhance or inhibit the function of different interneuron populations in preclinical disease models (*55*, *151*, *156*, *159*, *162*, *165*). These approaches are useful for understanding disease biology and the general effects of interneuron modulation but the clinical utility of these approaches remains unclear until genetic delivery of the actuators are proven safe in humans (*604*). Until then, identification of pharmacological targets with drugs or biologics that can be delivered systemically provide the best chances for clinical development. In Chapter IV, we found that $mGlu_1$ is expressed in SST interneurons in the rodent PFC and despite expression in other cell types, the functional effects of $mGlu_1$ activation were generally restricted to augmentation of SST interneuron activity and

consequently inhibitory transmission onto pyramidal neurons. As $mGlu_1$ is a GPCR expressed on the cell surface amenable to pharmacological intervention, we therefore have identified $mGlu_1$ as a druggable target that is enriched in a subtype of PFC interneurons and with the ongoing development of subtype selective PAMs, we were able to validate $mGlu_1$ as a potential target using preclinical models of schizophrenia.

Excitingly, we observed efficacy in reversing NMDA receptor antagonist-induced cognitive deficits relevant to schizophrenia. It will be essential in the future to test whether $mGlu_1$ PAMs have broad behavioral efficacy in other cognitive assays and in models of the negative symptoms of the disorder, as well as the extent of SST interneuron involvement in any of these effects. Consistent with our mechanistic work in brain slices, we identified that $mGlu_1$ PAM efficacy in the Y-maze task required PFC SST interneuron activity. This is consistent with the involvement of the PFC in spatial alternation (*158*, *161*). Interestingly, PFC SST interneurons themselves appear to be dispensable for this behavior, as optogenetic inhibition alone did not impair performance. This is in line with studies finding no effect of PFC SST interneuron ablation on Y-maze performance (*161*) and no effect of optogenetic inhibition on T-maze delayed alternation performance at short delays (*159*) which are similar to the time between arm entries in a spontaneous alternation task. On the other hand, ablation of PFC PV interneurons induces a deficit in Y-maze performance and based on *in vivo* electrophysiology studies (*356*), it is thought that PFC PV interneuron dysfunction produces cognitive deficits including impaired Y-maze performance induced by NMDA receptor antagonism. Contrary to this, optogenetic inhibition of PV neurons did not impair performance at any delay in a delayed alternation T-maze spatial working memory task (*159*) but the effects of real-time PV interneuron inhibition in the spontaneous alternation task have not been tested.

While modulation of SST interneurons is necessary for efficacy in the Y-maze task, the preferential actions of an $mGlu_1$ PAM on PFC SST interneurons might be predicted to disrupt the balance of inhibition mediated by SST and PV interneurons. The functional and behavioral consequences of perturbing this balance is unknown but we did not observe any behavioral

disruption in mice that were treated with the $mGlu_1$ PAM alone. Furthermore, optogenetically increasing or decreasing PFC PV interneuron activity in mice does not impair social interaction behavior (*151*, *156*) and optogenetic inhibition does not impair spatial working memory performance (*159*). A recent study also reported no social interaction or recognition deficits in a three-chamber task upon optogenetic inhibition of SST interneurons (*605*). However, enhancing PFC PV interneuron activity when there is a behavioral deficit is capable of rescuing cognitive and social deficits (*55*, *151*, *156*). Our results are consistent with these findings in that the $mGlu_1$ PAM alone has no effect on cognition but is able to rescue MK-801-induced deficits. Altogether, this would suggest that the range of acceptable balance between SST- and PV-mediated inhibition is fairly wide under normal conditions such that increasing or decreasing the activity of one subtype does not induce functional deficits alone. Conversely, under conditions of PFC dysfunction selective enhancement of one subtype appears sufficient to rescue behavioral deficits. Although our *in vivo* optogenetic results imply that PFC SST interneuron activity is necessary for $mGlu_1$ PAM efficacy in the Y-maze, we cannot also rule out the role of PV interneurons *in vivo* as we did not directly test for this. In slices, $mGlu_1$ activation affects PV interneurons and it is possible that these effects *in vivo* may be more substantial than observed *ex vivo* and this will be interesting to determine in future studies.

The observation that an $mGlu_1$ PAM can rescue cognitive deficits via actions on SST interneurons might suggest that the $mGlu_1$ PAM rescues inhibitory deficits *in vivo*. Systemic MK-801 administration results in a disinhibition of PFC pyramidal neurons (*356*) and aberrant gamma oscillations (*606*) *in vivo* modelling the cortical inhibitory deficits observed in schizophrenia. The majority of studies investigating these inhibitory deficits in animal models have been performed using *in vivo* techniques, therefore it is unclear if these deficits can be observed in *ex vivo* preparations more amenable to mechanistic studies. To address this, we initially prepared acute PFC slices shortly after *in vivo* administration of a high dose of MK-801 but did not observe any deficits in basal neurotransmission onto layer V pyramidal neurons in the PL cortex (Figure 33,

Page 143). We hypothesize that this lack of effect in slices could reflect a necessity for intact subcortical-cortical networks for NMDA receptor antagonism-induced deficits (*360*, *398*, *607*). Consistent with this, bath application of NMDA receptor antagonists in acute PFC slices affects both excitatory and inhibitory neurotransmission, resulting a reduced firing of pyramidal neurons (*577*) and implies that *ex vivo* preparations are not suitable for studying acute NMDA receptor antagonist effects of disinhibition. It will be necessary to use *in vivo* approaches in the future to study whether NMDA receptor-induced inhibitory deficits can be rescued by $mGlu_1$ PAMs. Our fMRI results demonstrate that VU6004909 can reverse broad cortical hyperactivity measured using BOLD signals and while this is consistent with MK-801-induced disinhibition, fMRI cannot discriminate between the activity of neuronal subtypes in the PFC. Interestingly, a recent report has observed SST interneuron dysfunction in the ACC after acute ketamine administration using two-photon *in vivo* Ca^{2+} imaging (*543*) but technical limitations prevented observation of SST dysfunction correlating with behavioral tasks. Future work utilizing freely-moving *in vivo* Ca^{2+} imaging techniques such as fiber photometry or miniscopes, as well as opto-tagged single-unit or *in vivo* whole-cell recordings will allow for the study of NMDA receptor antagonism on PFC SST interneuron function during behavioral tasks and whether an $mGlu_1$ PAM rescues physiological deficits *in vivo*.

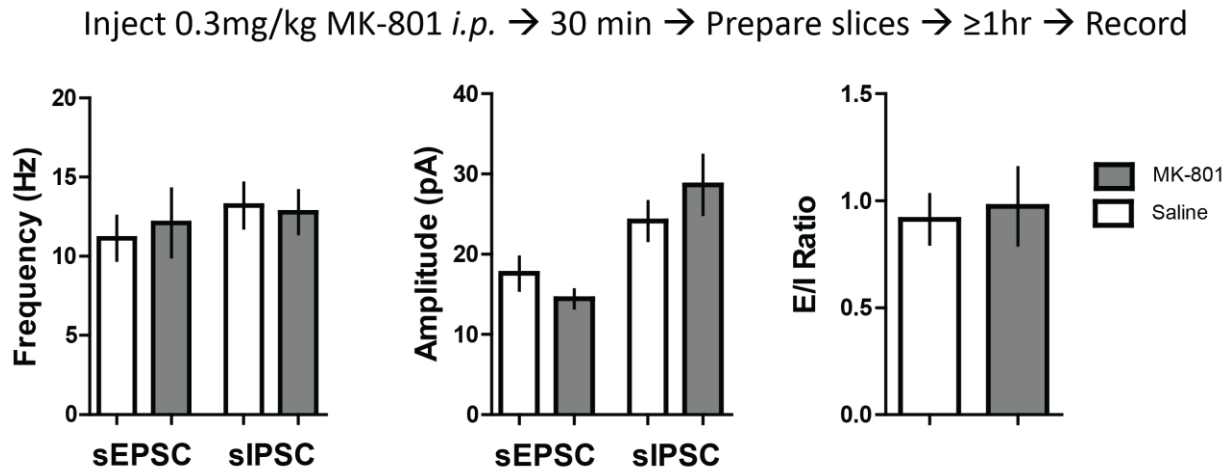

Figure 33: Effect of *in vivo* systemic MK-801 administration on basal synaptic properties of layer V pyramidal neurons in PL cortex slices. No effect on sEPSC frequency (unpaired Student's t-test, p = 0.71) or amplitude (p = 0.20) nor sIPSC frequency (p = 0.84) or amplitude (p = 0.32). The ratio of sEPSC to sIPSC ratio (E/I ratio) within each cell was also not different between groups (p = 0.78; n/N = 12 slices from 3 mice per group).

Although acute NMDA receptor antagonism clinically recapitulates positive, negative, and cognitive symptoms of schizophrenia in healthy volunteers and produces physiological changes consistent with those observed in schizophrenia patients, it is thought to mimic episodes of psychosis rather than the chronic disease (*398*). Furthermore, efficacy in preclinical studies using acute antagonist models could potentially reflect displacement of the antagonist rather than a rescue of functional deficits. Novel symptomatic treatments for schizophrenia will likely require chronic dosing and acute NMDA receptor antagonism precludes the ability to assess chronic efficacy. Therefore, in the future it will be necessary to determine the efficacy of $mGlu_1$ PAMs in reversing physiological and behavioral deficits in schizophrenia-like models aside from acute MK-801 administration. One such model involves mice in which the GluN1 subunit of the NMDA receptor has been knocked down to approximately 10-20% of wildtype levels (*608*). *In vivo* recordings demonstrate an increased firing rate of deep layer PFC neurons in these GluN1 knockdown mice (*441*), similar to acute NMDA receptor antagonism. To test if we could observe this in acute slices, we performed preliminary *ex vivo* experiments and found that layer V

pyramidal neurons in the PL cortex of GluN1 knockdown mice are hyperexcitable compared to cells from littermate controls (Figure 34). Thus, unlike acute MK-801, GluN1 knockdown mice may permit us to study PFC microcircuit dysfunction in a disease-like condition. Future studies will hopefully shed light on whether $mGlu_1$ PAMs are capable of rescuing physiological and behavioral deficits in this model and contribute to an improved mechanistic understanding of $mGlu_1$ PAM efficacy in various models of schizophrenia and cortical dysfunction.

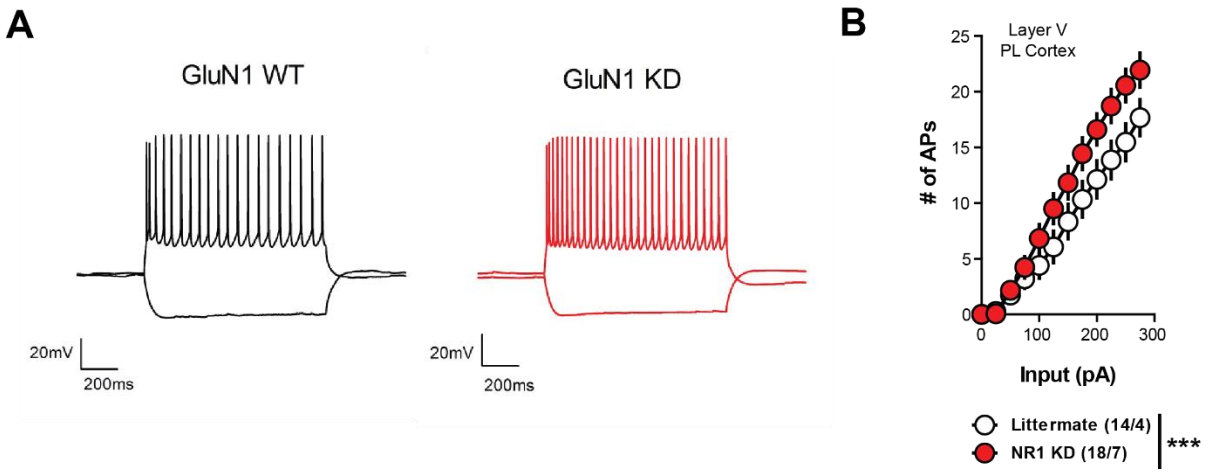

Figure 34: Genetic knockdown of the GluN1 NMDA receptor subunit produces cortical hyperexcitability. **(A)** Representative traces of action potential firing in response to current injection in layer V neurons. **(B)** Layer V pyramidal neurons in the PL cortex are hyperexcitable in GluN1 KD slices compared to littermate controls (two-way ANOVA, main effect of genotype, $F_{(1,372)} = 29.5$, $p < 0.0001$).

It will also be important to test $mGlu_1$ PAM efficacy in schizophrenia-like models that do not involve direct NMDA receptor manipulations including developmental manipulations such the MAM model and genetic models based on clinical data such as *Df(16)A*$^{+/-}$ mice (*609*). Efficacy observed across etiologically-distinct models would further support the hypothesis that $mGlu_1$ PAMs are efficacious therapeutics across all symptom domains of schizophrenia. Furthermore, the use of multiple models could improve future clinical trial design for $mGlu_1$ PAMs regarding patient and outcome selection. The hyperactivity we modelled in our work with NMDA receptor antagonism most closely recapitulates cortical hyperactivity and inhibitory deficits seen in the early stages of schizophrenia (*361*). Therefore, our results may support $mGlu_1$ PAM treatment for

schizophrenia patients early in disease progression but little is known about the potential effects of $mGlu_1$ potentiation in older patients. Chronic schizophrenia patients typically present with resting hypofunction of the dlPFC (*610*) therefore enhancing inhibition at these stages might not be as efficacious. Despite resting hypofrontality, the dlPFC in chronic schizophrenia patients still exhibits hyperactivity during working memory tasks (*611*) therefore an $mGlu_1$ PAM might still be effective. In fact, this might suggest that similar to M_1 (*437*) and $mGlu_5$ PAMs (*438*), the ideal $mGlu_1$ PAM clinical candidate would have pure PAM activity devoid of intrinsic agonism to avoid enhancing inhibition when $mGlu_1$ would not normally be activated by endogenous glutamate. Hopefully in the future an improved set of $mGlu_1$ PAM tool compounds will allow for the identification of the ideal pharmacodynamics properties that optimize efficacy and minimize any potential adverse effects of $mGlu_1$ PAMs.

It will also be critical to determine the molecular mechanism(s) mediating $mGlu_1$ PAM effects on physiology and behavior. This is especially important in light of recent observations of GPCR PAM signal bias and its relation to efficacy and toxicity (*248*, *612*, *613*). Furthermore, mGlu receptors function as homo- and heterodimers and there have been examples of differential pharmacology depending on the dimerization partners of certain mGlu receptors (*614*, *615*). Our work in Chapter IV focused on the circuit-level mechanism of $mGlu_1$ PAM action but future studies should investigate the molecular mechanism. The $mGlu_1$-mediated depolarization of SST interneurons likely involves either a closing of leak potassium channels or activation of TrpC channels, both of which have been shown to be downstream of $mGlu_1$ activation in other brain regions (*548*, *616*). Additionally, endogenous activation of $mGlu_1$ following high-frequency stimulation can elicit a slow EPSC in hippocampal interneurons and cerebellar neurons (*617*), but whether this occurs in PFC SST interneurons is unknown and would be relevant to $mGlu_1$ PAM action. We also only studied the short-term effects of $mGlu_1$ activation and potentiation therefore the long-term consequences of $mGlu_1$ activation remain to be explored. In other brain regions, $mGlu_1$ is involved in synaptic plasticity (*97*, *497*, *618*) and is known to mediate a form of LTP onto

hippocampal SST-positive oriens lacunosum-moleculare interneurons (*497*). Using extracellular field recordings, some groups have observed an LTD in the PFC upon group I mGlu receptor activation (*234*, *619*). It is possible that this observation reflects a network level effect of LTP onto SST interneurons although this remains untested. Understanding of the function of $mGlu_1$ in the brain has largely been hampered by a lack of subtype selective compounds but with the continued development of novel $mGlu_1$ PAM and NAM tool compounds, it will become possible to determine the function of $mGlu_1$ in various cell types and at multiple synapses. The ability to conditionally restrict $mGlu_1$ expression genetically will also improve our knowledge of $mGlu_1$ function in the brain. While *Grm1* KO mice exist, they display cognitive deficits and develop fatal ataxia during adolescence limiting their utility (*584*, *585*, *618*). Thus, generation of $mGlu_1$ floxed mice in the future will be essential to improving our understanding of the biology of $mGlu_1$ in discrete cells and circuits.

Relatedly, while we demonstrated that PFC SST interneuron function is necessary for the $mGlu_1$ PAM efficacy in reversing Y-maze deficits, this does not definitively demonstrate that $mGlu_1$ on SST interneurons is responsible. It is possible that $mGlu_1$ potentiation recruits circuit-level effects that require SST interneurons but that the locus of $mGlu_1$ activation is on a different cell type or in a different region. The development of $mGlu_1$ floxed mice and the subsequent conditional deletion of $mGlu_1$ from PFC SST interneurons will thus be required to definitively make the conclusion that $mGlu_1$ PAMs exert their effects through $mGlu_1$ activation on SST interneurons. Conditional mice will also allow us to determine the contribution of $mGlu_1$ modulation of PFC SST interneurons to the other effects of an $mGlu_1$ PAM observed previously (*486*). The efficacy of an $mGlu_1$ PAM in reversing positive symptom-like hyperlocomotion and deficits in PPI induced by amphetamine has been attributed to a local inhibition of dopamine release in the dorsal striatum, hypothesized to be mediated by $mGlu_1$ on dopamine D_1.receptor-expressing spiny projection neurons (*486*). NMDA receptor antagonists increase striatal dopamine release (*400*) and induce hyperlocomotion and deficits in PPI similar to amphetamine. It will be interesting in the future to

determine if $mGlu_1$ PAMs exert efficacy in reversing these deficits and if so, whether these effects are mediated by $mGlu_1$ in the dorsal striatum or in the PFC, but this will require $mGlu_1$ floxed mice. These mice would also be useful to explain the similar behavioral effects of $mGlu_1$ PAMs and NAMs in reversing hyperlocomotion and PPI deficits (*487*, *488*), potentially related to excitatory actions of $mGlu_1$ on dopaminergic neuron firing and inhibitory actions of $mGlu_1$ on striatal dopamine release.

Furthermore, our work described in Chapter IV may explain the cognition-disrupting effects of $mGlu_1$ NAMs that halted their development for the treatment of pain (*494*, *620*). Based on the procognitive effects of $mGlu_1$ PAMs described in our work, we would hypothesize that an $mGlu_1$ NAM might impair PFC SST interneuron function and produce deficits in cognition. Therefore, while $mGlu_1$ NAMs may have similar efficacy to $mGlu_1$ PAMs in positive symptom-like assays, we predict that they will exacerbate cognitive deficits in schizophrenia that would preclude their effectiveness. Alternatively, $mGlu_1$ NAMs may possess rapid, antidepressant-like efficacy based on $mGlu_1$ modulation of PFC SST interneurons. While the NMDA receptor antagonist ketamine produces psychotomimetic effects in healthy individuals, at low doses it results in a rapid and sustained antidepressant efficacy and is clinically-approved for treatment-resistant depression (*621*). Similarly, while M_1 PAMs are preclinically efficacious in schizophrenia-like models, scopolamine exerts rapid antidepressant efficacy in humans (*622*) and the M_1 selective antagonist VU0255035 recapitulates this in animal models (*511*). In mice lacking M_1 receptors in PFC SST interneurons, this antidepressant-like effect of scopolamine is absent, findings interpreted to mean that acute inhibition of PFC SST interneurons results in antidepressant-like effects similar to ketamine. Combined with our observation that $mGlu_1$ activation increases SST interneuron activity, we would predict that an $mGlu_1$ NAM might have rapid, antidepressant-like efficacy by engaging a similar mechanism. This is an exciting potential implication of our work and warrants future investigation.

Finally, although we focused on validating $mGlu_1$ PAM efficacy in the context of schizophrenia, $mGlu_1$ potentiation may have clinical utility in multiple disorders with perturbed excitation-inhibition balance or SST interneuron dysfunction. For example, a mouse model of the Dravet syndrome, a form of intractable epilepsy, exhibits deficits in cortical SST interneuron function that likely contribute to disease progression (*623*). Other forms of epilepsy also involve disruption of inhibitory transmission in the cortex and hippocampus (*587*). Therefore, enhancing SST interneuron function with an $mGlu_1$ PAM might have efficacy in Dravet and other epilepsy syndromes. Furthermore, $mGlu_1$ PAMs could be therapeutic for neurodegenerative disorders such as Alzheimer's disease and Parkinson's disease based on recent preclinical findings. In an Alzheimer's disease model, the morphology and function of SST-positive hippocampal interneurons are impaired by amyloid-beta (*624*) and optogenetic activation of SST interneurons can rescue amyloid-beta-induced physiological deficits (*625*). In a Parkinson's disease model, optogenetic activation of cortical SST interneurons alleviates motor symptoms (*626*). Thus, in addition to schizophrenia, $mGlu_1$ PAMs may have efficacy in treating multiple psychiatric and neurological disorders via their actions on SST interneurons.

5.3 Conclusion

The work presented in this dissertation identifies and validates two novel pharmacological targets for the treatment of psychiatric disorders based on an improved understanding PFC function and dysfunction. We have demonstrated that an M_1 PAM has efficacy in augmenting fear extinction, derived from our discovery that M_1 activation selectively modulates fear-related inputs to the PFC. Using this macrocircuit-level approach, we have validated M_1 PAMs as potential therapeutics to enhance the efficacy of clinical exposure therapy for the treatment of PTSD. We also identified that $mGlu_1$ activation preferentially enhances inhibitory transmission in the PFC microcircuit. Based on this, we found that an $mGlu_1$ PAM can reverse cortical hyperactivity and proceeded to validate $mGlu_1$ PAMs as potential treatments for schizophrenia that have broad

efficacy across positive, negative, and cognitive symptom models of the disease. With continued validation of these targets and an improved mechanistic understanding of their efficacy in the future, both M_1 PAMs and $mGlu_1$ PAMs may ultimately be able to provide therapeutic value to patients suffering from PTSD and schizophrenia. This dissertation therefore lays the groundwork for continued translational and clinical development focused on these targets to one day deliver more efficacious and safer treatments to patients.

REFERENCES

1. P. Rakic, Evolution of the neocortex: a perspective from developmental biology. *Nat. Rev. Neurosci.* **10**, 724–735 (2009).

2. J. K. Rilling, T. R. Insel, The primate neocortex in comparative perspective using magnetic resonance imaging. *J. Hum. Evol.* **37**, 191–223 (1999).

3. J. H. Balsters *et al.*, Evolution of the cerebellar cortex: the selective expansion of prefrontal-projecting cerebellar lobules. *Neuroimage*. **49**, 2045–2052 (2010).

4. J. M. Fuster, in *International encyclopedia of the social & behavioral sciences* (Elsevier, 2001), pp. 11969–11976.

5. A. F. T. Arnsten, B.-M. Li, Neurobiology of executive functions: catecholamine influences on prefrontal cortical functions. *Biol. Psychiatry*. **57**, 1377–1384 (2005).

6. J. M. Fuster, G. E. Alexander, Neuron activity related to short-term memory. *Science*. **173**, 652–654 (1971).

7. S. Funahashi, C. J. Bruce, P. S. Goldman-Rakic, Mnemonic coding of visual space in the monkey's dorsolateral prefrontal cortex. *J. Neurophysiol.* **61**, 331–349 (1989).

8. J. V. Pardo, P. T. Fox, M. E. Raichle, Localization of a human system for sustained attention by positron emission tomography. *Nature*. **349**, 61–64 (1991).

9. G. McCarthy *et al.*, Functional magnetic resonance imaging of human prefrontal cortex activation during a spatial working memory task. *Proc. Natl. Acad. Sci. USA*. **91**, 8690–8694 (1994).

10. J. M. Harlow, Passage of an iron rod through the head. *Publications of the Massachusetts Medical Society (Boston)* (1868).

11. K. O'Driscoll, J. P. Leach, No longer Gage": an iron bar through the head. Early observations of personality change after injury to the prefrontal cortex. *BMJ*. **317**, 1673–1674 (1998).

12. S. M. Szczepanski, R. T. Knight, Insights into human behavior from lesions to the prefrontal cortex. *Neuron*. **83**, 1002–1018 (2014).

13. J. H. Callicott *et al.*, Physiological dysfunction of the dorsolateral prefrontal cortex in schizophrenia revisited. *Cereb. Cortex*. **10**, 1078–1092 (2000).

14. S. Grimm *et al.*, Imbalance between left and right dorsolateral prefrontal cortex in major depression is linked to negative emotional judgment: an fMRI study in severe major depressive disorder. *Biol. Psychiatry*. **63**, 369–376 (2008).

15. R. L. Aupperle *et al.*, Dorsolateral prefrontal cortex activation during emotional anticipation and neuropsychological performance in posttraumatic stress disorder. *Arch. Gen. Psychiatry*. **69**, 360–371 (2012).

16. G. Dawson, A. N. Meltzoff, J. Osterling, J. Rinaldi, Neuropsychological correlates of early symptoms of autism. *Child Dev.* **69**, 1276–1285 (2008).

17. N. J. Gamo, A. F. T. Arnsten, Molecular modulation of prefrontal cortex: rational development of treatments for psychiatric disorders. *Behav. Neurosci.* **125**, 282–296 (2011).

18. M. F. Green, Cognitive impairment and functional outcome in schizophrenia and bipolar disorder. *J. Clin. Psychiatry*. **67**, e12 (2006).

19. J. Bobes, M. P. Garcia-Portilla, M. T. Bascaran, P. A. Saiz, M. Bousoño, Quality of life in schizophrenic patients. *Dialogues Clin Neurosci*. **9**, 215–226 (2007).

20. A. P. Husa *et al.*, Lifetime antipsychotic medication and cognitive performance in schizophrenia at age 43 years in a general population birth cohort. *Psychiatry Res.* **247**, 130–138 (2017).

21. A. Cipriani *et al.*, Comparative efficacy and acceptability of 21 antidepressant drugs for the acute treatment of adults with major depressive disorder: a systematic review and network meta-analysis. *Lancet*. **391**, 1357–1366 (2018).

22. M. Huhn *et al.*, Comparative efficacy and tolerability of 32 oral antipsychotics for the acute treatment of adults with multi-episode schizophrenia: a systematic review and network meta-analysis. *Lancet*. **394**, 939–951 (2019).

23. E. J. Nestler, S. E. Hyman, Animal models of neuropsychiatric disorders. *Nat. Neurosci.* **13**, 1161–1169 (2010).

24. C. J. Donahue, M. F. Glasser, T. M. Preuss, J. K. Rilling, D. C. Van Essen, Quantitative assessment of prefrontal cortex in humans relative to nonhuman primates. *Proc. Natl. Acad. Sci. USA*. **115**, E5183–E5192 (2018).

25. J. L. VandeBerg, S. Williams-Blangero, Advantages and limitations of nonhuman primates as animal models in genetic research on complex diseases. *J Med Primatol*. **26**, 113–119 (1997).

26. M. Laubach, L. M. Amarante, K. Swanson, S. R. White, What, if anything, is rodent prefrontal cortex? *Eneuro*. **5** (2018), doi:10.1523/ENEURO.0315-18.2018.

27. M. Carlén, What constitutes the prefrontal cortex? *Science*. **358**, 478–482 (2017).

28. K. Brodmann, Vergleichende Lokalisationslehre der Großhirnrinde (1909).

29. T. M. Preuss, Do rats have prefrontal cortex? The rose-woolsey-akert program reconsidered. *J. Cogn. Neurosci.* **7**, 1–24 (1995).

30. C. M. Leonard, The prefrontal cortex of the rat. I. cortical projection of the mediodorsal nucleus. II. efferent connections. *Brain Res.* **12**, 321–343 (1969).

31. C. M. Leonard, Finding prefrontal cortex in the rat. *Brain Res.* **1645**, 1–3 (2016).

32. W. O. Guldin, M. Pritzel, H. J. Markowitsch, Prefrontal cortex of the mouse defined as cortical projection area of the thalamic mediodorsal nucleus. *Brain Behav. Evol.* **19**, 93–107 (1981).

33. J. E. Rose, C. N. Woolsey, The orbitofrontal cortex and its connections with the mediodorsal nucleus in rabbit, sheep and cat. *Res. Publ. Assoc. Res. Nerv. Ment. Dis.* **27 (1 vol.)**, 210–232 (1948).

34. G. Paxinos, C. Watson, *The Rat Brain in Stereotaxic Coordinates* (Academic Press, 6th Edition., 2007).

35. W. B. Hoover, R. P. Vertes, Anatomical analysis of afferent projections to the medial prefrontal cortex in the rat. *Brain Struct. Funct.* **212**, 149–179 (2007).

36. R. P. Vertes, Interactions among the medial prefrontal cortex, hippocampus and midline thalamus in emotional and cognitive processing in the rat. *Neuroscience*. **142**, 1–20 (2006).

37. C. A. Heidbreder, H. J. Groenewegen, The medial prefrontal cortex in the rat: evidence for a dorso-ventral distinction based upon functional and anatomical characteristics. *Neurosci. Biobehav. Rev.* **27**, 555–579 (2003).

38. J. L. Bizon, T. C. Foster, G. E. Alexander, E. L. Glisky, Characterizing cognitive aging of working memory and executive function in animal models. *Front. Aging Neurosci.* **4**, 19 (2012).

39. M. A. Castro-Alamancos, B. W. Connors, Thalamocortical synapses. *Prog. Neurobiol.* **51**, 581–606 (1997).

40. F. Condé, E. Maire-Lepoivre, E. Audinat, F. Crépel, Afferent connections of the medial frontal cortex of the rat. II. Cortical and subcortical afferents. *J. Comp. Neurol.* **352**, 567–593 (1995).

41. H. J. Groenewegen, Organization of the afferent connections of the mediodorsal thalamic nucleus in the rat, related to the mediodorsal-prefrontal topography. *Neuroscience*. **24**, 379–431 (1988).

42. M. Kuroda *et al.*, Synaptic relationships between axon terminals from the mediodorsal thalamic nucleus and layer III pyramidal cells in the prelimbic cortex of the rat. *Brain Res.* **708**, 185–190 (1996).

43. J. P. Little, A. G. Carter, Subcellular synaptic connectivity of layer 2 pyramidal neurons in the medial prefrontal cortex. *J. Neurosci.* **32**, 12808–12819 (2012).

44. D. P. Collins, P. G. Anastasiades, J. J. Marlin, A. G. Carter, Reciprocal Circuits Linking the Prefrontal Cortex with Dorsal and Ventral Thalamic Nuclei. *Neuron*. **98**, 366–379.e4 (2018).

45. K. Delevich, J. Tucciarone, Z. J. Huang, B. Li, The mediodorsal thalamus drives feedforward inhibition in the anterior cingulate cortex via parvalbumin interneurons. *J. Neurosci.* **35**, 5743–5753 (2015).

46. S. J. Cruikshank *et al.*, Thalamic control of layer 1 circuits in prefrontal cortex. *J. Neurosci.* **32**, 17813–17823 (2012).

47. R. P. Vertes, W. B. Hoover, A. C. Do Valle, A. Sherman, J. J. Rodriguez, Efferent projections of reuniens and rhomboid nuclei of the thalamus in the rat. *J. Comp. Neurol.* **499**, 768–796 (2006).

48. G. V. Di Prisco, R. P. Vertes, Excitatory actions of the ventral midline thalamus (rhomboid/reuniens) on the medial prefrontal cortex in the rat. *Synapse*. **60**, 45–55 (2006).

49. K. D. Harris, G. M. G. Shepherd, The neocortical circuit: themes and variations. *Nat. Neurosci.* **18**, 170–181 (2015).

50. M. Kuroda, J. Yokofujita, K. Murakami, An ultrastructural study of the neural circuit between the prefrontal cortex and the mediodorsal nucleus of the thalamus. *Prog. Neurobiol.* **54**, 417–458 (1998).

51. S. Parnaudeau, S. S. Bolkan, C. Kellendonk, The mediodorsal thalamus: an essential partner of the prefrontal cortex for cognition. *Biol. Psychiatry*. **83**, 648–656 (2018).

52. A. E. Block, H. Dhanji, S. F. Thompson-Tardif, S. B. Floresco, Thalamic-prefrontal cortical-ventral striatal circuitry mediates dissociable components of strategy set shifting. *Cereb. Cortex*. **17**, 1625–1636 (2007).

53. K. A. Stokes, P. J. Best, Mediodorsal thalamic lesions impair radial maze performance in the rat. *Behav. Neurosci.* **102**, 294–300 (1988).

54. S. Parnaudeau *et al.*, Inhibition of mediodorsal thalamus disrupts thalamofrontal connectivity and cognition. *Neuron*. **77**, 1151–1162 (2013).

55. B. R. Ferguson, W.-J. Gao, Thalamic Control of Cognition and Social Behavior Via Regulation of Gamma-Aminobutyric Acidergic Signaling and Excitation/Inhibition Balance in the Medial Prefrontal Cortex. *Biol. Psychiatry*. **83**, 657–669 (2018).

56. F. Alcaraz *et al.*, Thalamocortical and corticothalamic pathways differentially contribute to goal-directed behaviors in the rat. *Elife*. **7** (2018), doi:10.7554/eLife.32517.

57. T. F. Marton, H. Seifikar, F. J. Luongo, A. T. Lee, V. S. Sohal, Roles of prefrontal cortex and mediodorsal thalamus in task engagement and behavioral flexibility. *J. Neurosci.* **38**, 2569–2578 (2018).

58. S. S. Bolkan *et al.*, Thalamic projections sustain prefrontal activity during working memory maintenance. *Nat. Neurosci.* **20**, 987–996 (2017).

59. K. R. Ramanathan, J. Jin, T. F. Giustino, M. R. Payne, S. Maren, Prefrontal projections to the thalamic nucleus reuniens mediate fear extinction. *Nat. Commun.* **9**, 4527 (2018).

60. T. M. Jay, M. P. Witter, Distribution of hippocampal CA1 and subicular efferents in the prefrontal cortex of the rat studied by means of anterograde transport of Phaseolus vulgaris-leucoagglutinin. *J. Comp. Neurol.* **313**, 574–586 (1991).

61. T. M. Jay, A.-M. Thierry, L. Wiklund, J. Glowinski, Excitatory Amino Acid Pathway from the Hippocampus to the Prefrontal Cortex. Contribution of AMPA Receptors in Hippocampo-prefrontal Cortex Transmission. *Eur. J. Neurosci.* **4**, 1285–1295 (1992).

62. P. L. Tierney, E. Dégenètais, A.-M. Thierry, J. Glowinski, Y. Gioanni, Influence of the hippocampus on interneurons of the rat prefrontal cortex. *Eur. J. Neurosci.* **20**, 514–524 (2004).

63. X. Liu, A. G. Carter, Ventral hippocampal inputs preferentially drive corticocortical neurons in the infralimbic prefrontal cortex. *J. Neurosci.* **38**, 7351–7363 (2018).

64. C. Varela, S. Kumar, J. Y. Yang, M. A. Wilson, Anatomical substrates for direct interactions between hippocampus, medial prefrontal cortex, and the thalamic nucleus reuniens. *Brain Struct. Funct.* **219**, 911–929 (2014).

65. L. M. McGarry, A. G. Carter, Inhibitory gating of basolateral amygdala inputs to the prefrontal cortex. *J. Neurosci.* **36**, 9391–9406 (2016).

66. S. B. Floresco, M. T. Tse, Dopaminergic regulation of inhibitory and excitatory transmission in the basolateral amygdala-prefrontal cortical pathway. *J. Neurosci.* **27**, 2045–2057 (2007).

67. J. Dilgen, H. A. Tejeda, P. O'Donnell, Amygdala inputs drive feedforward inhibition in the medial prefrontal cortex. *J. Neurophysiol.* **110**, 221–229 (2013).

68. S. R. Sesack, A. Y. Deutch, R. H. Roth, B. S. Bunney, Topographical organization of the efferent projections of the medial prefrontal cortex in the rat: an anterograde tract-tracing study with Phaseolus vulgaris leucoagglutinin. *J. Comp. Neurol.* **290**, 213–242 (1989).

69. T. Sigurdsson, S. Duvarci, Hippocampal-prefrontal interactions in cognition, behavior and psychiatric disease. *Front. Syst. Neurosci.* **9**, 190 (2015).

70. J. Jin, S. Maren, Prefrontal-Hippocampal Interactions in Memory and Emotion. *Front. Syst. Neurosci.* **9**, 170 (2015).

71. E. Likhtik, R. Paz, Amygdala-prefrontal interactions in (mal)adaptive learning. *Trends Neurosci.* **38**, 158–166 (2015).

72. J. C. Churchwell, R. P. Kesner, Hippocampal-prefrontal dynamics in spatial working memory: interactions and independent parallel processing. *Behav. Brain Res.* **225**, 389–395 (2011).

73. S. B. Floresco, J. K. Seamans, A. G. Phillips, Selective roles for hippocampal, prefrontal cortical, and ventral striatal circuits in radial-arm maze tasks with or without a delay. *J. Neurosci.* **17**, 1880–1890 (1997).

74. M. W. Jones, M. A. Wilson, Theta rhythms coordinate hippocampal-prefrontal interactions in a spatial memory task. *PLoS Biol.* **3**, e402 (2005).

75. A. G. Siapas, E. V. Lubenov, M. A. Wilson, Prefrontal phase locking to hippocampal theta oscillations. *Neuron*. **46**, 141–151 (2005).

76. T. Sigurdsson, K. L. Stark, M. Karayiorgou, J. A. Gogos, J. A. Gordon, Impaired hippocampal-prefrontal synchrony in a genetic mouse model of schizophrenia. *Nature*. **464**, 763–767 (2010).

77. T. Spellman *et al.*, Hippocampal-prefrontal input supports spatial encoding in working memory. *Nature*. **522**, 309–314 (2015).

78. M. L. Phillips, H. A. Robinson, L. Pozzo-Miller, Ventral hippocampal projections to the medial prefrontal cortex regulate social memory. *Elife*. **8** (2019), doi:10.7554/eLife.44182.

79. T. F. Giustino, S. Maren, The role of the medial prefrontal cortex in the conditioning and extinction of fear. *Front. Behav. Neurosci.* **9**, 298 (2015).

80. D. Sierra-Mercado, N. Padilla-Coreano, G. J. Quirk, Dissociable roles of prelimbic and infralimbic cortices, ventral hippocampus, and basolateral amygdala in the expression and extinction of conditioned fear. *Neuropsychopharmacology*. **36**, 529–538 (2011).

81. F. Sotres-Bayon, D. Sierra-Mercado, E. Pardilla-Delgado, G. J. Quirk, Gating of fear in prelimbic cortex by hippocampal and amygdala inputs. *Neuron*. **76**, 804–812 (2012).

82. V. Senn *et al.*, Long-range connectivity defines behavioral specificity of amygdala neurons. *Neuron*. **81**, 428–437 (2014).

83. A. Burgos-Robles *et al.*, Amygdala inputs to prefrontal cortex guide behavior amid conflicting cues of reward and punishment. *Nat. Neurosci.* **20**, 824–835 (2017).

84. O. Klavir, M. Prigge, A. Sarel, R. Paz, O. Yizhar, Manipulating fear associations via optogenetic modulation of amygdala inputs to prefrontal cortex. *Nat. Neurosci.* **20**, 836–844 (2017).

85. C. A. Orsini, J. H. Kim, E. Knapska, S. Maren, Hippocampal and prefrontal projections to the basal amygdala mediate contextual regulation of fear after extinction. *J. Neurosci.* **31**, 17269–17277 (2011).

86. R. Marek *et al.*, Hippocampus-driven feed-forward inhibition of the prefrontal cortex mediates relapse of extinguished fear. *Nat. Neurosci.* **21**, 384–392 (2018).

87. N. Padilla-Coreano *et al.*, Direct Ventral Hippocampal-Prefrontal Input Is Required for Anxiety-Related Neural Activity and Behavior. *Neuron*. **89**, 857–866 (2016).

88. G. M. Parfitt *et al.*, Bidirectional Control of Anxiety-Related Behaviors in Mice: Role of Inputs Arising from the Ventral Hippocampus to the Lateral Septum and Medial Prefrontal Cortex. *Neuropsychopharmacology*. **42**, 1715–1728 (2017).

89. A. C. Felix-Ortiz, A. Burgos-Robles, N. D. Bhagat, C. A. Leppla, K. M. Tye, Bidirectional modulation of anxiety-related and social behaviors by amygdala projections to the medial prefrontal cortex. *Neuroscience*. **321**, 197–209 (2016).

90. M. E. Joffe, B. A. Grueter, Cocaine Experience Enhances Thalamo-Accumbens N-Methyl-D-Aspartate Receptor Function. *Biol. Psychiatry*. **80**, 671–681 (2016).

91. P. O'Donnell, A. A. Grace, Synaptic interactions among excitatory afferents to nucleus accumbens neurons: hippocampal gating of prefrontal cortical input. *J. Neurosci.* **15**, 3622–3639 (1995).

92. J. P. Britt *et al.*, Synaptic and behavioral profile of multiple glutamatergic inputs to the nucleus accumbens. *Neuron*. **76**, 790–803 (2012).

93. Y.-Y. Ma *et al.*, Bidirectional modulation of incubation of cocaine craving by silent synapse-based remodeling of prefrontal cortex to accumbens projections. *Neuron*. **83**, 1453–1467 (2014).

94. A. T. Lee, D. Vogt, J. L. Rubenstein, V. S. Sohal, A class of GABAergic neurons in the prefrontal cortex sends long-range projections to the nucleus accumbens and elicits acute avoidance behavior. *J. Neurosci.* **34**, 11519–11525 (2014).

95. V. Vialou *et al.*, Prefrontal cortical circuit for depression- and anxiety-related behaviors mediated by cholecystokinin: role of ΔFosB. *J. Neurosci.* **34**, 3878–3887 (2014).

96. V. Pascoli *et al.*, Contrasting forms of cocaine-evoked plasticity control components of relapse. *Nature*. **509**, 459–464 (2014).

97. B. D. Turner, J. M. Rook, C. W. Lindsley, P. J. Conn, B. A. Grueter, mGlu1 and mGlu5 modulate distinct excitatory inputs to the nucleus accumbens shell. *Neuropsychopharmacology*. **43**, 2075–2082 (2018).

98. L. Chanes, L. F. Barrett, Redefining the role of limbic areas in cortical processing. *Trends Cogn. Sci. (Regul. Ed.)*. **20**, 96–106 (2016).

99. J. Jackson, M. M. Karnani, B. V. Zemelman, D. Burdakov, A. K. Lee, Inhibitory control of prefrontal cortex by the claustrum. *Neuron*. **99**, 1029–1039.e4 (2018).

100. S. F. Logue, T. J. Gould, The neural and genetic basis of executive function: attention, cognitive flexibility, and response inhibition. *Pharmacol. Biochem. Behav.* **123**, 45–54 (2014).

101. M. E. Ragozzino, The effects of dopamine D(1) receptor blockade in the prelimbic-infralimbic areas on behavioral flexibility. *Learn. Mem.* **9**, 18–28 (2002).

102. S. B. Floresco, O. Magyar, S. Ghods-Sharifi, C. Vexelman, M. T. L. Tse, Multiple dopamine receptor subtypes in the medial prefrontal cortex of the rat regulate set-shifting. *Neuropsychopharmacology*. **31**, 297–309 (2006).

103. J. Zahrt, J. R. Taylor, R. G. Mathew, A. F. Arnsten, Supranormal stimulation of D1 dopamine receptors in the rodent prefrontal cortex impairs spatial working memory performance. *J. Neurosci.* **17**, 8528–8535 (1997).

104. M. Koch, M. Bubser, Deficient sensorimotor gating after 6-hydroxydopamine lesion of the rat medial prefrontal cortex is reversed by haloperidol. *Eur. J. Neurosci.* **6**, 1837–1845 (1994).

105. D. J. Lodge, The medial prefrontal and orbitofrontal cortices differentially regulate dopamine system function. *Neuropsychopharmacology*. **36**, 1227–1236 (2011).

106. J. A. Milstein, O. Lehmann, D. E. H. Theobald, J. W. Dalley, T. W. Robbins, Selective depletion of cortical noradrenaline by anti-dopamine beta-hydroxylase-saporin impairs attentional function and enhances the effects of guanfacine in the rat. *Psychopharmacology*. **190**, 51–63 (2007).

107. M. D. S. Lapiz, D. A. Morilak, Noradrenergic modulation of cognitive function in rat medial prefrontal cortex as measured by attentional set shifting capability. *Neuroscience*. **137**, 1039–1049 (2006).

108. E. Seu, J. D. Jentsch, Effect of acute and repeated treatment with desipramine or methylphenidate on serial reversal learning in rats. *Neuropharmacology*. **57**, 665–672 (2009).

109. B. Xing, Y.-C. Li, W.-J. Gao, Norepinephrine versus dopamine and their interaction in modulating synaptic function in the prefrontal cortex. *Brain Res.* **1641**, 217–233 (2016).

110. T. Alkam *et al.*, Evaluation of object-based attention in mice. *Behav. Brain Res.* **220**, 185–193 (2011).

111. M. D. S. Lapiz-Bluhm, A. E. Soto-Piña, J. G. Hensler, D. A. Morilak, Chronic intermittent cold stress and serotonin depletion induce deficits of reversal learning in an attentional set-shifting test in rats. *Psychopharmacology*. **202**, 329–341 (2009).

112. A. A. Harrison, B. J. Everitt, T. W. Robbins, Central 5-HT depletion enhances impulsive responding without affecting the accuracy of attentional performance: interactions with dopaminergic mechanisms. *Psychopharmacology*. **133**, 329–342 (1997).

113. J. W. Dalley, J. P. Roiser, Dopamine, serotonin and impulsivity. *Neuroscience*. **215**, 42–58 (2012).

114. D. J. Chandler, C. S. Lamperski, B. D. Waterhouse, Identification and distribution of projections from monoaminergic and cholinergic nuclei to functionally differentiated subregions of prefrontal cortex. *Brain Res.* **1522**, 38–58 (2013).

115. J. von Engelhardt, M. Eliava, A. H. Meyer, A. Rozov, H. Monyer, Functional characterization of intrinsic cholinergic interneurons in the cortex. *J. Neurosci.* **27**, 5633–5642 (2007).

116. L. Zaborszky, R. P. Gaykema, D. J. Swanson, W. E. Cullinan, Cortical input to the basal forebrain. *Neuroscience*. **79**, 1051–1078 (1997).

117. F. Passetti, J. W. Dalley, M. T. O'Connell, B. J. Everitt, T. W. Robbins, Increased acetylcholine release in the rat medial prefrontal cortex during performance of a visual attentional task. *Eur. J. Neurosci.* **12**, 3051–3058 (2000).

118. V. Parikh, R. Kozak, V. Martinez, M. Sarter, Prefrontal acetylcholine release controls cue detection on multiple timescales. *Neuron*. **56**, 141–154 (2007).

119. T. M. Gill, M. Sarter, B. Givens, Sustained visual attention performance-associated prefrontal neuronal activity: evidence for cholinergic modulation. *J. Neurosci.* **20**, 4745–4757 (2000).

120. Y. Chudasama, J. W. Dalley, F. Nathwani, P. Bouger, T. W. Robbins, Cholinergic modulation of visual attention and working memory: dissociable effects of basal forebrain 192-IgG-saporin lesions and intraprefrontal infusions of scopolamine. *Learn. Mem.* **11**, 78–86 (2004).

121. K. C. Chen, M. G. Baxter, J. S. Rodefer, Central blockade of muscarinic cholinergic receptors disrupts affective and attentional set-shifting. *Eur. J. Neurosci.* **20**, 1081–1088 (2004).

122. D. Riga *et al.*, Optogenetic dissection of medial prefrontal cortex circuitry. *Front. Syst. Neurosci.* **8**, 230 (2014).

123. B. Rudy, G. Fishell, S. Lee, J. Hjerling-Leffler, Three groups of interneurons account for nearly 100% of neocortical GABAergic neurons. *Dev. Neurobiol.* **71**, 45–61 (2011).

124. Y. Kawaguchi, Pyramidal cell subtypes and their synaptic connections in layer 5 of rat frontal cortex. *Cereb. Cortex*. **27**, 5755–5771 (2017).

125. K. I. van Aerde, D. Feldmeyer, Morphological and physiological characterization of pyramidal neuron subtypes in rat medial prefrontal cortex. *Cereb. Cortex*. **25**, 788–805 (2015).

126. G. Buzsáki, A. Draguhn, Neuronal oscillations in cortical networks. *Science*. **304**, 1926–1929 (2004).

127. G. Gonzalez-Burgos, R. Y. Cho, D. A. Lewis, Alterations in cortical network oscillations and parvalbumin neurons in schizophrenia. *Biol. Psychiatry*. **77**, 1031–1040 (2015).

128. H. Hu, J. Gan, P. Jonas, Interneurons. Fast-spiking, parvalbumin^{+} GABAergic interneurons: from cellular design to microcircuit function. *Science*. **345**, 1255263 (2014).

129. B. R. Ferguson, W.-J. Gao, PV Interneurons: Critical Regulators of E/I Balance for Prefrontal Cortex-Dependent Behavior and Psychiatric Disorders. *Front. Neural Circuits*. **12**, 37 (2018).

130. Y. Wang, P. Zhang, D. R. Wyskiel, Chandelier cells in functional and dysfunctional neural circuits. *Front. Neural Circuits*. **10**, 33 (2016).

131. T. Miyamae, K. Chen, D. A. Lewis, G. Gonzalez-Burgos, Distinct Physiological Maturation of Parvalbumin-Positive Neuron Subtypes in Mouse Prefrontal Cortex. *J. Neurosci.* **37**, 4883–4902 (2017).

132. J. Szabadics *et al.*, Excitatory effect of GABAergic axo-axonic cells in cortical microcircuits. *Science*. **311**, 233–235 (2006).

133. A. R. Woodruff *et al.*, State-dependent function of neocortical chandelier cells. *J. Neurosci.* **31**, 17872–17886 (2011).

134. A. M. Packer, R. Yuste, Dense, unspecific connectivity of neocortical parvalbumin-positive interneurons: a canonical microcircuit for inhibition? *J. Neurosci.* **31**, 13260–13271 (2011).

135. M. Galarreta, S. Hestrin, A network of fast-spiking cells in the neocortex connected by electrical synapses. *Nature*. **402**, 72–75 (1999).

136. P. G. Anastasiades, J. J. Marlin, A. G. Carter, Cell-Type Specificity of Callosally Evoked Excitation and Feedforward Inhibition in the Prefrontal Cortex. *Cell Rep.* **22**, 679–692 (2018).

137. F. Alherz, M. Alherz, H. Almusawi, NMDAR hypofunction and somatostatin-expressing GABAergic interneurons and receptors: A newly identified correlation and its effects in schizophrenia. *Schizophr. Res. Cogn.* **8**, 1–6 (2017).

138. Z. Tan, H. Hu, Z. J. Huang, A. Agmon, Robust but delayed thalamocortical activation of dendritic-targeting inhibitory interneurons. *Proc. Natl. Acad. Sci. USA*. **105**, 2187–2192 (2008).

139. T. Riedemann, Diversity and Function of Somatostatin-Expressing Interneurons in the Cerebral Cortex. *Int. J. Mol. Sci.* **20** (2019), doi:10.3390/ijms20122952.

140. N. Tamamaki, R. Tomioka, Long-Range GABAergic Connections Distributed throughout the Neocortex and their Possible Function. *Front. Neurosci.* **4**, 202 (2010).

141. B. Tasic *et al.*, Shared and distinct transcriptomic cell types across neocortical areas. *Nature*. **563**, 72–78 (2018).

142. Y. Kubota *et al.*, Selective coexpression of multiple chemical markers defines discrete populations of neocortical GABAergic neurons. *Cereb. Cortex*. **21**, 1803–1817 (2011).

143. D. Shlosberg, S. L. Patrick, Y. Buskila, Y. Amitai, Inhibitory effect of mouse neocortex layer I on the underlying cellular network. *Eur. J. Neurosci.* **18**, 2751–2759 (2003).

144. A. Naka, H. Adesnik, Inhibitory circuits in cortical layer 5. *Front. Neural Circuits*. **10**, 35 (2016).

145. T. K. Berger, G. Silberberg, R. Perin, H. Markram, Brief bursts self-inhibit and correlate the pyramidal network. *PLoS Biol.* **8** (2010), doi:10.1371/journal.pbio.1000473.

146. G. Silberberg, H. Markram, Disynaptic inhibition between neocortical pyramidal cells mediated by Martinotti cells. *Neuron*. **53**, 735–746 (2007).

147. E. E. Fanselow, K. A. Richardson, B. W. Connors, Selective, state-dependent activation of somatostatin-expressing inhibitory interneurons in mouse neocortex. *J. Neurophysiol.* **100**, 2640–2652 (2008).

148. H.-J. Pi *et al.*, Cortical interneurons that specialize in disinhibitory control. *Nature*. **503**, 521–524 (2013).

149. R. Tremblay, S. Lee, B. Rudy, Gabaergic interneurons in the neocortex: from cellular properties to circuits. *Neuron*. **91**, 260–292 (2016).

150. B. Schuman *et al.*, Four unique interneuron populations reside in neocortical layer 1. *J. Neurosci.* **39**, 125–139 (2019).

151. O. Yizhar *et al.*, Neocortical excitation/inhibition balance in information processing and social dysfunction. *Nature*. **477**, 171–178 (2011).

152. A. Benn *et al.*, Optogenetic stimulation of prefrontal glutamatergic neurons enhances recognition memory. *J. Neurosci.* **36**, 4930–4939 (2016).

153. M. M. Diehl *et al.*, Active avoidance requires inhibitory signaling in the rodent prelimbic prefrontal cortex. *Elife*. **7** (2018), doi:10.7554/eLife.34657.

154. M. R. Gilmartin, H. Miyawaki, F. J. Helmstetter, K. Diba, Prefrontal activity links nonoverlapping events in memory. *J. Neurosci.* **33**, 10910–10914 (2013).

155. H. Cardoso-Cruz, P. Paiva, C. Monteiro, V. Galhardo, Selective optogenetic inhibition of medial prefrontal glutamatergic neurons reverses working memory deficits induced by neuropathic pain. *Pain*. **160**, 805–823 (2019).

156. A. Selimbeyoglu *et al.*, Modulation of prefrontal cortex excitation/inhibition balance rescues social behavior in CNTNAP2-deficient mice. *Sci. Transl. Med.* **9** (2017), doi:10.1126/scitranslmed.aah6733.

157. J. Courtin *et al.*, Prefrontal parvalbumin interneurons shape neuronal activity to drive fear expression. *Nature*. **505**, 92–96 (2014).

158. M. A. Rossi *et al.*, Prefrontal cortical mechanisms underlying delayed alternation in mice. *J. Neurophysiol.* **108**, 1211–1222 (2012).

159. A. I. Abbas *et al.*, Somatostatin Interneurons Facilitate Hippocampal-Prefrontal Synchrony and Prefrontal Spatial Encoding. *Neuron*. **100**, 926–939.e3 (2018).

160. D. Kim *et al.*, Distinct Roles of Parvalbumin- and Somatostatin-Expressing Interneurons in Working Memory. *Neuron*. **92**, 902–915 (2016).

161. A. J. Murray *et al.*, Parvalbumin-positive interneurons of the prefrontal cortex support working memory and cognitive flexibility. *Sci. Rep.* **5**, 16778 (2015).

162. A. Soumier, E. Sibille, Opposing effects of acute versus chronic blockade of frontal cortex somatostatin-positive inhibitory neurons on behavioral emotionality in mice. *Neuropsychopharmacology*. **39**, 2252–2262 (2014).

163. A. T. Lee *et al.*, VIP Interneurons Contribute to Avoidance Behavior by Regulating Information Flow across Hippocampal-Prefrontal Networks. *Neuron*. **102**, 1223–1234.e4 (2019).

164. M. Lundqvist *et al.*, Gamma and beta bursts underlie working memory. *Neuron*. **90**, 152–164 (2016).

165. V. S. Sohal, F. Zhang, O. Yizhar, K. Deisseroth, Parvalbumin neurons and gamma rhythms enhance cortical circuit performance. *Nature*. **459**, 698–702 (2009).

166. S. H. Bitzenhofer *et al.*, Layer-specific optogenetic activation of pyramidal neurons causes beta-gamma entrainment of neonatal networks. *Nat. Commun.* **8**, 14563 (2017).

167. J. Veit, R. Hakim, M. P. Jadi, T. J. Sejnowski, H. Adesnik, Cortical gamma band synchronization through somatostatin interneurons. *Nat. Neurosci.* **20**, 951–959 (2017).

168. G. Chen *et al.*, Distinct Inhibitory Circuits Orchestrate Cortical beta and gamma Band Oscillations. *Neuron*. **96**, 1403–1418.e6 (2017).

169. M. J. Niciu, B. Kelmendi, G. Sanacora, Overview of glutamatergic neurotransmission in the nervous system. *Pharmacol. Biochem. Behav.* **100**, 656–664 (2012).

170. R. T. Fremeau, S. Voglmaier, R. P. Seal, R. H. Edwards, VGLUTs define subsets of excitatory neurons and suggest novel roles for glutamate. *Trends Neurosci.* **27**, 98–103 (2004).

171. R. J. Vandenberg, R. M. Ryan, Mechanisms of glutamate transport. *Physiol. Rev.* **93**, 1621–1657 (2013).

172. G. Sanacora, C. A. Zarate, J. H. Krystal, H. K. Manji, Targeting the glutamatergic system to develop novel, improved therapeutics for mood disorders. *Nat. Rev. Drug Discov.* **7**, 426–437 (2008).

173. S. F. Traynelis *et al.*, Glutamate receptor ion channels: structure, regulation, and function. *Pharmacol. Rev.* **62**, 405–496 (2010).

174. Ionotropic glutamate receptors | Ion channels | IUPHAR/BPS Guide to PHARMACOLOGY, (available at https://www.guidetopharmacology.org/GRAC/FamilyDisplayForward?familyId=75).

175. M. M. Jacobs, R. L. Fogg, R. B. Emeson, G. D. Stanwood, ADAR1 and ADAR2 expression and editing activity during forebrain development. *Dev Neurosci*. **31**, 223–237 (2009).

176. D. E. Jane, D. Lodge, G. L. Collingridge, Kainate receptors: pharmacology, function and therapeutic potential. *Neuropharmacology*. **56**, 90–113 (2009).

177. C. M. Niswender, P. J. Conn, Metabotropic glutamate receptors: physiology, pharmacology, and disease. *Annu. Rev. Pharmacol. Toxicol.* **50**, 295–322 (2010).

178. A. Schousboe, H. S. Waagepetersen, GABA: homeostatic and pharmacological aspects. *Prog. Brain Res.* **160**, 9–19 (2007).

179. N. M. Rowley, K. K. Madsen, A. Schousboe, H. Steve White, Glutamate and GABA synthesis, release, transport and metabolism as targets for seizure control. *Neurochem. Int.* **61**, 546–558 (2012).

180. D. F. Owens, A. R. Kriegstein, Is there more to GABA than synaptic inhibition? *Nat. Rev. Neurosci.* **3**, 715–727 (2002).

181. J. Bormann, The “ABC” of GABA receptors. *Trends Pharmacol. Sci.* **21**, 16–19 (2000).

182. W. Sieghart, M. M. Savić, International Union of Basic and Clinical Pharmacology. CVI: GABAA Receptor Subtype- and Function-selective Ligands: Key Issues in Translation to Humans. *Pharmacol. Rev.* **70**, 836–878 (2018).

183. B. Bettler, K. Kaupmann, J. Mosbacher, M. Gassmann, Molecular structure and physiological functions of GABA(B) receptors. *Physiol. Rev.* **84**, 835–867 (2004).

184. A. Pinard, R. Seddik, B. Bettler, GABAB receptors: physiological functions and mechanisms of diversity. *Adv. Pharmacol.* **58**, 231–255 (2010).

185. S. Zhou, Y. Yu, Synaptic E-I Balance Underlies Efficient Neural Coding. *Front. Neurosci.* **12**, 46 (2018).

186. V. S. Sohal, J. L. R. Rubenstein, Excitation-inhibition balance as a framework for investigating mechanisms in neuropsychiatric disorders. *Mol. Psychiatry*. **24**, 1248–1257 (2019).

187. C. N. J. Meunier, P. Chameau, P. M. Fossier, Modulation of synaptic plasticity in the cortex needs to understand all the players. *Front. Synaptic Neurosci.* **9**, 2 (2017).

188. A. Citri, R. C. Malenka, Synaptic plasticity: multiple forms, functions, and mechanisms. *Neuropsychopharmacology*. **33**, 18–41 (2008).

189. Y. Goto, C. R. Yang, S. Otani, Functional and dysfunctional synaptic plasticity in prefrontal cortex: roles in psychiatric disorders. *Biol. Psychiatry*. **67**, 199–207 (2010).

190. R. S. Zucker, W. G. Regehr, Short-term synaptic plasticity. *Annu. Rev. Physiol.* **64**, 355–405 (2002).

191. C. Gemmell, S. M. O'Mara, Long-term potentiation and paired-pulse facilitation in the prelimbic cortex of the rat following stimulation in the contralateral hemisphere in vivo. *Exp. Brain Res.* **132**, 223–229 (2000).

192. Y. Izaki, M. Takita, M. Nomura, Mouse hippocampo-prefrontal paired-pulse facilitation and long-term potentiation in vivo. *Neuroreport*. **12**, 1191–1193 (2001).

193. S. B. Floresco, A. A. Grace, Gating of hippocampal-evoked activity in prefrontal cortical neurons by inputs from the mediodorsal thalamus and ventral tegmental area. *J. Neurosci.* **23**, 3930–3943 (2003).

194. J. P. Little, A. G. Carter, Synaptic mechanisms underlying strong reciprocal connectivity between the medial prefrontal cortex and basolateral amygdala. *J. Neurosci.* **33**, 15333–15342 (2013).

195. M. E. Joffe, C. I. Santiago, J. L. Engers, C. W. Lindsley, P. J. Conn, Metabotropic glutamate receptor subtype 3 gates acute stress-induced dysregulation of amygdalo-cortical function. *Mol. Psychiatry*. **24**, 916–927 (2019).

196. M. A. Parent, L. Wang, J. Su, T. Netoff, L.-L. Yuan, Identification of the hippocampal input to medial prefrontal cortex in vitro. *Cereb. Cortex*. **20**, 393–403 (2010).

197. A. E. Hernan, G. L. Holmes, D. Isaev, R. C. Scott, E. Isaeva, Altered short-term plasticity in the prefrontal cortex after early life seizures. *Neurobiol. Dis.* **50**, 120–126 (2013).

198. Y. Goto, A. A. Grace, Dopamine modulation of hippocampal-prefrontal cortical interaction drives memory-guided behavior. *Cereb. Cortex*. **18**, 1407–1414 (2008).

199. C. M. Hempel, K. H. Hartman, X. J. Wang, G. G. Turrigiano, S. B. Nelson, Multiple forms of short-term plasticity at excitatory synapses in rat medial prefrontal cortex. *J. Neurophysiol.* **83**, 3031–3041 (2000).

200. C. E. Young, C. R. Yang, Dopamine D1-like receptor modulates layer- and frequency-specific short-term synaptic plasticity in rat prefrontal cortical neurons. *Eur. J. Neurosci.* **21**, 3310–3320 (2005).

201. A. Ishikawa, S. Nakamura, Convergence and interaction of hippocampal and amygdalar projections within the prefrontal cortex in the rat. *J. Neurosci.* **23**, 9987–9995 (2003).

202. H. A. Tejeda, P. O'Donnell, Amygdala inputs to the prefrontal cortex elicit heterosynaptic suppression of hippocampal inputs. *J. Neurosci.* **34**, 14365–14374 (2014).

203. B. Esmaeili, A. A. Grace, Afferent drive of medial prefrontal cortex by hippocampus and amygdala is altered in MAM-treated rats: evidence for interneuron dysfunction. *Neuropsychopharmacology*. **38**, 1871–1880 (2013).

204. D. R. Thomases, D. K. Cass, J. D. Meyer, A. Caballero, K. Y. Tseng, Early adolescent MK-801 exposure impairs the maturation of ventral hippocampal control of basolateral amygdala drive in the adult prefrontal cortex. *J. Neurosci.* **34**, 9059–9066 (2014).

205. T. V. Bliss, T. Lomo, Long-lasting potentiation of synaptic transmission in the dentate area of the anaesthetized rabbit following stimulation of the perforant path. *J. Physiol. (Lond.)*. **232**, 331–356 (1973).

206. J. Larson, D. Wong, G. Lynch, Patterned stimulation at the theta frequency is optimal for the induction of hippocampal long-term potentiation. *Brain Res.* **368**, 347–350 (1986).

207. Y. Dan, M.-M. Poo, Spike timing-dependent plasticity: from synapse to perception. *Physiol. Rev.* **86**, 1033–1048 (2006).

208. K. P. Giese, N. B. Fedorov, R. K. Filipkowski, A. J. Silva, Autophosphorylation at Thr286 of the alpha calcium-calmodulin kinase II in LTP and learning. *Science*. **279**, 870–873 (1998).

209. D. S. Bredt, R. A. Nicoll, AMPA receptor trafficking at excitatory synapses. *Neuron*. **40**, 361–379 (2003).

210. K. G. Reymann, J. U. Frey, The late maintenance of hippocampal LTP: requirements, phases, "synaptic tagging", "late-associativity" and implications. *Neuropharmacology*. **52**, 24–40 (2007).

211. J. Lisman, A mechanism for the Hebb and the anti-Hebb processes underlying learning and memory. *Proc. Natl. Acad. Sci. USA*. **86**, 9574–9578 (1989).

212. S. Tomita, V. Stein, T. J. Stocker, R. A. Nicoll, D. S. Bredt, Bidirectional synaptic plasticity regulated by phosphorylation of stargazin-like TARPs. *Neuron*. **45**, 269–277 (2005).

213. S. J. Coultrap *et al.*, Autonomous CaMKII mediates both LTP and LTD using a mechanism for differential substrate site selection. *Cell Rep.* **6**, 431–437 (2014).

214. C. Lüscher, K. M. Huber, Group 1 mGluR-dependent synaptic long-term depression: mechanisms and implications for circuitry and disease. *Neuron*. **65**, 445–459 (2010).

215. Z. Nusser, E. Mulvihill, P. Streit, P. Somogyi, Subsynaptic segregation of metabotropic and ionotropic glutamate receptors as revealed by immunogold localization. *Neuroscience*. **61**, 421–427 (1994).

216. L. J. Volk, B. E. Pfeiffer, J. R. Gibson, K. M. Huber, Multiple Gq-coupled receptors converge on a common protein synthesis-dependent long-term depression that is affected in fragile X syndrome mental retardation. *J. Neurosci.* **27**, 11624–11634 (2007).

217. S. M. Fitzjohn *et al.*, A characterisation of long-term depression induced by metabotropic glutamate receptor activation in the rat hippocampus in vitro. *J. Physiol. (Lond.)*. **537**, 421–430 (2001).

218. N. Holbro, A. Grunditz, T. G. Oertner, Differential distribution of endoplasmic reticulum controls metabotropic signaling and plasticity at hippocampal synapses. *Proc. Natl. Acad. Sci. USA*. **106**, 15055–15060 (2009).

219. Y. Zhang *et al.*, The tyrosine phosphatase STEP mediates AMPA receptor endocytosis after metabotropic glutamate receptor stimulation. *J. Neurosci.* **28**, 10561–10566 (2008).

220. C. M. Gladding, S. M. Fitzjohn, E. Molnár, Metabotropic glutamate receptor-mediated long-term depression: molecular mechanisms. *Pharmacol. Rev.* **61**, 395–412 (2009).

221. S. Laroche, T. M. Jay, A. M. Thierry, Long-term potentiation in the prefrontal cortex following stimulation of the hippocampal CA1/subicular region. *Neurosci. Lett.* **114**, 184–190 (1990).

222. T. M. Jay, F. Burette, S. Laroche, NMDA receptor-dependent long-term potentiation in the hippocampal afferent fibre system to the prefrontal cortex in the rat. *Eur. J. Neurosci.* **7**, 247–250 (1995).

223. M. Takita, Y. Izaki, T. M. Jay, H. Kaneko, S. S. Suzuki, Induction of stable long-term depression in vivo in the hippocampal-prefrontal cortex pathway. *Eur. J. Neurosci.* **11**, 4145–4148 (1999).

224. C. Herry, R. M. Vouimba, R. Garcia, Plasticity in the mediodorsal thalamo-prefrontal cortical transmission in behaving mice. *J. Neurophysiol.* **82**, 2827–2832 (1999).

225. M. Maroun, G. Richter-Levin, Exposure to acute stress blocks the induction of long-term potentiation of the amygdala-prefrontal cortex pathway in vivo. *J. Neurosci.* **23**, 4406–4409 (2003).

226. S. Hugues, R. Garcia, Reorganization of learning-associated prefrontal synaptic plasticity between the recall of recent and remote fear extinction memory. *Learn. Mem.* **14**, 520–524 (2007).

227. L. S. Bueno-Junior *et al.*, Interaction between hippocampal-prefrontal plasticity and thalamic-prefrontal activity. *Sci. Rep.* **8**, 1382 (2018).

228. A. Caballero, D. R. Thomases, E. Flores-Barrera, D. K. Cass, K. Y. Tseng, Emergence of GABAergic-dependent regulation of input-specific plasticity in the adult rat prefrontal cortex during adolescence. *Psychopharmacology*. **231**, 1789–1796 (2014).

229. J. C. Hirsch, F. Crepel, Use-dependent changes in synaptic efficacy in rat prefrontal neurons in vitro. *J. Physiol. (Lond.)*. **427**, 31–49 (1990).

230. J. C. Hirsch, F. Crepel, Postsynaptic calcium is necessary for the induction of LTP and LTD of monosynaptic EPSPs in prefrontal neurons: an in vitro study in the rat. *Synapse*. **10**, 173–175 (1992).

231. R. M. Vickery, S. H. Morris, L. J. Bindman, Metabotropic glutamate receptors are involved in long-term potentiation in isolated slices of rat medial frontal cortex. *J. Neurophysiol.* **78**, 3039–3046 (1997).

232. D. Law-Tho, J. M. Desce, F. Crepel, Dopamine favours the emergence of long-term depression versus long-term potentiation in slices of rat prefrontal cortex. *Neurosci. Lett.* **188**, 125–128 (1995).

233. S. Otani, O. Blond, J. M. Desce, F. Crépel, Dopamine facilitates long-term depression of glutamatergic transmission in rat prefrontal cortex. *Neuroscience*. **85**, 669–676 (1998).

234. S. Otani, N. Auclair, J. M. Desce, M. P. Roisin, F. Crépel, Dopamine receptors and groups I and II mGluRs cooperate for long-term depression induction in rat prefrontal cortex through converging postsynaptic activation of MAP kinases. *J. Neurosci.* **19**, 9788–9802 (1999).

235. A. G. Walker *et al.*, Metabotropic glutamate receptor 3 activation is required for long-term depression in medial prefrontal cortex and fear extinction. *Proc. Natl. Acad. Sci. USA*. **112**, 1196–1201 (2015).

236. L. Di Menna *et al.*, Functional partnership between mGlu3 and mGlu5 metabotropic glutamate receptors in the central nervous system. *Neuropharmacology*. **128**, 301–313 (2018).

237. M. E. Joffe *et al.*, Mechanisms underlying prelimbic prefrontal cortex mGlu3/mGlu5-dependent plasticity and reversal learning deficits following acute stress. *Neuropharmacology*. **144**, 19–28 (2019).

238. Y. Matsuda, A. Marzo, S. Otani, The presence of background dopamine signal converts long-term synaptic depression to potentiation in rat prefrontal cortex. *J. Neurosci.* **26**, 4803–4810 (2006).

239. C. N. J. Meunier, M. Amar, L. Lanfumey, M. Hamon, P. Fossier, 5-HT(1A) receptors direct the orientation of plasticity in layer 5 pyramidal neurons of the mouse prefrontal cortex. *Neuropharmacology*. **71**, 37–45 (2013).

240. C. N. J. Meunier, J. Callebert, J.-M. Cancela, P. Fossier, Effect of dopaminergic D1 receptors on plasticity is dependent of serotoninergic 5-HT1A receptors in L5-pyramidal neurons of the prefrontal cortex. *PLoS One*. **10**, e0120286 (2015).

241. C. N. J. Meunier, J. M. Cancela, P. Fossier, Lack of GSK3β activation and modulation of synaptic plasticity by dopamine in 5-HT1A-receptor KO mice. *Neuropharmacology*. **113**, 124–136 (2017).

242. C.-C. Huang, K.-S. Hsu, Activation of muscarinic acetylcholine receptors induces a nitric oxide-dependent long-term depression in rat medial prefrontal cortex. *Cereb. Cortex*. **20**, 982–996 (2010).

243. D. A. Caruana, E. C. Warburton, Z. I. Bashir, Induction of activity-dependent LTD requires muscarinic receptor activation in medial prefrontal cortex. *J. Neurosci.* **31**, 18464–18478 (2011).

244. A. Ghoshal *et al.*, Potentiation of M1 muscarinic receptor reverses plasticity deficits and negative and cognitive symptoms in a schizophrenia mouse model. *Neuropsychopharmacology*. **41**, 598–610 (2016).

245. L. Wang, L.-L. Yuan, Activation of M2 muscarinic receptors leads to sustained suppression of hippocampal transmission in the medial prefrontal cortex. *J. Physiol. (Lond.)*. **587**, 5139–5147 (2009).

246. A. Ghoshal *et al.*, Role of mGlu5 receptors and inhibitory neurotransmission in M1 dependent muscarinic LTD in the prefrontal cortex: implications in schizophrenia. *ACS Chem. Neurosci.* **8**, 2254–2265 (2017).

247. H. G. S. Martin *et al.*, Endocannabinoids Mediate Muscarinic Acetylcholine Receptor-Dependent Long-Term Depression in the Adult Medial Prefrontal Cortex. *Front. Cell Neurosci.* **9**, 457 (2015).

248. S. P. Moran *et al.*, Biased M1 receptor-positive allosteric modulators reveal role of phospholipase D in M1-dependent rodent cortical plasticity. *Sci. Signal.* **12** (2019), doi:10.1126/scisignal.aax2057.

249. P. E. Castillo, T. J. Younts, A. E. Chávez, Y. Hashimotodani, Endocannabinoid signaling and synaptic function. *Neuron*. **76**, 70–81 (2012).

250. C. Q. Chiu, N. Puente, P. Grandes, P. E. Castillo, Dopaminergic modulation of endocannabinoid-mediated plasticity at GABAergic synapses in the prefrontal cortex. *J. Neurosci.* **30**, 7236–7248 (2010).

251. C. Q. Chiu *et al.*, Input-Specific NMDAR-Dependent Potentiation of Dendritic GABAergic Inhibition. *Neuron*. **97**, 368–377.e3 (2018).

252. A. Kerkhofs *et al.*, Adenosine A2A receptors control glutamatergic synaptic plasticity in fast spiking interneurons of the prefrontal cortex. *Front. Pharmacol.* **9**, 133 (2018).

253. J. Maksymetz *et al.*, Targeting metabotropic glutamate receptors for novel treatments of schizophrenia. *Mol. Brain* (2017).

254. S. P. Moran, J. Maksymetz, P. J. Conn, Targeting muscarinic acetylcholine receptors for the treatment of psychiatric and neurological disorders. *Trends Pharmacol. Sci.* **40**, 1006–1020 (2019).

255. B. S. McEwen, J. H. Morrison, The brain on stress: vulnerability and plasticity of the prefrontal cortex over the life course. *Neuron*. **79**, 16–29 (2013).

256. E. G. Karam *et al.*, The role of criterion A2 in the DSM-IV diagnosis of posttraumatic stress disorder. *Biol. Psychiatry*. **68**, 465–473 (2010).

257. Z. Steel *et al.*, Association of torture and other potentially traumatic events with mental health outcomes among populations exposed to mass conflict and displacement: a systematic review and meta-analysis. *JAMA*. **302**, 537–549 (2009).

258. American Psychiatric Association, *Diagnostic and statistical manual of mental disorders* (American Psychiatric Association, ed. 5th, 2013).

259. W. Berger *et al.*, Pharmacologic alternatives to antidepressants in posttraumatic stress disorder: a systematic review. *Prog. Neuropsychopharmacol. Biol. Psychiatry*. **33**, 169–180 (2009).

260. S. Qin, E. J. Hermans, H. J. F. van Marle, J. Luo, G. Fernández, Acute psychological stress reduces working memory-related activity in the dorsolateral prefrontal cortex. *Biol. Psychiatry*. **66**, 25–32 (2009).

261. M. Gärtner, L. Rohde-Liebenau, S. Grimm, M. Bajbouj, Working memory-related frontal theta activity is decreased under acute stress. *Psychoneuroendocrinology*. **43**, 105–113 (2014).

262. S.-Y. Moon, Y. B. Choi, H. K. Jung, Y. I. Lee, S.-H. Choi, Increased Frontal Gamma and Posterior Delta Powers as Potential Neurophysiological Correlates Differentiating Posttraumatic Stress Disorder from Anxiety Disorders. *Psychiatry Investig*. **15**, 1087–1093 (2018).

263. C. A. Morgan, A. Doran, G. Steffian, G. Hazlett, S. M. Southwick, Stress-induced deficits in working memory and visuo-constructive abilities in Special Operations soldiers. *Biol. Psychiatry*. **60**, 722–729 (2006).

264. K. C. Koenen *et al.*, Measures of prefrontal system dysfunction in posttraumatic stress disorder. *Brain Cogn.* **45**, 64–78 (2001).

265. E. B. Ansell, K. Rando, K. Tuit, J. Guarnaccia, R. Sinha, Cumulative adversity and smaller gray matter volume in medial prefrontal, anterior cingulate, and insula regions. *Biol. Psychiatry*. **72**, 57–64 (2012).

266. C. Liston, B. S. McEwen, B. J. Casey, Psychosocial stress reversibly disrupts prefrontal processing and attentional control. *Proc. Natl. Acad. Sci. USA*. **106**, 912–917 (2009).

267. P. Kim *et al.*, Effects of childhood poverty and chronic stress on emotion regulatory brain function in adulthood. *Proc. Natl. Acad. Sci. USA*. **110**, 18442–18447 (2013).

268. F. Tian *et al.*, Prefrontal responses to digit span memory phases in patients with post-traumatic stress disorder (PTSD): a functional near infrared spectroscopy study. *Neuroimage Clin.* **4**, 808–819 (2014).

269. T. Jovanovic *et al.*, Reduced neural activation during an inhibition task is associated with impaired fear inhibition in a traumatized civilian sample. *Cortex*. **49**, 1884–1891 (2013).

270. S. Kühn, J. Gallinat, Gray matter correlates of posttraumatic stress disorder: a quantitative meta-analysis. *Biol. Psychiatry*. **73**, 70–74 (2013).

271. S. E. Holmes *et al.*, Cerebellar and prefrontal cortical alterations in PTSD: structural and functional evidence. *Chronic Stress (Thousand Oaks)*. **2** (2018), doi:10.1177/2470547018786390.

272. J. N. Perusini *et al.*, Induction and expression of fear sensitization caused by acute traumatic stress. *Neuropsychopharmacology*. **41**, 45–57 (2016).

273. M. Koenigs, J. Grafman, Posttraumatic stress disorder: the role of medial prefrontal cortex and amygdala. *Neuroscientist*. **15**, 540–548 (2009).

274. D. V. Zuj, M. A. Palmer, M. J. J. Lommen, K. L. Felmingham, The centrality of fear extinction in linking risk factors to PTSD: A narrative review. *Neurosci. Biobehav. Rev.* **69**, 15–35 (2016).

275. E. A. Hembree *et al.*, Do patients drop out prematurely from exposure therapy for PTSD? *J. Trauma. Stress*. **16**, 555–562 (2003).

276. S. Maren, A. Holmes, Stress and fear extinction. *Neuropsychopharmacology*. **41**, 58–79 (2016).

277. S. Maren, K. L. Phan, I. Liberzon, The contextual brain: implications for fear conditioning, extinction and psychopathology. *Nat. Rev. Neurosci.* **14**, 417–428 (2013).

278. S. B. Sartori, N. Singewald, New pharmacological strategies for augmenting extinction learning in anxiety disorders. *e-Neuroforum*. **23** (2017), doi:10.1515/nf-2017-A011.

279. E. Shvil *et al.*, Sex differences in extinction recall in posttraumatic stress disorder: a pilot fMRI study. *Neurobiol. Learn. Mem.* **113**, 101–108 (2014).

280. M. R. Milad *et al.*, Neurobiological basis of failure to recall extinction memory in posttraumatic stress disorder. *Biol. Psychiatry*. **66**, 1075–1082 (2009).

281. C. Linnman, T. A. Zeffiro, R. K. Pitman, M. R. Milad, An fMRI study of unconditioned responses in post-traumatic stress disorder. *Biol. Mood Anxiety Disord.* **1**, 8 (2011).

282. J. D. Bremner *et al.*, Positron emission tomographic imaging of neural correlates of a fear acquisition and extinction paradigm in women with childhood sexual-abuse-related post-traumatic stress disorder. *Psychol. Med.* **35**, 791–806 (2005).

283. R. K. Sripada, S. N. Garfinkel, I. Liberzon, Avoidant symptoms in PTSD predict fear circuit activation during multimodal fear extinction. *Front. Hum. Neurosci.* **7**, 672 (2013).

284. G. Richter-Levin, O. Stork, M. V. Schmidt, Animal models of PTSD: a challenge to be met. *Mol. Psychiatry*. **24**, 1135–1156 (2019).

285. N. Singewald, A. Holmes, Rodent models of impaired fear extinction. *Psychopharmacology*. **236**, 21–32 (2019).

286. D. Knox *et al.*, Single prolonged stress disrupts retention of extinguished fear in rats. *Learn. Mem.* **19**, 43–49 (2012).

287. D. Knox *et al.*, Neural circuits via which single prolonged stress exposure leads to fear extinction retention deficits. *Learn. Mem.* **23**, 689–698 (2016).

288. R. Reznikov *et al.*, Prefrontal Cortex Deep Brain Stimulation Improves Fear and Anxiety-Like Behavior and Reduces Basolateral Amygdala Activity in a Preclinical Model of Posttraumatic Stress Disorder. *Neuropsychopharmacology*. **43**, 1099–1106 (2018).

289. J. Shallcross *et al.*, The divergent effects of CDPPB and cannabidiol on fear extinction and anxiety in a predator scent stress model of PTSD in rats. *Front. Behav. Neurosci.* **13**, 91 (2019).

290. L. S. Hwa *et al.*, Predator odor increases avoidance and glutamatergic synaptic transmission in the prelimbic cortex via corticotropin-releasing factor receptor 1 signaling. *Neuropsychopharmacology*. **44**, 766–775 (2019).

291. P. J. Fitzgerald, J. R. Seemann, S. Maren, Can fear extinction be enhanced? A review of pharmacological and behavioral findings. *Brain Res. Bull.* **105**, 46–60 (2014).

292. M. J. Girgenti, S. Ghosal, D. LoPresto, J. R. Taylor, R. S. Duman, Ketamine accelerates fear extinction via mTORC1 signaling. *Neurobiol. Dis.* **100**, 1–8 (2017).

293. M. Davis, K. Ressler, B. O. Rothbaum, R. Richardson, Effects of D-cycloserine on extinction: translation from preclinical to clinical work. *Biol. Psychiatry*. **60**, 369–375 (2006).

294. A. Holmes, G. J. Quirk, Pharmacological facilitation of fear extinction and the search for adjunct treatments for anxiety disorders--the case of yohimbine. *Trends Pharmacol. Sci.* **31**, 2–7 (2010).

295. J. van Os, S. Kapur, Schizophrenia. *Lancet*. **374**, 635–645 (2009).

296. D. L. Segal, in *The corsini encyclopedia of psychology*, I. B. Weiner, W. E. Craighead, Eds. (John Wiley & Sons, Inc., Hoboken, NJ, USA, 2010).

297. M. F. Green, What are the functional consequences of neurocognitive deficits in schizophrenia? *Am. J. Psychiatry*. **153**, 321–330 (1996).

298. J. P. McEvoy, The costs of schizophrenia. *J. Clin. Psychiatry*. **68 Suppl 14**, 4–7 (2007).

299. J. A. Lieberman *et al.*, Effectiveness of antipsychotic drugs in patients with chronic schizophrenia. *N. Engl. J. Med.* **353**, 1209–1223 (2005).

300. H. Y. Meltzer, Update on typical and atypical antipsychotic drugs. *Annu. Rev. Med.* **64**, 393–406 (2013).

301. J. Lally, J. H. MacCabe, Antipsychotic medication in schizophrenia: a review. *Br Med Bull*. **114**, 169–179 (2015).

302. S. Miyamoto, G. E. Duncan, C. E. Marx, J. A. Lieberman, Treatments for schizophrenia: a critical review of pharmacology and mechanisms of action of antipsychotic drugs. *Mol. Psychiatry*. **10**, 79–104 (2005).

303. W. W. Shen, A history of antipsychotic drug development. *Compr. Psychiatry*. **40**, 407–414 (1999).

304. H. Hippius, A historical perspective of clozapine. *J. Clin. Psychiatry*. **60 Suppl 12**, 22–23 (1999).

305. I. Creese, D. R. Burt, S. H. Snyder, Dopamine receptor binding predicts clinical and pharmacological potencies of antischizophrenic drugs. *Science*. **192**, 481–483 (1976).

306. P. Seeman, T. Lee, M. Chau-Wong, K. Wong, Antipsychotic drug doses and neuroleptic/dopamine receptors. *Nature*. **261**, 717–719 (1976).

307. H. Y. Meltzer, S. Matsubara, J. C. Lee, Classification of typical and atypical antipsychotic drugs on the basis of dopamine D-1, D-2 and serotonin2 pKi values. *J. Pharmacol. Exp. Ther.* **251**, 238–246 (1989).

308. A. Carlsson, M. Lindqvist, Effect of chlorpromazine or haloperidol on formation of 3methoxytyramine and normetanephrine in mouse brain. *Acta Pharmacol. Toxicol. (Copenh.)*. **20**, 140–144 (1963).

309. R. A. McCutcheon, A. Abi-Dargham, O. D. Howes, Schizophrenia, dopamine and the striatum: from biology to symptoms. *Trends Neurosci.* **42**, 205–220 (2019).

310. M. Toru *et al.*, Neurotransmitters, receptors and neuropeptides in post-mortem brains of chronic schizophrenic patients. *Acta Psychiatr. Scand.* **78**, 121–137 (1988).

311. F. Owen *et al.*, Increased dopamine-receptor sensitivity in schizophrenia. *Lancet*. **2**, 223–226 (1978).

312. E. D. Bird *et al.*, Increased brain dopamine and reduced glutamic acid decarboxylase and choline acetyl transferase activity in schizophrenia and related psychoses. *Lancet*. **2**, 1157–1158 (1977).

313. T. J. Crow *et al.*, Monoamine mechanisms in chronic schizophrenia: post-mortem neurochemical findings. *Br. J. Psychiatry*. **134**, 249–256 (1979).

314. R. McCutcheon, K. Beck, S. Jauhar, O. D. Howes, Defining the Locus of Dopaminergic Dysfunction in Schizophrenia: A Meta-analysis and Test of the Mesolimbic Hypothesis. *Schizophr. Bull.* **44**, 1301–1311 (2018).

315. L. S. Kegeles *et al.*, Increased synaptic dopamine function in associative regions of the striatum in schizophrenia. *Arch. Gen. Psychiatry*. **67**, 231–239 (2010).

316. O. D. Howes *et al.*, Midbrain dopamine function in schizophrenia and depression: a post-mortem and positron emission tomographic imaging study. *Brain*. **136**, 3242–3251 (2013).

317. F. da Silva Alves, M. Figee, T. van Amelsvoort, D. Veltman, L. de Haan, The revised dopamine hypothesis of schizophrenia: evidence from pharmacological MRI studies with atypical antipsychotic medication. *Psychopharmacol Bull*. **41**, 121–132 (2008).

318. D. M. Barch, A. Ceaser, Cognition in schizophrenia: core psychological and neural mechanisms. *Trends Cogn. Sci. (Regul. Ed.)*. **16**, 27–34 (2012).

319. M. Slifstein *et al.*, Deficits in prefrontal cortical and extrastriatal dopamine release in schizophrenia: a positron emission tomographic functional magnetic resonance imaging study. *JAMA Psychiatry*. **72**, 316–324 (2015).

320. Y. Okubo *et al.*, Decreased prefrontal dopamine D1 receptors in schizophrenia revealed by PET. *Nature*. **385**, 634–636 (1997).

321. A. Abi-Dargham *et al.*, Prefrontal dopamine D1 receptors and working memory in schizophrenia. *J. Neurosci.* **22**, 3708–3719 (2002).

322. A. Abi-Dargham *et al.*, Increased prefrontal cortical D_1 receptors in drug naive patients with schizophrenia: a PET study with [^{11}C]NNC112. *J. Psychopharmacol. (Oxford)*. **26**, 794–805 (2012).

323. D. M. Barch, C. S. Carter, Amphetamine improves cognitive function in medicated individuals with schizophrenia and in healthy volunteers. *Schizophr. Res.* **77**, 43–58 (2005).

324. J. A. Lieberman, J. M. Kane, J. Alvir, Provocative tests with psychostimulant drugs in schizophrenia. *Psychopharmacology*. **91**, 415–433 (1987).

325. B. Moghaddam, D. Javitt, From revolution to evolution: the glutamate hypothesis of schizophrenia and its implication for treatment. *Neuropsychopharmacology*. **37**, 4–15 (2012).

326. J. T. Coyle, Glutamate and schizophrenia: beyond the dopamine hypothesis. *Cell Mol. Neurobiol.* **26**, 365–384 (2006).

327. J. Cosgrove, T. G. Newell, Recovery of neuropsychological functions during reduction in use of phencyclidine. *J. Clin. Psychol.* **47**, 159–169 (1991).

328. D. C. Javitt, S. R. Zukin, Recent advances in the phencyclidine model of schizophrenia. *Am. J. Psychiatry*. **148**, 1301–1308 (1991).

329. J. H. Krystal *et al.*, Subanesthetic effects of the noncompetitive NMDA antagonist, ketamine, in humans. Psychotomimetic, perceptual, cognitive, and neuroendocrine responses. *Arch. Gen. Psychiatry*. **51**, 199–214 (1994).

330. J. Dalmau *et al.*, Anti-NMDA-receptor encephalitis: case series and analysis of the effects of antibodies. *Lancet Neurol.* **7**, 1091–1098 (2008).

331. Schizophrenia Working Group of the Psychiatric Genomics Consortium, Biological insights from 108 schizophrenia-associated genetic loci. *Nature*. **511**, 421–427 (2014).

332. M. Beneyto, J. H. Meador-Woodruff, Lamina-specific abnormalities of NMDA receptor-associated postsynaptic protein transcripts in the prefrontal cortex in schizophrenia and bipolar disorder. *Neuropsychopharmacology*. **33**, 2175–2186 (2008).

333. C. S. Weickert *et al.*, Molecular evidence of N-methyl-D-aspartate receptor hypofunction in schizophrenia. *Mol. Psychiatry*. **18**, 1185–1192 (2013).

334. M. Beneyto, J. H. Meador-Woodruff, Lamina-specific abnormalities of AMPA receptor trafficking and signaling molecule transcripts in the prefrontal cortex in schizophrenia. *Synapse*. **60**, 585–598 (2006).

335. B. P. Sokolov, Expression of NMDAR1, GluR1, GluR7, and KA1 glutamate receptor mRNAs is decreased in frontal cortex of “neuroleptic-free” schizophrenics: evidence on reversible up-regulation by typical neuroleptics. *J. Neurochem.* **71**, 2454–2464 (1998).

336. S. Akbarian *et al.*, Selective alterations in gene expression for NMDA receptor subunits in prefrontal cortex of schizophrenics. *J. Neurosci.* **16**, 19–30 (1996).

337. S. Dracheva *et al.*, N-methyl-D-aspartic acid receptor expression in the dorsolateral prefrontal cortex of elderly patients with schizophrenia. *Am. J. Psychiatry*. **158**, 1400–1410 (2001).

338. S. Dracheva, S. R. McGurk, V. Haroutunian, mRNA expression of AMPA receptors and AMPA receptor binding proteins in the cerebral cortex of elderly schizophrenics. *J. Neurosci. Res.* **79**, 868–878 (2005).

339. D. J. Healy *et al.*, AMPA receptor binding and subunit mRNA expression in prefrontal cortex and striatum of elderly schizophrenics. *Neuropsychopharmacology*. **19**, 278–286 (1998).

340. C. Corti *et al.*, Altered levels of glutamatergic receptors and Na+/K+ ATPase-α1 in the prefrontal cortex of subjects with schizophrenia. *Schizophr. Res.* **128**, 7–14 (2011).

341. L. V. Kristiansen, M. Beneyto, V. Haroutunian, J. H. Meador-Woodruff, Changes in NMDA receptor subunits and interacting PSD proteins in dorsolateral prefrontal and anterior cingulate cortex indicate abnormal regional expression in schizophrenia. *Mol. Psychiatry*. **11**, 737–47, 705 (2006).

342. M. A. Geyer, K. Krebs-Thomson, D. L. Braff, N. R. Swerdlow, Pharmacological studies of prepulse inhibition models of sensorimotor gating deficits in schizophrenia: a decade in review. *Psychopharmacology*. **156**, 117–154 (2001).

343. C. A. Jones, D. J. G. Watson, K. C. F. Fone, Animal models of schizophrenia. *Br. J. Pharmacol.* **164**, 1162–1194 (2011).

344. B. Moghaddam, B. Adams, A. Verma, D. Daly, Activation of glutamatergic neurotransmission by ketamine: a novel step in the pathway from NMDA receptor blockade to dopaminergic and cognitive disruptions associated with the prefrontal cortex. *J. Neurosci.* **17**, 2921–2927 (1997).

345. E. M. P. Poels *et al.*, Glutamatergic abnormalities in schizophrenia: a review of proton MRS findings. *Schizophr. Res.* **152**, 325–332 (2014).

346. J. E. Black *et al.*, Pathology of layer V pyramidal neurons in the prefrontal cortex of patients with schizophrenia. *Am. J. Psychiatry*. **161**, 742–744 (2004).

347. K. Broadbelt, W. Byne, L. B. Jones, Evidence for a decrease in basilar dendrites of pyramidal cells in schizophrenic medial prefrontal cortex. *Schizophr. Res.* **58**, 75–81 (2002).

348. P. Kalus, T. J. Müller, W. Zuschratter, D. Senitz, The dendritic architecture of prefrontal pyramidal neurons in schizophrenic patients. *Neuroreport*. **11**, 3621–3625 (2000).

349. L. A. Glantz, D. A. Lewis, Decreased dendritic spine density on prefrontal cortical pyramidal neurons in schizophrenia. *Arch. Gen. Psychiatry*. **57**, 65–73 (2000).

350. N. Kolluri, Z. Sun, A. R. Sampson, D. A. Lewis, Lamina-specific reductions in dendritic spine density in the prefrontal cortex of subjects with schizophrenia. *Am. J. Psychiatry*. **162**, 1200–1202 (2005).

351. L. J. Garey *et al.*, Reduced dendritic spine density on cerebral cortical pyramidal neurons in schizophrenia. *J. Neurol. Neurosurg. Psychiatry*. **65**, 446–453 (1998).

352. T. Hajszan, C. Leranth, R. H. Roth, Subchronic phencyclidine treatment decreases the number of dendritic spine synapses in the rat prefrontal cortex. *Biol. Psychiatry*. **60**, 639–644 (2006).

353. R. M. Ruddy, Y. Chen, M. Milenkovic, A. J. Ramsey, Differential effects of NMDA receptor antagonism on spine density. *Synapse*. **69**, 52–56 (2015).

354. S. K. Ultanir *et al.*, Regulation of spine morphology and spine density by NMDA receptor signaling in vivo. *Proc. Natl. Acad. Sci. USA*. **104**, 19553–19558 (2007).

355. L. M. DeVito *et al.*, Serine racemase deletion disrupts memory for order and alters cortical dendritic morphology. *Genes Brain Behav.* **10**, 210–222 (2011).

356. H. Homayoun, B. Moghaddam, NMDA receptor hypofunction produces opposite effects on prefrontal cortex interneurons and pyramidal neurons. *J. Neurosci.* **27**, 11496–11500 (2007).

357. O. M. Doyle *et al.*, Quantifying the attenuation of the ketamine pharmacological magnetic resonance imaging response in humans: a validation using antipsychotic and glutamatergic agents. *J. Pharmacol. Exp. Ther.* **345**, 151–160 (2013).

358. A. Breier, A. K. Malhotra, D. A. Pinals, N. I. Weisenfeld, D. Pickar, Association of ketamine-induced psychosis with focal activation of the prefrontal cortex in healthy volunteers. *Am. J. Psychiatry*. **154**, 805–811 (1997).

359. F. X. Vollenweider *et al.*, Metabolic hyperfrontality and psychopathology in the ketamine model of psychosis using positron emission tomography (PET) and [18F]fluorodeoxyglucose (FDG). *Eur. Neuropsychopharmacol.* **7**, 9–24 (1997).

360. Y. Suzuki, E. Jodo, S. Takeuchi, S. Niwa, Y. Kayama, Acute administration of phencyclidine induces tonic activation of medial prefrontal cortex neurons in freely moving rats. *Neuroscience*. **114**, 769–779 (2002).

361. D. S. Manoach *et al.*, Schizophrenic subjects activate dorsolateral prefrontal cortex during a working memory task, as measured by fMRI. *Biol. Psychiatry*. **45**, 1128–1137 (1999).

362. A. Anticevic *et al.*, Early-course unmedicated schizophrenia patients exhibit elevated prefrontal connectivity associated with longitudinal change. *J. Neurosci.* **35**, 267–286 (2015).

363. K. Nakazawa *et al.*, GABAergic interneuron origin of schizophrenia pathophysiology. *Neuropharmacology*. **62**, 1574–1583 (2012).

364. M. M. Behrens *et al.*, Ketamine-induced loss of phenotype of fast-spiking interneurons is mediated by NADPH-oxidase. *Science*. **318**, 1645–1647 (2007).

365. S. M. Cochran *et al.*, Induction of metabolic hypofunction and neurochemical deficits after chronic intermittent exposure to phencyclidine: differential modulation by antipsychotic drugs. *Neuropsychopharmacology*. **28**, 265–275 (2003).

366. D. Rujescu *et al.*, A pharmacological model for psychosis based on N-methyl-D-aspartate receptor hypofunction: molecular, cellular, functional and behavioral abnormalities. *Biol. Psychiatry*. **59**, 721–729 (2006).

367. D. S. Ling, L. S. Benardo, Recruitment of GABAA inhibition in rat neocortex is limited and not NMDA dependent. *J. Neurophysiol.* **74**, 2329–2335 (1995).

368. H. C. Grunze *et al.*, NMDA-dependent modulation of CA1 local circuit inhibition. *J. Neurosci.* **16**, 2034–2043 (1996).

369. Q. Li, S. Clark, D. V. Lewis, W. A. Wilson, NMDA receptor antagonists disinhibit rat posterior cingulate and retrosplenial cortices: a potential mechanism of neurotoxicity. *J. Neurosci.* **22**, 3070–3080 (2002).

370. C. Hull, J. S. Isaacson, M. Scanziani, Postsynaptic mechanisms govern the differential excitation of cortical neurons by thalamic inputs. *J. Neurosci.* **29**, 9127–9136 (2009).

371. A. J. Widman, L. L. McMahon, Disinhibition of CA1 pyramidal cells by low-dose ketamine and other antagonists with rapid antidepressant efficacy. *Proc. Natl. Acad. Sci. USA*. **115**, E3007–E3016 (2018).

372. N. V. Povysheva, J. W. Johnson, Effects of memantine on the excitation-inhibition balance in prefrontal cortex. *Neurobiol. Dis.* **96**, 75–83 (2016).

373. K. Nakazawa, K. Sapkota, The origin of NMDA receptor hypofunction in schizophrenia. *Pharmacol. Ther.*, 107426 (2019).

374. S. Akbarian *et al.*, Gene expression for glutamic acid decarboxylase is reduced without loss of neurons in prefrontal cortex of schizophrenics. *Arch. Gen. Psychiatry*. **52**, 258–266 (1995).

375. D. W. Volk, M. C. Austin, J. N. Pierri, A. R. Sampson, D. A. Lewis, Decreased glutamic acid decarboxylase67 messenger RNA expression in a subset of prefrontal cortical gamma-aminobutyric acid neurons in subjects with schizophrenia. *Arch. Gen. Psychiatry*. **57**, 237–245 (2000).

376. A. A. Curley *et al.*, Cortical deficits of glutamic acid decarboxylase 67 expression in schizophrenia: clinical, protein, and cell type-specific features. *Am. J. Psychiatry*. **168**, 921–929 (2011).

377. A. Guidotti *et al.*, Decrease in reelin and glutamic acid decarboxylase67 (GAD67) expression in schizophrenia and bipolar disorder: a postmortem brain study. *Arch. Gen. Psychiatry*. **57**, 1061–1069 (2000).

378. T. Hashimoto *et al.*, Alterations in GABA-related transcriptome in the dorsolateral prefrontal cortex of subjects with schizophrenia. *Mol. Psychiatry*. **13**, 147–161 (2008).

379. S. J. Fung *et al.*, Expression of interneuron markers in the dorsolateral prefrontal cortex of the developing human and in schizophrenia. *Am. J. Psychiatry*. **167**, 1479–1488 (2010).

380. J. J. Thune, H. B. Uylings, B. Pakkenberg, No deficit in total number of neurons in the prefrontal cortex in schizophrenics. *J. Psychiatr. Res.* **35**, 15–21 (2001).

381. B. R. Rocco, D. A. Lewis, K. N. Fish, Markedly lower glutamic acid decarboxylase 67 protein levels in a subset of boutons in schizophrenia. *Biol. Psychiatry*. **79**, 1006–1015 (2016).

382. T. Hashimoto *et al.*, Gene expression deficits in a subclass of GABA neurons in the prefrontal cortex of subjects with schizophrenia. *J. Neurosci.* **23**, 6315–6326 (2003).

383. S. H. Arif, A Ca(2+)-binding protein with numerous roles and uses: parvalbumin in molecular biology and physiology. *Bioessays*. **31**, 410–421 (2009).

384. S. Marenco *et al.*, Prefrontal GABA levels measured with magnetic resonance spectroscopy in patients with psychosis and unaffected siblings. *Am. J. Psychiatry*. **173**, 527–534 (2016).

385. L. M. Rowland *et al.*, Frontal Glutamate and γ-Aminobutyric Acid Levels and Their Associations With Mismatch Negativity and Digit Sequencing Task Performance in Schizophrenia. *JAMA Psychiatry*. **73**, 166–174 (2016).

386. C.-M. A. Chen *et al.*, GABA level, gamma oscillation, and working memory performance in schizophrenia. *Neuroimage Clin.* **4**, 531–539 (2014).

387. D. Ongür, A. P. Prescot, J. McCarthy, B. M. Cohen, P. F. Renshaw, Elevated gamma-aminobutyric acid levels in chronic schizophrenia. *Biol. Psychiatry*. **68**, 667–670 (2010).

388. C. de la Fuente-Sandoval *et al.*, Prefrontal and Striatal Gamma-Aminobutyric Acid Levels and the Effect of Antipsychotic Treatment in First-Episode Psychosis Patients. *Biol. Psychiatry*. **83**, 475–483 (2018).

389. M. W. Howard *et al.*, Gamma oscillations correlate with working memory load in humans. *Cereb. Cortex*. **13**, 1369–1374 (2003).

390. R. Y. Cho, R. O. Konecky, C. S. Carter, Impairments in frontal cortical gamma synchrony and cognitive control in schizophrenia. *Proc. Natl. Acad. Sci. USA*. **103**, 19878–19883 (2006).

391. M. J. Minzenberg *et al.*, Gamma oscillatory power is impaired during cognitive control independent of medication status in first-episode schizophrenia. *Neuropsychopharmacology*. **35**, 2590–2599 (2010).

392. P. J. Uhlhaas, W. Singer, Abnormal neural oscillations and synchrony in schizophrenia. *Nat. Rev. Neurosci.* **11**, 100–113 (2010).

393. S. J. Dienel, D. A. Lewis, Alterations in cortical interneurons and cognitive function in schizophrenia. *Neurobiol. Dis.* **131**, 104208 (2019).

394. J. E. Belforte *et al.*, Postnatal NMDA receptor ablation in corticolimbic interneurons confers schizophrenia-like phenotypes. *Nat. Neurosci.* **13**, 76–83 (2010).

395. K. Nakao *et al.*, Schizophrenia-Like Dopamine Release Abnormalities in a Mouse Model of NMDA Receptor Hypofunction. *Schizophr. Bull.* **45**, 138–147 (2019).

396. M. Carlén *et al.*, A critical role for NMDA receptors in parvalbumin interneurons for gamma rhythm induction and behavior. *Mol. Psychiatry*. **17**, 537–548 (2012).

397. T. Korotkova, E. C. Fuchs, A. Ponomarenko, J. von Engelhardt, H. Monyer, NMDA receptor ablation on parvalbumin-positive interneurons impairs hippocampal synchrony, spatial representations, and working memory. *Neuron*. **68**, 557–569 (2010).

398. J. E. Lisman, H. J. Pi, Y. Zhang, N. A. Otmakhova, A thalamo-hippocampal-ventral tegmental area loop may produce the positive feedback that underlies the psychotic break in schizophrenia. *Biol. Psychiatry*. **68**, 17–24 (2010).

399. K. A. Feigenson, A. W. Kusnecov, S. M. Silverstein, Inflammation and the two-hit hypothesis of schizophrenia. *Neurosci. Biobehav. Rev.* **38**, 72–93 (2014).

400. D. W. Miller, E. D. Abercrombie, Effects of MK-801 on spontaneous and amphetamine-stimulated dopamine release in striatum measured with in vivo microdialysis in awake rats. *Brain Res. Bull.* **40**, 57–62 (1996).

401. A. Balla, R. Koneru, J. Smiley, H. Sershen, D. C. Javitt, Continuous phencyclidine treatment induces schizophrenia-like hyperreactivity of striatal dopamine release. *Neuropsychopharmacology*. **25**, 157–164 (2001).

402. K. Y. Tseng, R. A. Chambers, B. K. Lipska, The neonatal ventral hippocampal lesion as a heuristic neurodevelopmental model of schizophrenia. *Behav. Brain Res.* **204**, 295–305 (2009).

403. B. K. Lipska, D. N. Lerman, Z. Z. Khaing, C. S. Weickert, D. R. Weinberger, Gene expression in dopamine and GABA systems in an animal model of schizophrenia: effects of antipsychotic drugs. *Eur. J. Neurosci.* **18**, 391–402 (2003).

404. P. O'Donnell, B. L. Lewis, D. R. Weinberger, B. K. Lipska, Neonatal hippocampal damage alters electrophysiological properties of prefrontal cortical neurons in adult rats. *Cereb. Cortex*. **12**, 975–982 (2002).

405. Y. Gulchina, S.-J. Xu, M. A. Snyder, F. Elefant, W.-J. Gao, Epigenetic mechanisms underlying NMDA receptor hypofunction in the prefrontal cortex of juvenile animals in the MAM model for schizophrenia. *J. Neurochem.* **143**, 320–333 (2017).

406. H. Lacaille *et al.*, Impaired interneuron development in a novel model of neonatal brain injury. *Eneuro*. **6** (2019), doi:10.1523/ENEURO.0300-18.2019.

407. A. Mukherjee, F. Carvalho, S. Eliez, P. Caroni, Long-Lasting Rescue of Network and Cognitive Dysfunction in a Genetic Schizophrenia Model. *Cell*. **178**, 1387–1402.e14 (2019).

408. M. R. Picciotto, M. J. Higley, Y. S. Mineur, Acetylcholine as a neuromodulator: cholinergic signaling shapes nervous system function and behavior. *Neuron*. **76**, 116–129 (2012).

409. M. Sarter, C. Lustig, W. M. Howe, H. Gritton, A. S. Berry, Deterministic functions of cortical acetylcholine. *Eur. J. Neurosci.* **39**, 1912–1920 (2014).

410. J. Wess, R. M. Eglen, D. Gautam, Muscarinic acetylcholine receptors: mutant mice provide new insights for drug development. *Nat. Rev. Drug Discov.* **6**, 721–733 (2007).

411. M. E. Hasselmo, M. Sarter, Modes and models of forebrain cholinergic neuromodulation of cognition. *Neuropsychopharmacology*. **36**, 52–73 (2011).

412. N. C. Bodick *et al.*, Effects of xanomeline, a selective muscarinic receptor agonist, on cognitive function and behavioral symptoms in Alzheimer disease. *Arch. Neurol.* **54**, 465–473 (1997).

413. A. Shekhar *et al.*, Selective muscarinic receptor agonist xanomeline as a novel treatment approach for schizophrenia. *Am. J. Psychiatry*. **165**, 1033–1039 (2008).

414. A. M. Bender, C. K. Jones, C. W. Lindsley, Classics in chemical neuroscience: xanomeline. *ACS Chem. Neurosci.* **8**, 435–443 (2017).

415. J. A. Berman, D. A. Talmage, L. W. Role, Cholinergic circuits and signaling in the pathophysiology of schizophrenia. *Int Rev Neurobiol*. **78**, 193–223 (2007).

416. T. J. Raedler, F. P. Bymaster, R. Tandon, D. Copolov, B. Dean, Towards a muscarinic hypothesis of schizophrenia. *Mol. Psychiatry*. **12**, 232–246 (2007).

417. E. Scarr *et al.*, Low levels of muscarinic M1 receptor-positive neurons in cortical layers III and V in Brodmann areas 9 and 17 from individuals with schizophrenia. *J. Psychiatry Neurosci.* **43**, 338–346 (2018).

418. B. Dean, M. McLeod, D. Keriakous, J. McKenzie, E. Scarr, Decreased muscarinic1 receptors in the dorsolateral prefrontal cortex of subjects with schizophrenia. *Mol. Psychiatry*. **7**, 1083–1091 (2002).

419. F. Yi *et al.*, Direct excitation of parvalbumin-positive interneurons by M1 muscarinic acetylcholine receptors: roles in cellular excitability, inhibitory transmission and cognition. *J. Physiol. (Lond.)*. **592**, 3463–3494 (2014).

420. D. B. Carr, D. J. Surmeier, M1 muscarinic receptor modulation of Kir2 channels enhances temporal summation of excitatory synaptic potentials in prefrontal cortex pyramidal neurons. *J. Neurophysiol.* **97**, 3432–3438 (2007).

421. J. K. Shirey *et al.*, A selective allosteric potentiator of the M1 muscarinic acetylcholine receptor increases activity of medial prefrontal cortical neurons and restores impairments in reversal learning. *J. Neurosci.* **29**, 14271–14286 (2009).

422. A. T. Gulledge, D. J. Bucci, S. S. Zhang, M. Matsui, H. H. Yeh, M1 receptors mediate cholinergic modulation of excitability in neocortical pyramidal neurons. *J. Neurosci.* **29**, 9888–9902 (2009).

423. S. G. Anagnostaras *et al.*, Selective cognitive dysfunction in acetylcholine M1 muscarinic receptor mutant mice. *Nat. Neurosci.* **6**, 51–58 (2003).

424. R. W. Gould *et al.*, Role for the M1 Muscarinic Acetylcholine Receptor in Top-Down Cognitive Processing Using a Touchscreen Visual Discrimination Task in Mice. *ACS Chem. Neurosci.* **6**, 1683–1695 (2015).

425. M. J. Marino, S. T. Rouse, A. I. Levey, L. T. Potter, P. J. Conn, Activation of the genetically defined m1 muscarinic receptor potentiates N-methyl-D-aspartate (NMDA) receptor currents in hippocampal pyramidal cells. *Proc. Natl. Acad. Sci. USA*. **95**, 11465–11470 (1998).

426. C. Sur *et al.*, N-desmethylclozapine, an allosteric agonist at muscarinic 1 receptor, potentiates N-methyl-D-aspartate receptor activity. *Proc. Natl. Acad. Sci. USA*. **100**, 13674–13679 (2003).

427. L. Ma *et al.*, Selective activation of the M1 muscarinic acetylcholine receptor achieved by allosteric potentiation. *Proc. Natl. Acad. Sci. USA*. **106**, 15950–15955 (2009).

428. C. Chambon, C. Jatzke, N. Wegener, A. Gravius, W. Danysz, Using cholinergic M1 receptor positive allosteric modulators to improve memory via enhancement of brain cholinergic communication. *Eur. J. Pharmacol.* **697**, 73–80 (2012).

429. K. H. C. Choy *et al.*, Positive allosteric modulation of the muscarinic M1 receptor improves efficacy of antipsychotics in mouse glutamatergic deficit models of behavior. *J. Pharmacol. Exp. Ther.* **359**, 354–365 (2016).

430. A. I. Levey, Muscarinic acetylcholine receptor expression in memory circuits: implications for treatment of Alzheimer disease. *Proc. Natl. Acad. Sci. USA*. **93**, 13541–13546 (1996).

431. A. I. Levey, C. A. Kitt, W. F. Simonds, D. L. Price, M. R. Brann, Identification and localization of muscarinic acetylcholine receptor proteins in brain with subtype-specific antibodies. *J. Neurosci.* **11**, 3218–3226 (1991).

432. H. S. Lange, C. E. Cannon, J. T. Drott, S. D. Kuduk, J. M. Uslaner, The M1 muscarinic positive allosteric modulator PQCA improves performance on translatable tests of memory and attention in rhesus monkeys. *J. Pharmacol. Exp. Ther.* **355**, 442–450 (2015).

433. J. M. Uslaner *et al.*, The muscarinic M1 receptor positive allosteric modulator PQCA improves cognitive measures in rat, cynomolgus macaque, and rhesus macaque. *Psychopharmacology*. **225**, 21–30 (2013).

434. D. C. Beshore *et al.*, MK-7622: A First-in-Class M_1 Positive Allosteric Modulator Development Candidate. *ACS Med. Chem. Lett.* **9**, 652–656 (2018).

435. J. E. Davoren *et al.*, Design and Synthesis of γ- and δ-Lactam M1 Positive Allosteric Modulators (PAMs): Convulsion and Cholinergic Toxicity of an M1-Selective PAM with Weak Agonist Activity. *J. Med. Chem.* **60**, 6649–6663 (2017).

436. S. P. Moran *et al.*, PF-06827443 Displays Robust Allosteric Agonist and Positive Allosteric Modulator Activity in High Receptor Reserve and Native Systems. *ACS Chem. Neurosci.* **9**, 2218–2224 (2018).

437. S. P. Moran *et al.*, M1-positive allosteric modulators lacking agonist activity provide the optimal profile for enhancing cognition. *Neuropsychopharmacology*. **43**, 1763–1771 (2018).

438. J. M. Rook *et al.*, Unique signaling profiles of positive allosteric modulators of metabotropic glutamate receptor subtype 5 determine differences in in vivo activity. *Biol. Psychiatry*. **73**, 501–509 (2013).

439. S. Vijayraghavan, A. J. Major, S. Everling, Muscarinic M1 receptor overstimulation disrupts working memory activity for rules in primate prefrontal cortex. *Neuron*. **98**, 1256–1268.e4 (2018).

440. T. Voss *et al.*, Randomized, controlled, proof-of-concept trial of MK-7622 in Alzheimer's disease. *Alzheimers Dement (N Y)*. **4**, 173–181 (2018).

441. M. D. Grannan *et al.*, Prefrontal Cortex-Mediated Impairments in a Genetic Model of NMDA Receptor Hypofunction Are Reversed by the Novel M1 PAM VU6004256. *ACS Chem. Neurosci.* **7**, 1706–1716 (2016).

442. J. M. Rook *et al.*, A Novel M1 PAM VU0486846 Exerts Efficacy in Cognition Models without Displaying Agonist Activity or Cholinergic Toxicity. *ACS Chem. Neurosci.* **9**, 2274–2285 (2018).

443. V. Puri, X. Wang, J. D. Vardigan, S. D. Kuduk, J. M. Uslaner, The selective positive allosteric M1 muscarinic receptor modulator PQCA attenuates learning and memory deficits in the Tg2576 Alzheimer's disease mouse model. *Behav. Brain Res.* **287**, 96–99 (2015).

444. S. J. Bradley *et al.*, M1 muscarinic allosteric modulators slow prion neurodegeneration and restore memory loss. *J. Clin. Invest.* **127**, 487–499 (2017).

445. C. K. Jones *et al.*, Novel selective allosteric activator of the M1 muscarinic acetylcholine receptor regulates amyloid processing and produces antipsychotic-like activity in rats. *J. Neurosci.* **28**, 10422–10433 (2008).

446. D. P. Holschneider, Y. Guo, Z. Wang, M. Vidal, O. U. Scremin, Positive Allosteric Modulation of Cholinergic Receptors Improves Spatial Learning after Cortical Contusion Injury in Mice. *J. Neurotrauma* (2019), doi:10.1089/neu.2018.6036.

447. M. Thomsen *et al.*, Contribution of both M1 and M4 receptors to muscarinic agonist-mediated attenuation of the cocaine discriminative stimulus in mice. *Psychopharmacology*. **220**, 673–685 (2012).

448. C. Puddifoot *et al.*, PGC-1α negatively regulates extrasynaptic NMDAR activity and excitotoxicity. *J. Neurosci.* **32**, 6995–7000 (2012).

449. M. M. Zeron *et al.*, Increased sensitivity to N-methyl-D-aspartate receptor-mediated excitotoxicity in a mouse model of Huntington's disease. *Neuron*. **33**, 849–860 (2002).

450. D. T. Monaghan, M. W. Irvine, B. M. Costa, G. Fang, D. E. Jane, Pharmacological modulation of NMDA receptor activity and the advent of negative and positive allosteric modulators. *Neurochem. Int.* **61**, 581–592 (2012).

451. D. H. Hackos *et al.*, Positive Allosteric Modulators of GluN2A-Containing NMDARs with Distinct Modes of Action and Impacts on Circuit Function. *Neuron*. **89**, 983–999 (2016).

452. A. M. Kaufman *et al.*, Opposing roles of synaptic and extrasynaptic NMDA receptor signaling in cocultured striatal and cortical neurons. *J. Neurosci.* **32**, 3992–4003 (2012).

453. Y. Iwata *et al.*, Effects of glutamate positive modulators on cognitive deficits in schizophrenia: a systematic review and meta-analysis of double-blind randomized controlled trials. *Mol. Psychiatry*. **20**, 1151–1160 (2015).

454. H. Wu *et al.*, Structure of a class C GPCR metabotropic glutamate receptor 1 bound to an allosteric modulator. *Science*. **344**, 58–64 (2014).

455. K. Hemstapat *et al.*, A novel family of potent negative allosteric modulators of group II metabotropic glutamate receptors. *J. Pharmacol. Exp. Ther.* **322**, 254–264 (2007).

456. J. A. Christopher *et al.*, Fragment and Structure-Based Drug Discovery for a Class C GPCR: Discovery of the mGlu5 Negative Allosteric Modulator HTL14242 (3-Chloro-5-[6-(5-fluoropyridin-2-yl)pyrimidin-4-yl]benzonitrile). *J. Med. Chem.* **58**, 6653–6664 (2015).

457. K. M. Houamed *et al.*, Cloning, expression, and gene structure of a G protein-coupled glutamate receptor from rat brain. *Science*. **252**, 1318–1321 (1991).

458. M. Masu, Y. Tanabe, K. Tsuchida, R. Shigemoto, S. Nakanishi, Sequence and expression of a metabotropic glutamate receptor. *Nature*. **349**, 760–765 (1991).

459. T. Abe *et al.*, Molecular characterization of a novel metabotropic glutamate receptor mGluR5 coupled to inositol phosphate/Ca2+ signal transduction. *J. Biol. Chem.* **267**, 13361–13368 (1992).

460. L. Aniksztejn, P. Bregestovski, Y. Ben-Ari, Selective activation of quisqualate metabotropic receptor potentiates NMDA but not AMPA responses. *Eur. J. Pharmacol.* **205**, 327–328 (1991).

461. J. Harvey, G. L. Collingridge, Signal transduction pathways involved in the acute potentiation of NMDA responses by 1S,3R-ACPD in rat hippocampal slices. *Br. J. Pharmacol.* **109**, 1085–1090 (1993).

462. S. P. Yu, S. L. Sensi, L. M. Canzoniero, A. Buisson, D. W. Choi, Membrane-delimited modulation of NMDA currents by metabotropic glutamate receptor subtypes 1/5 in cultured mouse cortical neurons. *J. Physiol. (Lond.)*. **499 (Pt 3)**, 721–732 (1997).

463. S. M. Fitzjohn *et al.*, Activation of group I mGluRs potentiates NMDA responses in rat hippocampal slices. *Neurosci. Lett.* **203**, 211–213 (1996).

464. M. J. Higley, Localized GABAergic inhibition of dendritic Ca(2+) signalling. *Nat. Rev. Neurosci.* **15**, 567–572 (2014).

465. C. Romano, A. N. van den Pol, K. L. O'Malley, Enhanced early developmental expression of the metabotropic glutamate receptor mGluR5 in rat brain: protein, mRNA splice variants, and regional distribution. *J. Comp. Neurol.* **367**, 403–412 (1996).

466. J. S. Lum *et al.*, Neurodevelopmental Expression Profile of Dimeric and Monomeric Group 1 mGluRs: Relevance to Schizophrenia Pathogenesis and Treatment. *Sci. Rep.* **6**, 34391 (2016).

467. M. A. Ayoub *et al.*, Deleterious GRM1 mutations in schizophrenia. *PLoS One*. **7**, e32849 (2012).

468. R. A. W. Frank *et al.*, Clustered coding variants in the glutamate receptor complexes of individuals with schizophrenia and bipolar disorder. *PLoS One*. **6**, e19011 (2011).

469. D. W. Volk, S. M. Eggan, D. A. Lewis, Alterations in metabotropic glutamate receptor 1α and regulator of G protein signaling 4 in the prefrontal cortex in schizophrenia. *Am. J. Psychiatry*. **167**, 1489–1498 (2010).

470. S. A. Brody, F. Conquet, M. A. Geyer, Disruption of prepulse inhibition in mice lacking mGluR1. *Eur. J. Neurosci.* **18**, 3361–3366 (2003).

471. H. P. Cho *et al.*, Chemical modulation of mutant mGlu1 receptors derived from deleterious GRM1 mutations found in schizophrenics. *ACS Chem. Biol.* **9**, 2334–2346 (2014).

472. F. Knoflach *et al.*, Positive allosteric modulators of metabotropic glutamate 1 receptor: characterization, mechanism of action, and binding site. *Proc. Natl. Acad. Sci. USA*. **98**, 13402–13407 (2001).

473. E. Vieira *et al.*, 9H-Xanthene-9-carboxylic acid [1,2,4]oxadiazol-3-yl- and (2H-tetrazol-5-yl)-amides as potent, orally available mGlu1 receptor enhancers. *Bioorg. Med. Chem. Lett.* **15**, 4628–4631 (2005).

474. P. M. Garcia-Barrantes *et al.*, Development of Novel, CNS Penetrant Positive Allosteric Modulators for the Metabotropic Glutamate Receptor Subtype 1 (mGlu1), Based on an N-(3-Chloro-4-(1,3-dioxoisoindolin-2-yl)phenyl)-3-methylfuran-2-carboxamide Scaffold, That Potentiate Wild Type and Mutant mGlu1 Receptors Found in Schizophrenics. *J. Med. Chem.* **58**, 7959–7971 (2015).

475. P. M. Garcia-Barrantes *et al.*, Lead optimization of the VU0486321 series of mGlu(1) PAMs. Part 2: SAR of alternative 3-methyl heterocycles and progress towards an in vivo tool. *Bioorg. Med. Chem. Lett.* **26**, 751–756 (2016).

476. P. M. Garcia-Barrantes *et al.*, Lead optimization of the VU0486321 series of mGlu1 PAMs. Part 1: SAR of modifications to the central aryl core. *Bioorg. Med. Chem. Lett.* **25**, 5107–5110 (2015).

477. P. M. Garcia-Barrantes *et al.*, Lead optimization of the VU0486321 series of mGlu1 PAMs. Part 3. Engineering plasma stability by discovery and optimization of isoindolinone analogs. *Bioorg. Med. Chem. Lett.* **26**, 1869–1872 (2016).

478. P. M. Garcia-Barrantes *et al.*, Re-exploration of the $mGlu_1$ PAM Ro 07-11401 scaffold: Discovery of analogs with improved CNS penetration despite steep SAR. *Bioorg. Med. Chem. Lett.* **26**, 2289–2292 (2016).

479. K. L. Davis, R. S. Kahn, G. Ko, M. Davidson, Dopamine in schizophrenia: a review and reconceptualization. *Am. J. Psychiatry*. **148**, 1474–1486 (1991).

480. O. D. Howes *et al.*, Elevated striatal dopamine function linked to prodromal signs of schizophrenia. *Arch. Gen. Psychiatry*. **66**, 13–20 (2009).

481. A. Verma, B. Moghaddam, Regulation of striatal dopamine release by metabotropic glutamate receptors. *Synapse*. **28**, 220–226 (1998).

482. J. M. Campusano, J. Abarca, M. I. Forray, K. Gysling, G. Bustos, Modulation of dendritic release of dopamine by metabotropic glutamate receptors in rat substantia nigra. *Biochem. Pharmacol.* **63**, 1343–1352 (2002).

483. S. Chaki, R. Yoshikawa, S. Okuyama, Group II metabotropic glutamate receptor-mediated regulation of dopamine release from slices of rat nucleus accumbens. *Neurosci. Lett.* **404**, 182–186 (2006).

484. H. Zhang, D. Sulzer, Glutamate spillover in the striatum depresses dopaminergic transmission by activating group I metabotropic glutamate receptors. *J. Neurosci.* **23**, 10585–10592 (2003).

485. D. J. Foster *et al.*, Antipsychotic-like Effects of M4 Positive Allosteric Modulators Are Mediated by CB2 Receptor-Dependent Inhibition of Dopamine Release. *Neuron*. **91**, 1244–1252 (2016).

486. S. E. Yohn *et al.*, Activation of the mGlu1 metabotropic glutamate receptor has antipsychotic-like effects and is required for efficacy of M4 muscarinic receptor allosteric modulators. *Mol. Psychiatry* (2018), doi:10.1038/s41380-018-0206-2.

487. A. Satow *et al.*, Pharmacological effects of the metabotropic glutamate receptor 1 antagonist compared with those of the metabotropic glutamate receptor 5 antagonist and metabotropic glutamate receptor 2/3 agonist in rodents: detailed investigations with a selective allosteric metabotropic glutamate receptor 1 antagonist, FTIDC [4-[1-(2-fluoropyridine-3-yl)-5-methyl-1H-1,2,3-triazol-4-yl]-N-isopropyl-N-methyl-3,6-dihydropyridine-1(2H)-carboxamide]. *J. Pharmacol. Exp. Ther.* **326**, 577–586 (2008).

488. A. Satow *et al.*, Unique antipsychotic activities of the selective metabotropic glutamate receptor 1 allosteric antagonist 2-cyclopropyl-5-[1-(2-fluoro-3-pyridinyl)-5-methyl-1H-1,2,3-triazol-4-yl]-2,3-dihydro-1H-isoindol-1-one. *J. Pharmacol. Exp. Ther.* **330**, 179–190 (2009).

489. S. Prisco, S. Natoli, G. Bernardi, N. B. Mercuri, Group I metabotropic glutamate receptors activate burst firing in rat midbrain dopaminergic neurons. *Neuropharmacology*. **42**, 289–296 (2002).

490. A. Tozzi *et al.*, Involvement of transient receptor potential-like channels in responses to mGluR-I activation in midbrain dopamine neurons. *Eur. J. Neurosci.* **18**, 2133–2145 (2003).

491. E. Guatteo, N. B. Mercuri, G. Bernardi, T. Knöpfel, Group I metabotropic glutamate receptors mediate an inward current in rat substantia nigra dopamine neurons that is independent from calcium mobilization. *J. Neurophysiol.* **82**, 1974–1981 (1999).

492. G. Renoldi, E. Calcagno, F. Borsini, R. W. Invernizzi, Stimulation of group I mGlu receptors in the ventrotegmental area enhances extracellular dopamine in the rat medial prefrontal cortex. *J. Neurochem.* **100**, 1658–1666 (2007).

493. A. Ledonne *et al.*, Neuregulin 1 signalling modulates mGluR1 function in mesencephalic dopaminergic neurons. *Mol. Psychiatry*. **20**, 959–973 (2015).

494. O. El-Kouhen *et al.*, Blockade of mGluR1 receptor results in analgesia and disruption of motor and cognitive performances: effects of A-841720, a novel non-competitive mGluR1 receptor antagonist. *Br. J. Pharmacol.* **149**, 761–774 (2006).

495. F. Ferraguti *et al.*, Immunohistochemical localization of the mGluR1beta metabotropic glutamate receptor in the adult rodent forebrain: evidence for a differential distribution of mGluR1 splice variants. *J. Comp. Neurol.* **400**, 391–407 (1998).

496. F. Ferraguti *et al.*, Immunolocalization of metabotropic glutamate receptor 1alpha (mGluR1alpha) in distinct classes of interneuron in the CA1 region of the rat hippocampus. *Hippocampus*. **14**, 193–215 (2004).

497. C. Le Duigou, E. Savary, D. M. Kullmann, R. Miles, Induction of Anti-Hebbian LTP in CA1 Stratum Oriens Interneurons: Interactions between Group I Metabotropic Glutamate Receptors and M1 Muscarinic Receptors. *J. Neurosci.* **35**, 13542–13554 (2015).

498. S. M. Paluszkiewicz, J. L. Olmos-Serrano, J. G. Corbin, M. M. Huntsman, Impaired inhibitory control of cortical synchronization in fragile X syndrome. *J. Neurophysiol.* **106**, 2264–2272 (2011).

499. H. Sun, V. Neugebauer, mGluR1, but not mGluR5, activates feed-forward inhibition in the medial prefrontal cortex to impair decision making. *J. Neurophysiol.* **106**, 960–973 (2011).

500. J. Maksymetz *et al.*, M1 Muscarinic Receptors Modulate Fear-Related Inputs to the Prefrontal Cortex: Implications for Novel Treatments of Posttraumatic Stress Disorder. *Biol. Psychiatry*. **85**, 989–1000 (2019).

501. P. S. Goldman-Rakic, Cellular basis of working memory. *Neuron*. **14**, 477–485 (1995).

502. A. Gazzaley, A. C. Nobre, Top-down modulation: bridging selective attention and working memory. *Trends Cogn. Sci. (Regul. Ed.)*. **16**, 129–135 (2012).

503. E. K. Miller, J. D. Cohen, An integrative theory of prefrontal cortex function. *Annu. Rev. Neurosci.* **24**, 167–202 (2001).

504. A. F. T. Arnsten, Stress signalling pathways that impair prefrontal cortex structure and function. *Nat. Rev. Neurosci.* **10**, 410–422 (2009).

505. A. F. T. Arnsten, L. E. Jin, Molecular influences on working memory circuits in dorsolateral prefrontal cortex. *Prog Mol Biol Transl Sci*. **122**, 211–231 (2014).

506. S. Chattarji, A. Tomar, A. Suvrathan, S. Ghosh, M. M. Rahman, Neighborhood matters: divergent patterns of stress-induced plasticity across the brain. *Nat. Neurosci.* **18**, 1364–1375 (2015).

507. M. A. Wilson, J. R. Fadel, Cholinergic regulation of fear learning and extinction. *J. Neurosci. Res.* **95**, 836–852 (2017).

508. J. J. Pilcher, G. R. Sessions, S. A. McBride, Scopolamine impairs spatial working memory in the radial maze: an analysis by error type and arm choice. *Pharmacol. Biochem. Behav.* **58**, 449–459 (1997).

509. N. R. Mirza, I. P. Stolerman, The role of nicotinic and muscarinic acetylcholine receptors in attention. *Psychopharmacology*. **148**, 243–250 (2000).

510. E. Santini, M. Sepulveda-Orengo, J. T. Porter, Muscarinic receptors modulate the intrinsic excitability of infralimbic neurons and consolidation of fear extinction. *Neuropsychopharmacology*. **37**, 2047–2056 (2012).

511. A. Navarria *et al.*, Rapid antidepressant actions of scopolamine: Role of medial prefrontal cortex and M1-subtype muscarinic acetylcholine receptors. *Neurobiol. Dis.* **82**, 254–261 (2015).

512. G. J. Digby *et al.*, Novel allosteric agonists of M1 muscarinic acetylcholine receptors induce brain region-specific responses that correspond with behavioral effects in animal models. *J. Neurosci.* **32**, 8532–8544 (2012).

513. D. J. Sheffler *et al.*, A novel selective muscarinic acetylcholine receptor subtype 1 antagonist reduces seizures without impairing hippocampus-dependent learning. *Mol. Pharmacol.* **76**, 356–368 (2009).

514. J. E. Marlo *et al.*, Discovery and characterization of novel allosteric potentiators of M1 muscarinic receptors reveals multiple modes of activity. *Mol. Pharmacol.* **75**, 577–588 (2009).

515. S. E. Hamilton *et al.*, Disruption of the m1 receptor gene ablates muscarinic receptor-dependent M current regulation and seizure activity in mice. *Proc. Natl. Acad. Sci. USA*. **94**, 13311–13316 (1997).

516. A. Kamsler, T. J. McHugh, D. Gerber, S. Y. Huang, S. Tonegawa, Presynaptic m1 muscarinic receptors are necessary for mGluR long-term depression in the hippocampus. *Proc. Natl. Acad. Sci. USA*. **107**, 1618–1623 (2010).

517. A. Burgos-Robles, I. Vidal-Gonzalez, G. J. Quirk, Sustained conditioned responses in prelimbic prefrontal neurons are correlated with fear expression and extinction failure. *J. Neurosci.* **29**, 8474–8482 (2009).

518. L. A. Bell, K. A. Bell, A. R. McQuiston, Synaptic muscarinic response types in hippocampal CA1 interneurons depend on different levels of presynaptic activity and different muscarinic receptor subtypes. *Neuropharmacology*. **73**, 160–173 (2013).

519. Z. Xiang, A. D. Thompson, C. K. Jones, C. W. Lindsley, P. J. Conn, Roles of the M1 muscarinic acetylcholine receptor subtype in the regulation of basal ganglia function and

implications for the treatment of Parkinson's disease. *J. Pharmacol. Exp. Ther.* **340**, 595–603 (2012).

520. M. Bubser, N. Byun, M. R. Wood, C. K. Jones, Muscarinic receptor pharmacology and circuitry for the modulation of cognition. *Handb Exp Pharmacol*, 121–166 (2012).

521. M. Yamasaki, M. Matsui, M. Watanabe, Preferential localization of muscarinic M1 receptor on dendritic shaft and spine of cortical pyramidal cells and its anatomical evidence for volume transmission. *J. Neurosci.* **30**, 4408–4418 (2010).

522. E. S. Wohleb *et al.*, GABA interneurons mediate the rapid antidepressant-like effects of scopolamine. *J. Clin. Invest.* (2016).

523. B. M. Graham, M. R. Milad, The study of fear extinction: implications for anxiety disorders. *Am. J. Psychiatry*. **168**, 1255–1265 (2011).

524. B. P. Godsil, J. P. Kiss, M. Spedding, T. M. Jay, The hippocampal-prefrontal pathway: the weak link in psychiatric disorders? *Eur. Neuropsychopharmacol.* **23**, 1165–1181 (2013).

525. A. Ghoshal, P. J. Conn, The hippocampo-prefrontal pathway: a possible therapeutic target for negative and cognitive symptoms of schizophrenia. *Future Neurol.* **10**, 115–128 (2015).

526. S. L. Rauch, L. M. Shin, E. A. Phelps, Neurocircuitry models of posttraumatic stress disorder and extinction: human neuroimaging research--past, present, and future. *Biol. Psychiatry*. **60**, 376–382 (2006).

527. S. A. Allsop, C. M. Vander Weele, R. Wichmann, K. M. Tye, Optogenetic insights on the relationship between anxiety-related behaviors and social deficits. *Front. Behav. Neurosci.* **8**, 241 (2014).

528. J. A. Gordon, On being a circuit psychiatrist. *Nat. Neurosci.* **19**, 1385–1386 (2016).

529. E. A. Phelps, M. R. Delgado, K. I. Nearing, J. E. LeDoux, Extinction learning in humans: role of the amygdala and vmPFC. *Neuron*. **43**, 897–905 (2004).

530. P. Tovote, J. P. Fadok, A. Lüthi, Neuronal circuits for fear and anxiety. *Nat. Rev. Neurosci.* **16**, 317–331 (2015).

531. E. Santini, G. J. Quirk, J. T. Porter, Fear conditioning and extinction differentially modify the intrinsic excitability of infralimbic neurons. *J. Neurosci.* **28**, 4028–4036 (2008).

532. E. Scarr *et al.*, The distribution of muscarinic M1 receptors in the human hippocampus. *J Chem Neuroanat*. **77**, 187–192 (2016).

533. A. A. Disney, K. V. Domakonda, C. Aoki, Differential expression of muscarinic acetylcholine receptors across excitatory and inhibitory cells in visual cortical areas V1 and V2 of the macaque monkey. *J. Comp. Neurol.* **499**, 49–63 (2006).

534. M. B. Young, S. A. Thomas, M1-muscarinic receptors promote fear memory consolidation via phospholipase C and the M-current. *J. Neurosci.* **34**, 1570–1578 (2014).

535. M. R. Milad *et al.*, A role for the human dorsal anterior cingulate cortex in fear expression. *Biol. Psychiatry*. **62**, 1191–1194 (2007).

536. B. J. Stansley *et al.*, Contextual fear extinction induces hippocampal metaplasticity mediated by metabotropic glutamate receptor 5. *Cereb. Cortex*. **28**, 4291–4304 (2018).

537. J. Park, J.-W. Chun, H.-J. Park, E. Kim, J.-J. Kim, Involvement of amygdala-prefrontal dysfunction in the influence of negative emotion on the resolution of cognitive conflict in patients with schizophrenia. *Brain Behav.* **8**, e01064 (2018).

538. D. J. Holt *et al.*, Extinction memory is impaired in schizophrenia. *Biol. Psychiatry*. **65**, 455–463 (2009).

539. S. K. Hill, J. R. Bishop, D. Palumbo, J. A. Sweeney, Effect of second-generation antipsychotics on cognition: current issues and future challenges. *Expert Rev Neurother*. **10**, 43–57 (2010).

540. M. F. Green, Impact of cognitive and social cognitive impairment on functional outcomes in patients with schizophrenia. *J. Clin. Psychiatry*. **77 Suppl 2**, 8–11 (2016).

541. D. A. Lewis, A. A. Curley, J. R. Glausier, D. W. Volk, Cortical parvalbumin interneurons and cognitive dysfunction in schizophrenia. *Trends Neurosci.* **35**, 57–67 (2012).

542. K. A. Cummings, R. L. Clem, Prefrontal somatostatin interneurons encode fear memory. *Nat. Neurosci.* **23**, 61–74 (2020).

543. F. Ali *et al.*, Ketamine disinhibits dendrites and enhances calcium signals in prefrontal dendritic spines. *Nat. Commun.* **11**, 72 (2020).

544. M. Tsubomoto *et al.*, Expression of Transcripts Selective for GABA Neuron Subpopulations across the Cortical Visuospatial Working Memory Network in the Healthy State and Schizophrenia. *Cereb. Cortex*. **29**, 3540–3550 (2019).

545. E. C. Muly, M. Maddox, Y. Smith, Distribution of mGluR1alpha and mGluR5 immunolabeling in primate prefrontal cortex. *J. Comp. Neurol.* **467**, 521–535 (2003).

546. G. López-Bendito, R. Shigemoto, A. Fairén, R. Luján, Differential distribution of group I metabotropic glutamate receptors during rat cortical development. *Cereb. Cortex*. **12**, 625–638 (2002).

547. A. Baude *et al.*, The metabotropic glutamate receptor (mGluR1 alpha) is concentrated at perisynaptic membrane of neuronal subpopulations as detected by immunogold reaction. *Neuron*. **11**, 771–787 (1993).

548. G. Mannaioni, M. J. Marino, O. Valenti, S. F. Traynelis, P. J. Conn, Metabotropic glutamate receptors 1 and 5 differentially regulate CA1 pyramidal cell function. *J. Neurosci.* **21**, 5925–5934 (2001).

549. J. Schindelin *et al.*, Fiji: an open-source platform for biological-image analysis. *Nat. Methods*. **9**, 676–682 (2012).

550. H. Hu, J. Z. Cavendish, A. Agmon, Not all that glitters is gold: off-target recombination in the somatostatin-IRES-Cre mouse line labels a subset of fast-spiking interneurons. *Front. Neural Circuits*. **7**, 195 (2013).

551. N. E. Byun *et al.*, Antipsychotic drug-like effects of the selective M4 muscarinic acetylcholine receptor positive allosteric modulator VU0152100. *Neuropsychopharmacology*. **39**, 1578–1593 (2014).

552. M. S. Moehle *et al.*, Cholinergic Projections to the Substantia Nigra Pars Reticulata Inhibit Dopamine Modulation of Basal Ganglia through the M4 Muscarinic Receptor. *Neuron*. **96**, 1358–1372.e4 (2017).

553. J. B. Mandeville *et al.*, Dynamic functional imaging of relative cerebral blood volume during rat forepaw stimulation. *Magn. Reson. Med.* **39**, 615–624 (1998).

554. H. Markram *et al.*, Interneurons of the neocortical inhibitory system. *Nat. Rev. Neurosci.* **5**, 793–807 (2004).

555. J. C. Magee, Dendritic integration of excitatory synaptic input. *Nat. Rev. Neurosci.* **1**, 181–190 (2000).

556. S. M. Cohen, R. W. Tsien, D. C. Goff, M. M. Halassa, The impact of NMDA receptor hypofunction on GABAergic neurons in the pathophysiology of schizophrenia. *Schizophr. Res.* **167**, 98–107 (2015).

557. E. A. Hackler *et al.*, Selective potentiation of the metabotropic glutamate receptor subtype 2 blocks phencyclidine-induced hyperlocomotion and brain activation. *Neuroscience*. **168**, 209–218 (2010).

558. A. Guidotti *et al.*, GABAergic dysfunction in schizophrenia: new treatment strategies on the horizon. *Psychopharmacology*. **180**, 191–205 (2005).

559. D. A. Lewis, D. W. Volk, T. Hashimoto, Selective alterations in prefrontal cortical GABA neurotransmission in schizophrenia: a novel target for the treatment of working memory dysfunction. *Psychopharmacology*. **174**, 143–150 (2004).

560. U. Rudolph, H. Möhler, GABAA receptor subtypes: Therapeutic potential in Down syndrome, affective disorders, schizophrenia, and autism. *Annu. Rev. Pharmacol. Toxicol.* **54**, 483–507 (2014).

561. M.-Y. Xu, A. H. C. Wong, GABAergic inhibitory neurons as therapeutic targets for cognitive impairment in schizophrenia. *Acta Pharmacol Sin*. **39**, 733–753 (2018).

562. D. A. Lewis *et al.*, Subunit-selective modulation of GABA type A receptor neurotransmission and cognition in schizophrenia. *Am. J. Psychiatry*. **165**, 1585–1593 (2008).

563. K. M. Gill, D. J. Lodge, J. M. Cook, S. Aras, A. A. Grace, A novel α5GABA(A)R-positive allosteric modulator reverses hyperactivation of the dopamine system in the MAM model of schizophrenia. *Neuropsychopharmacology*. **36**, 1903–1911 (2011).

564. T. D. Prevot *et al.*, Novel Benzodiazepine-Like Ligands with Various Anxiolytic, Antidepressant, or Pro-Cognitive Profiles. *Mol. Neuropsychiatry*. **5**, 84–97 (2019).

565. T. M. Ballard *et al.*, RO4938581, a novel cognitive enhancer acting at GABAA alpha5 subunit-containing receptors. *Psychopharmacology*. **202**, 207–223 (2009).

566. Y. Geffen, R. Keefe, J. Rabinowitz, R. Anand, M. Davidson, Bl-1020, a new γ-aminobutyric acid-enhanced antipsychotic: results of 6-week, randomized, double-blind, controlled, efficacy and safety study. *J. Clin. Psychiatry*. **73**, e1168–74 (2012).

567. E. Burke, J. Wojcik, L. J. Seidman, A. Green, T.-U. W. Woo, F43. potentiation of inhibitory neurotransmission in the treatment of recent-onset schizophrenia by modification of developmental pruning of prefrontal circuitry. *Schizophr. Bull.* **44**, S235–S236 (2018).

568. J. M. Schulz, F. Knoflach, M.-C. Hernandez, J. Bischofberger, Dendrite-targeting interneurons control synaptic NMDA-receptor activation via nonlinear α5-GABAA receptors. *Nat. Commun.* **9**, 3576 (2018).

569. M. T. Koh, S. Rosenzweig-Lipson, M. Gallagher, Selective GABA(A) α5 positive allosteric modulators improve cognitive function in aged rats with memory impairment. *Neuropharmacology*. **64**, 145–152 (2013).

570. R. B. Poorthuis *et al.*, Layer-specific modulation of the prefrontal cortex by nicotinic acetylcholine receptors. *Cereb. Cortex*. **23**, 148–161 (2013).

571. J. Haam, J. Zhou, G. Cui, J. L. Yakel, Septal cholinergic neurons gate hippocampal output to entorhinal cortex via oriens lacunosum moleculare interneurons. *Proc. Natl. Acad. Sci. USA*. **115**, E1886–E1895 (2018).

572. J. J. Lawrence, J. M. Statland, Z. M. Grinspan, C. J. McBain, Cell type-specific dependence of muscarinic signalling in mouse hippocampal stratum oriens interneurones. *J. Physiol. (Lond.)*. **570**, 595–610 (2006).

573. J. R. Tregellas, K. P. Wylie, Alpha7 nicotinic receptors as therapeutic targets in schizophrenia. *Nicotine Tob. Res.* **21**, 349–356 (2019).

574. A. C. Conley *et al.*, Cognitive and electrophysiological measures of a phase 1 single ascending dose study of the muscarinic positive allosteric modulator vu319. *Alzheimers Dement.* **15**, P253 (2019).

575. D. J. Lodge, M. M. Behrens, A. A. Grace, A loss of parvalbumin-containing interneurons is associated with diminished oscillatory activity in an animal model of schizophrenia. *J. Neurosci.* **29**, 2344–2354 (2009).

576. H.-X. Wang, W.-J. Gao, Cell type-specific development of NMDA receptors in the interneurons of rat prefrontal cortex. *Neuropsychopharmacology*. **34**, 2028–2040 (2009).

577. D. C. Rotaru, H. Yoshino, D. A. Lewis, G. B. Ermentrout, G. Gonzalez-Burgos, Glutamate receptor subtypes mediating synaptic activation of prefrontal cortex neurons: relevance for schizophrenia. *J. Neurosci.* **31**, 142–156 (2011).

578. M. E. Horn, R. A. Nicoll, Somatostatin and parvalbumin inhibitory synapses onto hippocampal pyramidal neurons are regulated by distinct mechanisms. *Proc. Natl. Acad. Sci. USA*. **115**, 589–594 (2018).

579. L. V. Moran, L. E. Hong, High vs low frequency neural oscillations in schizophrenia. *Schizophr. Bull.* **37**, 659–663 (2011).

580. S. J. Fung, S. G. Fillman, M. J. Webster, C. Shannon Weickert, Schizophrenia and bipolar disorder show both common and distinct changes in cortical interneuron markers. *Schizophr. Res.* **155**, 26–30 (2014).

581. T. Kroon *et al.*, Group I mGluR-Mediated Activation of Martinotti Cells Inhibits Local Cortical Circuitry in Human Cortex. *Front. Cell Neurosci.* **13**, 315 (2019).

582. D. M. Gerhard *et al.*, GABA interneurons are the cellular trigger for ketamine's rapid antidepressant actions. *J. Clin. Invest.* (2020).

583. B. Kirkpatrick, W. S. Fenton, W. T. Carpenter, S. R. Marder, The NIMH-MATRICS consensus statement on negative symptoms. *Schizophr. Bull.* **32**, 214–219 (2006).

584. A. Aiba *et al.*, Reduced hippocampal long-term potentiation and context-specific deficit in associative learning in mGluR1 mutant mice. *Cell*. **79**, 365–375 (1994).

585. A. Aiba *et al.*, Deficient cerebellar long-term depression and impaired motor learning in mGluR1 mutant mice. *Cell*. **79**, 377–388 (1994).

586. R. Gao, P. Penzes, Common mechanisms of excitatory and inhibitory imbalance in schizophrenia and autism spectrum disorders. *Curr. Mol. Med.* **15**, 146–167 (2015).

587. J.-M. Fritschy, Epilepsy, E/I balance and GABA(A) receptor plasticity. *Front. Mol. Neurosci.* **1**, 5 (2008).

588. M. A. Busche, A. Konnerth, Impairments of neural circuit function in Alzheimer's disease. *Philos. Trans. R. Soc. Lond. B, Biol. Sci.* **371** (2016), doi:10.1098/rstb.2015.0429.

589. M. Bubser *et al.*, Selective activation of M4 muscarinic acetylcholine receptors reverses MK-801-induced behavioral impairments and enhances associative learning in rodents. *ACS Chem. Neurosci.* **5**, 920–942 (2014).

590. R. W. Gould *et al.*, Cognitive enhancement and antipsychotic-like activity following repeated dosing with the selective M4 PAM VU0467154. *Neuropharmacology*. **128**, 492–502 (2018).

591. F. R. Schneier *et al.*, Combined prolonged exposure therapy and paroxetine for PTSD related to the World Trade Center attack: a randomized controlled trial. *Am. J. Psychiatry*. **169**, 80–88 (2012).

592. M. C. Mithoefer, M. T. Wagner, A. T. Mithoefer, L. Jerome, R. Doblin, The safety and efficacy of {+/-}3,4-methylenedioxymethamphetamine-assisted psychotherapy in subjects with chronic, treatment-resistant posttraumatic stress disorder: the first randomized controlled pilot study. *J. Psychopharmacol. (Oxford)*. **25**, 439–452 (2011).

593. M. C. Mithoefer *et al.*, Durability of improvement in post-traumatic stress disorder symptoms and absence of harmful effects or drug dependency after 3,4-methylenedioxymethamphetamine-assisted psychotherapy: a prospective long-term follow-up study. *J. Psychopharmacol. (Oxford)*. **27**, 28–39 (2013).

594. K. J. Ressler *et al.*, Cognitive enhancers as adjuncts to psychotherapy: use of D-cycloserine in phobic individuals to facilitate extinction of fear. *Arch. Gen. Psychiatry*. **61**, 1136–1144 (2004).

595. N. Singewald, C. Schmuckermair, N. Whittle, A. Holmes, K. J. Ressler, Pharmacology of cognitive enhancers for exposure-based therapy of fear, anxiety and trauma-related disorders. *Pharmacol. Ther.* **149**, 150–190 (2015).

596. R. A. de Kleine, G.-J. Hendriks, W. J. C. Kusters, T. G. Broekman, A. van Minnen, A randomized placebo-controlled trial of D-cycloserine to enhance exposure therapy for posttraumatic stress disorder. *Biol. Psychiatry*. **71**, 962–968 (2012).

597. J. Difede *et al.*, D-cycloserine augmentation of exposure therapy for post-traumatic stress disorder: a pilot randomized clinical trial. *Neuropsychopharmacology*. **39**, 1052–1058 (2014).

598. D. J. Holt, G. Coombs, M. A. Zeidan, D. C. Goff, M. R. Milad, Failure of neural responses to safety cues in schizophrenia. *Arch. Gen. Psychiatry*. **69**, 893–903 (2012).

599. D. L. Uliana, L. B. M. Resstel, A. A. Grace, Fear extinction disruption in a developmental rodent model of schizophrenia correlates with an impairment in basolateral amygdala-medial prefrontal cortex plasticity. *Neuropsychopharmacology*. **43**, 2459–2467 (2018).

600. R. W. Buchanan *et al.*, A randomized clinical trial of MK-0777 for the treatment of cognitive impairments in people with schizophrenia. *Biol. Psychiatry*. **69**, 442–449 (2011).

601. J. P. Redrobe *et al.*, Negative modulation of GABAA α5 receptors by RO4938581 attenuates discrete sub-chronic and early postnatal phencyclidine (PCP)-induced cognitive deficits in rats. *Psychopharmacology*. **221**, 451–468 (2012).

602. Y. Geffen *et al.*, BL-1020: a novel antipsychotic drug with GABAergic activity and low catalepsy, is efficacious in a rat model of schizophrenia. *Eur. Neuropsychopharmacol.* **19**, 1–13 (2009).

603. A. Nudelman *et al.*, A mutual prodrug ester of GABA and perphenazine exhibits antischizophrenic efficacy with diminished extrapyramidal effects. *J. Med. Chem.* **51**, 2858–2862 (2008).

604. J. G. English, B. L. Roth, Chemogenetics-A Transformational and Translational Platform. *JAMA Neurol.* **72**, 1361–1366 (2015).

605. D. Scheggia *et al.*, Somatostatin interneurons in the prefrontal cortex control affective state discrimination in mice. *Nat. Neurosci.* **23**, 47–60 (2020).

606. T. Hakami *et al.*, NMDA receptor hypofunction leads to generalized and persistent aberrant gamma oscillations independent of hyperlocomotion and the state of consciousness. *PLoS One*. **4**, e6755 (2009).

607. E. Jodo *et al.*, Activation of medial prefrontal cortex by phencyclidine is mediated via a hippocampo-prefrontal pathway. *Cereb. Cortex*. **15**, 663–669 (2005).

608. A. R. Mohn, R. R. Gainetdinov, M. G. Caron, B. H. Koller, Mice with reduced NMDA receptor expression display behaviors related to schizophrenia. *Cell*. **98**, 427–436 (1999).

609. K. L. Stark *et al.*, Altered brain microRNA biogenesis contributes to phenotypic deficits in a 22q11-deletion mouse model. *Nat. Genet.* **40**, 751–760 (2008).

610. K. Hill *et al.*, Hypofrontality in schizophrenia: a meta-analysis of functional imaging studies. *Acta Psychiatr. Scand.* **110**, 243–256 (2004).

611. J. H. Callicott *et al.*, Complexity of prefrontal cortical dysfunction in schizophrenia: more than up or down. *Am. J. Psychiatry*. **160**, 2209–2215 (2003).

612. J. M. Rook *et al.*, Biased mGlu5-Positive Allosteric Modulators Provide In Vivo Efficacy without Potentiating mGlu5 Modulation of NMDAR Currents. *Neuron*. **86**, 1029–1040 (2015).

613. Z. Xiang *et al.*, mGlu5 Positive Allosteric Modulators Facilitate Long-Term Potentiation via Disinhibition Mediated by mGlu5-Endocannabinoid Signaling. *ACS Pharmacol. Transl. Sci.* **2**, 198–209 (2019).

614. S. Yin *et al.*, Selective actions of novel allosteric modulators reveal functional heteromers of metabotropic glutamate receptors in the CNS. *J. Neurosci.* **34**, 79–94 (2014).

615. D. Moreno Delgado *et al.*, Pharmacological evidence for a metabotropic glutamate receptor heterodimer in neuronal cells. *Elife*. **6** (2017), doi:10.7554/eLife.25233.

616. C. E. Gee, P. Benquet, U. Gerber, Group I metabotropic glutamate receptors activate a calcium-sensitive transient receptor potential-like conductance in rat hippocampus. *J. Physiol. (Lond.)*. **546**, 655–664 (2003).

617. J. Hartmann, H. A. Henning, A. Konnerth, mGluR1/TRPC3-mediated Synaptic Transmission and Calcium Signaling in Mammalian Central Neurons. *Cold Spring Harb. Perspect. Biol.* **3** (2011), doi:10.1101/cshperspect.a006726.

618. F. Conquet *et al.*, Motor deficit and impairment of synaptic plasticity in mice lacking mGluR1. *Nature*. **372**, 237–243 (1994).

619. H. G. S. Martin, O. Lassalle, O. J. Manzoni, Differential Adulthood Onset mGlu5 Signaling Saves Prefrontal Function in the Fragile X Mouse. *Cereb. Cortex*. **27**, 5592–5602 (2017).

620. S. Chiechio, Modulation of chronic pain by metabotropic glutamate receptors. *Adv. Pharmacol.* **75**, 63–89 (2016).

621. N. D. Iadarola *et al.*, Ketamine and other N-methyl-D-aspartate receptor antagonists in the treatment of depression: a perspective review. *Ther. Adv. Chronic Dis.* **6**, 97–114 (2015).

622. W. C. Drevets, C. A. Zarate, M. L. Furey, Antidepressant effects of the muscarinic cholinergic receptor antagonist scopolamine: a review. *Biol. Psychiatry*. **73**, 1156–1163 (2013).

623. C. Tai, Y. Abe, R. E. Westenbroek, T. Scheuer, W. A. Catterall, Impaired excitability of somatostatin- and parvalbumin-expressing cortical interneurons in a mouse model of Dravet syndrome. *Proc. Natl. Acad. Sci. USA*. **111**, E3139–48 (2014).

624. L. C. Schmid *et al.*, Dysfunction of Somatostatin-Positive Interneurons Associated with Memory Deficits in an Alzheimer's Disease Model. *Neuron*. **92**, 114–125 (2016).

625. K. Park *et al.*, Optogenetic activation of parvalbumin and somatostatin interneurons selectively restores theta-nested gamma oscillations and oscillation-induced spike timing-dependent long-term potentiation impaired by amyloid β oligomers. *BMC Biol.* **18**, 7 (2020).

626. M. Vandecasteele *et al.*, Opto-activation of cortical somatostatin interneurons alleviates parkinsonian symptoms. *BioRxiv* (2018), doi:10.1101/460535.